

SSD

SCIENCE FOR A SUSTAINABLE DEVELOPMENT



POLICY SUPPORT SYSTEM FOR CARBON CAPTURE AND STORAGE AND COLLABORATION BETWEEN BELGIUM-THE NETHERLANDS

"PSS-CCS"

K. PIESSENS, K. WELKENHUYSEN, B. LAENEN, H. FERKET, W. NIJS,
J. DUERINCK, E. COCHEZ, PH. MATHIEU, D. VALENTINY, J.-M.
BAELE, N. DUPONT, CH. HENDRIKS



ENERGY



TRANSPORT AND MOBILITY



AGRO-FOOD



HEALTH AND ENVIRONMENT



CLIMATE



BIODIVERSITY



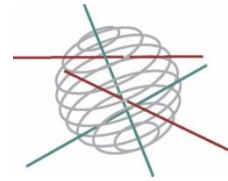
ATMOSPHERE AND TERRESTRIAL AND MARINE ECOSYSTEMS



TRANSVERSAL ACTIONS



SCIENCE FOR A SUSTAINABLE DEVELOPMENT
(SSD)



Climate

FINAL REPORT
**POLICY SUPPORT SYSTEM FOR CARBON CAPTURE AND
STORAGE AND COLLABORATION BETWEEN BELGIUM-
THE NETHERLANDS**
“PSS-CCS”

Promotors

Kris Piessens

Royal Belgian Institute of Natural Sciences
Geological Survey of Belgium

Ben Laenen

Vlaamse Instelling voor Technologisch Onderzoek (VITO)

Wouter Nijs

Vlaamse Instelling voor Technologisch Onderzoek (VITO)

Philippe Mathieu
Université de Liège

Jean-Marc Baele
Faculté Polytechnique de Mons

Authors

Kris Piessens, Kris Welkenhuysen (RBINS)

Ben Laenen, Helga Ferket, Wouter Nijs, Jan Duerinck, Evelien Cochez (VITO)

Philippe Mathieu, David Valentiny (ULg)

Jean-Marc Baele, Nicolas Dupont (UMons)

Chris Hendriks (ECOFYS)





D/2012/1191/7

Published in 2012 by the Belgian Science Policy

Avenue Louise 231

Louizalaan 231

B-1050 Brussels

Belgium

Tel: +32 (0)2 238 34 11 – Fax: +32 (0)2 230 59 12

<http://www.belspo.be>

Contact person: Sophie Verheyden

+32 (0)2 238 34 11

Neither the Belgian Science Policy nor any person acting on behalf of the Belgian Science Policy is responsible for the use which might be made of the following information. The authors are responsible for the content.

No part of this publication may be reproduced, stored in a retrieval system, or transmitted in any form or by any means, electronic, mechanical, photocopying, recording, or otherwise, without indicating the reference:

K. PIESSENS, K. WELKENHUYSEN, B. LAENEN, H. FERKET, W. NIJS, J. DUERINCK, E. COCHEZ, PH. MATHIEU, D. VALENTINY, J.-M. BAELE, N. DUPONT, CH. HENDRIKS. ***Policy Support System for Carbon Capture and Storage and collaboration between Belgium-the Netherlands - "PSS-CCS"***. Final Report. Brussels: Belgian Science Policy 2009 – 335 p. (Research Programme Science for a Sustainable Development)

TABLE OF CONTENT

TABLE OF CONTENT	3
SUMMARY.....	7
Context	7
Objectives.....	7
Conclusions	8
Contribution of the project in a context of scientific support to a sustainable development policy.....	9
Key-words	10
1. INTRODUCTION	11
2. METHODOLOGY AND RESULTS.....	13
2.1. Policy support system	13
2.1.1. PSS Simulator introduction	13
2.1.2. PSS Simulator structure & operation	13
2.1.3. Capture.....	18
2.1.4. Transport	20
2.1.5. Storage	25
2.1.6. Project decisions	30
2.1.7. Link with TIMES-BE	38
2.1.8. Scenarios.....	38
2.2. Risks and monitoring challenges for CO ₂ sequestration in coal	42
2.2.1. introduction.....	42
2.2.2. Risk assessment in coal-bearing strata.....	45
2.2.3. CO ₂ sequestration in coal in belgium	68
2.2.4. Coal sequences in the Hainaut Basin.....	77
2.2.5. Aquifers in the Hainaut Basin	89
2.2.6. Monitoring of gas leakage from coal strata	91
2.2.7. Cost of monitoring and safety	110
2.3. Data collection for carbon capture in power and non-power sectors.....	121
2.3.1. Summary	121
2.3.2. Introduction.....	124
2.3.3. CO ₂ Capturing technologies	124
2.3.4. CO ₂ capture in the power sector.	138
2.3.5. CO ₂ capture in the cement industry.....	155

2.3.6.	capture in the iron and steel making industry	170
2.3.7.	CO ₂ capture in the hydrogen industry	185
2.3.8.	CO ₂ capture in the ammonia industry	198
2.3.9.	CO ₂ capture in the refinery industry	209
2.3.10.	CO ₂ capture from industrial boilers	237
3.	POLICY SUPPORT	251
3.1.	Results of the PSS II simulator	251
3.1.1.	Power sector.....	251
3.1.2.	Iron & steel sector.....	275
3.1.3.	Transport	281
3.1.4.	CO ₂ storage	284
3.1.5.	Conclusions: key messages.....	291
3.2.	The European and Belgian TIMES model.....	293
3.2.1.	Overview of the scenarios	293
3.2.2.	The EU climate policy perspectives and their implications for Belgium.....	295
3.2.3.	Uncertainty issues with TIMES.....	295
3.2.4.	Setting up links with PSS II	295
3.3.	Comparison of some conclusions from the TIMES BE and PSS II models	296
3.3.1.	Results of the Reference scenario	297
3.3.2.	Results for the NoNucGoCCS scenario.....	300
3.3.3.	The message behind the differences	304
4.	DISSEMINATION AND VALORISATION	307
4.1.	Introduction.....	307
4.2.	PSS-CCS phase I	307
4.2.1.	Organisation of dissemination events	307
4.2.2.	Presentations at other events	307
4.3.	PSS-CCS phase II and BeNe	308
4.3.1.	Organisation of dissemination events	308
4.3.2.	Presentations at other events	308
4.4.	Dissemination and valorisation trough other projects	309
5.	PUBLICATIONS	311
5.1.	PSS-CCS phase I	311
5.1.1.	Peer reviewed publications	311
5.1.2.	Other publications.....	311

- 5.2. PSS-CCS phase II and BeNe312
 - 5.2.1. Peer reviewed publications 312
 - 5.2.2. Other publications..... 313
- 6. ACKNOWLEDGEMENTS317
- 7. REFERENCES.....319
- 8. ANNEXES..... 335

SUMMARY

Context

The climate on Earth is changing due to the increased emissions of CO₂ into the atmosphere, and these changes are expected to have a predominantly negative impact, with potentially dramatic economic, social and environmental consequences. The increased concentrations of CO₂ are already resulting in acidification of the oceans, which adds further to the environmental pressure. Reducing the emissions of CO₂ is therefore of prime importance. CO₂ Capture and Storage (CCS) is considered as an essential element in the portfolio of measures, and has the potential to reduce the CO₂ emissions from large industrial facilities to nearly zero. This has been recognised by the international community and especially Europe is being proactive in stimulating the development and implementation of CCS. Policy related research on CCS in Belgium has been centralised in the PSS-CCS projects (Policy Support System for Carbon Capture and Storage). Phase one (PSS-CCS I) started at the end of 2005 and the results were integrally published in 2009 (Piessens et al., 2009). This work was continued in the projects PSS-CCS II, the actual phase two, and the international valorisation project PSS-CCS BeNe which extended the scope to the Netherlands and created official bridges between the national CCS projects in Belgium and the Netherlands (CATO-2).

Objectives

From the start, the PSS-CCS projects (Policy Support System for Carbon Capture and Storage) have promised to provide detailed and objective insights in the role that CCS can play in the CO₂ mitigation efforts of Belgium. Achieving this central objective is only possible by bringing together information, data and methodologies from widely different fields. The list below gives a brief overview of these activities, which have often resulted in deliverables which are usually to be regarded as important achievements in their own right.

- Inventory of the industrial emission sources for CO₂ in Belgium at plant and sector level, for providing an actual view on these emissions and the need to replace aging infrastructure.
- Economic and technical analysis of the different technologies and their performance that allow capturing CO₂ from power plants and other industrial facilities.
- Development and calibration of a least-cost routing application for transport of CO₂ by pipeline.

- Summary of the geological data to identify geological reservoirs (aquifers and coal related storage options) that are potentially suited for geological storage of CO₂.
- Risk evaluation of different types of reservoirs and a techno-economic overview of the different techniques to monitor a CO₂ reservoir.
- Overview of the storage options in neighbouring countries accessible from Belgium, and an assessment on the domestic use of these reservoirs in those countries.
- Analysis of the production, conversion and consumption of energy in Belgium using the TIMES-BE model, including CCS technologies.
- Development of the PSS II simulator for detailed and ad-hoc predictions of CCS implementation in Belgium.
- Evaluating the simulation results of the two models regarding the economic and environmental role that CCS can play under different scenarios.

Conclusions

The PSS-CCS projects have looked into the different, but related aspects of CCS.

Capture of CO₂ in the power sector is retaken and update in this report, but particular attention is given to how capture technologies can be integrated in industrial production processes. Particular attention is given to the production of cement, iron and steel, hydrogen, ammonia, refineries and industrial boilers, making this report a reference document for the capture from industrial sources. Cost estimates of those technologies are provided where possible, often indicating that capture can be more cost efficiently than in the power sector (e.g. steel, hydrogen...). For others, such as refineries, it may be quite challenging because of the complexity of such installations.

The storage of CO₂ is only of secondary importance when considering only costs, but is essential in the project planning and communication. This is why, now demonstration projects in neighbouring countries have become a reality, this topic is attracting an increasing amount of attention. This report in particular looks at storage in coal bearing sequences by evaluating the different potential migration routes of CO₂. In an attempt to quantify the amounts of CO₂ that may migrate to the surface, a comparison is made with published estimates. Conservative estimates for leakage along abandoned wells would be below the health concentration of CO₂, and vertical migration of CO₂ in the Campine Basin in absence of such wells or conductive faults would be below meter scale at a 100y time resolution. Migration of CO₂ out of the coal-bearing strata would be even more difficult, since coal acts as both a reservoir and seal, and additional sealing layers are present within the heterogeneous sequence. Nevertheless, as also required by

European law, extensive monitoring is required. A portfolio of different technologies is required to achieve a the resolution required for confirming that CO₂ is not leaking from the reservoir, leading to relatively high monitoring costs for small reservoirs or reservoirs with low injectivity.

A comprehensive overview of the coal sequences in the Hainaut Basin indicates a storage potential of 500 to 700 Mt in this area. Injection strategies for coal are discussed acknowledging the geological particularities of this coal basin. The capacity of the Dinantian aquifer in this area is comparable to that of coal, but of particularly interest because of the high injectivity.

The databases of the PSS simulator have been updated and extended according to the newly acquired data in this project, and have been calibrated for pipeline routing against confidential data from industry. Together with the important improvements, the current version (PSS II) produces realistic and reliable forecasts on power technologies based on coal, natural gas and biomass, as well as for the steel sector. PSS II is used in parallel with TIMES-BE, using large the same databases to make the results compatible.

These models show that CCS will be a likely economic option in the power sector, but especially in industry. However, relatively high ETS prices for CO₂ emissions are required to trigger large scale implementation of CCS in especially the power sector. An essential factor in assuring that very low emission targets are realised by 2050, a portfolio of technologies is required: if technologies are left out, the probability that the low targets are reached decreases dramatically. Technology lock-in additionally poses a real threat, but can be mitigated with appropriate policy measures. When it comes to storage, the development of domestic storage capacity is justified, although Belgium will additionally have to rely on the export of CO₂.

Contribution of the project in a context of scientific support to a sustainable development policy

During the more or less five years during which the PSS-CCS projects have been active, they have been able to fill the need for information and follow-up on the topic of CCS in Belgium. This resulted in a large and active follow-up committee representing over 30 institutes, including many administrations and stakeholders that weigh on environmental and economic policy. The different valorisation events of the project were initially strongly focussed on the dissemination of correct and objective information on CCS, for which the international interest was strongly growing. This was in line with the activities within the project of which the earliest tasks were focussed on gathering and organising the data required for modelling the role of CCS. Energy models in Belgium were at that time also looking to include data on CCS technologies as a future option, leading to a

direct feed of information into e.g. the Belgian TIMES- BE model. Also the reports of the Federal Planning Bureau (PRIMES model) cite PSS-CCS as a main reference. An important surge for information was during the preparation of the European CCS directive (Directive 2009/31/EC). Technical information regarded mainly the storage of CO₂, the prime focus of the directive, but also the outlooks produced by the project were used to consider the scale and relevance of CCS for Belgium. Also other organisations and networks called upon the PSS-CCS partners for direct advice, or for presentations on the topic. The reader is referred to chapter 4 (DISSEMINATION AND VALORISATION) for an overview of the main and official valorisation activities originating from the PSS-CCS projects. Within Belgium and its regions, CCS is a well-known and documented option in mid- and long-term energy projections thanks to the catalytic role of the PSS-CCS projects. The now fully mature PSS II simulator and its databases currently play an important role in exchange activities with other countries through European collaboration and network projects (e.g. Welkenhuysen & Piessens, 2011b). This export of expertise may result in an impact in those countries, comparable to that of the PSS-CCS projects in Belgium.

Key-words

CO₂ capture and storage, CO₂ capture, pipeline transport, CO₂ geological storage, climate change, uncertainty

1. INTRODUCTION

In the phase I report of the PSS-CCS projects (Piessens et al., 2009), the state-of-the-art for 2008 was given regarding the scientific basis for climate change, its consequences, and the international and Belgian policy. Since then, the fact that the climate is changing has been confirmed, as well as its dominantly negative impacts. In spite of the success of the Kyoto protocol, no world-wide agreement has been reached on how to achieve the required deep reductions in greenhouse gas emissions. This delay consequently means that the portfolio of measures needed, representing the total effort to limit global warming, has increased (Pacala & Socolow, 2004; Socolow, 2011). Or simply put: the longer the wait, the larger the effort. This is in particular true for CO₂ Capture and Storage (CCS).

The results in this combined report of the projects PSS-CCS II and PSS-CCS BeNe are a direct continuation of the achievements in PSS-CCS I. We indeed picks up where PSS-CCS phase 1 came to an end in 2008, offering us: a full database on the actual sources, a technology description and database on future CCS relevant technologies for the power sector, a methodology and implementation for pipeline economics, an overview of the storage potential for Belgium, an evaluation of the economics of CO₂ storage, an evaluation of CCS technology using Markal, and the development of the ad-hoc CCS simulator PSS I.

The interruption between the projects was used for orientation and evaluation, so that PSS-CCS II/BeNe could be focussed efficiently to complete the achievements of PSS-CCS I, and at the same time would address the issues that had been identified as critical (Figure 1.1). As was the case for PSS-CCS I, also PSS-CCS II would become a truly multidisciplinary project, aiming to update the datasets already available and extending these with descriptive data on the capture potential and technologies in different industrial sectors. The geological database has been further completed especially with information on coal related storage scenarios in the Walloon Region. The risk perception of geological storage, crucial in any actual CCS project, was indirectly covered by evaluating the monitoring technologies for in particular coal bearing sequences. Important changes were made to the PSS simulator, including the introduction of a new investment decision scheme allowing much more realistic projections of the implementation of CCS technology. In parallel, similar exercises were made using Times BE, allowing for a cross-comparison of the projections and models. The international dimension was emphasised through the PSS-CCS BeNe project, which allowed through the Cato-2 project (ANNEX 4: CATO-2 LETTER OF INTENT) to include the Dutch storage options in a very direct and detailed way in the model.

Policy Support System for Carbon Capture and Storage (PSS-CCS)

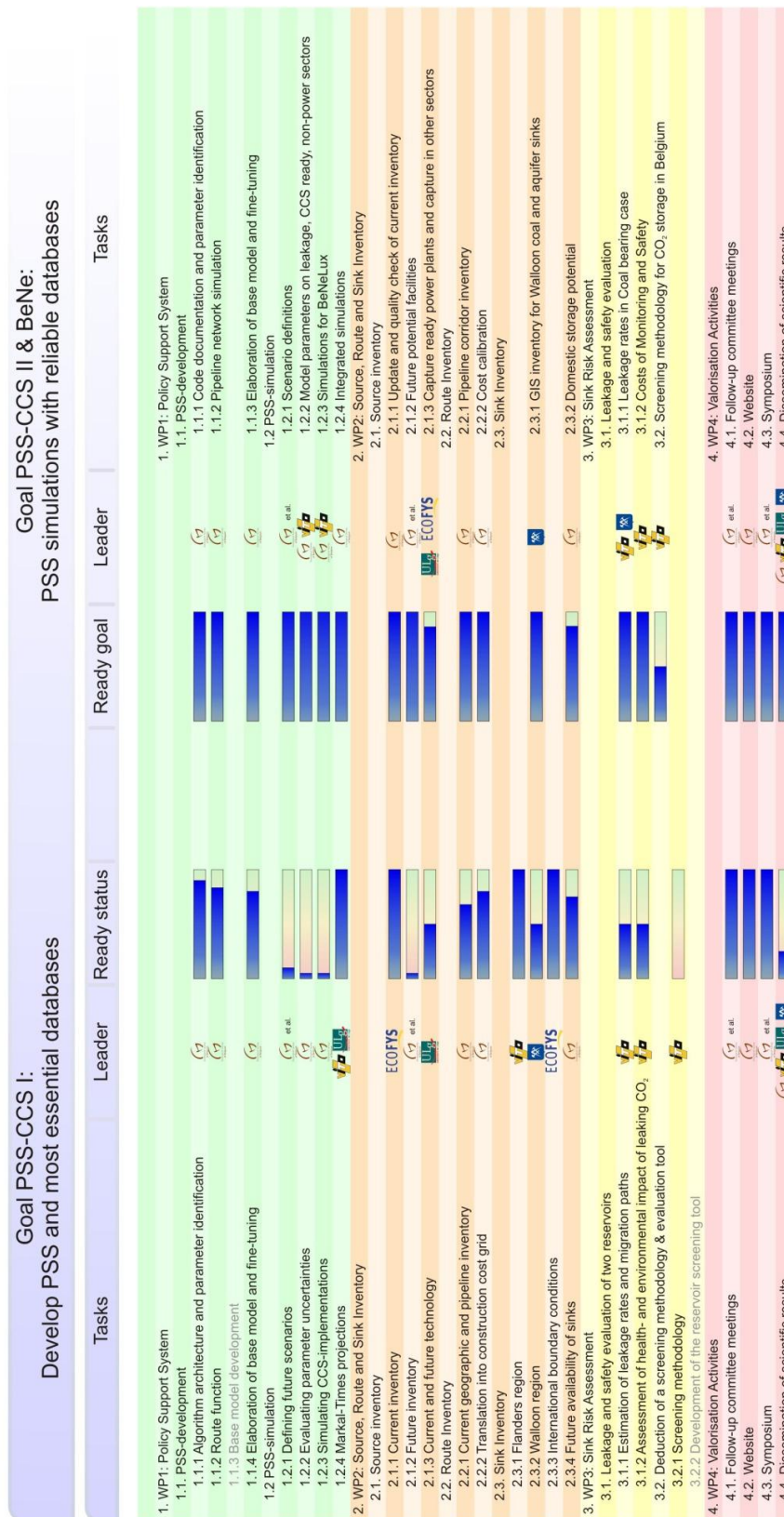


Figure 1.1. The PSS-CCS projects were temporarily discontinued between PSS-CCS I and PSS-CCS II/BeNe allowing for time to reorient and refocus. This figure gives an overview before the start of phase II, summarizing the achievements of PSS-CCS I and the goals of PSS-CCS II/BeNe.

2. METHODOLOGY AND RESULTS

2.1. Policy support system

The PSS II Simulator has a central position in the PSS-CCS projects. Data on capture, transport and storage discussed in previous chapters are essential as input for making projections on the deployment and operation of the CCS-relevant industry.

Phase I of the project delivered an operational version I of the PSS simulator (Piessens et al., 2009). It was further developed and expanded during phase II, retaining most of its basic philosophy although thorough changes were made in the program's code and structure. The methodology described hereafter is that of PSS II, the most recent version developed in the frame of the PSS-CCS II and PSS-CCS BeNe projects.

2.1.1. PSS Simulator introduction

The PSS II Simulator is a techno-economic computer simulator that is purpose-built to address policy-related questions regarding the future of CCS. It is a true simulator since in essence it uses input data and a set of equations to calculate a probable future result. A bottom-up approach was chosen to make realistic project decisions with high detail in particular fields. This opposes to a top-down model, where the total system is analysed from the highest level down, in general without ever reaching the detailed bottom level which is used as input for the bottom-up method.

PSS II is an ad-hoc CCS simulator. It was specially designed for making projections regarding the future of CCS, and while CO₂ capture is generally associated with the power sector, other industrial sectors can be entered into the simulator. PSS II will produce meaningful results for CCS relevant production and capture technologies. For power industry that means fossil fuel and biomass plants can be considered; other renewables and nuclear technologies cannot be added.

2.1.2. PSS Simulator structure & operation

Because PSS II is a recent and in-house developed simulator, no documentation is currently available. The basic structure and operation of the simulator will be explained in the following paragraphs. Further on, the most important parts and processes are discussed into more detail.

Throughout the PSS projects, industrial installations producing or emitting CO₂ and relevant for the simulator are called sources, whereas suited geological reservoirs for CO₂ storage are called sinks. PSS II discriminates CO₂ sources (production, emission and capture), pipelines (transport) and sinks/borders (for storage/export) as main simulation components.

2.1.2.1. Handling uncertainty

CO₂ capture, transport and geological storage is applied in just a few commercial or demonstration projects today. Although the idea itself is not new, policy and technology are still immature and comprise many uncertainties. These uncertainties only grow larger when looking towards the future. On the other hand geological reservoirs are needed for storage. Worldwide these are explored in different levels of detail. Poorly explored areas have very large uncertainties regarding storage, while very well-known reservoirs may still hold a few unknowns.

The PSS II Simulator was specially designed to be able to handle almost any range of uncertainty. To introduce uncertainty in PSS II, each parameter is given a range of possible values. One value will be chosen for one calculation, as explained in the following paragraph.

A distribution is appointed to each stochastic parameter. In its simplest form only one value is available (with a probability of 100 %). This is the exact distribution. When a minimum and maximum value are defined and all interlaying values have the same probability, a block distribution is formed. A normal distribution is also possible. Here, a minimum and maximum value with accompanying probabilities are defined. The chosen value will always lie inside the minimum-maximum interval to avoid outliers. The same method is also used for the lognormal distribution.

The value that is chosen for one calculation of PSS II is set using a random generator, considering the parameter's distribution. The pseudo-random number function embedded in Microsoft (MS) Office is not being used by PSS II. Instead, a set of 160 MB of true random binary data based generated from natural fluctuations in atmospheric noise (provided by [random.org](http://www.random.org)¹) is used to set the stochastic parameters.

After finishing one PSS II calculation, the simulator will return to setting the stochastic parameters, choose another random number and set a slightly different set of values. This method will produce each time a different result, based on the uncertainties that exist. This repetition of calculations using random input values (within a certain range) to determine the uncertainty of the result is called a stochastic or Monte-Carlo (MC) analysis.

¹ Random.org, true random generator; <http://www.random.org>.

2.1.2.2. Structure

The core of the PSS II Simulator is a MS Access file in the 2000 version format containing several Visual Basic for Applications (VBA) modules that are executed during PSS II operation. The VBA language was chosen to have an easy interaction between different MS Access tables and the simulator itself, because of its native integration in the MS Office package.

Next to this main file, several databases are needed with input parameters. These files and a short description of their contents are listed in **Error! Reference source not found..**

Table 2.I.Databases with input data for the PSS II Simulator.

Database filename	Description
HinderData.mdb	Vector objects, for pipeline routing
ObjectDataOthers.mdb	Sinks, borders and existing pipelines
ObjectDataSources.mdb	Future sources with technical parameters
ScenarioData.mdb	Economic and general technical parameters
SinkProb.mdb	Reservoir capacities and probabilities
SourceData.mdb	Existing CO ₂ emitting industry
TerrainFactorData.mdb	Raster data, for pipeline routing
TerrainModel.mdb	Raster data, for pipeline routing

PSS Explorer is a separate VBA assisted MS Excel calculation sheet wherein capacity and probability of the geological reservoirs are calculated. The results from this sheet are used as direct input for the PSS II Simulator (SinkProb.mdb database). PSS explorer is explained in more detail in chapter 2.1.5 (Storage).

The structure of the PSS II Simulator program is given in Figure 2.1. After initialisation, data from the input databases is read. Because of the two nested Monte-Carlo loops, the largest one is called outer Monte-Carlo, while the smallest one is called inner Monte-Carlo. In general, when a Monte-Carlo simulation is mentioned, the outer MC is meant. In the outer MC loop first the stochastic parameters are set. The time loop is repeated for each year from 2010 to 2050, simulating decisions being taken in that year.

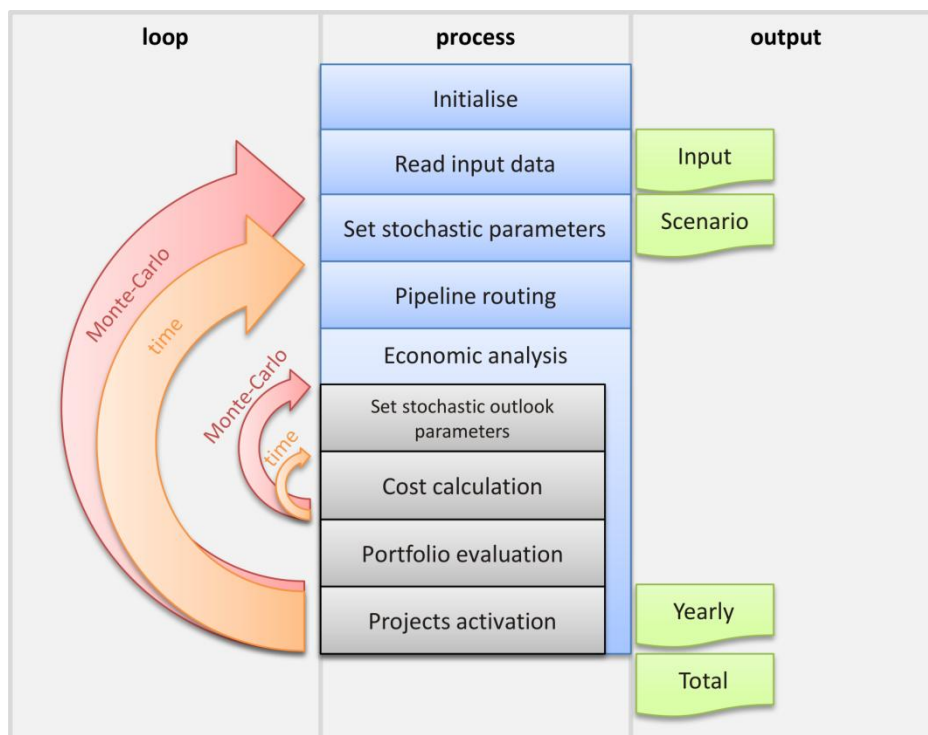


Figure 2.1. Structure of the PSS II Simulator. After initialisation all input data is read and written to a single output file. Two nested Monte-Carlo loops are present, each with a time loop. Stochastic parameters are set at the start of each MC calculation. Each year the cheapest route from each reservoir or border to any location is calculated. In the economic analysis the options for building capacity to meet demand are calculated and the best ones are chosen based on production cost using portfolio analysis. True production cost calculation requires considering changes in parameters, such as CO₂ price, over the project's lifetime, hence the inner Monte-Carlo and time loops. Each year an output file is generated containing data on yearly parameters and project evaluation. After each time loop, at the end of an outer MC calculation, a total file is produced containing the results of this and all previous MC calculations.

In each year the routing module calculates the cheapest route from each reservoir or border to any location (chapter 2.1.4 Transport). The economic module will consider all existing industrial installations for retrofitting and all possible future installations and their technology options, per sector. This is explained in more detail in chapter 2.1.6.3 (Technology options and Real Options Analysis).

PSS II makes decisions based on production cost. These will be calculated using Real Options Analysis (Brekke & Schieldrop, 2000), and decisions are made with the Modern Portfolio Theory (Markowitz, 1987). Important is that the actual future costs and benefits that the projects will be confronted with in PSS II, are different from the cost and benefit outlooks at the time project decisions are taken. This method comes close to real life where decisions are based on current knowledge, but actual values of technology parameters and political/economic circumstances such as costs and performance and CO₂ price are not exactly known in advance.

2.1.2.3. Operation

The PSS II Simulator is optimised for use on a high-end personal computer with the MS Windows operating system and an MS Office version 2007 or 2010 with MS Access. On a typical modern computer one Monte-Carlo simulation for Belgium will take about 3 hours. Therefore, to produce any meaningful results, at least one week-end of simulation is needed. The PSS II architecture allows for simple parallel computing using several computers or individual processor cores, drastically increasing the computing power. Typically between 10 and 15 cores are used during several days for final calculations. A more detailed description on operating the simulator is given in Annex 5 & 6.

2.1.2.4. Output

PSS's output consists of MS Excel or ASCII text files. The first version of the PSS Simulator was capable of only producing MS Excel output files, which was time consuming. Therefore it was chosen to create by default ASCII text files. Test runs have indicated that on a single Monte-Carlo run a speed gain of 20 minutes was achieved. In ASCII output mode a second content file is created for each output file to enable insertion in sheets into MS Excel.

At first an input file is created in which all data that is read is structured and outputted, mainly for verification. For each MC loop a scenario file is created where the values of the stochastic parameters are given that are chosen for this MC loop. Next, for each year a yearly output file is created with all projects considered and chosen for that year. Lastly, a total file is created after each MC loop, containing all output data of the current and all previous MC loops.

2.1.3. Capture

2.1.3.1. Cost factors for capture

Capture is for most sources the most expensive part of the whole CCS chain. Several capital and operational costs are to be considered when calculating the production cost listed in Table 2.II. Parameters used for production and capture cost calculation in PSS II.

Table 2.II. Parameters used for production and capture cost calculation in PSS II.

Parameter	Unit	Description
INV	M€	Capital cost (investment cost)
FOM	M€/y	Fixed operation and maintenance cost
VOM	€/UoP	Variable operation and maintenance cost
AvF	%	Availability factor
ProdEff	UoP/kj	Production efficiency
ProdCap	UoP/y	Production capacity
DiscRate	%	Discount rate
FuelEm	tCO ₂ /kj	Fuel emissions
CaptEff	%	Capture efficiency
FuelPrice	€/kj	Fuel price
CarbPrice	€/t	CO ₂ price

2.1.3.2. Cost calculation for capture

PSS II decisions are based on minimising production cost and maximising investment return (project risk is a second decision parameter, and is discussed in chapter 2.1.6.4 Portfolio choices). Production costs are regarded as the average production costs over all years of operation. In order to do so, the costs for each year of operation in the future need to be considered. Therefore the investment cost is annualised. Because retrofitting an industrial installation may cause changes in production capacity, the production capacity of each year needs to be discounted, and annualised again to obtain a yearly value. The same operation of discounting and annualisation is needed for the costs. The discounted production cost for year y per unit of production (UoP) is:

$$\begin{aligned}
 &ProdCost_{UoP,y} \\
 &= Decr_y \cdot (INV_{UoP} + FOM_{UoP} + VOM_{UoP} + FuelCost_{UoP} + CarbCost_{UoP})
 \end{aligned}$$

With

$$INV_{UoP} = \frac{INV \cdot FCF}{AvF \cdot ProdCap_y}$$

$$FCF = \frac{DiscRate}{1 - (1 + DiscRate)^{-DiscTime}}$$

$$FuelCost_{UoP} = \frac{FuelPrice}{ProdEff}$$

$$FOM_{UoP} = \frac{FOM_y}{AvF \cdot ProdCap_y}$$

$$CarbCost_{UoP} = CarbPrice \cdot \frac{CarbEmNet}{ProdCap_y \cdot AvF}$$

$$CarbEmNet = \frac{ProdCap_y \cdot AvF}{ProdEff} \cdot FuelEm \cdot (1 - CaptEff)$$

$$Decr_y = \frac{1}{(1 + DiscRate)^{(y - ystart)}}$$

To account for changes in production capacity these annual production costs need to be multiplied by the fraction of the true yearly production capacity and the discounted and annualised production capacity.

$$\begin{aligned} ProdCostTot_{UoP,y} \\ = (ProdCost_{UoP,y} + TransCost_{UoP,y} + StorCost_{UoP,y}) \cdot \frac{ProdCap_y}{ProdCapDisc} \end{aligned}$$

With

$$ProdCapDisc = FCF \cdot \frac{ProdCap_y \cdot AvF \cdot Decr_y}{y}$$

The final discounted and annualised production cost per unit of production is:

$$ProdCost_{UoP} = FCF \cdot \frac{ProdCostTot_{UoP,y}}{y}$$

Production costs calculated using these formulas are used for project activation decisions (chapter 2.1.6 Project decisions). The actual production cost of activated projects may differ from this value as is also explained in chapter 2.1.6 (Project decisions). The individual cost factor values are stored as follows: the value of the parameter in the year of activation is stored for each year the project is active. These values may change only in case of a retrofit.

2.1.4. Transport

The Router module responsible for the correct cost estimation of transport of CO₂ by pipeline was a key-element of the PSS I Simulator and is well described in the phase 1 report of the PSS-CCS projects (chapters 4.3 and 8.4 in Piessens et al., 2009). The Router module is capable of finding in an efficient way (relying on an advanced spreading algorithm) the least cost pathway between sources and sinks, taking into account the required capacity, general terrain factors and specific cost factors for large linear infrastructure (railways, main roads...). The Router module has been improved on several points, which are detailed below. Important is that the routing parameters were verified and further calibrated using confidential data from industry during the preparation of the cost report on transport by the European Technology Platform for Zero Emission Fossil Fuel Power Plants (ZEP, 2011b).

2.1.4.1. Pipeline diameter

Calculating the least-cost pipeline requires an optimal pressure and diameter ratio. The formula for estimating the technical and economic optimal pipeline diameter was derived in Piessens et al. (2009), and published by Vandeginste & Piessens (2008) (included in Annex 1). These publications contain a misprint which is corrected in the erratum below.

In both publications, a formula is proposed to calculate the optimal pipeline diameter for a CO₂ pipeline (Piessens et al., 2009, formula 38; Vandeginste & Piessens, 2008, formula 16). After comparing this formula with the formula present in the PSS-simulator and the working documents from which these publications resulted, an error was found in the denominator of the a and b fractions. The denominator must be multiplied by the square of the density (ρ), thus the a and b fractions should be:

$$D = E^{3/4} = \left(\frac{1}{2} \sqrt{t_1 + t_2} + \frac{1}{2} \sqrt{-t_1 - t_2 - \frac{2b}{\sqrt{t_1 + t_2}}} \right)^{3/4}$$

with

$$t_1 = \frac{4\sqrt[3]{2/3}a}{\sqrt[3]{9b^2 + \sqrt{3}\sqrt{27b^4 - 256a^3}}}$$

$$t_2 = \frac{\sqrt[3]{9b^2 + \sqrt{3}\sqrt{27b^4 - 256a^3}}}{3^{2/3}\sqrt[3]{2}}$$

$$a = -\frac{4^{10/3}n^2LQ^2}{\rho^2\pi^2(z_1 - z_2 + ((p_1 - p_2)/\rho g))}$$

$$b = -\frac{8Q^2\Sigma_i\zeta_i}{\rho^2g\pi^2(z_1 - z_2 + ((p_1 - p_2)/\rho g))}$$

2.1.4.2. Booster stations to compensate topographic height difference

PSS I produced errors in the pipeline dimensioning function in the rare situation when the uphill height difference between a CO₂ source and sink was too large (typically larger than 250 m).

A sensitivity analysis was conducted, revealing that the pipeline diameter increases exponentially towards a limit when the pressure difference is lowered and /or if the height difference is increased uphill. Below this limit, the CO₂ cannot be pumped upwards with the given pressure difference, no matter how large the pipeline diameter is. For a certain height difference, the hydrostatic pressure at the lowest point of the pipeline is:

$$P_h = \rho * g * \Delta h$$

With

P_h = hydrostatic pressure

ρ = CO₂ density

g = gravitational acceleration (9.81 $\frac{m}{s^2}$)

Δh = height difference

The pressure difference applied for pumping the CO₂ should be at least larger than the hydrostatic pressure. In the PSS I calculations, this was sometimes not the case, and it produced an error. Boosters (compressors) were already added by PSS Simulator to maintain CO₂ pressure in pipelines for long distance transportation. For horizontal transport, this situation was managed well. For downhill transport, less booster stations were needed because of the additional gravitational force. For uphill transport additional height boosters are implemented in PSS Simulator.

A second problem was revealed during the MS Excel sensitivity analysis: if the pressure difference and the height difference between two pipeline ends are both 0, there is a division by 0 and the diameter could not be calculated. Therefore, if the pressure difference is initially 0, the source pressure is set to the maximum pipeline pressure. After diameter calculations, the pressure is reset to its original value. Other formula's concerning the pipeline size and properties were checked and don't give any error when both pressure difference and height difference are 0.

2.1.4.3. Cost calibration

The cost estimations in PSS I were based on empirical and semi-empirical equations for material, labour, right-of-way and miscellaneous costs for pipeline construction. These were derived from annual overviews in the Oil & Gas Journal Pipeline Economics reports, estimates of the amount of steel used and discussions with industry and authorities. Confidential reference data was obtained during PSS-CCS BeNe to detail the calibration parameters of the different equations, and the recent cost report from the European Technology Platform for Zero Emission Fossil Fuel Power Plants (ZEP, 2011a&b) was used as final verification of the accurateness of the cost predictions. Cost estimations now correspond to the construction of high-grade steel (X70) of which the material cost when used in pipelines averages 1300€/t, for pipelines constructed in Belgium and the Netherlands.

2.1.4.4. Pipeline corridors

In the Netherlands, preferred or obligatory routes for pipelines, called pipeline corridors, are common. While rules in Belgium are less strict, pipelines will not be constructed randomly but will e.g. follow existing pipeline trajectories. Since routing applications are cost driven, such effects of preferred routes are usually translated into cost factors. This is however not correct, since costs for pipeline construction will not differ much inside or outside the corridor. In PSS II an additional parameter has therefore been embedded in the router application, which is called a 'phony (cost) parameter'. This parameter will weigh on (reduce) the minimal cost route used to select the optimal route, but is excluded from the final cost calculation. As such, pipelines will be drawn towards pipeline corridors in a measure depending on the phony cost parameters inside the corridor, without affecting the actual cost parameters, which will lead to more realistic cost predictions.

2.1.4.5. Pipeline networks

It will be likely that once CCS becomes a mature technology, a CO₂ pipeline transport network will emerge to operate more cost-efficient (Kuby et al., 2011). PSS II has the ability to create networks in two different ways. A first method is creating networks within a single time step. Several new CO₂ producing facilities can be connected to a number of geological reservoirs to form a truly optimised (least-cost) network. This method essentially comes down to finding the optimal branching points for a pipeline network. For a simple 2-sources – 1-sink configuration the least-cost route from sources and sink are calculated to any point on the raster grid (Figure 2.2a). When these three cost grids are stacked and the three costs are added for each raster cell, the cost to build the three pipelines to that cell is found. The optimised network will then be the cell with the lowest value, and the three corresponding least-cost pipeline routes.

This calculation is fairly easy since transport capacities at all points are known. If one source is however connected to two or more sinks, the capacity needs to be divided between the sinks. In most cases the least-cost sink will be used at its maximum, followed by the second and so on. An approximation can thus be made. The same method can be applied for a n-source – n-sink configuration (Figure 2.2b).

The limiting factor for this single time step optimised network calculation is calculation time. On a typical computer one routing calculation takes about one second. For the 2-source – 1-sink configuration this takes about 46 times more. Bearing in mind that the PSS II Simulator relies on repeated calculations, a typical PSS simulation with n-source – n-sink networks applicable to Belgium would take at least 200 days to calculate instead of one weekend (Welkenhuysen & Piessens, 2011a). This clearly limits its practical use.

This method would create the optimised, least-cost pipeline network for different projects, which would produce unrealistic over-optimised predictions which is in violation with the PSS approach of producing realistic, project based forecasts. Therefore, in PSS II this method is limited to connecting two new CO₂ producers to one reservoir in combination with a more efficient and realistic approach, detailed below.

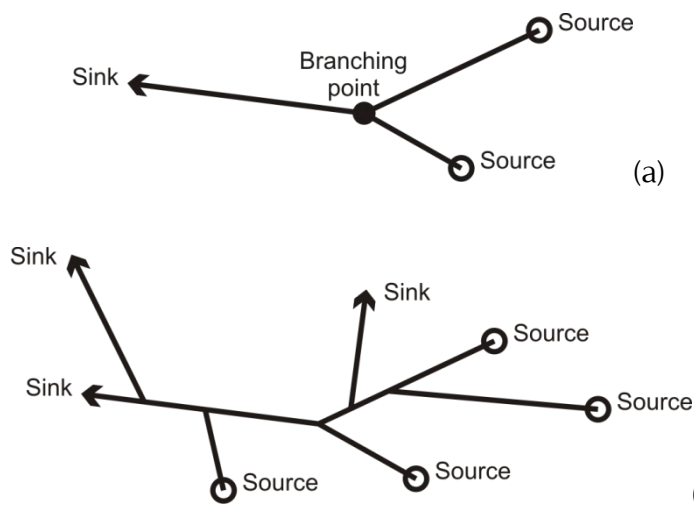


Figure 2.2. Least-cost pipeline network calculation in a single time step. The most basic network connects two sources and one sink (a). The least-cost route to each raster cell is calculated from these three points. Adding these three costs for each cell gives the cost of a network branching on a particular cell. The optimal branching point is the cell with the lowest cost. A PSS II simulation using calculations for a least-cost network for an n-source – n-sink configuration (b) would demand an unrealistic calculation time of about 200 days. Therefore only the 2-source – 1-sink configuration is implemented in PSS II and will only be used to address specific issues.

This alternative simulates the construction of a network over different time steps. It might be cost-effective for a CCS project to use (part of) the same route of an existing project (Figure 2.3a). In this case the jointly used segment will be pretended to have been built enlarged (Figure 2.3b). To account for discounting, the additional investment costs will be discounted backwards, and added to the new project's investment costs. Critical is the time elapsed between the construction of the first and second pipeline. If the first pipeline is relatively recent, then it is more likely that the assumed overdimensioned pipeline segment is the cheaper option. The up-front investment in overdimensioned pipelines (simulated by the backward discounting) becomes more expensive the longer it takes for the second pipeline to become active.

This method does not fundamentally influence the calculation time, since only one route is calculated per project. It is however not possible to create a network of several interlinked sources and sinks in one step, but this is not a fundamental problem since the time steps taken by PSS II are small (one year by default). It should also be noted that the algorithm is not limited to two pipelines, but is designed to simulate complex networks of virtually an unlimited number of pipelines and pipeline intersections.

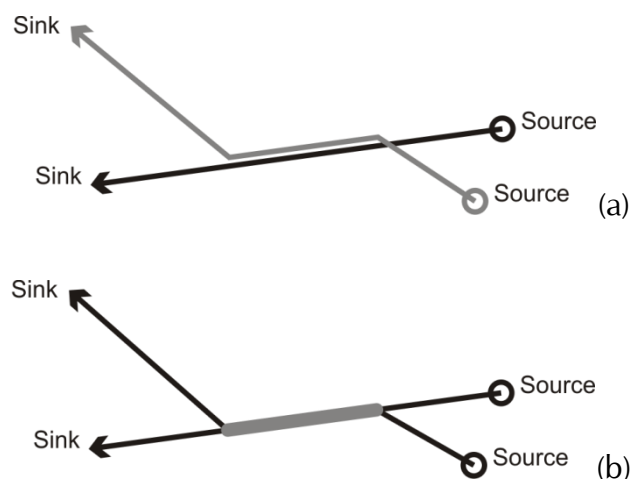


Figure 2.3. Building a least-cost pipeline network over different time steps. It might be cost-effective for a CCS project to use (part of) the same trajectory of an existing pipeline (a). This pipeline will be assumed to have been oversized to allow transporting the combined emissions of two (or more) sources. The additional investment costs will also be backwards discounted as if the investment was made with the first pipeline.

2.1.5. Storage

2.1.5.1. Storage reservoirs and uncertainty

Regional CCS simulations will in general only account for geological storage reservoirs that are sufficiently known. For regions without a good deep subsurface exploration history, this means no storage capacity would be available.

Considering however the resource pyramid by Bachu et al. (2007), storage capacity can be assessed, although at different levels of accuracy. In case local or regional storage capacity is well known, due to extensive geological exploration, reliable estimates can be made regarding storage costs using current rates on drilling, tubing, monitoring etc. On the resource pyramid these capacity estimates lie in the practical or matched capacity range. If storage capacity is less well-known, uncertainty on costs increases dramatically and, if it is even possible to calculate. The capacity estimates will be located in the bottom most layer of the resource pyramid, the theoretical capacity.

If deep reservoir geology is not well known in a certain area, such as is in general the case for Belgium, a method specially developed within the PSS framework, PSS Explorer, can be applied to upgrade capacity estimates to the practical capacity level. The PSS II Simulator will then use these estimates in CCS project calculations, generating the matched capacity (Piessens & Welkenhuysen, 2010).

2.1.5.2. Storage cost and capacity input

To make cost estimations with PSS Explorer, a storage project is condensed into a conceptual model (Piessens, 2011). This can be simplified to two decision moments. A decision is first made whether or not to start exploration of a reservoir. When exploration is finished, a second decision is made if the storage project is started or not. At both decision moments the project can be cancelled. If a project is cancelled after exploration, exploration investments are lost.

Geological storage of CO₂ is very complex. In this study we assume the uncertainty on geotechnical parameters outweighs that of other parameters. Therefore a simplified generic model is used which describes a storage reservoir with three parameters: whether or not it will be able to trap CO₂, how much CO₂ can be stored in total, and lastly at which rate CO₂ can be injected into the reservoir. These parameters are defined as stochastic parameters with an uncertainty distribution.

Still, some data is needed for capacity calculation. If data quality is poor in quality and quantity, experts can still form an opinion on basic reservoir properties. Also, experts may have insights in other research fields or confidential data that is not available to everyone.

The experts are given three basic questions to answer:

- What is the chance a reservoir will not be suited for storing CO₂ (in percentage)?
- What is the total capacity of the reservoir (as a probability distribution)?
- What is the yearly injection capacity at a typical injection site (as a probability distribution)?

2.1.5.3. Cost calculation for storage

PSS Explorer is basically a real options calculation scheme embedded in MS Excel calculation sheets. The actual calculation takes into account required rates of return, discount times, time and budgetary constraints etc. and discriminates for each project exploration, R&D and development phases. The methodology which is used in PSS Explorer is discussed in detail in chapter 8.7 of Piessens et al. (2009). In the course of PSS-CCS BeNe a short course for PSS Explorer was written (ANNEX 5: PSS EXPLORER SHORT COURSE).

2.1.5.4. Results

PSS Explorer generates two complementary tables, total reservoir capacity and yearly injection capacity. These tables were visualised in phase I of the PSS-CCS projects as Figure 2.4 (see chapters 8.7.4 and 8.7.5 in Piessens et al., 2009). An alternative and more intuitive way of presenting these results is as histograms. This approach is used for estimating the total storage capacity of Belgium (Piessens, 2009; Piessens et al., 2010; Piessens, 2011). The practical capacity (Bachu et al., 2007) estimates obtained by PSS Explorer can be expressed per reservoir or for a whole region, such as Belgium. The price of CO₂ that is assumed to be available for geological storage is a determining factor. This is evident from

Figure 2.5a which shows the probability that exploration in Belgium leads to at least one economically viable reservoir. This increases quickly and approaches 100% above prices of 10€/t, even if at present no reservoirs have been identified with certainty. Also the practical storage capacity increases with the price for storage.

Figure 2.5b shows the yearly and total practical storage capacity of Belgium assuming a storage cost of 15€/t. At this price, the average capacities is 15Mt on an annual basis, or 620Mt in total. The uncertainty range is quite large: the 95% confidence intervals for the annual and total capacity are respectively 3 to 35Mt/y and 150 to 1400Mt. Increasing the price above 15€/t will not increase the capacities, which means that the physical storage limits are met. Assuming a lower and possibly more realistic storage price of 5€/t lowers the average capacities to 5Mt/y and 225Mt.

Before these new estimates were known, the storage potential of Belgium was estimated by national experts at around 1Gt (Welkenhuysen et al., 2011). In view of the degree of knowledge of the reservoirs, this estimate should be considered as a mostly theoretical capacity. As can be expected, the estimated practical capacity is considerably lower, although still well within range of the confidence interval.

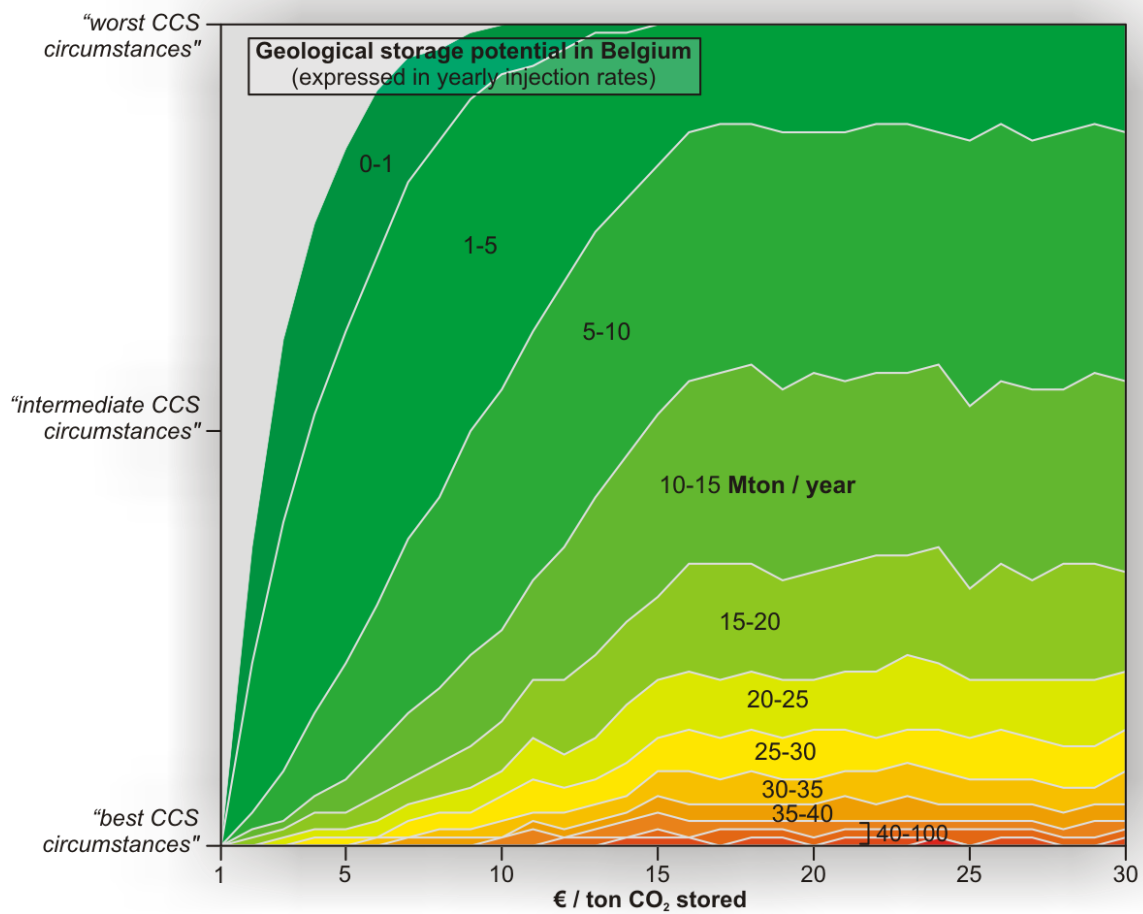


Figure 2.4. Yearly storage capacity of Belgium expressed as million tonnes per year, in function of the price one is willing to pay for storage (horizontal axis) and an uncertainty factor (vertical axis). If one is willing to pay 15 €/t CO₂ stored, there will be, in intermediate circumstances, about 10 Mt yearly capacity. Above 15 Euro per tonne, storage capacity stops increasing with costs because at this point the physical limits of the reservoirs are reached.

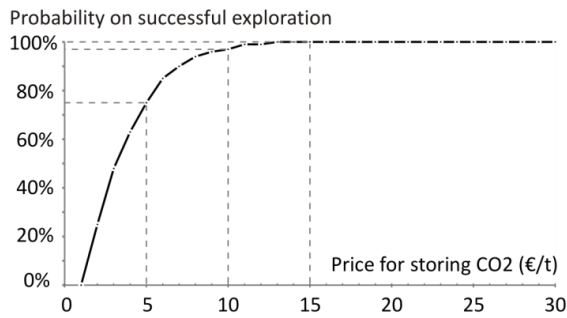


Figure 2.5a. The probability that exploration for CO₂ reservoirs is successful in identifying economic reservoirs depends on the price at which CO₂ will be stored.

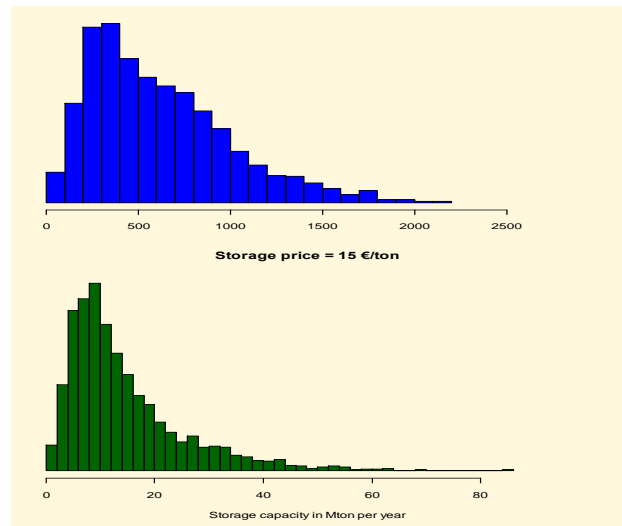


Figure 2.5b. Estimates of the storage capacity of Belgium expressed as yearly injection rate and total capacity. A storage cost of 15€/tCO₂ is assumed.

2.1.5.5. Dutch reservoirs

Because of confidentiality, no detailed data on the Dutch reservoirs is freely available. More general data per region was provided by the University of Utrecht in the frame of the PSS-CCS BeNe project which valorised the link between the Belgian PSS-CCS projects and the Dutch CATO-2 project. Eight regions with generalised storage cost and capacity data were added to the PSS II Simulator. PSS calculates least-cost pipelines up to the Rotterdam harbour area. The geographic centre of the regions were calculated and transport costs from this centre to the individual reservoirs were averaged and added to the storage costs, as were the transport costs from the Rotterdam harbour area (Zuid-Holland region centre) to the region's centres (Figure 2.6). These regions are:

- Groningen
- Northern Offshore
- Southern Offshore
- Noord-Holland
- Zuid-Holland
- Twente
- Wadden
- Utsira (the Dutch export option)

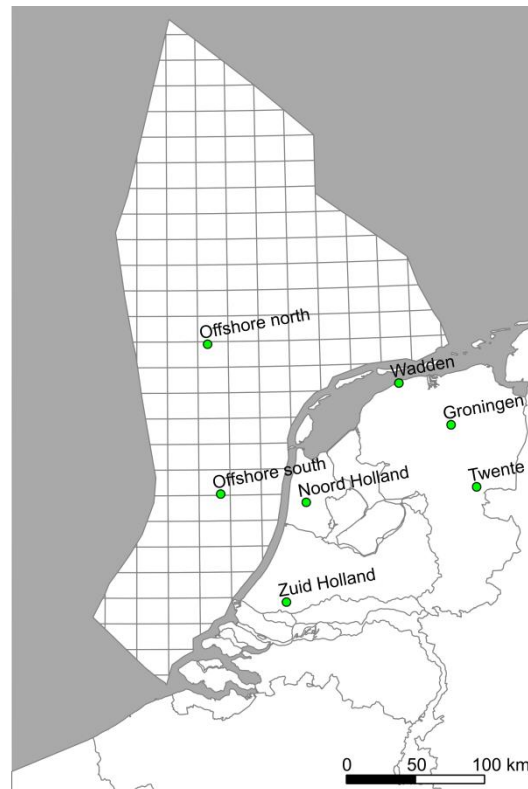


Figure 2.6. Geographic centres of the storage regions in the Netherlands. Because detailed data on the potential Dutch reservoirs is mostly confidential, summarised data by the Dutch partner in the PSS-CCS BeNe project is used for simulations. CO₂ is transported from the Rotterdam harbour area to these centres. Storage costs for the Dutch reservoirs include costs for this transport, and transport from the centres to the individual reservoirs.

2.1.6. Project decisions

2.1.6.1. Introduction

Basic to a bottom-up simulator such as PSS is the ability to make realistic project decisions. In essence this is a selection of the technologies with the lowest production cost, until the demand is satisfied. In the first version of PSS, NPV (Net Present Value) was calculated by discounting production cost, although assuming that all parameters remained constant through time. PSS II now calculates production cost with future projection of cost parameters (such as investment cost, CO₂ price), using uncertainties on future projections. It additionally considers the existing energy portfolio, as well as the benefits of optionality of capture readiness and retrofitting.

While in the first version PSS made least-cost decisions based on one installation, it now takes into consideration the risk on return and all active installations of a certain industrial sector, and other possible new projects. This comes close to how project decisions in the real world are influenced by external factors, and introduces optimisation into a bottom-up simulator.

2.1.6.2. Stochastic outlook parameters

As is visualised in Figure 2.1, two nested Monte-Carlo loops are present in PSS. The first, outer, loop uses stochastic parameters explained in chapter 2.1.2.2 (Structure). These calculations represent the variations in the "real world at present time" for PSS. To mimic the increase of uncertainty when looking into the future, a second level of uncertainty and stochastic parameters is introduced: the stochastic outlook parameters. This is the uncertainty level where the different branches of the Real Options tree are calculated repeatedly (chapter 2.1.6.3. Technology options and Real Options Analysis).

In general these operate in the same way as the higher level stochastic parameters. The most important difference is that at input level, a value is defined with which the parameter's value can rise or fall each year (Figure 2.7, black lines). In order to clip unrealistic values, a 90% probability interval is defined (red lines) that contains 90% of all possible future pathways (based on random walk).

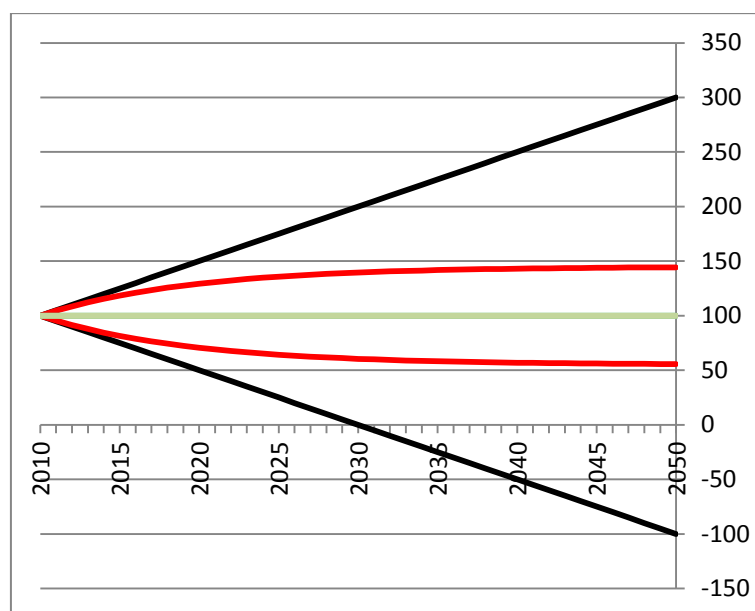


Figure 2.7. Example of a stochastic outlook parameter's value evolution. To simulate future uncertainty a yearly uncertainty range (black lines) is defined around the parameter's value (green line). In order to avoid unrealistic outliers, a 90% probability interval is defined (red lines). The outlook values for each year will be defined as a random walk within this red envelope.

For specific situations it is possible to bias these stochastic outlook parameters on which investment decisions are taken. This is done by the bias parameter that was introduced to "steer" the outlook parameter up or down from the parameter's original value (Figure 2.8).

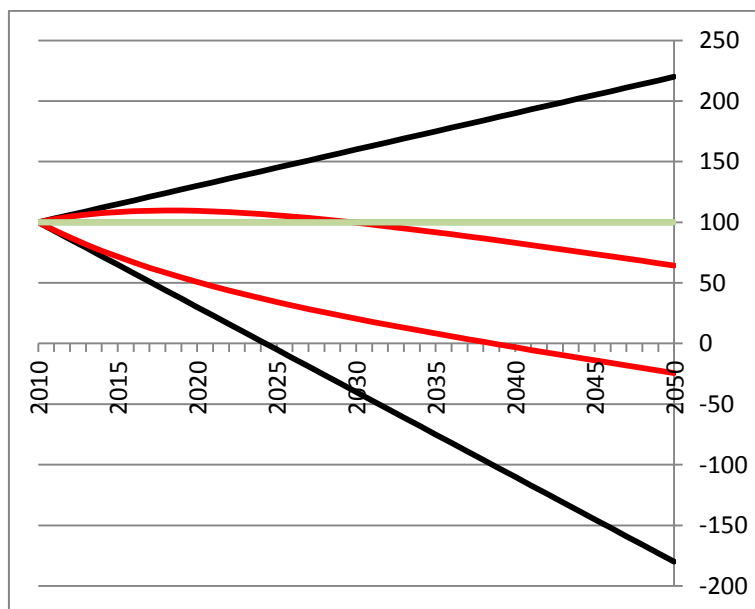


Figure 2.8. Example of a stochastic outlook parameter's value evolution with a negative bias. Using this bias parameter the simulator can be made to believe a parameter will be on average lower or higher than its actual future value (in green). Compared to Figure 2.7, a negative bias is applied, and the outlook values for each year will be defined as a random walk within this red envelope, getting well below the actual future parameter values (green line).

2.1.6.3. Technology options and Real Options Analysis

Real option analysis is a technique to estimate the economic value of a series of future investment decisions (Brekke & Schieldrop, 2000 & Moel & Tufano, 2000), and is used by PSS II to determine the return and investment risk of different assets (such as power plants with or without CCS). It does this by discounting the future investments towards a present value, an approach shared by many economic evaluations, which simply allows comparing their economic value to other investment options. The uncertainty which is intrinsic to future projections, is included by making the relevant parameters stochastic. The most transparent and flexible way of doing this is by using Monte-Carlo techniques, which means that a model is repeatedly calculated, each time varying parameters randomly within a probability range. The variance of the results will show the influence of the uncertainty on the input parameters.

Fundamental to a real options assessment is that also project decisions are embedded in the calculation scheme in such a way that real option models produce more realistic outcomes than e.g. standard net present value evaluations. This can be easily illustrated with the bidding process for a geological asset, such as an exploitation license for a mine or hydrocarbon field. The existing results of the exploration will be made available to the potential buyers, and they can evaluate from these the probability that the concession will be profitable. In a standard evaluation, the potential investment returns and losses are calculated directly from these probabilities, assuming intrinsically e.g. that a mine will be developed and remain in operation even if further exploration proves that it can only be operated at a loss. This leads to a significant overestimation of the risk on losses. In order to overcome this very conservative approach, real options schemes include at least one phase of exploration. It is assumed that after the exploration the current uncertainty is completely resolved. If it is unfavourable to develop the concession, then only the (very limited) exploration costs are considered as losses. Such a very simple scheme will also be used in the model for exploring and developing CO₂ geological reservoirs.

Applied to industrial facilities, PSS II identifies available technologies which may be non-CCS, CCS-ready and CCS-operational and takes into account that CCS retrofit technologies can be applied to a non-CCS plant. All these options should be considered when calculating the lowest production cost using real options analysis. The real-options analysis refers to the ability to change the current investment in the future, which in this case means retrofitting an existing CO₂ source to capture (more) CO₂ or increase efficiency. Retrofits can also be applied at different times in the future. Mapping all these options will generate a tree of technology options in which each branch represents a different technology choice in time (Figure 2.9). It is this tree that forms the basis for calculating the production cost of the actual technology choices.

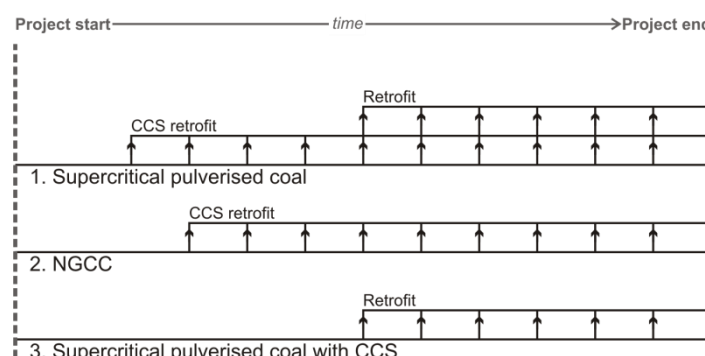


Figure 2.9. A typical technology tree in PSS II, for a technology choice of a new power plant. Three options are available now, each with their own retrofit options through time. Retrofitting is possible at all years after it becomes available, and each pathway or branch will result in a different production cost.

2.1.6.4. Portfolio choices

When making investments, the optimal balance is sought between risk and return. By creating a portfolio of investment options, the risk can be significantly reduced. The central question is what the optimal risk-return balance is, and which portfolio meets this optimal balance. The Modern Portfolio Theory (Markowitz, 1987) provides an answer to this question.

All possible investment options can be plotted on a risk-return graph to form a cloud of assets (Figure 2.10). A combination in shares of any of these options will lie in an area which has a boundary called the efficient front. A third parameter is also needed: the correlation coefficient between two assets. Positively correlated assets can be e.g. two power plants running both on pulverised coal.

While the return of a portfolio will always lie between the return of the individual assets, the same relation does not apply to the risk; it has a cubic relation. This means a portfolio of assets can have a smaller risk than the individual assets. This also makes sense in the real world, and is in fact the reason for investing in a portfolio. The correlation coefficient of two assets will further influence this relation: the lower the correlation coefficient, the lower the risk for this portfolio.

The optimal investment will lie on this efficient front (EF). In a total risk averse situation, the best investment lies on the leftmost point on this front. There is however another option for investment in a total risk aversion situation: short-dated government securities. These have a close to zero risk, and are called the risk free rate (RFR).

The CAL (Capital Allocation Line) describes the combination of two assets: the risk free rate and the tangent point on the efficient front. Optimal investments are made somewhere along this line, depending on the risk aversion of the investor. Since PSS II is demand driven, investments can only be made in new projects; the optimal portfolio for investment thus lies on the tangent point. Different shares for different projects are defined in this point.

In Figure 2.11 an actual example of a portfolio from a PSS II calculation is given. All assets are indicated, grouped per technology option. The circles indicate the assets chosen by the simulator.

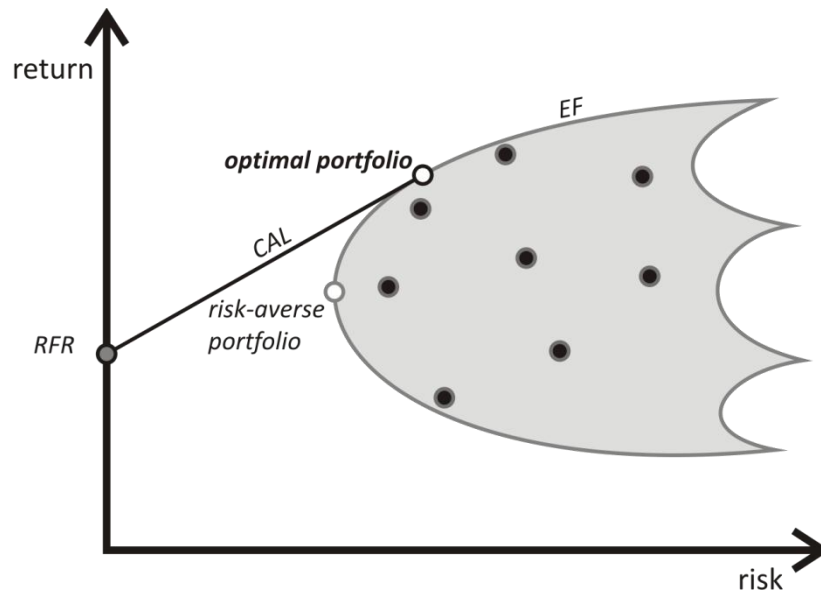


Figure 2.10. Graphical representation of the Optimal Portfolio Theory decision algorithm used in PSS II. All investment options are plotted in a risk versus return graph. The grey area represents all possible combinations of these assets, the line delineating this area is called the efficient front (EF). The best risk-averse investment option is then the leftmost point on this EF. However, outside this portfolio the risk free rate (RFR, identified with short-term state bonds) presents a better risk versus return option. Taking this into account, the optimal investment considering both risk and return lies somewhere on the tangent line between the RFR and the EF, the Capital Allocation Line (CAL). This line represents a combination of portfolio assets and the RFR. In PSS II investments can only be made in industrial installations, thus the optimal investment is the point where the CAL touches the EF. This optimal portfolio consists of one or a combination of assets.

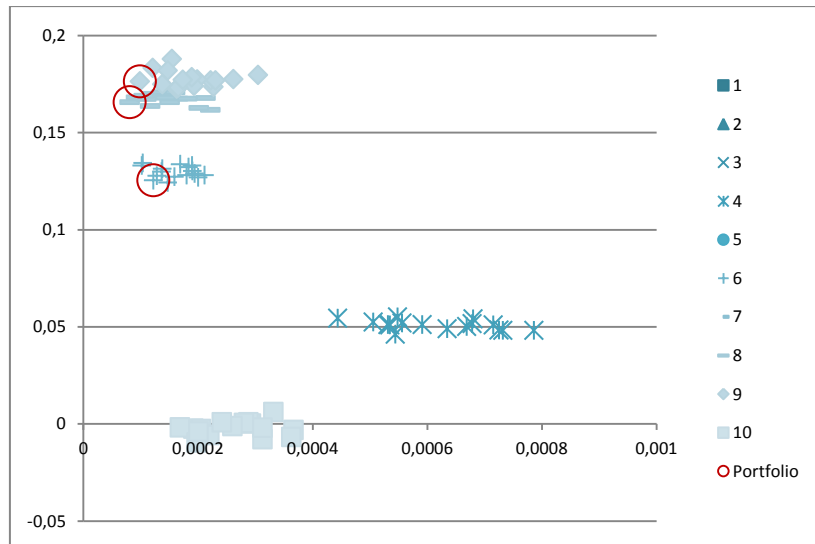


Figure 2.11. A real example of a portfolio in PSS II with risk on the horizontal and return on the vertical axis. Assets are grouped by technology (1 to 10) and the best investment options of this portfolio are circled. An imaginary efficient front and capital allocation line, and risk free rate of 0.10 (Figure 2.10) reveals the choice of the two topmost circled assets. Because of the urge to spread the risk, the same technology is not chosen twice, and the next best option has a lower return.

While the Optimal Portfolio Theory uses risk and return, the production cost calculation with real options analysis will produce a mean cost and a variance. Variance can directly be regarded as a measure of risk.

In order to transform production cost into production return an average selling price needs to be known. In PSS, the sector's average selling price is calculated as follows:

$$SellingPrice_s = ProdCost_s + ProdCost_s \cdot Return_s$$

With

$$ProdCost_s = Sector's \ average \ production \ cost$$

$$Return_s = Sector's \ average \ return \ rate$$

The sector's average production cost is determined from the existing portfolio. For the first year of simulation an existing portfolio is not available, and the average production cost of the portfolio under evaluation is used here. The return of the installation under evaluation is then calculated:

$$Return = \frac{SellingPrice_s - ProdCost}{ProdCost}$$

With

ProdCost

= *Production cost as calculated in chapter 2.1.3.2. Cost calculation for capture*

Some adjustment had to be made to the original portfolio algorithm to make it fit for the PSS simulator. Next to the two existing constraints (all shares must be positive and the sum of all shares is 1), the following additional constraint is essential: existing industrial facilities are added to the constraints to fix existing production. The remaining gap between production and demand can be filled with new assets. Also, shares will have a lower and upper size, since normally any share of an asset can be chosen, while in reality e.g. the size of a certain type of power plant is constrained by a minimal and maximal capacity.

The portfolio analysis runs a first time with all installations. Though, only selected non-CCS and CCS projects with domestic storage will be activated. A second time the portfolio analysis runs with these projects as activated projects, and projects with cross-border storage are evaluated and activated. This is done to favour domestic storage in a realistic way.

2.1.6.5. Regions

PSS II is able to simulate different regions or countries. A separate set of economic parameters can be defined for separate regions. In the portfolio analysis all installations of all regions are evaluated together, but for each region an additional constraint for demand is added. This way the portfolio analysis is conducted cross-border, while demand for each separate region will be full-filled.

2.1.6.6. Correlation matrix

Certain technologies may have one or more correlations (same fuel etc.; chapter 2.1.6.4 Portfolio choices). These correlations are used by the portfolio module and are therefore combined into one correlation coefficient, which was constructed as follows: equal technologies were given a correlation of 100%, with CCS or without CCS. Different technologies using the same kind of fuel were given a correlation of 50%. Other correlations were set to 0% (not correlated).

2.1.6.7. Presentation of results

Presenting results from stochastic calculations presents some difficulties. If results (e.g. CO₂ emissions) are plotted as lines onto one graph, a crisscross of results emerges, giving a first impression of the diversity and spread. A coloured density plot can be made of these lines. This produces a graph with red colours representing high and blue colours low probability. A uniform scale bar for all years and graphs cannot be made, but the colours must be interpreted as follows. The rainbow-coloured graphs (e.g. Figure 3.14) consist of different segments per year. The highest number of lines going through a segment is chosen maximum for a particular year and is assigned red as colour. For smoothing not just one segment is regarded, but a 20-segment interval is chosen for the graphs presented here for the power sector and a 30-segment interval for iron & steel. If a graph is constructed using the results of several Monte-Carlo calculations, the number of calculations is given within the graph as $n = \#MC's$.

2.1.7. Link with TIMES-BE

To make reliable predictions on energy systems, an economy-wide evaluation is needed. As mentioned, PSS II is only able to handle the CCS-relevant industry and therefore parallel simulations are executed with the Belgian TIMES model (chapter 3.2. The European and Belgian TIMES model). This TIMES model is able to handle an entire energy system. The same technological input data is used for both simulators. PSS II however needs e.g. demand (production), fuel prices and CO₂ price as input, which will be calculated with the TIMES model. Parallel simulation and exchange of results will also provide a more solid background for the PSS II Simulator, as the TIMES models are widely used and recognised.

2.1.8. Scenarios

A framework of policy and economy related parameters with their future evolution is needed for making techno-economic projections. One set of such parameter values is called a scenario. Four scenarios were defined for this project and run in PSS II and TIMES-BE. These scenarios are based on four parameters: the availability of technologies, the fuel prices, the demand for production and the price of CO₂. A listing of the scenarios is given in Table 2.III, followed by the individual parameters and a scenario description.

Table 2.III. Four scenarios are used for the PSS II and TIMES-BE simulations. A short description of these scenarios is given here.

Scenario	Short description
1 Reference	Only existing climate restrictions, with nuclear phase-out
2 NoNucGoCCS	2050 climate restrictions, with nuclear phase-out
5 GoNucGoCCS	2050 climate restrictions, no nuclear phase-out
7 LowDem	2050 climate restrictions, low demand for power

The availability of technologies (as well as all routing and storage data) is kept the same throughout all scenarios to leave technology choices completely to the simulator, based on production cost and the existing portfolio. TIMES-BE simulation results for fuel prices indicate only minor differences for hard coal, natural gas and biomass up to 2050 between the scenarios. It was therefore decided to keep them the same for all four scenarios in PSS II. Figure 2.12 shows the price evolution of the fuels used for PSS II simulations. Coal prices rise and stabilise after 2025. The price of biomass rises gradually while the natural gas price rises faster until 2050.

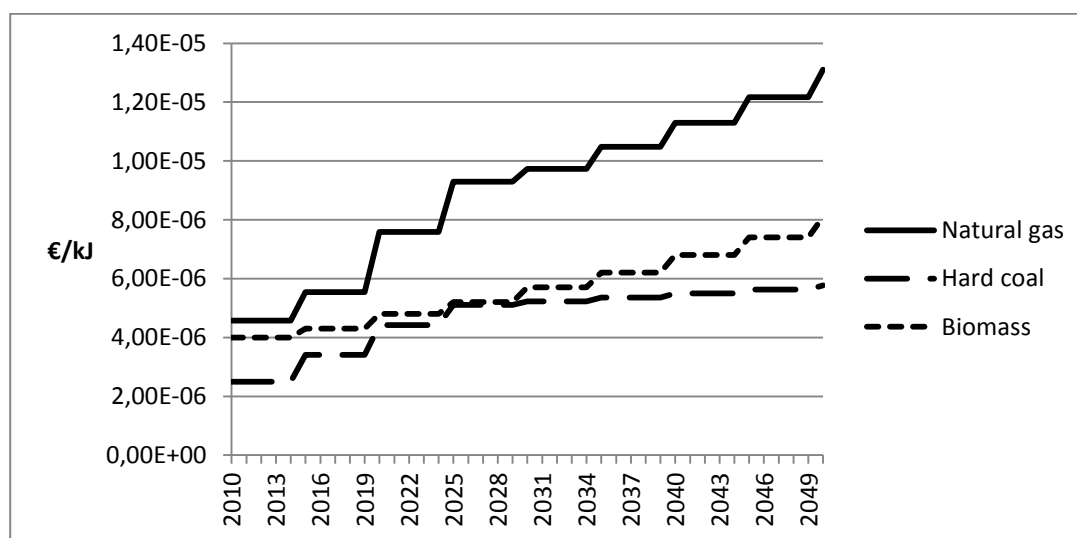


Figure 2.12. Fuel price evolution from 2010 to 2050 for hard coal, natural gas and biomass. Fuel prices are kept the same in all four scenarios.

CO₂ price and demand differ in each scenario. The curves are determined with help of TIMES-BE calculations. In the Reference scenario the CO₂ price remains constant at 20 €/tonne (outlook values for this parameters will change when looking in the future (see 2.1.6.2 Stochastic outlook parameters), the real-world value will remain constant). In the other scenarios prices rise up to 600 to 788 €/tonne (Figure 2.13), starting from 15 €/tonne in 2010 for scenarios 2 and 5, and 0 €/tonne for scenario 7.

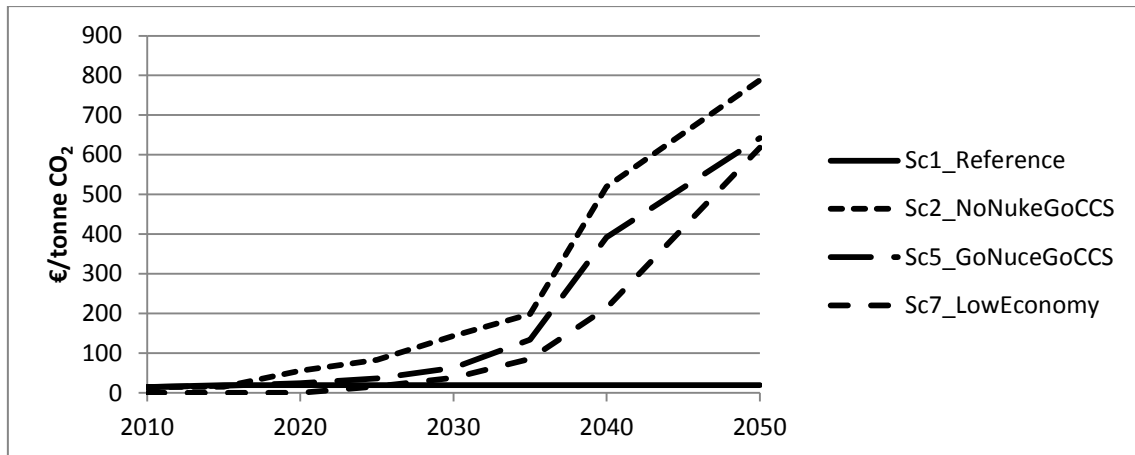


Figure 2.13. Input values of CO₂ price for the four scenarios. In scenario 1 it remains constant at 20 €/tonne while in the scenarios with climate restrictions (2, 5 & 7) prices rise up to 600-788 €/tonne.

Since the PSS II Simulator will simulate only the CCS relevant industry, demand for the power sector is formulated as the demand for fossil fuels and biomass centralised energy production only (thus excluding other renewables and nuclear). In scenario 1 and 2 the share of CCS relevant power production becomes large after 2020 (Figure 2.14a&b). If nuclear energy production is allowed, the share of CCS relevant production becomes very small, diminishing towards 2035 and rising again a little towards 2050 (Figure 2.14c). In the low demand scenario this share lies somewhere in between and total electricity demand remains low (Figure 2.14d).

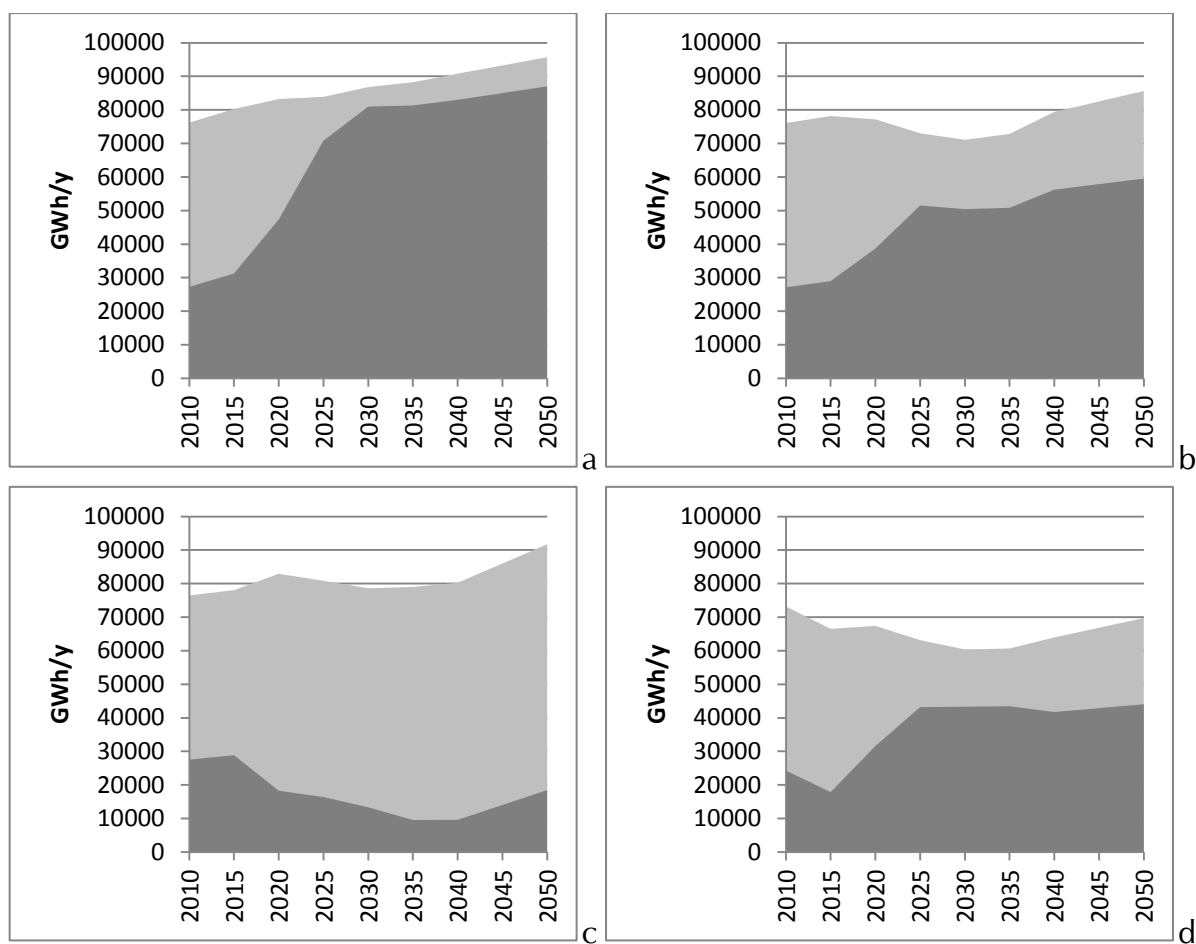


Figure 2.14. Renewable and nuclear electricity demand, not simulated in PSS (light grey) and fossil and biomass electricity demand, used in PSS (dark grey) for (a) scenario 1 (reference), (b) 2 (no nuclear), (c) 5 (with nuclear) and (d) 7 (low demand). It is this dark grey wedge of demand for which the technology portfolio will be predicted by PSS II.

Demand for the iron & steel sector was kept the same for all scenarios, and was kept constant through time at 10Mt/y. Technological data was added from chapter 2.3.6 (capture in the iron and steel making industry) and if necessary recalculations were made for some parameters.

The different scenarios reflect realistic economic evolutions and policy decisions which affect the CO₂-emitting industry. The Reference scenario includes only current climate and energy policy: the projected nuclear phase-out is maintained, and no additional (post-Kyoto) climate goals are set. This results in a high demand for fossil and biomass fuelled power production after the closure of nuclear plants, and a low CO₂ price. In the NoNucGoCCS scenario this nuclear phase-out is maintained, but additional climate targets are set (58% emission reduction target for 2050, which corresponds to the Belgian effort in the European 70% reduction target by 2050). This climate constraint will result in a steep rise of the CO₂ price. When the option of nuclear energy production is kept, in the GoNucGoCCS scenario, electricity demand from fossil fuels and biomass is low. Because the 58% reduction target is retained the CO₂ price will still rise high. In the last scenario, a low energy demand will obviously result in a low electricity demand. The emission reduction target of 58% provides a rising CO₂ price. Because of the low general energy demand, the CO₂ price will start at 0 and the increase is delayed compared to the previous scenarios.

2.2. Risks and monitoring challenges for CO₂ sequestration in coal

Assessing the risks associated with CO₂ geological storage in Belgium runs against several uncertainties due to insufficient knowledge of the reservoirs. This reveals again the necessity of more geological exploration of the Belgian subsurface.

In the first phase of the PSS-CCS project, two detailed case studies on risk assessment were worked out for aquifer storage in the Carboniferous limestone and the Westphalian sandstone. The sequestration option in coal-bearing strata has not been covered before. Therefore, during this second phase of the project, the focus is put on the coal-bearing case.

2.2.1. introduction

There are two main options for geological storage of CO₂ in Belgium: saline aquifers and unmined coal seams.

Deep aquifers are of interest also for seasonal natural gas storage and for geothermal energy extraction. These conflicts of use require a regulating policy for subsurface applications. If subsurface reservoirs can be of economic value it is less probable that they will be attributed a license for CO₂ storage. Sometimes different applications might be possible in the same reservoir, e.g. combined geothermy and CO₂ storage, but the synergy then must be controlled.

Apart from the aquifer storage option, unmined coal reserves and unmineable coal layers represent a large total reservoir capacity (~400 Mton of CO₂, Laenen et al., 2004). Moreover, residual coalbed methane gas (CBM reserves estimated at ~53-79 . 10⁹ m³ CH₄) can be extracted in combination with CO₂ sequestration whereby methane production is enhanced by adding CO₂ as a flue gas. This enhanced CBM production (ECBM) is based on the preferential adsorption of CO₂ on the coal surface compared to CH₄.

The low injectivity of CO₂ (now estimated at 5-10kton/y/well based on classical techniques) and the complex geology in coal sequences still forms a challenge. Notwithstanding the large amount of mine archives focusing on coal content, more ECBM-directed exploration, targeted coal research and alternative drilling techniques are needed in order to develop ECBM in Belgium. The LRM² is currently investigating the possibility of CBM production in Limburg.

In order to assess the CCS-perspectives for Belgium, the following questions need to be answered: "How much can we store?", "How safe is it?" and "Can we prove (monitor) the containment?".

2.2.1.1. Leakage and safety evaluation

In general, CO₂-storage in coal is considered a safe option for several reasons:

- Coal seams have held CH₄ for millions of years;
- CO₂ is adsorbed more easily on the coal surface than CH₄ and N₂;
- Because of this differential adsorption capacity of coal, less free CO₂ is expected;
- The geology of coal basins (interbedding of coal seams, shales, sandstones,...) provides a stack of local reservoirs and seals, which slows down upward migration and encourages lateral flow. This in turn leads to multiple trapping opportunities: structural, hydrodynamic, dissolution, ionic, mineral and adsorption trapping.

But, at the same time, it is also true that:

- safety aspects in coal are less well studied. There have been a few field tests worldwide, but mainly in higher permeable and thicker coal seams and in geologically less complex areas. In most cases CO₂-injection had place under sub-critical conditions (shallow depth).

² LRM: Limburgse Reconversie Maatschappij (<http://www.lrm.be/en>)

- there are still some uncertainties relating to swelling effects, wettability, fracturing, mechanical behavior of natural faults/fractures, stress-strain path and effects in mined zones;
- monitoring in complex geological reservoirs with low injection rates, and hence small volumes of CO₂, is not easy and so far there are not yet ready solutions that foresee in reliable and cost-effective monitoring for small CO₂ - CH₄ leaks.

Current research targets these challenges and efforts focus mainly on:

- integrity of ECBM systems
 - accurate simulations
 - more field data
- optimization of the ECBM process
- reliable and cost-effective monitoring and CO₂ - CH₄ verification systems appropriate to the special conditions of CO₂ storage and flow in coals
- Swelling under different (coal and geologic) conditions
- Effect of wettability
- Effect of pressure conditions pre- and syn-injection
- Permeability-evolution during and after injection (often in pulses, rebound after initial reduction) and how injectivity can be influenced
- Geomechanical behavior and stress conditions (coal weakening, changed slip/failure barriers?)
- Conductivity of fault zones crossing coal and overburden

2.2.1.2. Results from ECBM field tests

Several ECBM field tests have been performed around the world during the last 15 years. These pilots proved the feasibility of CO₂ sequestration in unmined coal strata, the containment of CO₂ after the tests and they provided learning about the ongoing processes like swelling, shrinkage, interconnection of hydrofractures, pressure evolution, etc. ECBM field tests were organized so far in several coal basins in the United States of America, in Poland, China, Japan and Canada.

Several lessons can be learnt from these experiments:

- The wettability (water-wet or CO₂-wet) of the coal plays a crucial role in degassing of CH₄ and adsorption of CO₂. Preferentially, a production phase should precede CO₂-injection. If CO₂ is injected in water-wet coal, the CO₂ will easily by-pass the coal surface and migrate via the cleat highways and cause early CO₂ break-through in monitoring wells.

- Increased pore pressures during high-pressure injection keep natural fractures open. Each fall-off or production period is then a relaxation period where coal swelling becomes more important reducing the permeability of the coal.
- If large-scale CBM production over the reservoir is more important than the local CO₂ injection, then the overall reservoir pressure decreases and CO₂ injectivity increases.
- In all test cases the net CO₂ storage wins, even if small portions of CO₂ were produced or back-produced after the test. This means that even if adsorption does not completely take place (e.g. due to initially water-wet coal), anyway, a large portion of the injected CO₂ remains in the reservoir (and the reproduced CO₂ might be reinjected in CO₂-wet coal).
- There seems to be an evolution in injectivity through time due to redistribution of adsorbed CO₂. Often a decrease in injectivity is observed after a first period of adsorption. This trend is later reversed again on the long term. This could relate to excess CO₂ around the injector being redistributed laterally. Spreading could be controlled by coeval production (pressure sinks) in smart producer-injector grids, although initial permeability and specific geological conditions may require location-specific strategies.
- Current numerical models are able to produce simulation output explaining large part of the field data, but there are still problems to accurately model the reservoir behavior, (Reeves, 2005).
- There is still a scale-problem between lab and field observations and some physical processes are not completely understood (e.g. Reeves, 2005; Reeves et al., 2008).

2.2.2. Risk assessment in coal-bearing strata

2.2.2.1. Type of risks

The same type of risks apply for CO₂ storage projects in coal than for those in aquifers, although risks are not equal and some particularities of coal ask for different monitoring strategies. In this section the type of risks are summarized. The next section zooms in on some specificities of coal that result in different risk levels.

Risk assessment (RA) can be divided according to three levels (Figure 2.15): geological risks relating to failure in the reservoir – seal concept, historical risks relating to leaking old subsurface infrastructure (wells and mines) and mechanical risks relating to failing (sub)surface infrastructure operated for the storage project. Each level requires its own monitoring strategy and equipment.

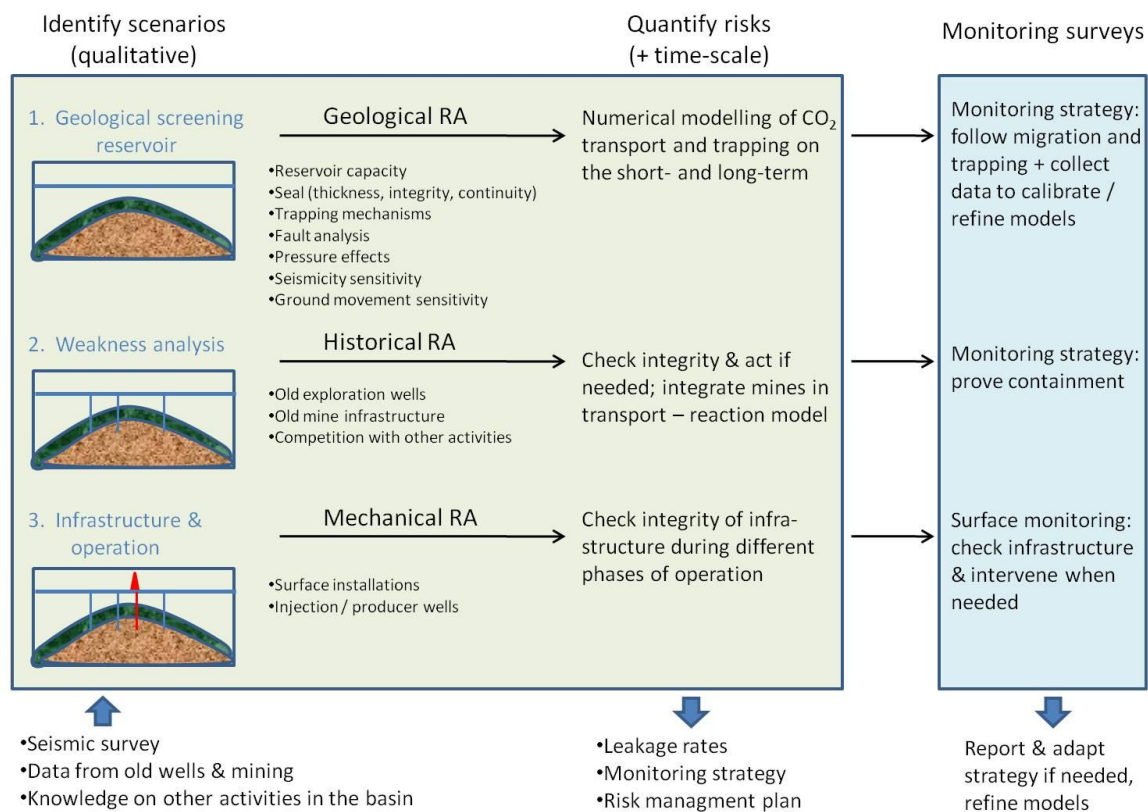


Figure 2.15. overview of risk assessment and monitoring strategy.

2.2.2.1.1. Leakage of CO₂

Most concern goes to leakage of CO₂. There can be several potential migration pathways for CO₂ in a reservoir, which need special attention and in some cases direct monitoring to make sure that CO₂ is not migrating out of the reservoir boundaries.

CO₂ could migrate:

- along abandoned wells or old mine infrastructure

The economic interest in a basin often determines the number of exploration wells and subsurface infrastructure. A safety distance from these features should be considered. Stuffken (1957) calculated the extent of fractured wall rock around mine galleries. For old wells, the aging and the emplacement of the wellbore cement need to be checked. Also the sealing method after abandonment should be known. Note that old cements were not designed for CO₂ interaction aspects. If there are doubts about the cement integrity, an extra sealing intervention should be planned. Nevertheless, CO₂ migration through locally imperfect cement seals is slow and in most cases large distances need to be travelled before CO₂ is reaching out of the reservoir. It can thus be considered as a long-term risk (Celia & Bachu, 2003) for which the leakage rates then need to be monitored.

The leakage rates can be computed by applying analytical solutions, although solving them becomes extremely complex when several aquifers and aquitards and multiple wells are involved. In the latter case, approximations to the well function and appropriate simplification of the convolution integral can be introduced (Nordbotten et al., 2004). Zhou et al. (2005) calculated a maximum leakage rate of 0.012 kg/day at 5000 years along abandoned wells for the Weyburn project using overestimated values and conservative assumptions. This value if emitted at a point source would not exceed the health CO₂ concentration norms in case no secondary accumulation of CO₂ takes place.

The effect of past mining activity is discussed below.

Old subsurface infrastructure that is situated within the reservoir needs to be screened for wellbore integrity. Old mines should be integrated in the transport – reaction models and could be used as monitoring sites by following up changes in water chemistry.

- along newly drilled wells

Also new infrastructure needs to be screened during different stages of operation for leaks. Worst case scenario is a wellhead failure with acute leaking of CO₂. Wellbore integrity tests, blow out prevention, safety valves, vents and other measures are standard for safety management. Imperfect cementing of wells, deformation around the wellbore, failure of casing and debonding of cement could cause leakage through the annulus between casing and wall rock. The risk is lower than for wellhead failure because of the slow migration process leaving time for monitoring to detect the problem and intervene.

There are several monitoring opportunities for detection of leaks at the surface.

- out of the coal-bearing reservoir by insufficient sealing at top

The integrity of the primary sealing layer is a crucial aspect in safety assessment. Nevertheless, coal-bearing reservoirs depend to a lesser degree on the top seal than aquifers because the coal-bearing reservoir in itself contains numerous interlayered secondary seals composed of low permeable argillaceous rocks. Also, coal layers act as sink (reservoir) and seal at the same time. Because of the stratigraphic heterogeneity inherent to coal basins, the spatial definition of reservoir and seal is not as straightforward as it is for aquifers. These aspects are discussed in more detail below.

The integrity of the regional seal can be checked by monitoring at crucial positions in the geology (faults, overlying aquifers or mines, control wells...).

- along faults with reach out of the reservoir

Faults can play very different roles, as fluid conduits or even preferential flow pathways, but they can also form barriers for fluid flow. Compartmentalization might be interesting in case of large aquifer storage when lateral sealing prevents further spreading out of CO₂. In case of thin-layered coal reservoirs compartmentalization can strongly limit storage capacity. The role of faults needs to be evaluated for each specific location. Active faults require special attention and a safety distance (determined in function of the reservoir permeability versus the kinetics of CO₂-trapping mechanisms) must be considered. Fault positions can be checked by seismic surveys. The actual role of faults can be checked with high confidence only during pump tests implying two wells at both sides of the fault.

Subsurface monitoring of water chemistry at crucial positions (e.g. at the crossing of the fault with an overlying aquifer) should be performed to check the main faults hydraulic integrity.

- lateral migration out of reservoir

CO₂ can migrate out of the reservoir if lateral migration is too fast and lateral seals are lacking, for example by outcropping or subcropping (juxtaposition of aquifers) of CO₂-bearing strata. The velocity of CO₂ migration is determined by the permeability of the reservoir and by the kinetics of the CO₂-rock reactions.

The lateral spread of CO₂ can be monitored by control wells or by seismic techniques.

2.2.2.1.2. Leakage of CH₄

Besides leakage of CO₂, there is also a risk on leakage of CH₄ in case of storage in coal-bearing reservoirs. CO₂ and/or CH₄ are naturally produced during burial and maturation of coal-prone organic material. Depending on the degree of coalification, different ratios of CO₂/CH₄ are produced. The higher the coal rank, the more CH₄ is adsorbed on the coal surface.

When CO₂ is injected into CH₄-mature coal an exchange reaction will take place, because of preferential adsorption of CO₂ compared to CH₄. The desorbed CH₄ molecules are displaced through the cleat and fracture system and can flow according to prevailing pressure gradients to producing wells or to control wells. CH₄ leaks could potentially occur:

- along abandoned wells
- along non-active producers
- along faults

The desorbed CH₄ can be extracted by producer wells, in some cases economically (ECBM). Anyway, producer wells are recommended to control the permeability and pressure distribution, and thus indirectly, injectivity in such low-permeable reservoirs. These producer wells then act at the same time as monitoring points.

The leakage of CH₄ is a concern, because it has a global warming potential 25 times higher than CO₂ (http://cdiac.ornl.gov/pns/current_ghg.html).

2.2.2.1.3. Pressure effects on aquifers

- Intrusion of saline water in fresh water aquifers

Apart from in-situ and near-situ risks, there is also a far-distance risk relating to pressure effects which extend much farther than the direct reservoir influence around the injector. In case of injection into saline aquifers, it should be avoided that saline water would intrude other aquifers and affect groundwater quality. Hydrological modeling together with aquifer monitoring is required to ensure hydrological integrity.

In case of CO₂-injection in coal, the volumetric capacity is limited and there are multiple hydrological barriers within the reservoir, which make pressure communication with other aquifers rather unlikely. Only in case of important conductive faults crossing the coal reservoir there is a risk of saline water escape.

Overpressures can be avoided by coeval production of water (with desorbed CH₄) from the reservoir. Hydrological communication can be monitored by measuring pressure and water chemistry at crucial points in the aquifers. Note that pressure measurements have a higher chance to detect changes because they are detectable over a wide area, in contrast to chemical anomalies which would build up locally. In order to detect changes in water chemistry the monitoring tools or water sampling should be placed/carried out on the right spot, which cannot always be adequately predicted.

- Competition with other activities in the same basin

Pressure effects are to be considered also when possible conflicts of use occur. A same basin can host several subsurface activities (e.g. geothermal energy extraction, seasonal gas storage, mining, CO₂ storage...) at the same time, in different zones or at different depths and stratigraphic intervals. Hydrogeological modeling is required, as well as specific monitoring. Based on these models and measurements, safety distances can be set more precisely.

The parallel activities, if interfering, are not necessarily negatively impacting each other; a positive synergy is possible in some cases. The operation of ECBM extraction in the coal layers could possibly benefit from geothermal energy extraction in deeper parts (e.g. the Dinantian aquifer). In the CBM pilot test at Peer in the early nineties excess water production was maintained during more than 1 year as a result of water inflow from a fault zone. If a geothermal production well would catch this water at a deeper level along the fault zone, pressure reduction and hence degassing would become much easier. On the other hand, pressure reduction higher along the fault zone would stimulate flow towards the fault zone which should result in more efficient geothermal production.

CO₂-storage in coal can only be envisaged for deep unminable coal deposits. Later mining of coal beds that were used for CO₂ sequestration would release the earlier adsorbed CO₂ back to the surface. A safety distance should also be kept from potential future mine zones because of related pressure reductions that might liberate CH₄ and CO₂ from the storage site.

2.2.2.1.4. Ground movements

In rare cases, there is a risk of minor ground movements (local uplift) due to pressure changes and swelling of the reservoir. Movements, such as regional subsidence, have been registered for example during large-scale gas extraction in the Netherlands or during large-scale mining activity in Limburg. Although instability of collapsed mine infrastructure has caused locally significant surface subsidence during the period of mine operation, the subsequent flooding of the mines with water caused only slow, uniform and very minor uplift of the mine region. The amount of rebound after mine abandonment has been calculated for the Dutch coal mines to be in the order of 2-4% of the former subsidence (Pöttgens & Van Herk, 2000). For the Belgian coal mines, we can thus expect an uplift of 8-16 cm in the western subbasin and 16-32 cm in the eastern subbasin as a result of minewater flooding and elastic rebound (Devleeschouwer et al., 2007).

Injection of limited volumes of CO₂ in coal would cause local swelling of the coal surface, but this is not expected to be large enough to cause measurable uplift of the surface. The expected effects from coal swelling are on the small-scale and local. They could possibly lead to failure or slip deformation of overlying layers. If this slip would be large enough to juxtapose two aquifers, then flow could occur from high to lower pressure. The lithology of coal basins, however, favors the formation of clay gauges and coal powdering, which decrease the permeability of faults. Even in case of locally changed flow paths, the stratigraphic heterogeneity of the reservoir would limit the overall effect.

2.2.2.1.5. Induced earthquakes

Seismic risks are directly related to pressure effects. If pressure effects lead to non-elastic deformation of the subsurface, displacement can occur which can be accompanied by seismic waves. A certain formation can have a specific overpressure (extra pressure above the prevailing reservoir pressure) without causing failure or slip, depending on the confining pressure, the fluid pressure, the presence of weakness surfaces (older fractures, faults, heterogeneities with different geomechanical competences) and the stress field. The chance of causing failure or slip can be calculated if these parameters are known.

Special attention to overpressures must be paid when preparing fracking activities to stimulate productivity or injectivity of a well.

Geomechanical measurements and stress analysis should be performed prior to completion and injection. During operation, monitoring can be done by laying out geophones or by standard seismologic recording bases.

2.2.2.2. Particular characteristics of coal

Many risks are similar for CO₂-storage in coal as for storage in saline aquifers (e.g. well-bore integrity), but coal represents some specificities and associated different risk levels. These particularities are discussed in the section below.

2.2.2.2.1. Permeability of coal

The most important factor in geological risk assessment is the permeability of the concerned lithologies (reservoir – seal definition). These values determine the hydrological properties of the storage site, or in other words the flow and primary trapping conditions. The lower the flow velocities in the reservoir and the more internal and external flow barriers present, the safer the storage (Nelson et al., 2005).

The permeability of coal is quite different than permeability from classical reservoirs (aquifers). It is not straightforward to quantify coal permeability, which is much dependent on other properties, such as gas saturation, depth, tectonic setting, stress changes, etc. Coal always is characterized by dual porosity, called "matrix" and "fracture/cleat" porosity or primary and secondary porosity, with very different characteristics. The primary (matrix) porosity is composed of micropores which contain the gas in place (GIP). These pores ensure the sequestration capacity by adsorption. When coal does not show significant secondary porosity, it can be classified as an 'impermeable' reservoir or seal. Mass transfer through the primary micropores is dominated by diffusion driven by a concentration gradient. Flow velocities thus are slow.

The secondary porosity relates to the cleat system, which is composed of two sets of fractures with almost perpendicular orientations (the face and butt cleats). They form conduits for fluid flow and thus bring desorbed gases to the well bore during CBM production. Mass transfer through the cleats is characterized by Darcian flow driven by a pressure gradient (BERR, 2004).

The secondary porosity of coal can be enhanced by development of hydrofractures (e.g. fracking to overcome injectivity problems).

Coal permeability is highly dependent on changes in effective stress and volumetric strain effects (shrinkage / swelling) associated with de- / ad-sorption. Pressure tests on cylindrical coal samples show a rapid closure of cleats and an exponential permeability-decline with increasing confining pressures. At shallow depths coal permeability can be better than that in sandstones at similar depth. At deeper zones it is comparable rather to that of mudstones. Because cleats are often vertical and coal is highly stress-dependent, changes in horizontal stress (e.g. compressional or tensile regime) may strongly impact the secondary porosity of coal. In addition, changes in concentration of gases (CH₄ versus CO₂) also impact the coal permeability by differential swelling/shrinkage.

The secondary permeability of coal is further determined by diagenesis, e.g. mineral infills in cleats and by external changes (CBM production / CO₂ injection changing the hydraulic pressure and sorption leading to volumetric strain effects).

Most European coal basins show low porosity and permeability values below 1 mD under normal reservoir pressure conditions (UK: Olroyd et al., 1971, BERR 2004; Campine Basin: Wolf et al., 2001).

2.2.2.2.2. Permeability of adjacent / overlying strata

Coal layers by themselves act as sink and trap at the same time. The special characteristics of coal make them particularly suitable for CO₂ sequestration. But coal layers are generally thin and thus represent only limited storage capacity. Practically, the complex play of stacked reservoir and seal lithologies in a coal basin can be targeted for CO₂ storage. Intercalated sandstone layers with higher permeabilities enhance the injectivity and storage capacity, while intercalated coal and shales contribute to the overall sealing and trapping capacity. Stratigraphic heterogeneity in both vertical and lateral direction is typical for all coal basins (Figure 2.16). The typical lithologic assemblage is composed of repetitions of arenaceous and argillaceous strata.

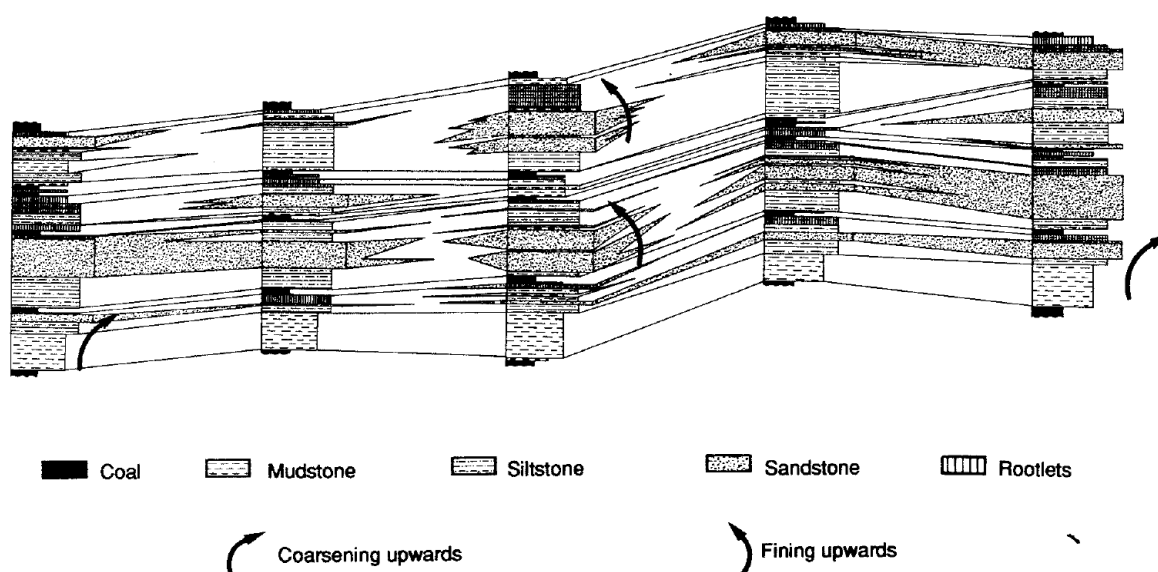


Figure 2.16. Typical lithological heterogeneity in coal basin deposits. Example from the Campine Basin (Dreesen, 1993).

This stratigraphic heterogeneity can be regarded as an advantage with respect to CO₂-storage, because it involves extra barriers to vertical fluid escape and thus slows down upward migration (e.g. Gibson-Poole et al., 2006). Instead, lateral migration is encouraged (Figure 2.17). The length of the migration path and the fluid volume moved through increase. Hereby more trapping opportunities are created favoring dissolution, residual, ionic and mineral trapping. Note that migration through the reservoir does not necessarily mean "leakage". By defining the reservoir as a stacked body, the CO₂-storage capacity is enlarged and at the same time the multiple local seals help secure containment. This results in less reliance on the regional top seal, which however should be present also. In the Campine Basin, the Cretaceous marls form a first regional seal, but additional clay seals are present also in the Tertiary sequence.



Figure 2.17. Sketch of final CO₂ spread (shown in white) in a hypothetical storage project in the Westphalian coal-bearing sequence of the Campine Basin. Lateral migration is more important than vertical migration and multiple trapping mechanisms are activated (structural, hydromechanical, solution, ionic, mineral, adsorption).

If the overall permeability is too low this results in an early stop of the injection capacity in the basin. If, on the contrary, the permeability of interlayered aquifers is very well connected, a better storage capacity is reached but high flow velocities would occur that enlarge the risk of leakage. Dynamic reservoir modeling must prove the safe containment and monitoring must confirm the containment within the set boundaries.

Monitoring in case of multiple layer storage in a coal basin should cover a relatively large area according to the expected lateral spreading. Reservoir models would typically include more uncertainties in simulations because of the complexity at different scales. The challenge in this kind of storage options is to define the boundaries of the reservoir, or in other words: where we don't want to have migration (e.g. some faults). These positions would then become obliged monitoring points.

Note that the concentration of CBM gas in place (GIP) can be regarded as a measure for the sealing capacity of the coal sequence and overburden. It is assumed that the coal was initially (at maximum burial and gas generation) CH₄-saturated and lost part of its gas content during subsequent uplift and erosion. The CH₄-content measured in the CBM-test well at Peer shows a depletion around the depth where a conducting fault is cutting the well. Probably, part of the initial CH₄-content has been washed out by circulating formation waters. On the other hand, in areas where secondary gas accumulations have built up below the overburden covering the Westphalian sequence, this might indicate the sealing capacity of the overburden. Such data can be used as exploration guides for storage options.

2.2.2.2.3. Faults

In order to store CO₂ safely in an underground reservoir, understanding the hydrogeology of the reservoir is a prerequisite. It depends much on the presence of faults and fractures. These heterogeneities can either form barriers and thus create compartments in the reservoir, or transmit fluids while connecting several units which enlarge the reservoir capacity. Jin & Pashin (2008) studied fracture patterns and their connectivity for the Deerlick Creek coal field in the Black Warrior Basin (USA; Figure 2.18). These authors concluded that hydrologic communication is likely between closely spaced coal seams due to interconnecting networks of joints. Thick intercalations of marine shale between the coal seams, on the contrary, limit largely the risk of cross-formational fluid flow.

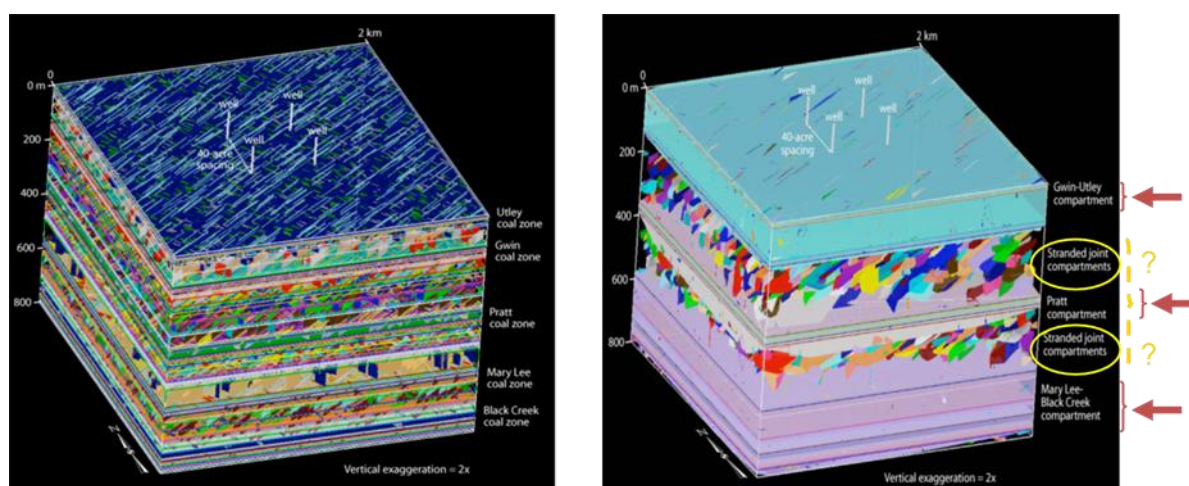


Figure 2.18. Discrete Fracture Network (DFN) model results (left) and compartmentalization analysis (right) for the Deerlick Creek Coal Field. Note the small, stranded joint compartments between the major reservoir compartments. From: Jin & Pashin (2008)

In Deerlick Creek, Groshong et al. (2003) could conclude that faults segment the reservoir into compartments showing different gas productivity. Moreover, from the results in this area it appears that moderate deformation (half grabens) may enhance fracture transmissivity relative to areas of no deformation (the horst), and that too much deformation (the full graben) reduces transmissivity (Groshong et al., 2003).

Pervasive cleat filling may also relate to fluid flow along faults and hence help forming flow compartments (Pashin et al., 2004; Figure 2.19). Fault-related fractures appear to have a higher potential to transmit fluids than hairline joints and most flow would be concentrated in few larger fractures (Pashin et al., 2003). The latter authors also demonstrated that bed-parallel flow is dominant in first order compartments around closely spaced coal seams, while cross-formational flow is favored in elongate compartments around faults. Clayton et al. (1994) showed that tangible leakage risk exists along normal faults when acidic CO₂-rich formation waters would dissolve significant amount of calcite cement in the coal cleats. In order to minimize leakage risks, CO₂ storage should thus be prioritized in blocks away from such faults.

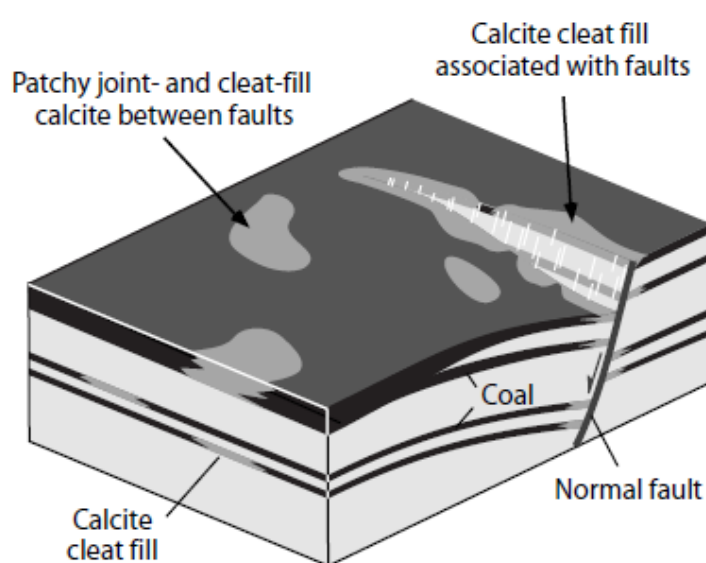


Figure 2.19. Generalized model of calcite mineralization in coal of the eastern Black Warrior basin (From Pashin et al., 2004; modified from Pitman et al., 2003).

2.2.2.2.4. Swelling

Adsorption of CH₄ or CO₂ on coal causes the coal matrix to swell. Adsorption of moisture also leads to swelling. Desorption, on the contrary, causes shrinkage of the coal matrix. Coal swelling engenders a reduction in cleat apertures and thus also in coal permeability. Due to different sorption capacity of coal for CH₄ and CO₂, differential swelling occurs when replacing CH₄ by CO₂ during ECBM operation (e.g. Mazumder & Wolf, 2008).

Sorption on the coal surface is stress-dependent (Pone, 2009). It also depends on the wettability conditions of the coal (see below; Mazumder & Wolf, 2008). In addition, van Bergen (2009) revealed through his PhD study that pre-compacted granular coal samples in the lab show a much stronger swelling effect than untreated samples. This is an important observation, in particular for low permeable coals that have undergone high tectonic stress and deep burial. Understanding the swelling effects is crucial for controlling injectivity problems.

2.2.2.2.5. Wettability

The presence of water appears from both laboratory and field studies to have a negative influence on methane recovery and CO₂ adsorption (Mazumder & Wolf, 2008). Under wet conditions the CO₂-CH₄ exchange in the coal matrix is impeded to a large degree which causes a fast bypass of CO₂ through the cleat system, due to CO₂ gravity override (buoyancy). When continuous CO₂ injection is maintained, water is flushed out of the cleat system and the coal matrix starts to desorb moisture (van Bergen, 2009). This gradual drying of the coal leads to a competition between on the one hand shrinkage with permeability enhancement and on the other hand swelling with permeability reduction due to improved CO₂ adsorption.

2.2.2.2.6. Geomechanical risks

There are various processes involved with CO₂ sequestration in coal that might cause changes in local stresses: drilling, stimulation, pumping, injecting, fluid flow, sorption, swelling, etc. Myer (2003) and Wo et al. (2005) wrote a good overview on related risks of generating new leakage paths for CO₂ by failure or slip along pre-existing discontinuities. The below paragraphs are mainly based on their analysis.

Pre-injection situation:

Drilling and completion are largely similar for aquifers and coal except for wellbore stability because shale and coal are weaker than sandstone or carbonate and manifest a higher risk on deformation around the well. A poor cementation job could on the long-term result in leakage along the cemented annulus between formation and casing. Therefore, a regular check for leakage is required, especially in case of old abandoned wells. Old coal exploration wells show a risk for cement integrity which may be imperfect and / or deteriorated through time. Especially when caving out of coal seams has occurred, the cementation may be incomplete locally. For new CO₂-injection wells additives can be used to achieve a better cement performance, but old wells were not adapted for this purpose. Acidic formation waters may corrode the cement creating additional pathways along the cemented wellbore.

Completion of wells also is more risky in coal because the thin seams might allow hydrofracture growth through the overburden. This depends on the horizontal stress (σ_H) in the overburden and in the coal. Most lithologies surrounding coal layers, however, possess higher σ_H and greater stiffness (Elastic modulus) and toughness impeding hydrofracture extension through surrounding layers. The vertical extent of hydrofractures should be controlled and monitored.

In case of open-cavity completion, failure and slip could occur potentially causing collapses in overlying strata, depending on the cavity width. Redistribution of in-situ stresses may further enhance fracture propagation (Myer, 2003).

Injection phase:

Production and injection cause changes in pressure and hence displacements in reservoir if failure or slip on pre-existing discontinuities occurs. Note that changes in pore pressure result in different effective stresses (shift of the Mohr circle), but not always to an equal degree for horizontal and vertical stresses (i.e. stress coupling effect, Addis, 1997; Hillis, 2001; Tingay et al., 2009). CBM production leads to increased differential stress (wider Mohr circle) and hence shear fracturing is promoted. CO₂ injection decreases the differential stress (smaller Mohr circle) which can result in tensile failure (Figure 2.20). Some effects may be irreversible due to complex stress redistribution (e.g. after initial phase of CBM draw down).

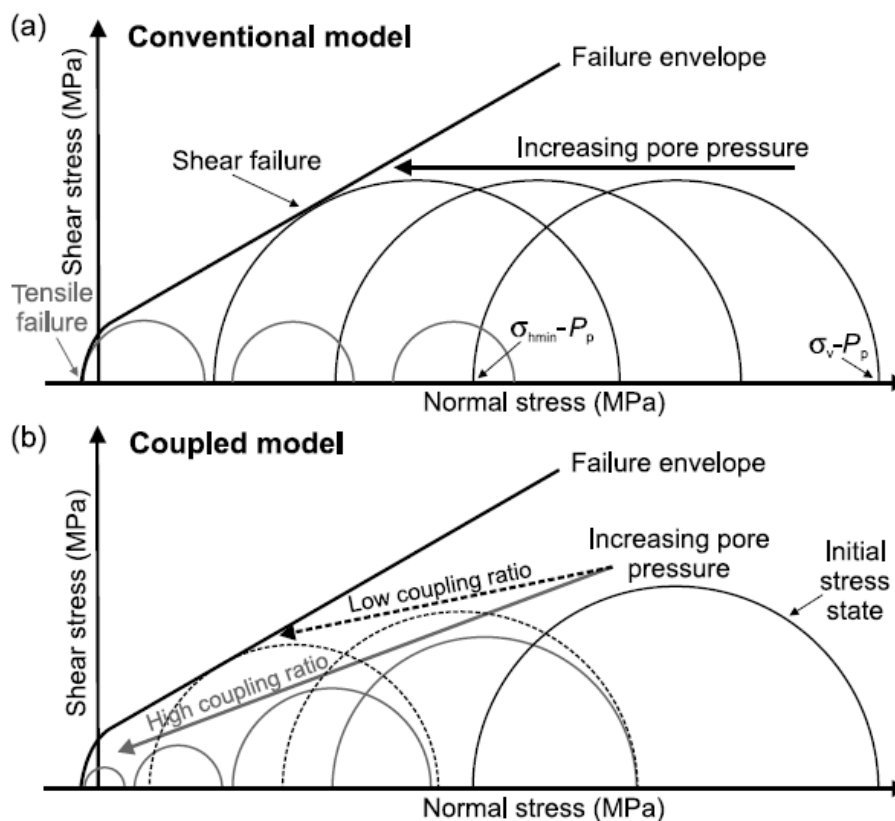


Figure 2.20. Schematic evolution of Mohr circles with increasing pore pressure (P_p) in a normal-faulting stress regime (modified from Hillis, 2001). (a) Conventional model where stresses are independent of pore pressure and brittle failure mode (shear versus tensile) is only controlled by the initial differential stress. (b) Model incorporating pore pressure-stress coupling. Source: Tingay et al. (2009)

Production and injection also cause volumetric changes in the reservoir which can affect the overburden depending on the compressibility and thickness of the reservoir rock. In some cases this might lead to minor subsidence or uplift. Coal is thin and compressible, but there is the additional effect of swelling / shrinkage due to sorption changes. When the effect is large enough, shear deformation may be expected at the top and bottom of the coal seam or elsewhere if the fluid pressure is not equally distributed (Figure 2.21).

When a pre-existing discontinuity cuts through the coal seam, then slip can occur also in the overburden. The risk of leakage then depends on the fluid flow (e.g. sandstone layers that become interconnected).

When slip takes place within the coal seam, then the risk depends on the degree of dilatancy. Nevertheless, formation of clay gouges makes the fracture surface less rough resulting in a lesser increase in permeability.

Although the risks on leakage are limited in case of CO₂ storage in coal, thanks to stratigraphic heterogeneity (see above) special attention should be paid to in-situ stress analysis, (micro)structural geology and hydrologic aspects. Sensitivity studies can be carried out to test and evaluate risks.

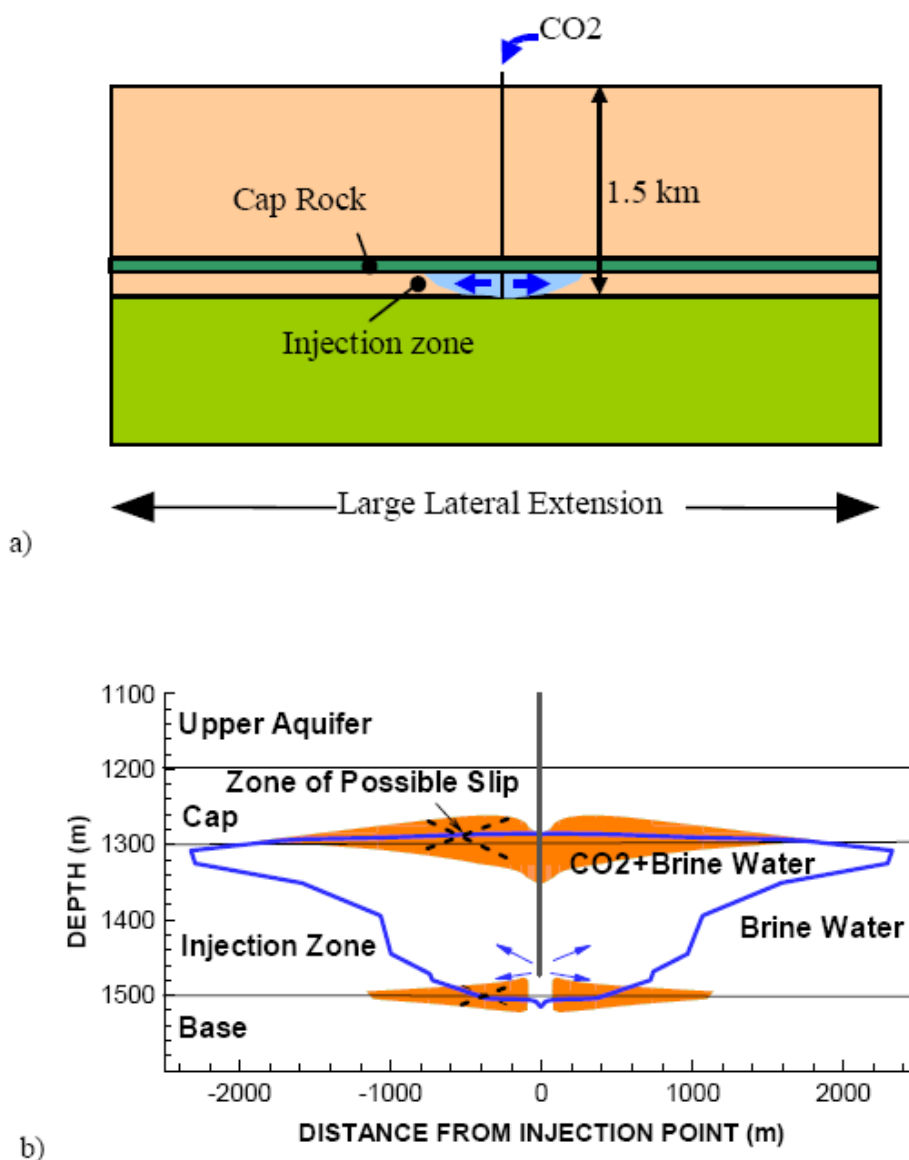


Figure 2.21. Result of numerical simulation of stresses and displacements due to injection of CO₂ into a brine saturated formation. The shaded area shows where shear stresses would develop (typically at heterogeneities such as the top and bottom of the layer where fluid pressures are unequally distributed); the blue line delimits the CO₂ plume. In the case of coal, swelling due to CO₂ adsorption can add to the possible volumetric expansion of the layer. After Rutqvist & Tsang, 2003 and retaken by Myer, 2003; Wo et al., 2005.

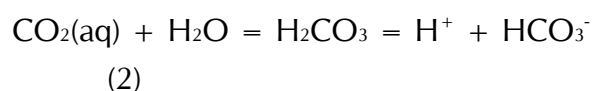
After all, most of the geomechanical aspects discussed come from desk and lab studies, while field evidences are still scarce. Furthermore, some of the physical behavior of coal, such as swelling and weakening under certain conditions still needs further study. Reeves et al. (2008) conducted uniaxial-strain experiments to better replicate in-situ conditions, whereby vertical stress (corresponding with the overburden) is kept constant and horizontal strain is kept zero (i.e. by keeping the diameter of the plug constant and adapting instead the horizontal stress). In this way, excess (or reduced) stress is caused because the sample is not allowed to swell (or shrink). Some experiments resulted in excess stress that became so large that the coal sample failed. This is surprising because it was not predicted by geomechanical laws. It can be explained only by a change in mechanical properties of the coal during injection which could relate to micro/hydro-fracturing, weakening or plasticization.

2.2.2.2.7. Geochemical interactions

When CO₂ is injected into a geological reservoir it tends to dissolve into the formation water that then becomes more acidic and eventually corrosive with respect to certain mineral phases. Other mineral phases precipitate according to the newly installed chemical equilibria in the pore fluid. These geochemical fluid-rock interactions ensure long-term mineral trapping of CO₂. The degree of interaction depends on the presence of reactive minerals and on the composition of the formation fluid.

Coal typically contains bicarbonate-rich formation waters that differ from the brines in most saline aquifers. As such it has less tendency to precipitate minerals when CO₂ is dissolved in the formation water. Coal formation water contains mainly HCO₃⁻, Cl⁻ and SO₄²⁻ as anions and Ca²⁺, Mg²⁺, Na⁺ and K⁺ as cations.

If the coal is not dewatered (dry coal), then the following reactions take place in the formation fluid after CO₂ injection:



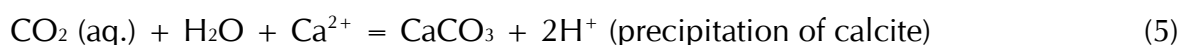
The formation of H⁺ results in a pH drop and in dissolution of calcite (most common mineral as cleat fill):



Combination of 2 and 3 gives:



However, if HCO_3^- is abundant over CO_2 or Ca^{2+} over calcite (e.g. after dissolution of calcite), the reverse reaction of (3) may occur resulting in:



Precipitation decreases the coal permeability by obstruction of the cleat system. Since the coal formation waters already tend to contain much CO_2 (HCO_3^-), the excess CO_2 probably will not cause mineral precipitation (Reeves & Schoeling, 2000).

The solubility of CO_2 in water is also pressure- (and temperature-) dependent (cfr. Henry's law). High pressure during injection may cause calcite (if present, e.g. as cleat-filling cement) to dissolve and lowered pressure around producer wells may cause calcite to precipitate around the wells. Nevertheless, the presence of other ions may buffer the reactions.

Smith & Reeves (2002) studied the effect of CO_2 injection by modeling the changes in saturation index for calcite in different formation waters. They concluded that no significant changes would occur and thus no dissolution is expected, neither precipitation near the injection wells. It should however be noted that they did not account for coal mineralogical composition or minor ion concentrations, neither for the effect of saline water intrusion from adjacent aquifers, and they also did not consider kinetic effects (timing).

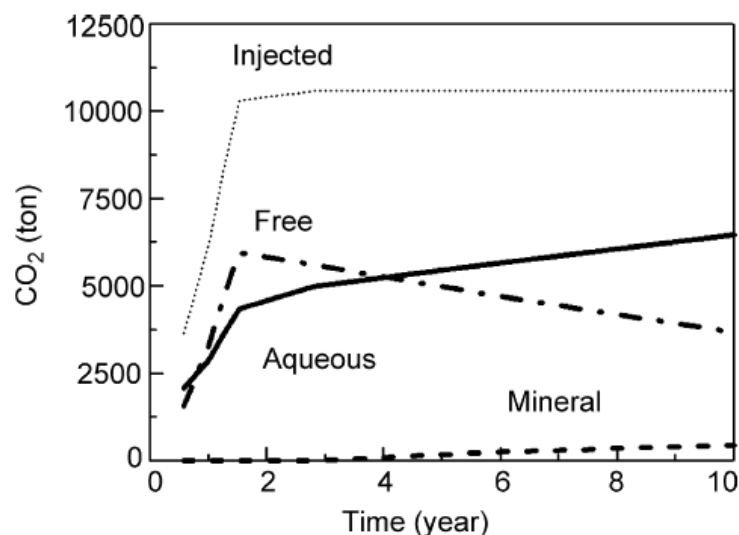


Figure 2.22. Amount of CO₂ sequestered by different mechanisms after injection into a sandstone reservoir, based on the Nagaoke pilot, Japan. From Mito et al. (2008).

Arenaceous strata within the coal-bearing sequence will react differently when CO₂ migrates through them. Water-rock reaction with reactive components (feldspars, carbonates, chlorite...) probably will help sequestering CO₂ by mineral trapping.

A good field example is the Nagaoke pilot in Japan where significant changes in chemistry were observed between formation waters sampled pre- and post-injection. The HCO₃⁻ concentration increased in a few years and mainly plagioclase and chlorite reacted to neutralize the CO₂-rich waters, which in turn could dissolve more CO₂ (Mito et al., 2008; Figure 2.22).

Another example is the Frio project where an increase in Ca, Mg and Mn was observed one day after arrival of CO₂ to the observation well (Kharaka et al., 2006). Despite the long-term (10000 years to sequester large part of CO₂ by mineral trapping) predictions by transport - reaction modeling, it is clear that mineral trapping starts already on the short-term. It depends of course on the reactivity of the reservoir, the amount of CO₂ injected, and the reservoir conditions. Most simulations and lab experiences show rapid reactions with respect to carbonates. (e.g. Hellevang, 2006).

2.2.2.2.8. Past mining activity

CO₂ sequestered in unmined coal could potentially migrate towards overlying or adjacent abandoned mines. These mines are characterized by zones with enlarged porosity and permeability in left open spaces (shafts, stonedrifts, galleries...), in back-filled or collapsed panels and in fractured zones around the cavings. Stuffken (1957) established some empirical relationships relating caving to fracturing of the surrounding rock massif. The effects of fracturing would be measurable until 120m above a mined out structure (Figure 2.23). This gives a minimum safety distance to be kept from the mined out zone. Where large pre-existing faults or fractures exist or where important collapses with surface subsidence have occurred, however, longer pathways for fluids might be present and hence a higher risk of leakage must be considered (Figure 2.24).

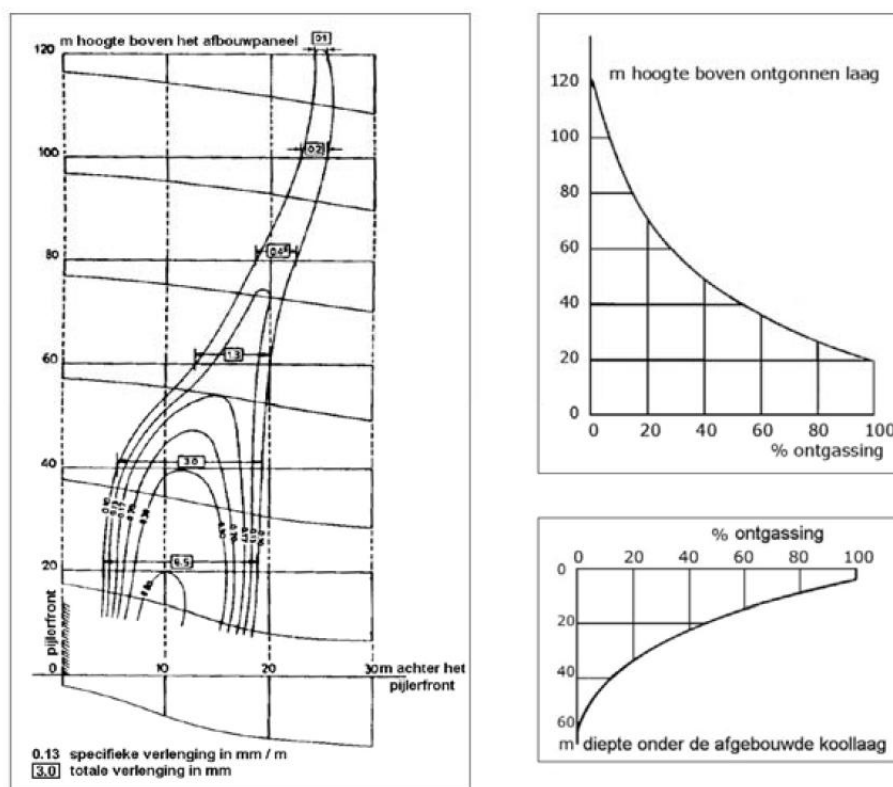


Figure 2.23. Relationships for fracturing around mined zones. Left: lines of equal specific stretching in the rock above (m) a progressing coal mining front. Right: Degassing of a coal layer as a result of fracturing versus height above / below (m) a mined part. From Stuffken, 1957.

Depending on the flooding history of the mine the inside pressure may be lower (i.e. underpressured) than the hydrostatic pressure within the surrounding rock massif; flow vectors are oriented towards the mine. When the inside pressure equals this surrounding hydrostatic pressure, the regional flow patterns may be restored. When CO₂ is added to the minewater, the system becomes overpressured with respect to the surrounding rock massif and CO₂ may migrate out of the mine along existing pathways. Since the existence of such features cannot be excluded the use of abandoned mines for permanent gas storage should be carefully considered (Piessens, in press.).

In case a geological storage site in the coal basin would leak, part of the leaked CO₂ would be trapped underway by dissolution trapping in formation fluids or by adsorption on coal and shale. The small quantities that would arrive to the mine would initially also dissolve into the mine water depending on prevailing pressure, temperature and composition of the water (Henry's law). Changes in chemical composition (pH, electric conductivity, HCO₃⁻...) and pressure and temperature can be monitored inside the mine. When the amount of CO₂ would become too large for the system to keep the CO₂ inside the mine, injection can be stopped and if needed a remediation (e.g. lowering the pressure by pumping part of the minewater out of the system) can be performed since the CO₂ leak can be localized. This is an advantage compared to aquifer storage where unexpected leaks would be less tangible and makes mines ideal points/areas for monitoring.

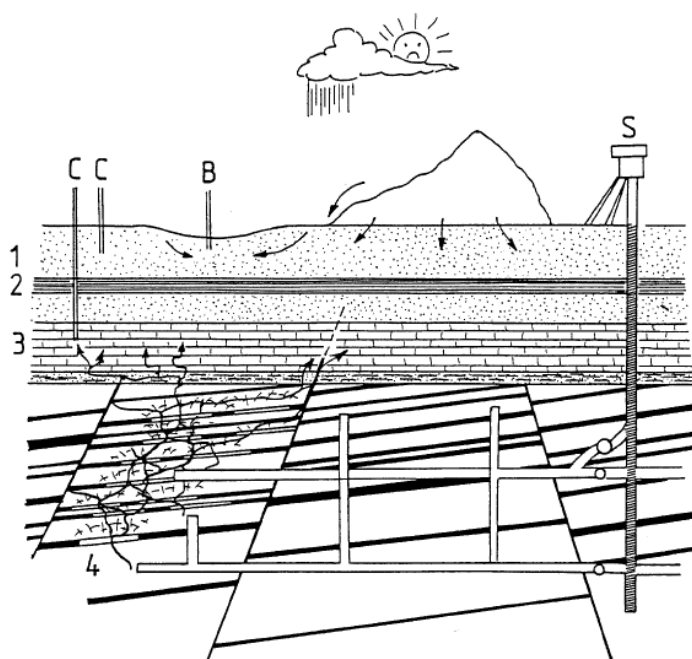


Figure 2.24. Sketch illustrating the potential effect of leakage along large fractured systems connecting the abandoned mine with an overlying aquifer. Source: VITO.

2.2.2.3. Leakage rates in coal-bearing cases

Although the mechanisms of CO₂ leakage are fairly well understood, quantifying leakage rates is still a challenge. The most straightforward quantification can be attempted for leakage along point sources such as wells. The leakage rates along abandoned wells (see above) can be computed by applying analytical solutions, although solving them becomes extremely complex when several aquifers and aquitards and multiple wells are involved. In the latter case, approximations to the well function and appropriate simplification of the convolution integral can be introduced (Nordbotten et al., 2004). Zhou et al. (2005) calculated a maximum leakage rate of 0.012 kg/day at 5000 years along abandoned wells for the Weyburn project using overestimated values and conservative assumptions. This value if emitted at a point source would not exceed the health CO₂ concentration norms in case no secondary accumulation of CO₂ takes place.

The only way to specify leakage rates from coal basin reservoirs is to look at natural analogues and field tests. Natural analogues for coal degassing are for example measurements of gas escape during mining (although circumstances are different), either directly (in shafts) or indirectly (soil). This gives an idea of release rates when CO₂ migrates close to the surface (at low pressure).

Another analogue is where coal occurs in outcrops and shallow subcrops (e.g. USA, the Netherlands, Germany). These situations give indications on the expected fluxes when CO₂ would migrate within the coal close to the surface and give an idea about expected interferences with other activities that involve pressure releases (e.g. future mining or CBM exploitation close to the storage site).

Field tests increase our learning about the reasons and circumstances of CO₂-breakthroughs between wells, and provide calibration data for testing conceptual models. Complete quantification requires independent estimates of the main parameters which depend highly on local conditions (pressure and porosity - permeability distribution, coal characteristics...). Such quantification often is not possible due to heterogeneity and small scale variations. So far, no commercial test data are available and results from demonstration projects show that the performance numbers are highly dependent on the combination with CBM production which largely controls the permeability and pressure distribution.

When sufficient data are available to set up a dynamic model of the coal reservoir, "leakage" (in the sense of "migration" out of the coal layer, not necessarily implying migration to the surface) through the overburden can be estimated by defining a maximum effective permeability for this overburden. This number can be deduced from the initial water production curves of the CBM wells. An example is given for the Deerlick Creek Field test in USA (Figure 2.25, Kieke, 2008, CCP2 final report). Here, a maximum value of 10^{-5} mD could be defined for the overburden resulting in m-scale vertical migration on a time scale of 100 years.

For the situation in the Campine Basin, vertical migration rates are expected to be even lower and would be acceptable on the long-term provided that no conductive faults are cutting through the reservoir, thanks to the thick Westphalian sequence and the depth of the coal layers.

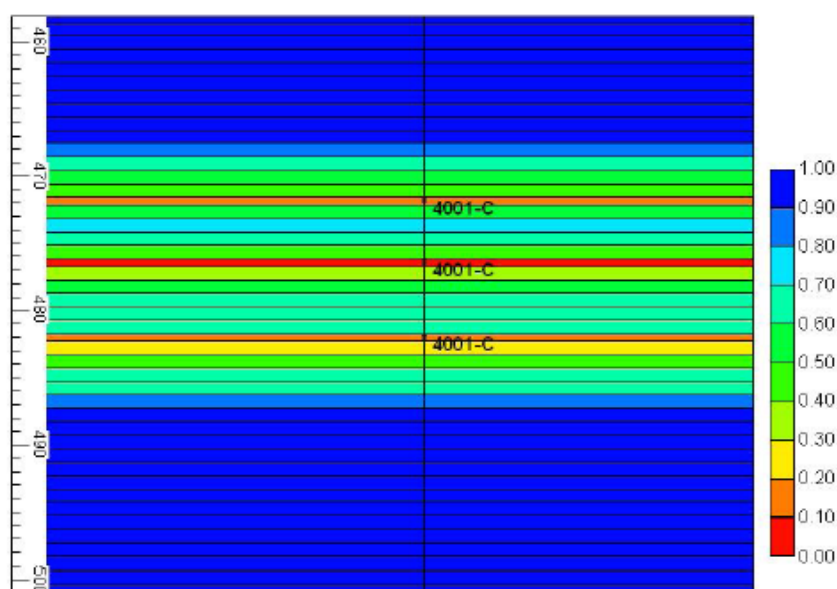


Figure 2.25. water saturation in the Mary Lee coal zone at the end of the simulation (after 90 years) by applying a maximum effective permeability for the overburden determined by initial water production rates. From Kieke, 2008, CCP2 final report.

2.2.3. CO₂ sequestration in coal in Belgium

2.2.3.1. The Campine Basin

2.2.3.1.1. Sedimentology

The advantage of stratigraphic heterogeneity for CO₂ sequestration in coal basins by stacking reservoir and seal units has been discussed already above (section 2.2.2. Risk assessment in coal-bearing strata). A comprehensive overview of the sedimentologic characteristics for the Westphalian-C strata within the Campine coal basin is given by Dreesen et al. (1995).

Coal seams can be regarded at the same time as reservoir and trap because of the long-term adsorption capacity of the coal matrix. Furthermore, sealing layers are present within the heterogeneous sequence. In addition, regional sealing formations are present in the Cretaceous (marls) and Tertiary (clays; Figure 2.26). The chemical sealing of the marls is not proven and needs more study. Also, the Cretaceous becomes more sandy towards the Roer Valley Graben in the east.

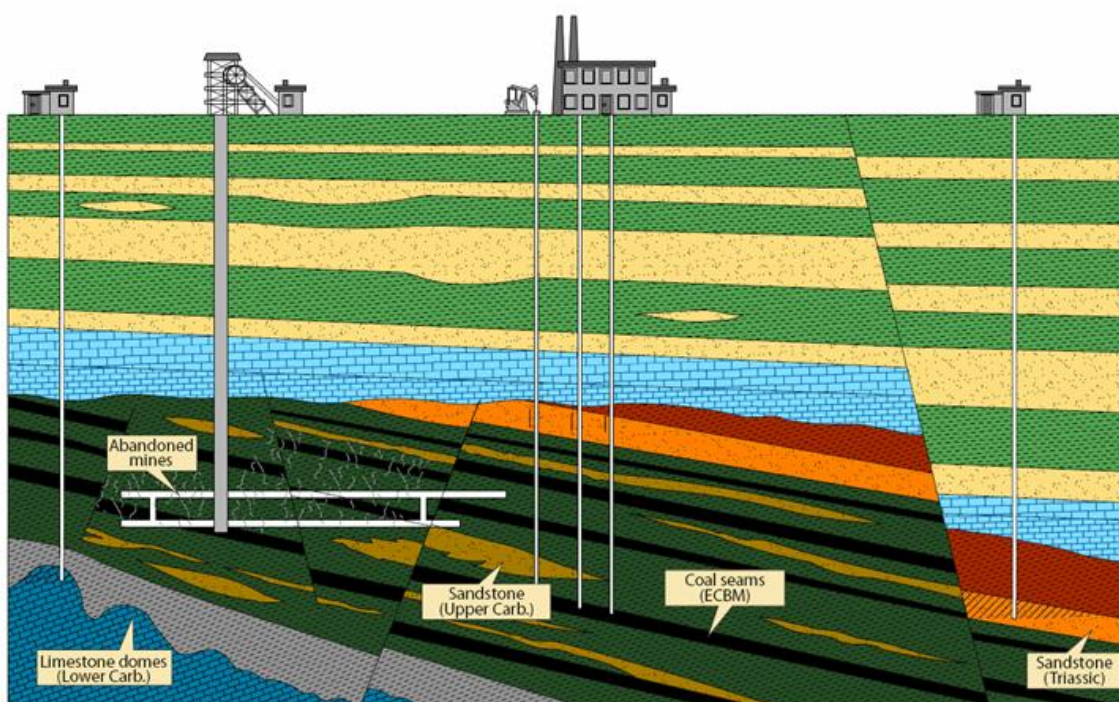


Figure 2.26. Sketch of the geology of the Campine Basin with indication of potential storage reservoirs. From top to bottom: green (clay-dominated strata), yellow (sand-dominated strata), blue (marl and chalk), red (Jurassic clay-dominated), orange (Triassic sand-dominated), alternated black, dark green and kaki (coal series with seams, clays and sandstones), gray (Namurian shales), dark blue (Carboniferous limestone). Modified after Lagrou (2002).

2.2.3.1.2. Structural setting - faults

A first division on inventarisation of faults started from the geological maps of the Campine Basin by Langenaeker (2000). The pre-Permian subcrop maps reveal a significant amount of faults throughout the basin. However, faults are more numerous in the eastern part, towards the Roer Valley Graben. The density of faults on the map is also biased by the density of seismic and other geological data. For instance, more smaller faults are drawn on the map in the area of former coal mines in Limburg.

The seismic data not only indicate the presence of faults, but also reveal their inclination, orientation (if faults are recognized on several seismic lines), and sense and amount of displacement.

The geological map (Figure 2.27) shows that on average, most faults are oriented roughly NW-SE. However, there are variations. Based on these differences, several sets of faults can be distinguished. Some faults have a curved trace on the map, suggesting they have incorporated another fault segment with a different orientation.

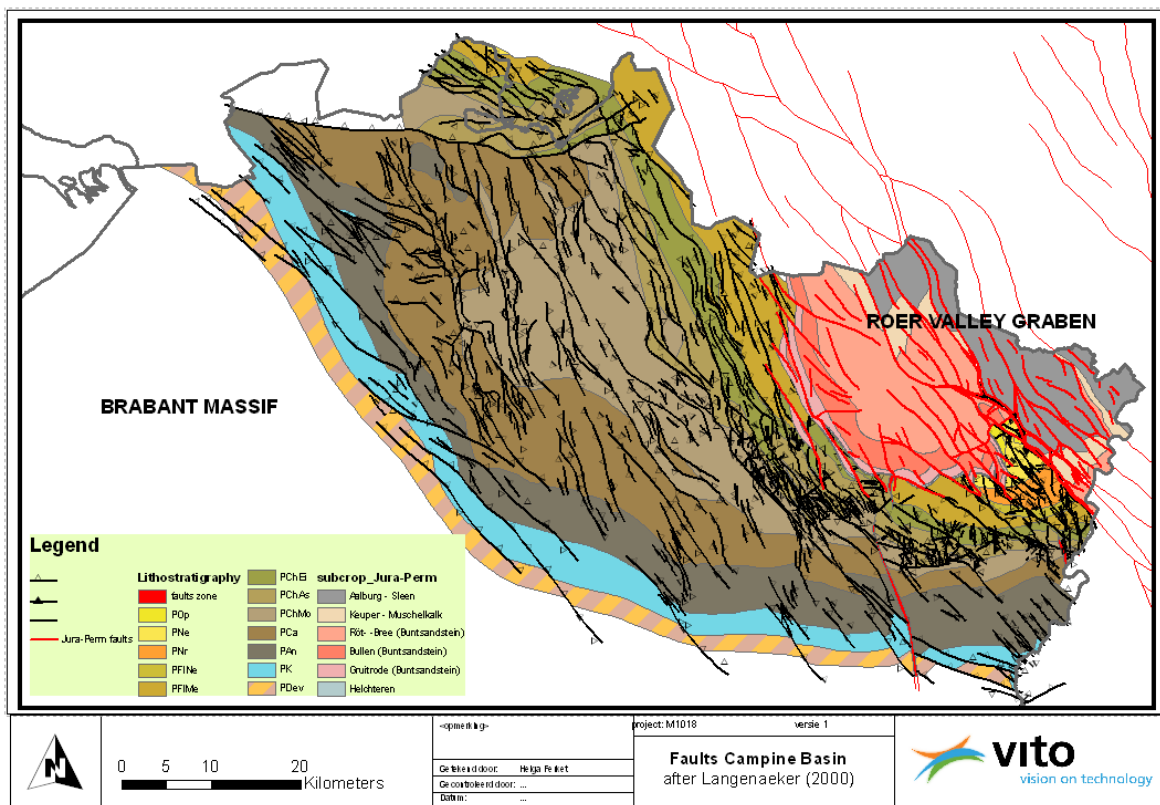


Figure 2.27. Subcrop map of the Campine Basin modified after Langenaeker (2000) with indication of Paleozoic faults (black) and Permian-Jurassic faults (red) (source: VITO).

- Set 1

The main faults, which are the longest on the map, are oriented NNW-SSE. The dip direction is either between 070 and 080, or between 250 and 260. These faults occur throughout most of the Campine Basin.

- Set 2

A second set of faults occurs in the east to northeast of the Campine Basin. The strike of these faults is more NW-SE. The dip direction is between 040 and 060 (or 220 to 240).

- Set 3

In the northwestern part of the Campine Basin, there is a set of faults oriented WNW-ESE. The dip direction varies between 030 and 040 (210 to 220). This orientation of faults is also present in the north of the basin (Meer area). In the area of the seismic survey of Olmen (Olmen-Balen)

- Set 4

In the former coal mining area, a fourth set of faults is present. Their orientation varies from N-S to NE-SW. However, their occurrence is rather limited.

- Set 5

The Hoogstraten Fault in the north of the Campine Basin forms a set on its own. Unlike the other faults, this is a normal fault oriented E-W, dipping to the north.

The majority of the NW-SE oriented faults dip to the east to northeast. This is synthetic with the southwestern border faults of the Roer Valley Graben.

Older faults oriented NW-SE were oriented ideally for later reactivation during graben activity. This is the orientation of the majority of faults. The WNW-ESE faults appear to be an older generation of faults. Their orientation is less suitable for later reactivation. However, seismic data reveal that these faults often have a pronounced influence on the Cretaceous formations. The base of the Cretaceous is either offset, or these strata show an undulation or flexure above the fault. Hence, this set of faults is certainly not an older generation that has become inactive after Carboniferous to Permian times (Variscan Orogeny).

Intra-Carboniferous faults probably are not permeable, but might induce compartmentalization of the reservoir and hence affect reservoir capacity. Nevertheless, the CBM pilot test at Peer showed that the Carboniferous Donderslag Fault zone transmits water. Due to the extensional graben tectonics, old lineaments - especially those with an orientation close to the graben strike - have a high potential to be reactivated and to focus fluid flow. CO₂ sequestration should thus be controlled within larger blocks between such faults.

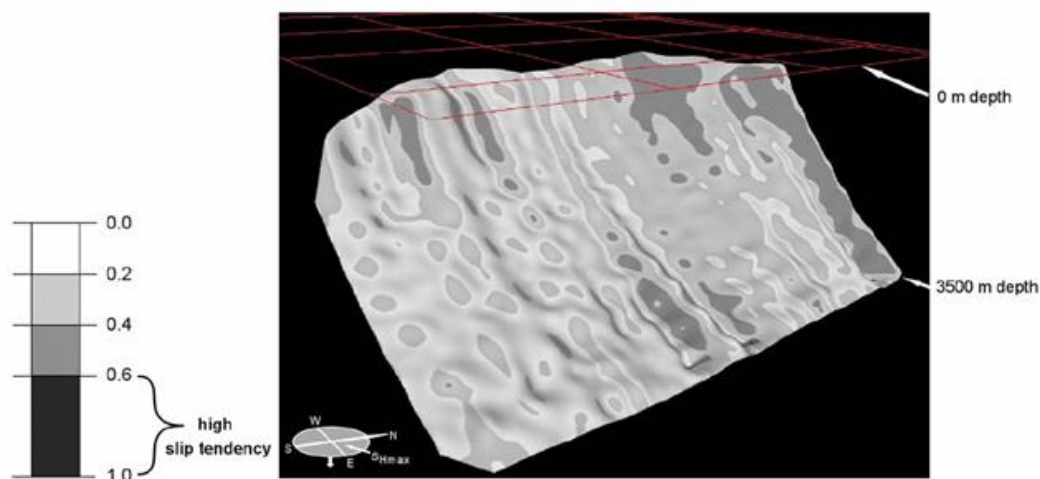


Figure 2.28. Slip tendency on a fault surface. The orientation of the fault surface is based on 3D seismic data. From Streit & Hillis (2004).

In order to control geomechanical integrity during CO₂ injection the location, orientation and behavior of the involved faults should be known. 3D fault orientation can be deduced from detailed seismic acquisition (Figure 2.28). In addition, the prevailing stress field should be known (principal stress axes and the magnitudes) so that the Mohr circles can be drawn. Then, also the actual pore fluid pressure (P_f) in the reservoir needs to be determined. In case of ECBM, P_f should be determined again after CBM field depletion to obtain the correct initial situation. With these data available, the fault slip tendency can be predicted and the maximum pore fluid pressure that the reservoir can take before causing slip on existing faults can be calculated (Figure 2.29). For one curved fault surface, this value will be different depending on the position on the surface (Figure 2.28). Therefore caution is required when using average fault orientations while in reality the fault displays variations in orientation.

For the Campine region there are some areas with denser seismic survey data, but many areas lack substantial seismic data displaying the 3D fault architecture.

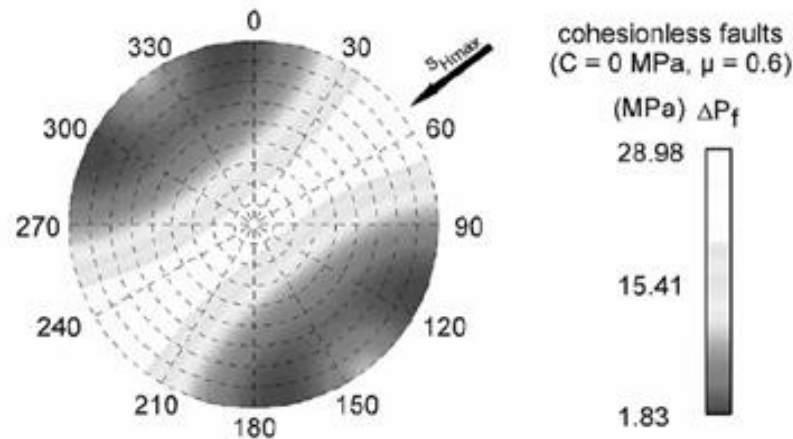


Figure 2.29. Stereographic projection showing P_f increases required to cause failure for any fault orientation (poles to fault planes) at 2 km depth using the same stress tensor as in Figure 2.28 . From Streit & Hillis (2004).

2.2.3.1.3. Stress field

The present-day regional stress field in the Campine area is related to late Alpine deformation. Deformation of the north foreland of the Alpine Orogeny is still ongoing with large-scale lithospheric folding and weakening of lithosphere in the Lower Rhine Graben (LRG) in contrast to the cold and thick lithosphere of the Brabant Massif (Cloething et al., 2006). In the LRG area, faults are mostly normal and strike-slip, with very minor thrust faulting (Figure 2.30). The stress field is dominated by NE-SW extension and NW-SE compression (Figure 2.31).

The Roer Valley Graben is superimposed on the Campine Basin and has caused reactivation of older faults. Active faults often show to be sealing at shallow depth by aquifer offsets, clay smears, grain reorientation and mineral precipitations (cfr. the large water table steps in Dutch Limburg; Bense & Van Balen, 2004). This does not imply, however, that they act as barriers at larger depths in the Westphalian series. One example just across the Belgian – Dutch border is the Benzenrader Fault which started leaking hot saline water in the mine during excavation workings cutting the fault zone.

As the Campine coal basin is actually in a normal fault regime, increases in pore pressure during injection of CO₂ would reduce the differential stress ($\Delta\sigma$) and could give rise to new extension fractures. Neotectonic movements at the border of the Roer Valley Graben are purely extensional with a NE-SW direction perpendicular to the graben axis (Cloething et al., 2006; Figure 2.31). Minor faults may have an impact on the kinematics of major faults and thus indirectly co-activate larger fault systems. In case significant slip or failure occurs, seismic activity may be triggered. In order to minimize the risk on microseismic activity, it is necessary to understand the stress system and the fault network, and to monitor the reservoir pressure. The injection pressure should at all times be kept below the critical values for failure and slip (when operating in the neighbourhood of faults).

Relatively large earthquakes in the intraplate domain of Northwest Europe have been registered since 1900, some related to human activities such as mining and CH₄ extraction (Figure 2.31). These earthquakes mainly related to pre-stressed faults that became reactivated by the changes in pressure and possibly weakened by fluid flow along them (Bense et al., 2003; Van Wees et al., 2003).

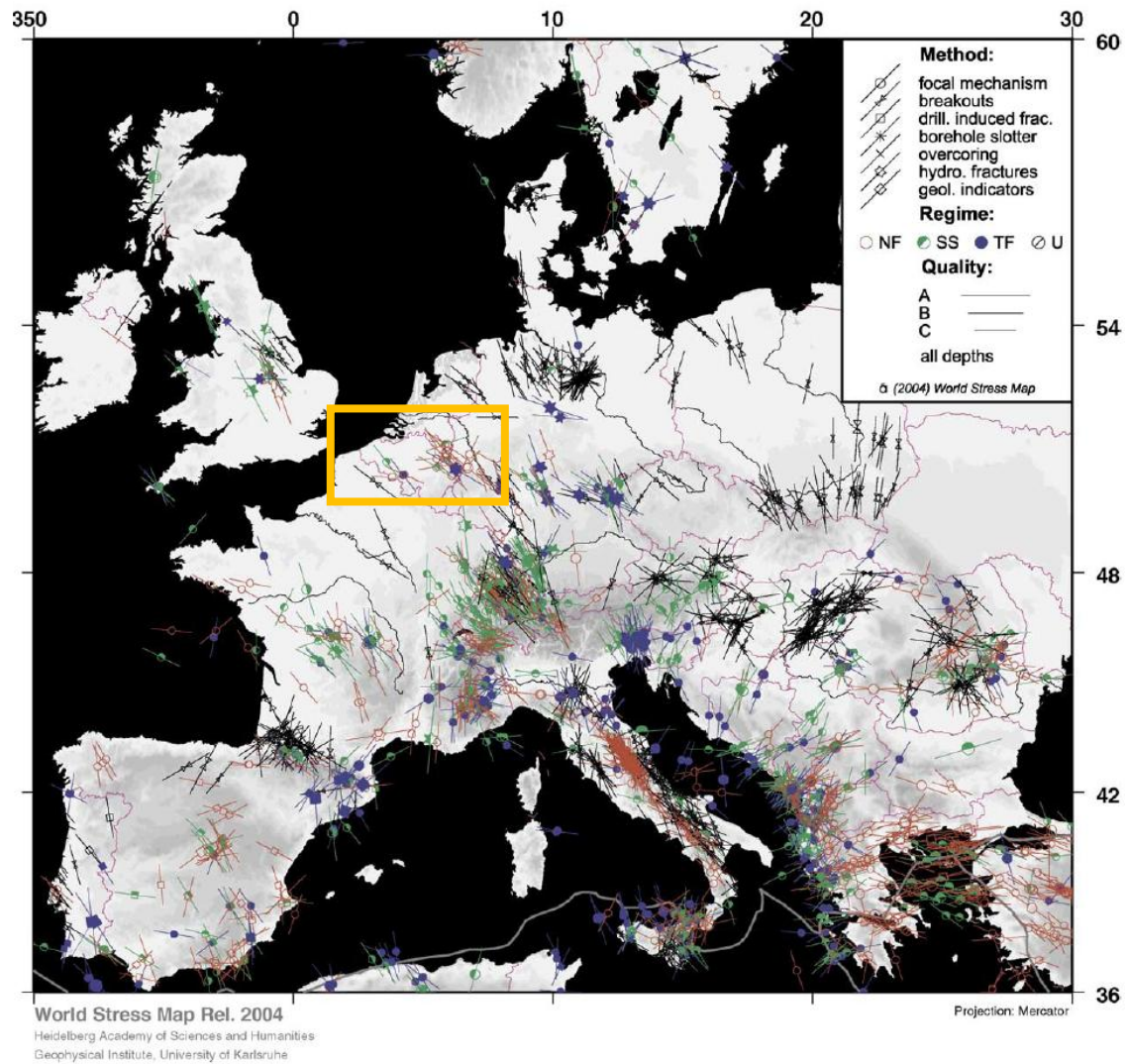


Figure 2.30. Stress map for northwestern Europe displaying the tectonic regimes as deduced from focal mechanisms of earthquakes and other stress indicators. The present-day orientation of maximum horizontal stress is indicated also. A zoom on Belgium is shown below.

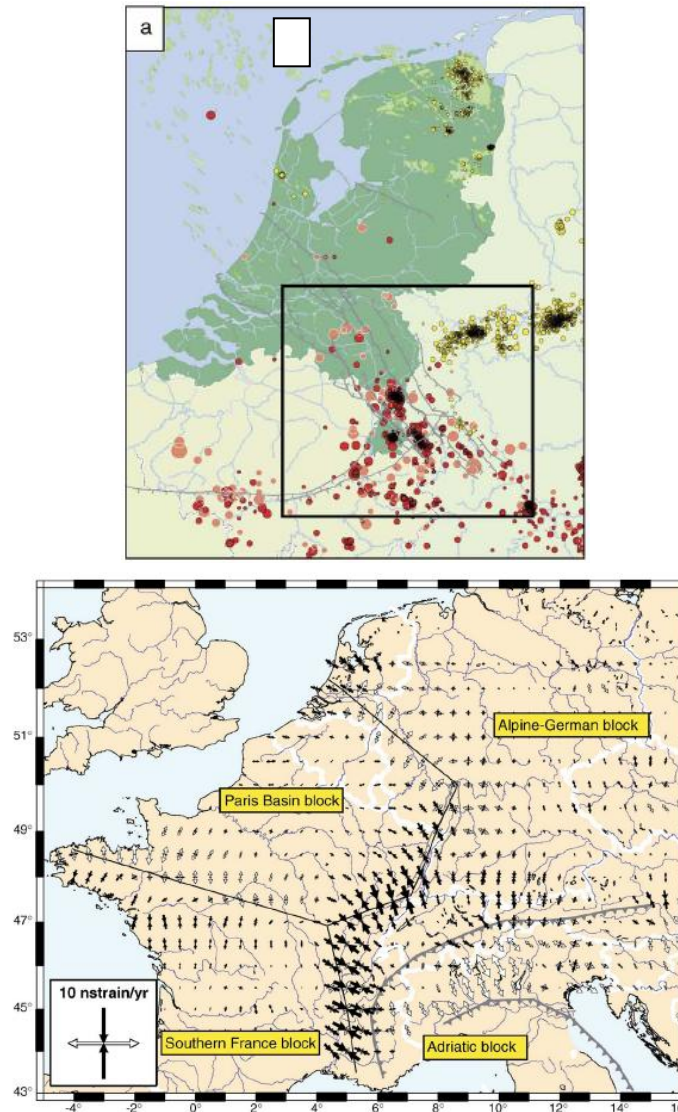


Figure 2.31. a) Registered seismic events since 1900 in the Lower Rhine Graben area. Red circles = natural seismicity, yellow circles = man-induced seismicity; scaled according to magnitude of the events. b) Principal axes and values of strain rates through Western Europe based on velocity solutions and a four block model. Compressional and extensional axes are in black and in white, respectively. From Cloethingh et al. (2006).

2.2.3.1.4. Exploration wells & mines

The past coal exploration and exploitation period has left behind some traces in the subsurface. The largest impact is caused by the mine collieries with their subsurface infrastructure and left open spaces. The location of mined out panels, galleries, stonedrifts and shafts is known through the Campine mines archives and has been digitized and integrated into a 3D database and model by VITO (the RAM-model; Figure 2.32).

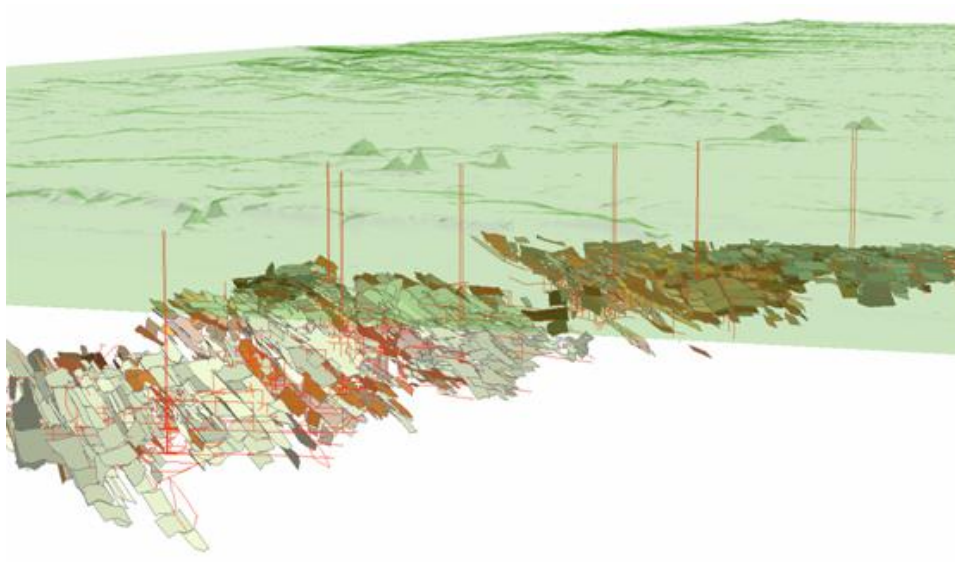


Figure 2.32. 3D visualisation of mined out panels, shafts and stonedrifts in the Campine collieries based on the RAM-database (model: VITO; data: LRM).

All shaft entrances to the Campine mines have been rigorously sealed after closure (Figure 2.33).

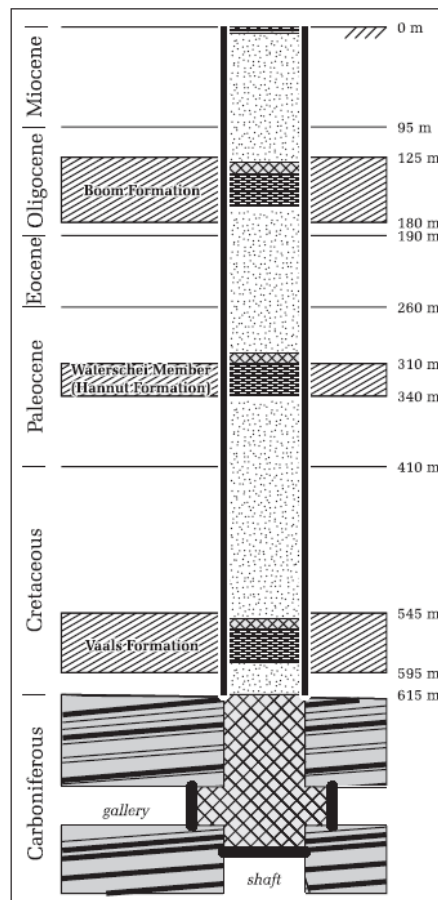


Figure 2.33. Schematic cross section through a shafts from the Beringen mine that was meticulously sealed, as is typical for Campine coal mines. From Piessens & Dusar (2004).

Besides old mines, there are a lot of abandoned exploration wells in the basin that could form potential leakage pathways if well integrity is not sufficient. The abandonment procedure at closure of wells mostly involved cementing of the open hole through the Carboniferous and Triassic sections, cementing of the remnant casing in the Cretaceous and filling up of the upper part with gravel. In some cases the wells were completely refilled with cement. If there are doubts about cement integrity, make-over should be considered and these points should be monitored. The density of exploration wells relates much to the former mine license areas. The location of old exploration wells is known through the mine archives and has been digitized and integrated in the Gekko-database by VITO.

2.2.4. Coal sequences in the Hainaut Basin

2.2.4.1. GIS database

The Hainaut basin and its extension to the East (Centre and Charleroi basins) is the most promising area for storing CO₂ in both coal sequences and deep aquifers (Piessens et al., 2009). A GIS database was built for this basin in ArcGIS® environment. The input data fall into three different categories: administrative, mining and geological data. An example output is given in Figure 2.34.

The administrative data set provides the essential administrative framework such as political boundaries (country, region, province and commune boundaries), main urbanized areas, roads and mining concession boundaries.

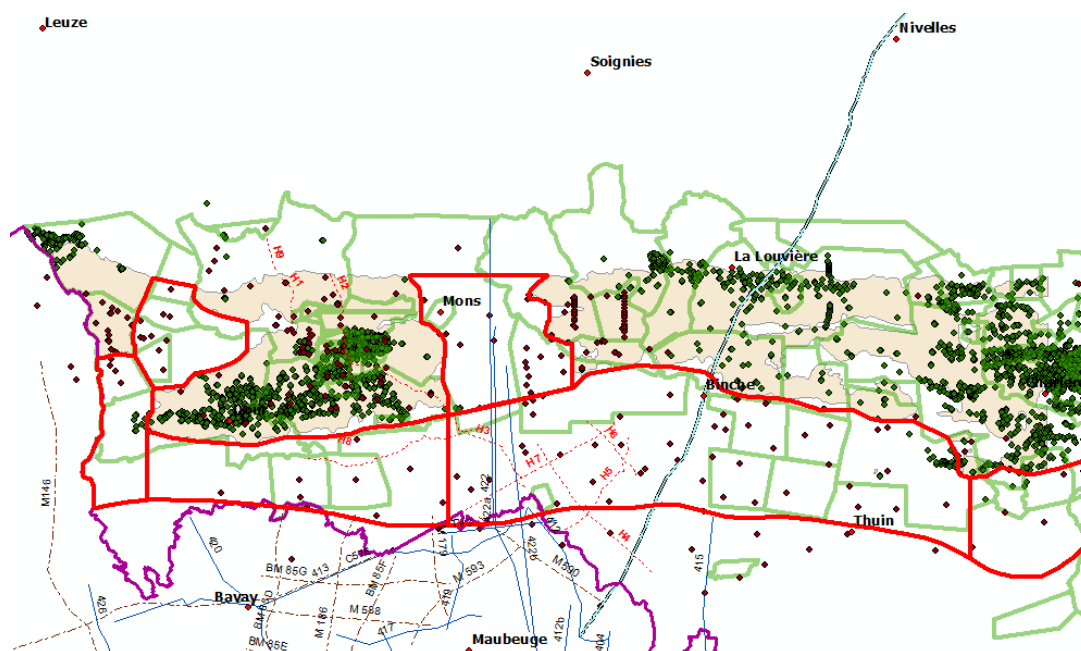


Figure 2.34. Example output of the GIS database for the sink inventory in the Walloon Region. Red polygons: target areas for storage in coal sequences; green polygons: mine concessions; shaded areas: mined zones; dark diamonds: exploration boreholes; green diamonds: abandoned shafts; thin lines: seismic surveys (the BELCORP survey (Bouckaert et al., 1988) is the thick, light blue line crossing the whole basin); purple line: political boundary. The map width is ca. 60 km.

The mining data set includes the extent of mined zones and an inventory of abandoned mine shafts. These elements are critical for the delineation of those areas where leakage risks are higher due to the presence of mine galleries and shafts but also where geological data might be found (i.e. in mine and shaft sections). Other data of interest for CCS research were collected in the available mine records, mainly the *Annales des Mines de Belgique* publications. These include records of gas shows and mine water, which can provide an indication on gas content, permeability and leakage risks for CO₂ storage. Information on gas shows was compiled as follows: date, location, local geology, type (vent, kick, burst), intensity and damaging effects (displaced rock volume, number of workers killed, etc.). A sample of the table for the "Agrappe" concession is given in Figure 2.35.

Biblio	N°	Date	Heu	Bassin	Concession	Puits	Etage	Localisation	Veine	Pendage	Ouverture	Déplacement	Excavation	Ouvrage	Etat massif	
										T	m°	T	m°			
4	Stassart et Lemare 1910, AMB T	2 0402/1892	12	Borinage	Agrappe	2	580	Sur la costresse (Est?) à 220m du bouveau de	Gde Veine l'Evêque	30	1	70	53	Costresse	Procs. faille(s)	
5	Stassart et Lemare 1910, AMB T	4 0909/1892	9,5	Borinage	Agrappe	2	630	E A 985mE et 26mN du puits d'aérage	Epusoire	20	1	130		Vallée	Faus-droit avec renflement veine (proc faille)	
6	Stassart et Lemare 1910, AMB T	4 5 0909/1892	15,5	Borinage	Agrappe	2	630	E A 985mE et 26mN du puits d'aérage	Epusoire	25	1	2		Vallée	Faus-droit avec renflement veine (proc faille)	
7	Stassart et Lemare 1910, AMB T	45 0909/1898	14	Borinage	Agrappe	2	630	V coupe chautier couche en dressant	Chaufournoise	45	1	19		Taille	petit pli sur toit - disparition face-banc	
8	Stassart et Lemare 1910, AMB T	47 2402/1898	13,5	Borinage	Agrappe	2	630	V coupe chautier couche en dressant	Chaufournoise	35	1	32		Taille	R.A.S.	
9	Stassart et Lemare 1910, AMB T	48 2009/1898	12,5	Borinage	Agrappe	2	630	V coupe chautier couche en dressant	Chaufournoise	37	1	17		Taille	R.A.S.	
10	Stassart et Lemare 1910, AMB T	49 2809/1898	9	Borinage	Agrappe	2	630	V coupe chautier couche en dressant	Chaufournoise	30	182	35		Taille	R.A.S.	
11	Stassart et Lemare 1910, AMB T	51 0802/1899	9	Borinage	Agrappe	2	630	V taille dressant (bèche montante)	Chaufournoise	40	0,88	0		Taille	voisinage étroite	
12	Stassart et Lemare 1910, AMB T	53 2302/1899	13	Borinage	Agrappe	2	630	V taille dressant (bèche montante)	Chaufournoise	20	0,9			Taille	voisinage crochon	
13	Stassart et Lemare 1910, AMB T	57 2802/1901	16	Borinage	Agrappe	2	630	V	Chaufournoise	25	0,75	30		12	Taille	Changement d'inclinaison - fissure
14	Stassart et Lemare 1910, AMB T	61 2009/1901	12	Borinage	Agrappe	2	630	V	Chaufournoise	25	0,8	76		50	Taille	piétement de la couche
15	Stassart et Lemare 1910, AMB T	74	10,3	Borinage	Agrappe	2	630	V 056m de prof. près du crochon-faille	Chaufournoise	45	1,06	44		Taille	voisinage crochon-faille	
16	Arnould 1880, ATPB T37	19 1869		Borinage	Agrappe	2	465	plateau	Petit-Saman	0,6				Taille	veine comprise entre terrains très durs et non-fissés	
17	Arnould 1880, ATPB T37	26 0809/1874		Borinage	Agrappe	2	550		Grande-Sézeuse	0,6				Chassage	proxième faille et étroite	
18	Arnould 1880, ATPB T37	27 2907/1874		Borinage	Agrappe	2	580	N bouveau Nord	Grande-Veine L'E.	25		150		Bouveau		
19	Arnould 1880, ATPB T37	39 1709/1879		Borinage	Agrappe	2	550	plateau	Grande-Sézeuse			10		Voie	serrement de la veine, broyée, proximité "oran"	
20	Arnould 1880, ATPB T37	41 1704/1879		Borinage	Agrappe	2	630	S	Epusoire	13	1,94	420		Montage	étroite	
21	Roberti-Linkermans 1895, ATPB	37 1805/1895	8,5	Borinage	Agrappe	2	640	V taille costresse couchant	Epusoire			220		Taille	veine irrégulière	
22	Roberti-Linkermans 1895, ATPB	38 3000/1896	11	Borinage	Agrappe	2	640	V un peu à l'V du précédent.	Epusoire	variable		61		Taille	ondulations au mur, proximité étroite, forte variat	
23	Roberti-Linkermans 1895, ATPB	39 1803/1897	16	Borinage	Agrappe	2	640	E terre voie plate levant	Epusoire	30		62		Taille		
24	Roberti-Linkermans 1895, ATPB	40 2004/1896		Borinage	Agrappe	2	640	E Deme voie plate en plateau	Epusoire			24		Taille	déclanchement	
25	Roberti-Linkermans 1895, ATPB	41 1805/1898		Borinage	Agrappe	2	640	E Deme voie plate	Epusoire			51		Taille	cloche de houille décolorée, dressant séparé d'un pi	
26	Roberti-Linkermans 1895, ATPB	42 2707/1898		Borinage	Agrappe	2	630		Epusoire			2		Montage	renflement	
27	Roberti-Linkermans 1895, ATPB	43 1809/1890		Borinage	Agrappe	2	520	E taille sous anciens travaux de 504 (prof 500m)	Croq-Palmes	variable				Taille	gement très tourmenté, grisou sort de deux car	
28	Roberti-Linkermans 1895, ATPB	44 2709/1891		Borinage	Agrappe	2	630	V taille en vallée en aval d'un crochon, le long du	Grande-Veine L'Evêque					Taille	aval crochon, le long du Grand Transport, toit post	
29	Arnould 1880, ATPB T37	20 1870		Borinage	Agrappe	3	459		Plate Veine					Taille		
30	Roberti-Linkermans 1895, ATPB	1 1302/1890		Borinage	Agrappe	3	600	E coupe levant du dressant	Chaufournoise					Taille	veine irrégulière	
31	Roberti-Linkermans 1895, ATPB	2 2004/1890		Borinage	Agrappe	3	600	E taille levant	5 Palmes / Hage	90	1,0			Taille		
32	Roberti-Linkermans 1895, ATPB	3 2005/1890		Borinage	Agrappe	3	600	E coupe levant	Chaufournoise			16		Taille		
33	Roberti-Linkermans 1895, ATPB	4 1206/1890		Borinage	Agrappe	3	600	coupe	Chaufournoise	variable		3		Taille	étroite	
34	Roberti-Linkermans 1895, ATPB	5 1808/1894	19	Borinage	Agrappe	3	640	V rete taille costresse couchant en plateau	Chaufournoise					Taille		
35	Roberti-Linkermans 1895, ATPB	6 2009/1890		Borinage	Agrappe	3	640	V rete taille costresse couchant en plateau	Chaufournoise					Taille		
36	Roberti-Linkermans 1895, ATPB	7 1805/1894	1	Borinage	Agrappe	3	640	V rete taille costresse couchant en plateau	Chaufournoise					Taille		
37	Roberti-Linkermans 1895, ATPB	8 2009/1890		Borinage	Agrappe	3	640	E plateau, taille montante n°3 partant de la Deme	Chaufournoise					Taille		
38	Roberti-Linkermans 1895, ATPB	9 1809/1894		Borinage	Agrappe	3	640	E voie n°7	Chaufournoise					Voie		
39	Roberti-Linkermans 1895, ATPB	8 2509/1894		Borinage	Agrappe	3	640	V taille n°9	Chaufournoise			6		Taille	léger rejet du toit	
40	Roberti-Linkermans 1895, ATPB	9 2809/1894		Borinage	Agrappe	3	640	V voie aérage couchant plateau	Chaufournoise			6		Voie		
41	Roberti-Linkermans 1895, ATPB	10 0609/1894	12,5	Borinage	Agrappe	3	640	V taille couchant plateau	Chaufournoise			50		Taille	renfoncement de 0.3m	
42	Roberti-Linkermans 1895, ATPB	11 3009/1894	9	Borinage	Agrappe	3	640	V voie n°4	Chaufournoise			99		Voie		
43	Roberti-Linkermans 1895, ATPB	12 1809/1894		Borinage	Agrappe	3	640	V tailles 11 et 12bis plateau	Chaufournoise			25		Taille		
44	Roberti-Linkermans 1895, ATPB	13 1809/1894		Borinage	Agrappe	3	640	E levant plateau	Chaufournoise			8		Taille		
45	Roberti-Linkermans 1895, ATPB	14 1002/1894		Borinage	Agrappe	3	640	E taille n°2	Chaufournoise					Taille		
46	Roberti-Linkermans 1895, ATPB	15 3002/1894		Borinage	Agrappe	3	640	V partie sup taille costresse au couchant	Chaufournoise			7		Taille	taille du troussage	

Figure 2.35. Sample of the database for the gas shows record in the Hainaut coal mines.

The number of gas shows in coal mines is considerably greater in the southern part of the mined area relative to its northern part (Figure 2.36). This would indicate that the large E-W extending target area south of the basin has a higher potential for CO₂ storage or ECBM. It is worth noting that most of the “gassy” mines were set in the Masse-Borinage tectonic unit overlying other units (Piessens et al., 2009) and there are uncertainties regarding the actual extent of this unit to the south. However, many gas shows occurred just below the Masse-Borinage unit, where the rocks are known to be extensively fractured over a thickness of tens to hundredths of meters. This heavily-fractured interval, which is called “nappe faillée”, is a geological peculiarity of the Hainaut coal basin. Its origin is still unclear but likely associated with anhydrite dissolution in the underlying Dinantian carbonates. Supporting evidence for this theory is that the “nappe faillée” has a greater thickness where the top Paleozoic surface is depressed, i.e. where it was subjected to higher subsidence rates than in other areas (Delmer, 2004). The “nappe faillée” has a basin-wide extent and lies largely within the suitable depth range for storing CO₂ (700-1300m or deeper). Hence it should be considered as a major prospect for gas production and/or CO₂ storage. The frequent occurrence of free gas is a good indication of either an enhanced porosity/permeability in this horizon and sealing capacity of the bounding formations. However, no reservoir data are available for the “nappe faillée” and hence no attempt was made to take it into account (i.e. an increased porosity and accessibility) in our storage capacity estimation.

Coal sequences are still found underlying the "nappe faillée" at depth exceeding 1200 m. They were subjected to restricted mining activities. Seismic surveys in the North of France strongly suggest that these deep coal units extent at least kilometers southwards. They too should be considered as a major prospect for CCS. Tectonic deformation is minimal in these units which belong to the para-autochthonous basement. This would facilitate injection operations within localized horizons (coal seams and/or sandstones bodies) in comparison to overlying units where the strata are much more disturbed. Their structure consists of a series of hectometric to kilometric-wide tilted blocks that are bounded by highly-dipping thrust faults ("massifs imbriqués"). This would limit the lateral migration of the injected CO₂ since the formation probability of sealing contacts due to faulting is very high (ca. 80 vol% of shales, the least permeable lithology in the coal sequence). Most of the target areas in this unit are underlying the Ardennes overthrust, for which virtually no reliable geological data are available. However, the Belcorp seismic survey (Bouckaert et al., 1988) provides a good indication on the continuity of coal sequences to the south (see Figure 2.40). Future exploration should focus on this region which extends from the Midi fault outcrop southwards to the French border.

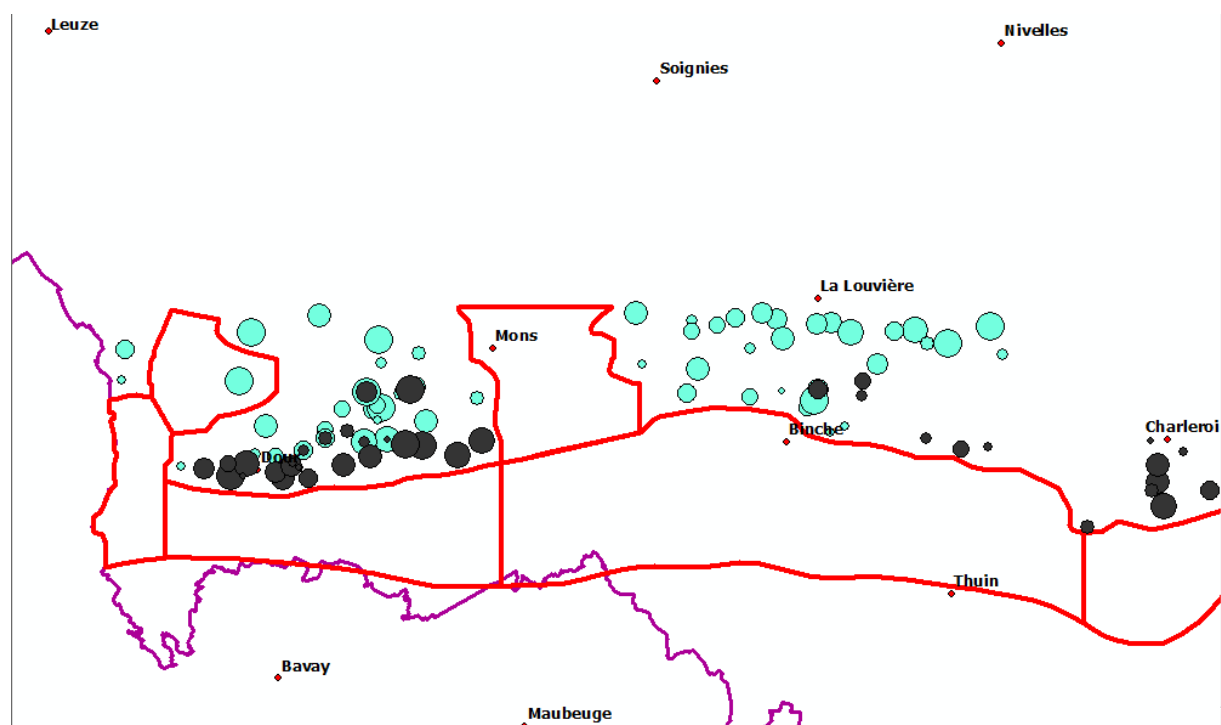


Figure 2.36. Example output for the gas shows and mine water database in the Hainaut coal mines. The total number of gas shows is plotted as dark disks with their diameter proportional to the number of shows. For the mine water, the pumping rate is plotted in light blue. The red polygons delineate the target areas for CO₂ storage in coal sequences. This map shows that the southern region of the coal basin has a greater gas content and/or permeability than the northern region.

Mine water data consist of pumping rates in the mines while they were operating. These data have less significance for CO₂- or gas-related projects since most of the water flows in the Hainaut coal mines originated from the overlying aquifers, not from the coal sequence itself, which was reputed "dry" in the Hainaut basin.

The geological data set in the GIS includes surface geology from geological maps and available compiled data on deep geology such as boreholes, top Paleozoic basement and the Ardennes overthrust (Figure 2.37). The top Paleozoic basement is not shown for the eastern part of the basin as it is outcropping in most of the area (data digitized from Delmer & Van Wichelen, 1980). Its very irregular topography is due to differential subsidence processes created by deep (>2500 m) solution in the anhydrite-bearing limestone sequence in the Lower Carboniferous (i.e. which underlies the coal sequences). These solution processes resulted in a series of collapse structures that formed at different scales: sinkholes (hm scale), subsidence centres (km scale) and a large depression at basin-wide scale. The deformation visible in Figure 2.37 is due to subsidence centres and is accompanied by downwarping of the overlying Cretaceous strata. The lower Ardennes overthrust, which is composed of Lower Devonian siliciclastics, has a smoother topography although it was subjected to similar but seemingly less intense solution-collapse deformations. Considering both the Cretaceous strata and the Lower Devonian overthrust as a (uppermost) caprock, the conclusion from the observation of these topographical data is that there is little chance to find anticline (dome-shaped) structural traps. However, as pointed out in the (Piessens et al., 2009), storing CO₂ in the coal sequences should rely first in the sealing capacity of the interbedded shales, which make up to 80 vol. % of the Westphalian strata. Thus, to our sense, the requirement for a "younger" sedimentary caprock overlying the reservoir, as reported in many classical storing schemes, is of secondary importance.

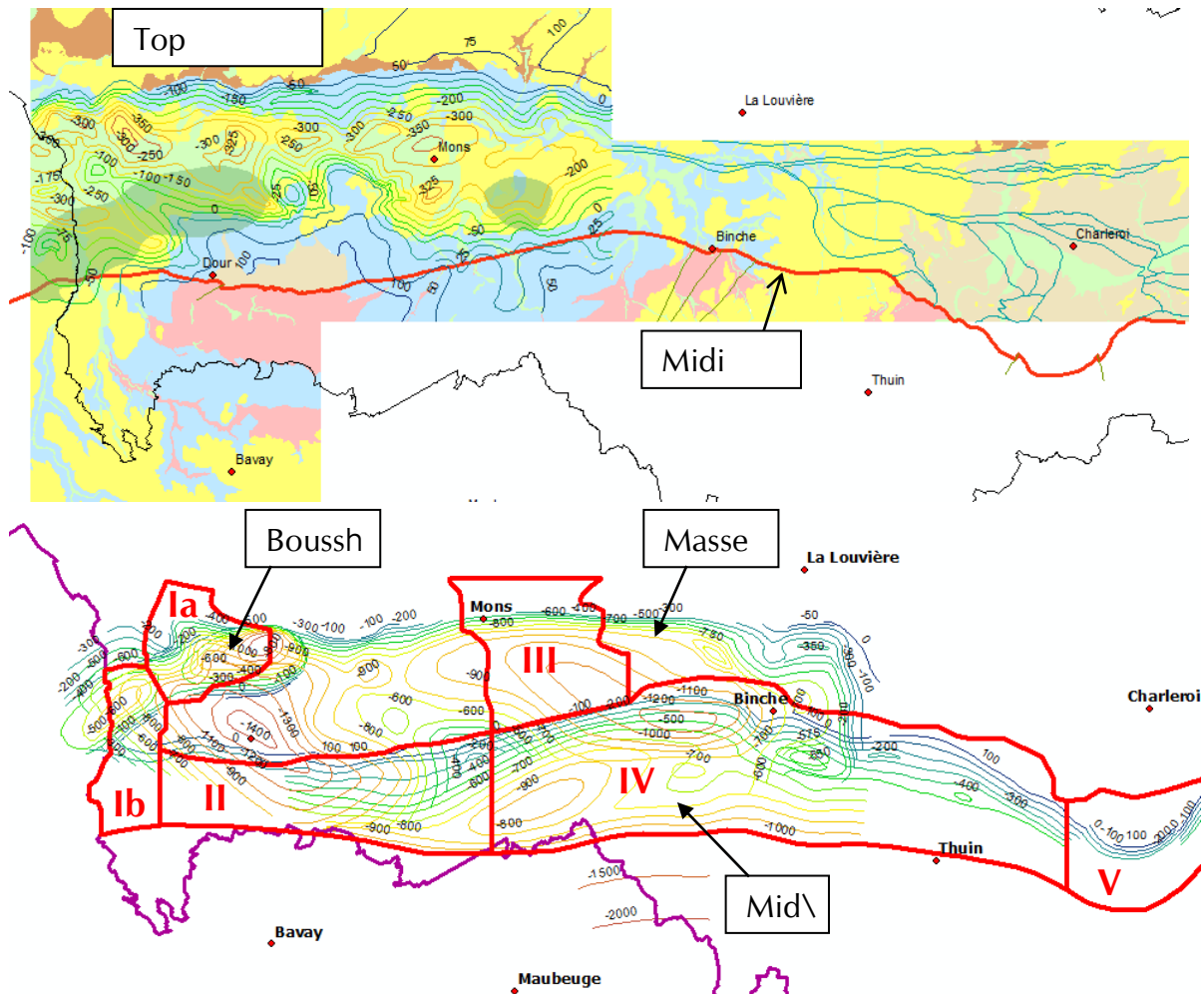


Figure 2.37. Topography of the top Paleozoic surface in the Hainaut basin (upper map) and of major fault surfaces (lower map). The red line in the upper map is the Midi fault outcrop. In the lower map, three fault surfaces are shown (from north to south): the Boussu fault and the Masse fault, and the Midi fault (to the south). The areas delineated by red lines and labeled are the different target areas for storing CO₂ (see Piessens et al., 2009 for details). Map width is ca. 60 km.

The Hainaut Paleozoic basin has specific geological features, most of which are due to the above-mentioned deep solution processes.

Sinkholes are the smallest-scale deformation structures induced by these processes. They consist of hectometric-wide pipes infilled with collapsed (brecciated) material originating from the overlying rocks (i.e. mostly Westphalian rocks). Their vertical extent ranges from several hundredths of meters to a few kilometers. A number of them reached the top Paleozoic surface. There is no clear indication in the mine records that the sinkholes have represented a particular hazard for mining activities. There were apparently no systematic major gas shows or floods when the miners breached them. But this may be biased by some lack of observation in the mine record. Over a total number of 139 known sinkholes (Figure 2.38), one was subjected to a gas show when it was breached, six to water flood and five behaved almost like the undisturbed surrounding rocks. There is unfortunately no information for the rest of the sinkholes (n=127). It is likely, however, that the occurrence of significant gas or water shows would have left more traces in the mine record than actually observed. One could indeed argue that the predominantly shaly infill would make these pipes rather compact and impervious and that they may therefore constitute only reservoirs of extremely limited capacity. However, a number of observations show that mineral deposits such as sulphides (pyrite) and carbonates often occur within the sinkholes and over a significant distance in the surrounding rocks. This indicates that sinkholes have been subjected to significant fluid flow and that they could constitute leakage pathways of possible importance for long-term CO₂ storage. That is why entries for these sinkholes were included in the GIS database (location, diameter, known depth, infill, gas or water shows, etc.). From the mapping in Figure 2.38 it can be seen that sinkholes are less abundant to the south of the Hainaut basin. This would make the large target area in the south safer regarding CCS if hazard associated with the presence of sinkholes is established.

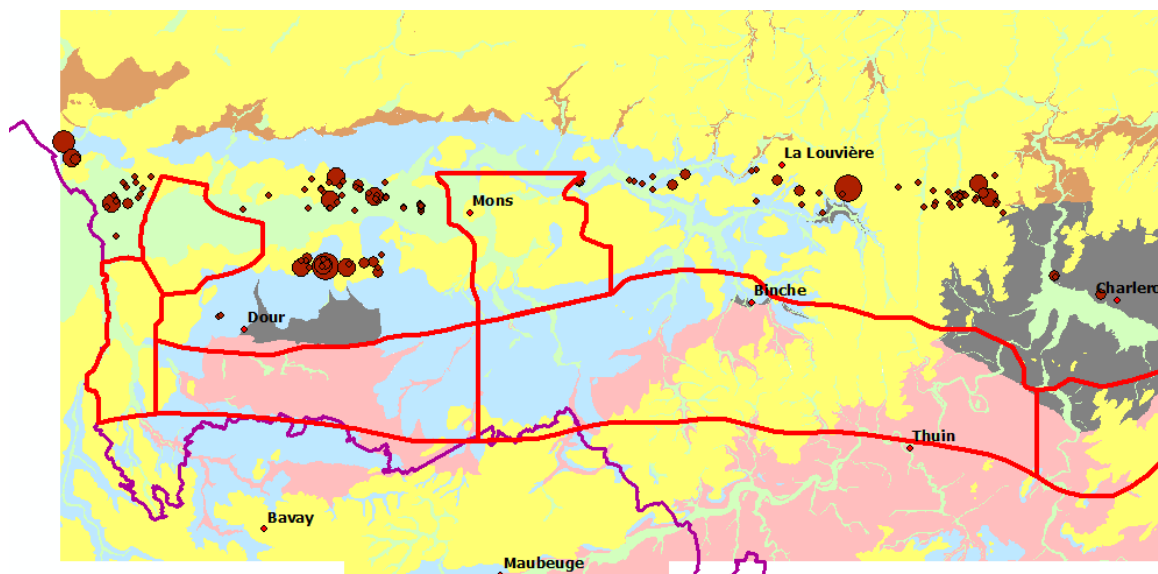


Figure 2.38. Distribution of the known sinkholes in the Hainaut basin (red circles). The diameter of the symbols is proportional to that of the sinkholes. Map width is ca. 60 km.

To conclude, most of the geological and anthropogenic factors that are relevant for site selection for storing CO₂ and associated techniques (ECBM, ...) in the Walloon Region, including the most prospective horizons and key-elements for risk assessment (leakage risk) were implemented in the GIS database.

2.2.4.2. Storage capacities

A methodology for estimating storage capacities in coal seams and mines has been developed in the PSS-CCS I project (Piessens et al., 2009). The approach was based on a comprehensive estimation of the contribution of all the potentially storing lithologies in the coal sequence: coal, sandstone and shales. The figures for base cases are a storage capacity lying between 1 and 1,5 MtCO₂/km² with more than 400 km² of potential reservoir surface area, which makes a total of 500 to 700 MtCO₂ that could be sequestered in coal sequences (plus a few tens of Mt in three selected coal mines).

Analysis of the result showed that 1) the storage capacity of coal alone is low compared to other lithologies (much less than 50%) and 2) capacity figures are varying dramatically with certain parameters that are difficult to estimate such as accessibility, i.e. the portion of the reservoir which effectively contributes to the storage.

The effect of other parameters such as mineral trapping in sandstone and shales was neglected due to a lack of data for the Hainaut basin. Mineral trapping in siliciclastics (sandstones and siltstones) was investigated, suggesting that this process has a storage capacity twice that in porosity (Dupont & Baele, 2009). Therefore, all the CO₂ that is injected in sandstone porosity could be trapped on the long-term by dissolution/precipitation. Attention was subsequently paid to shales, the far more dominant lithology (Reumont, 2011). The results show that the storage capacity of shales which was retained for the base case, i.e. 10 kg CO₂ per ton, is likely to be underestimated. This 10 kg CO₂ per ton capacity was deduced from sorption experiments in the Thermodynamic laboratory at UMons and is consistent with measurements on German shales from similar geological age and environment (Busch et al., 2008). A theoretical capacity lying between 50 and 80 kgCO₂/t can be obtained based on a detailed mineralogical analysis of representative shale samples from the Hainaut basin and the empirical storage capacity for the different minerals published by Xu et al. (2004).

Using this value and applying the same accessibility factor (1%) as for storage in porosity ($\phi = 0.05\%$) triples the total storage capacity (Figure 2.39). An experimental work in a closed-system reactor simulating storage conditions at 1000 m (45°C – 100 bars) showed that dissolved species (Ca²⁺, Mg²⁺, SO₄⁼) and precipitates (mainly iron oxide) can be detected in a CO₂-H₂O mixture after 3 months of soaking period. Note that the shale sample was not ground to increase its reactivity but consists in a single chip of ca. 1 cm³. Dissolution of iron and magnesium carbonate (ankerite and siderite) was also detected by powder XRD of the shale sample. A longer soaking period should be used for quantifying the dissolution and precipitation products and for detecting other reactions such as chlorite and feldspar dissolution. In flushing experiments (e.g. Bertier et al., 2005), reactions should also be accelerated as reactants are replenished continuously.

These results show that although solution and mineral trapping are the slowest trapping mechanisms, their effects can be detected in a few months under experimental conditions where reactivity is not artificially increased (closed system, no grinding of the sample). However, the time needed to have complete reaction is not known yet and, at the moment, the storage capacity of our shales (50 kgCO₂/t) should be considered for long-term storage only. Even in this case, the result is promising as the contribution of shales to the storage greatly exceeds that of coal and sandstones together (Figure 2.39). Shales are thus capable of trapping the CO₂ that would escape from the coal seams or sandstone bodies used for injection or from unexpected, cross-cutting fractures caused by fracturing.

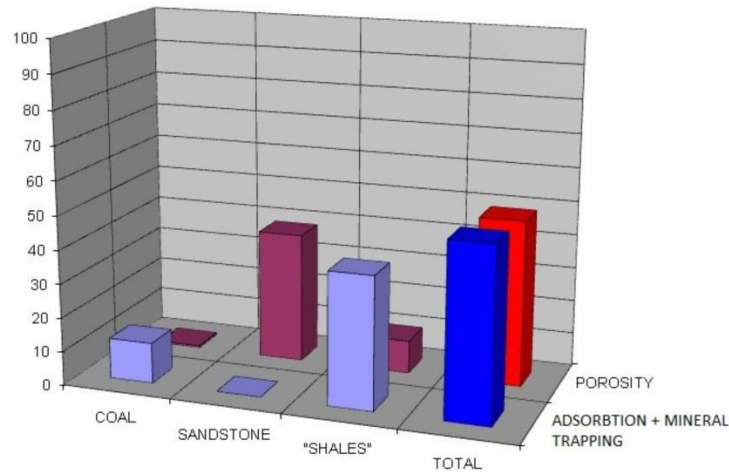
2.2.4.3. Injectivity and injection strategies

Injectivity in sandstones was estimated using the theoretical radial-flow model (Dupont & Baele, 2009). Taking into account realistic variations in reservoir properties, injectivity values between 0.1 and 10 MtCO₂/year were obtained for a typical sandstone formation of 10 m thick. Although there is a two-order of magnitude variations in this estimate, annual emissions from many common industrial plants such as power plants, cement factories, etc. lie in between.

Injectivity was not assessed for coal due to the lack of knowledge of its flowing properties, especially the effect of swelling, which dramatically reduces permeability as CO₂ becomes adsorbed. Inversely, the evolution of reservoir properties as injection proceeds would be positive in the case of sandstone since dissolution of minerals in the vicinity of the injection point will create additional porosity. It was estimated based on detailed mineralogical analysis that this porosity increase would be 50% due to dissolution of carbonate minerals alone. Injection operations could benefit from this process during their lifetime since batch experiments show that carbonate minerals are the first to dissolve in the presence of CO₂-H₂O. However, the actual effects of these reactions on permeability remain to be investigated at sample but also field scale.

Injectivity was not assessed for shales either due to the same reasons. In addition, bulk flow in shale would be extremely reduced due to the very low permeability of the clay matrix. Flow would concentrate into (induced?) fractures instead and assessing this necessitates well data that are not available for the Hainaut coal basin.

**CO₂ STORAGE IN THE HAINAUT SILESIAN :
RELATIVE CONTRIBUTION OF LITHOLOGIES
AND STORAGE PROCESSES**

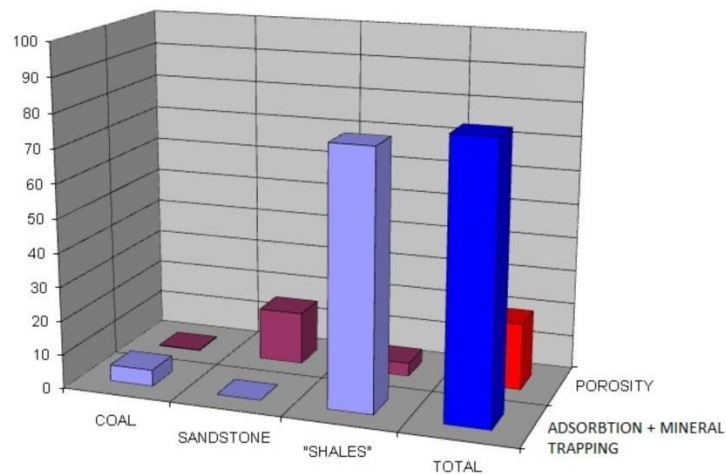


PARAMETERS:

COAL ADS: 60 - 80 - 100 kg/t
 COAL GIP: 15 - 20 - 25 Nm³/t
 COAL ACCESS: 0,2 - 0,4
 SANDSTONE PHI: 1 - 2%
 SANDSTONE ACCES: 0,4 - 0,6
 SHALES ADS: **10 kg/t**
 SHALES PHI: 0,05 %
 SHALES ACCES: 0,01

Total capacity for the 700-1300m depth range:

1.18 MtCO₂/km²



PARAMETERS:

COAL ADS: 60 - 80 - 100 kg/t
 COAL GIP: 15 - 20 - 25 Nm³/t
 COAL ACCESS: 0,2 - 0,4
 SANDSTONE PHI: 1 - 2%
 SANDSTONE ACCES: 0,4 - 0,6
 SHALES ADS: **50 kg/t**
 SHALES PHI: 0,05 %
 SHALES ACCES: 0,01

Total capacity for the 700-1300m depth range:

3.89 MtCO₂/km²

Figure 2.39. Storage capacity estimates using different mineral trapping capacities for the shales in the Hainaut coal basin. The upper graph shows the base case used in previous estimations, with 10 kgCO₂/t, and the lower graph, the theoretical case, with 50 kgCO₂/t. The effect on the total storage capacity is important but should be used only for long-term assessment. It can be seen that shales are capable of trapping more than all the CO₂ that could be injected in coal and sandstone together.

Different injection strategies can be drawn for the Walloon coal basin. Each of the three main lithologies: shales, sandstones and coal, has its own reservoir properties and pros and cons regarding CO₂ storage (Table 2.IV). Shales have the highest capacity on the long-term, mainly by mineral trapping, but the lowest on the short-term due to their very low porosity and permeability (injectivity would be very low as well). Sandstones have the highest short-term capacity and injectivity owing to their substantially better reservoir properties. Coal has rather poor reservoir properties. The long-term storage capacity should be appreciable due to the efficient adsorption process. Adsorption is here ranked as a long-term process but it could be mid-term. The Movecbm project³ showed that it is very difficult to find evidence of in-depth adsorption of the injected CO₂ in the coal matrix at field scale (it is likely that, on the short-term, adsorption is restricted to the external surface of the coal). However, storing CO₂ in coal has the advantage of releasing CH₄, which can be a valuable by-production (ECBM).

Table 2.IV. Ranking of the different trapping lithologies in the Walloon coal basin in terms of capacity and injectivity (the typical abundance in the Walloon basin is indicated in volume percent). Short-term capacity refers to storage in porosity whereas long-term capacity includes slower trapping processes such as adsorption, dissolution and mineral precipitation.

Lithology	Short-term capacity	Long-term capacity	Injectivity
Shales (~ 80%)	- -	+ +	- -
Sandstones (~ 20%)	+	+	+
Coal (1-5%)	-	+	-

The best injection strategy would be to use the sandstone as both reservoirs and conduits for an enhanced CO₂ flow into the other lithologies. Sandstone layers are usually thick (up to 40 m) and this would limit slanted and in-seam drilling. Additional flexibility is brought by the occurrence of different coal units with different structures and reservoir properties in the Hainaut basin. "Conventional", flat-lying coal sequences can be found in the deepest part of the basin. In shallower (but still suitable for CO₂ storage) depth, the extensive "nappe faillée" might provide a better reservoir in terms of flow properties along with an efficient sealing caprock (provided by the overlying coal sequence). Note that gas could still be produced in this scenario.

³ <http://www.movecbm.eu/>

2.2.5. Aquifers in the Hainaut Basin

2.2.5.1. Capacity

The Dinantian aquifer was identified as the main aquifer target for storing CO₂ in the RW and a preliminary assessment of its storage capacity has been undertaken (Piessens et al., 2009).

Geological data concerning this aquifer is very scarce and many uncertainties will remain until new seismic and/or coring data will be available. Note that reprocessing of previous seismic data could slightly improve the situation as shown by Eggermont (2010) on the "H1" seismic line crossing the Saint-Ghislain Borehole (Dejonghe et al., 1992). This line does not bring much geological information due to its location and length (only 3 km) but it was intentionally chosen as close as possible to the Saint-Ghislain borehole for calibration purposes. However, in the course of PSS-CCS II, more efforts were placed in the analysis of available seismic and borehole data for refining the storage assessment figures. Seismic data include the Belcorp (Bouckaert et al., 1988) and the M146 (Lacquement, 1997) lines. Borehole data include the Saint-Ghislain, Douvrain and Ghlin boreholes (Groessens et al., 1979; Leclerq, 1980 & Delmer et al., 1982, respectively) and the Jeumont-Marpent borehole (COPESEP, 1965).

The Dinantian aquifer is largely outcropping north of the Hainaut (including in the Tournaisis and the south Brabant regions) where it reaches 2000 to 3000 m in thickness. This formation is dipping southwards attaining a depth of 2500 m right below the Midi fault outcrop. The dip angle decreases southwards and strata are almost flat-lying 2 km from the outcrop. This situation is well depicted in the Belcorp seismic line (Figure 2.40) where the underlying Givetian limestone is well-marked by a strong reflector (as it is in the M146 line - see Figure 2.34 for its location). The Jeumont borehole provide valuable data of the aquifer but unfortunately no comprehensive reservoir characteristics (logs). The Dinantian in this borehole has a thickness of ca. 500 m and is composed of limestones, dolostones and brecciated horizons (which produced water). Porosities ranges from ~5 to ~8% in limestones and dolostones, respectively (we will however consider much lower porosities for the estimation). This aquifer can be traced northwards over more than 10 km until the seismic section is blurred probably due to the presence of a dense mine network in the overlying coal sequences. The aquifer is known a few kilometers northwards, where it was cored by the Saint-Ghislain exploration project. The Dinantian formation in this borehole has considerably gained in thickness (2000 to 3000 m) which is consistent with that of the coeval outcropping rocks (with the notable exception that thick evaporite beds occur in the Saint-Ghislain borehole).

The considerable thickness change over only a few km in distance remains unexplained. Among other explanations, a tectonic structure such as a synsedimentary fault (or several of them) might be responsible for it. This is of particular importance for CO₂ storage projects since faults (or other geological structures) may dramatically affect the lateral sealing properties of the formation. This aspect needs further research.

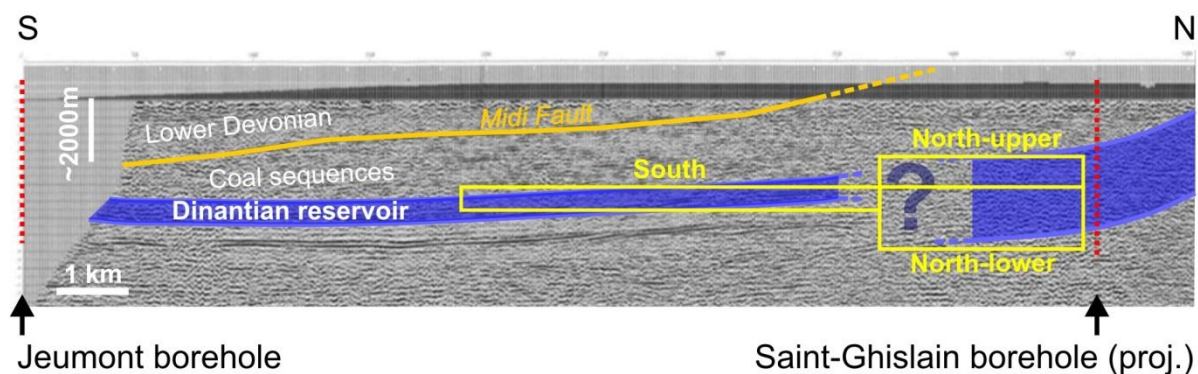


Figure 2.40. Location of the Dinantian reservoir and its compartments (in yellow) selected for CO₂ storage on the Belcorp seismic cross-section (the NE-SW Belcorp seismic line is shown in blue in Figure 2.34). The approximate depth is shown to the left. The Dinantian aquifer is shown in shaded blue and the underlying Devonian (Givetian) is visible on the left part of the section (dark reflector). The location of the southern Dinantian aquifer is based on seismic data (Belcorp, M146) and the Jeumont Borehole (shown to the left in dotted red). Data from the Saint-Ghislain borehole and from outcrops were used for its northern part (to the right). The question mark lies in a region where seismic data are blurred, making unclear the connection between the two parts of the aquifer (which show a very different thickness).

The Saint-Ghislain borehole shows that the Dinantian aquifer may be divided into two units.

The Upper unit which is ~1000 m thick and is very heterogeneous as it shows an alternation of permeable (brecciated/karstified rocks) and impermeable (anhydrite, compact limestones) horizons. The main geothermal productive horizon lies in this upper unit.

The lower unit has a thickness of ~1500 m and is much more homogeneous. The lithologies in this unit are dominated by massive dolostones. A detailed analysis of the neutron-porosity log shows that porosities are indeed highly variable in the upper unit : from 0 to more than 10%, with an average of 2,5%, and much more constant in the lower unit : from 1 to 4% - 1,5% in average (we will retain this lower porosity value for the estimation in the south aquifer).

The estimated capacity calculated using the classical methodology (accessible reservoir volume multiplied by porosity and CO₂ density) yields figures that are lower than previous estimations but still relevant for industrial applications (Table 2.V). The south reservoir unit alone can provide 200 Mt storage capacity. This unit may be considered as the safest relative to the others due its structure (flat-lying aquifer), depth and distance from the outcrops to the north. It is important to investigate aspects regarding flow in this reservoir including the potential of hydrodynamic or structural trapping.

Table 2.V. Approximated reservoir parameters for the three units selected in the Hainaut Dinantian aquifer. Even the « safer » reservoir (south) alone yields a significant storage capacity.

Reservoir	North-Upper	North-Lower	South
Thickness (m)	1000	1500	500
Top depth (m)	2000	3000	3000
Porosity (%)	2,5	1,5	1,5
Surface (km ²)	450	450	> 300
Capacity (MtCO ₂)	~ 300	300	> 200

2.2.5.2. Injectivity

The theoretical injectivity can be calculated using the radial-flow approach (Gaussens, 1986). A series of assumptions have to be made: homogeneous and isotropic infinite aquifer, steady injection, flow under Darcy conditions and no change in pressure. A key parameter in the calculation is the permeability, which is not known for each formation. However, transmissivity values are available from the geothermal production history at Saint-Ghislain (well tests, which yielded 7 to 9.10⁻⁴ m²/s). A minimum permeability of 10 to 15 mD may thus be assigned to most of the Dinantian reservoir (this figure is consistent with other similar carbonate aquifers).

Injectivity was found to be ca. 4 to 5 MtCO₂/y, which falls within the range of emission rate from many industrial plants.

2.2.6. Monitoring of gas leakage from coal strata

2.2.6.1. Introduction

Monitoring the fate of CO₂ during and after injection into the subsurface is a prerequisite to ensure containment and safe operation. There are many phases and aspects of monitoring during the life-cycle of a storage project. The guidance documents 1, 2 and 3 (EC, 2011a, b & c) to the EU CCS Directive (Directive 2009/31/EC) distinguishes 6 phases separated by clear milestones (Figure 2.41). Monitoring is involved from the pre-operational stage through the post-transfer, albeit in different ways.

Depending on the development stage, the focuses of the monitoring may be different and other techniques can be required. In general, three main groups of techniques, each comprising multiple technical solutions, can be distinguished according to the target:

- » Atmospheric techniques
 - » CO₂ detectors
 - » Remote sensing techniques
- » Near-surface monitoring
 - » Tracers (best way to follow hydrology)
 - » Remote: thermal hyperspectral imaging
 - » Tiltmeter
 - » Flux measurements
- » Sub-surface monitoring
 - » Seismic techniques (surface survey, VSP, CSP, passive)
 - » Non-seismic well-logging (e.g. EMR, gravity)
 - » Well monitoring (well-head + down-hole: e.g. annulus P-tests,...)
 - » Aqueous geochemistry
 - » Tracers + periodic sampling at control wells

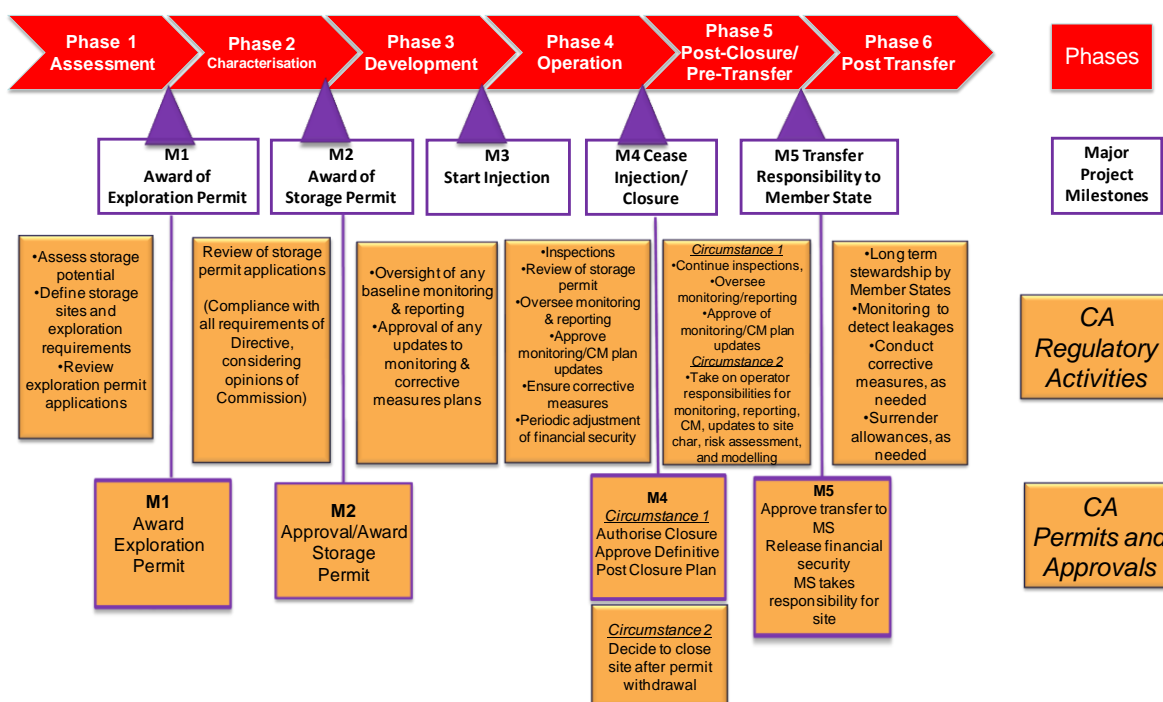


Figure 2.41. Summary of the CO₂ storage life-cycle phases and milestones from Guideline Document 1 to the EU CCS-directive (EC, 2011a).

In the following sections, first an overview of currently available monitoring tools is given with their remaining challenges for development and then an evaluation of the effectiveness to answer monitoring needs in coal is presented.

2.2.6.2. Overview of available monitoring techniques

A quite complete and comprehensive overview of presently available (or under development) monitoring techniques is given by NETL (2009) in their best practice guide for monitoring CO₂ storage. The summary lists of techniques available for monitoring at surface, near the surface in the soil and in the subsurface are given below in Table 2.VI to Table 2.VIII. Some techniques have been highlighted in grey to indicate what techniques would be most useful for the Belgian storage options. Note, however, that the focus of the NETL guide is on saline aquifers, because info on coal and especially ECBM field evidence is scarce.

The overview list from the EU CCS directive is presented in Table 2.IX.

In addition, the IEAGHG has developed a user-friendly monitoring selection tool (<http://www.ieaghg.org/index.php?/20091223131/monitoring-a-selection-tool.html>) that helps users to set up a monitoring protocol for a defined CO₂ storage project. It is a decision support tool and not prescriptive. It works well for large and simple storage projects, but cannot take into account challenges related to geological complexity and related specific resolution problems.

Table 2.VI. Proposed atmospheric monitoring methods for gas storage projects; from NETL (2009).

Atmospheric Monitoring Techniques	
Monitoring Technique	Description, Benefits, and Challenges
CO₂ Detectors	<i>Description:</i> Sensors for monitoring CO ₂ either intermittently or continuously in air.
	<i>Benefits:</i> Relatively inexpensive and portable. Mature and new technologies represented.
	<i>Challenges:</i> Detect leakage above ambient CO ₂ emissions (signal to noise).
Eddy Covariance	<i>Description:</i> Atmospheric flux measurement technique to measure atmospheric CO ₂ concentrations at a height above the ground surface.
	<i>Benefits:</i> Mature technology that can provide accurate data under continuous operation.
	<i>Challenges:</i> Very specialized equipment and robust data processing required. Signal to noise.
Advanced Leak Detection System	<i>Description:</i> A sensitive three-gas detector (CH ₄ , Total HC, and CO ₂) with a GPS mapping system carried by aircraft or terrestrial vehicles.
	<i>Benefits:</i> Good for quantification of CO ₂ fluxes from the soil.
	<i>Challenges:</i> Null result if no CO ₂ .
Laser Systems and LIDAR	<i>Description:</i> Open-path device that uses a laser to shine a beam – with a wavelength that CO ₂ absorbs – over many meters.
	<i>Benefits:</i> Highly accurate technique with large spatial range. Non-intrusive method of data collection over a large area in a short timeframe.
	<i>Challenges:</i> Needs favorable weather conditions. Interference from vegetation, requires time laps Signal to noise.
Tracers (Isotopes)	<i>Description:</i> Natural isotopic composition and/or compounds injected into the target formation along with the CO ₂ .
	<i>Benefits:</i> Used to determine the flow direction and early leak detection.
	<i>Challenges:</i> Samples need analyzed offsite if project team does not have the proper analytical equipment.

Table 2.VII. Proposed near-surface monitoring methods for gas storage projects (source: NETL, DOE).

Near-Surface Monitoring	
Monitoring Technique	Description, Benefits, and Challenges
Ecosystem Stress Monitoring	<i>Description:</i> Satellite or airplane-based optical method.
	<i>Benefits:</i> Easy and effective reconnaissance method.
	<i>Challenges:</i> Detection only after emission has occurred. Quantification of leakage rates difficult. Changes not related to CCS lead to false positives. Not all ecosystems equally sensitive to CO ₂ .
Tracers	<i>Description:</i> CO ₂ soluble compounds injected along with the CO ₂ into the target formation
	<i>Benefits:</i> Used to determine the hydrologic properties, flow direction and low-mass leak detection.
	<i>Challenges:</i> Many of the tested CO ₂ -soluble tracers are GHGs, and therefore, add to risk profile.
Groundwater Monitoring	<i>Description:</i> Sampling of water or vadose zone/soil (near surface) for basic chemical analysis.
	<i>Benefits:</i> Mature technology, easier detection than atmospheric. Early detection prior to large emissions.
	<i>Challenges:</i> Significant effort for null result (no CO ₂ leakage). Relatively late detection of leakage.
Thermal Hyperspectral Imaging	<i>Description:</i> An aerial remote-sensing approach primarily for enhanced coalbed methane recovery and sequestration.
	<i>Benefits:</i> Covers large areas; detects CO ₂ and CH ₄ .
	<i>Challenges:</i> Not a great deal of experience with this technique in GS.
Synthetic Aperture Radar (SAR & InSAR)	<i>Description:</i> A satellite-based technology in which radar waves are sent to the ground to detect surface deformation.
	<i>Benefits:</i> Large-scale monitoring (100 km x 100 km).
	<i>Challenges:</i> Best used in environments with minimal topography, minimal vegetation, and minimal land use. Only useful in time-laps.
Color Infrared (CIR) Transparency Films	<i>Description:</i> A vegetative stress technology deployed on satellites or aerially.
	<i>Benefits:</i> Good indicator of vegetative health, which can be an indicator of CO ₂ or

	brine leakage.
	<i>Challenges:</i> Detection only post-leakage. Need for deployment mechanism (i.e. aircraft).
Tiltmeter	<i>Description:</i> Measures small changes in elevation via mapping tilt, either on the surface or in subsurface.
	<i>Benefits:</i> Mature oil field technology for monitoring stream or water injection, CO ₂ flooding and hydrofracturing.
	<i>Challenges:</i> Access to surface and subsurface. Measurements are typically collected remotely.
Flux Accumulation Chamber	<i>Description:</i> Quantifies the CO ₂ flux from the soil, but only from a small, predetermined area.
	<i>Benefits:</i> Technology that can quickly and effectively determine CO ₂ fluxes from the soil at a predetermined area.
	<i>Challenges:</i> Only provides instantaneous measurements in a limited area.
Induced Polarization	<i>Description:</i> Geophysical imaging technology commonly used in conjunction with DC resistivity to distinguish metallic minerals and conductive aquifers from clay minerals in subsurface materials.
	<i>Benefits:</i> Detecting metallic materials in the subsurface with fair ability to distinguish between different types of mineralization. Also a useful technique in clays.
	<i>Challenges:</i> Does not accurately depict non-metallic based materials. Typically used only for characterization.
Spontaneous (Self) Potential	<i>Description:</i> Measurement of natural potential differences resulting from electrochemical reactions in the subsurface. Typically used in groundwater investigations and in geotechnical engineering applications for seepage studies.
	<i>Benefits:</i> Fast and inexpensive method for detecting metal in the near subsurface. Useful in rapid reconnaissance for base metal deposits when used in tandem with EM and geochemical techniques.
	<i>Challenges:</i> Should be used in conjunction with other technologies. Qualitative only.
Soil and Vadose Zone Gas Monitoring	<i>Description:</i> Sampling of gas in vadose zone/soil (near surface) for CO ₂ .
	<i>Benefits:</i> CO ₂ retained in soil gasses provides a longer residence time. Detection of elevated CO ₂ concentrations well above background levels provides indication of leak and migration from the target reservoir.

	<i>Challenges:</i> Significant effort for null result (no CO ₂ leakage). Relatively late detection of leakage.
Shallow 2-D Seismic	<i>Description:</i> Closely spaced geophones along a 2-D seismic line.
	<i>Benefits:</i> Mature technology that can provide high resolution images of the presence of gas phase CO ₂ . Can be used to locate "bright spots" that might indicate gas, also/ used in timelaps.
	<i>Challenges:</i> Semi-quantitative. Cannot be used for mass-balance CO ₂ dissolved or trapped as/mineral not monitored. Out of plane migration not monitored.

Table 2.VIII. Proposed sub-surface monitoring methods for gas storage projects (source: NETL, DOE)

Subsurface Monitoring	
Monitoring Technique	Description, Benefits, and Challenges
Multi-component 3-D Surface Seismic Timelapse Survey	<i>Description:</i> Periodic surface 3-D seismic surveys covering the CCS reservoir.
	<i>Benefits:</i> Mature technology that can provide high-quality information on distribution and migration of CO ₂ . Best technique for map view coverage. Can be used in multi-component form (ex. three, four, or nine component), to account for both compressional waves (P-waves) and shear waves (S-waves).
	<i>Challenges:</i> Semi-quantitative. Cannot be used for mass-balance CO ₂ dissolved or trapped as/mineral not monitored. Signal to noise, not sensitive to concentration. Thin plumes or low CO ₂ concentration may not be detectable.
Vertical Seismic Profile (VSP)	<i>Description:</i> Seismic survey performed in a wellbore with multi-component processes. Can be implemented in a "walk-away" fashion in order to monitor the footprint of the plume as it migrates away from the injection well and in time-lapse application.
	<i>Benefits:</i> Mature technology that can provide robust information on CO ₂ concentration and migration. More resolution than surface seismic by use of a single wellbore. Can be used for calibration of a 2-D or 3-D seismic.
	<i>Challenges:</i> Application limited by geometry surrounding a wellbore.
Magnetotelluric Sounding	<i>Description:</i> Changes in electromagnetic field resulting from variations in electrical properties of CO ₂ and formation fluids.
	<i>Benefits:</i> Can probe the Earth to depths of several tens of kilometers.
	<i>Challenges:</i> Immature technology for monitoring of CO ₂ movement. Relatively low resolution.
Electromagnetic Resistivity	<i>Description:</i> Measures the electrical conductivity of the subsurface including soil, groundwater, and rock.
	<i>Benefits:</i> Rapid data collection.
	<i>Challenges:</i> Strong response to metal. Sensitivity to CO ₂ .
Electromagnetic Induction Tomography (EMIT)	<i>Description:</i> Utilizes differences in how electromagnetic fields are induced within various materials.
	<i>Benefits:</i> Provides greater resolution and petrophysical information than ERT.
	<i>Challenges:</i> Difficult to execute. Requires non-conductive casing downhole to

	obtain high– frequency data. Esoteric technique, not proven for GS.
Injection Well Logging (Wireline Logging)	<i>Description:</i> Wellbore measurement using a rock parameter, such as resistivity or temperature, to monitor fluid composition in wellbore.
	<i>Benefits:</i> Easily deployed technology and very useful for wellbore leakage.
	<i>Challenges:</i> Area of investigation limited to immediate wellbore. Sensitivity of tool to fluid change.
Annulus Pressure Monitoring	<i>Description:</i> A mechanical integrity test on the annular volume of a well to detect leakage from the casing, packer or tubing. Can be done constantly.
	<i>Benefits:</i> Reliable test with simple equipment. Engineered components are known to be areas of high frequency.
	<i>Challenges:</i> Periodic mechanical integrity testing requires stopping the injection process during testing. Limited to constructed system.
Pulsed Neutron Capture	<i>Description:</i> A wireline tool capable of depicting oil saturation, lithology, porosity, oil, gas, and water by implementing pulsed neutron techniques.
	<i>Benefits:</i> High resolution tool for identifying specific geologic parameters around the well casing. Most quantitative to CO ₂ saturation in time-lapse.
	<i>Challenges:</i> Geologic characteristics identified only in the vicinity of the wellbore. Not sensitive to dissolution trapped and mineral trapped CO ₂ . Sensitive to borehole conditions, fluid invasion because of workover. Decreased sensitivity in lower salinity water, at low saturation.
Electrical Resistance Tomography (ERT)	<i>Description:</i> Use of vertical arrays of electrodes in two or more wells to monitor CO ₂ as a result of changes in layer resistivity.
	<i>Benefits:</i> Potential high resolution technique to monitor CO ₂ movement between wells.
	<i>Challenges:</i> Immature technology for monitoring of CO ₂ movement. Processes such as massbalance and dissolution/mineral trapping difficult to interpret. Poor resolution and limited testing in GS applications.
Sonic (Acoustic) Logging	<i>Description:</i> A wireline log used to characterize lithology, determine porosity, and travel time of the reservoir rock.
	<i>Benefits:</i> Oil field technology that provides high resolution. Can be used to time seismic sections.
	<i>Challenges:</i> Does not yield data on hydraulic seal. May have to make slight corrects for borehole eccentricity. Not a “stand alone” technology. Should be used in conjunction with other techniques.

2-D Seismic Survey	<i>Description:</i> Acoustic energy, delivered by explosive charges or vibroseis trucks (at the surface) is reflecting back to a straight line of recorders (geophones). After processing, the reflected acoustic signature of various lithologies is presented as a 2-D graphical display.
	<i>Benefits:</i> Can be used to monitor "bright spots" of CO ₂ in the subsurface. Excellent for shallow plumes as resolution decreases with depth.
	<i>Challenges:</i> Coverage limited to lines.
Time-lapse Gravity	<i>Description:</i> Use of gravity to monitor changes in density of fluid resulting from injection of CO ₂ .
	<i>Benefits:</i> Effective technology.
	<i>Challenges:</i> Limited detection and resolution unless gravimeters are located just above reservoir, which significantly increases cost. Sensitivity.
Density Logging (RHOB Log)	<i>Description:</i> Continuous record of a formation bulk density as a function of depth by accounting for both the density of matrix and density of liquid in the pore space.
	<i>Benefits:</i> Effective technology that can estimate formation density and porosity at varying depths.
	<i>Challenges:</i> Lower resolution log compared to other wireline methods.
Optical Logging	<i>Description:</i> Device equipped with optical imaging tools is lowered down the length of the wellbore to provide detailed digital images of the well casing.
	<i>Benefits:</i> Simple and cheap technology that provides qualitative well integrity verification at depth.
	<i>Challenges:</i> Does not provide information beyond what is visible inside the well casing.
Cement Bond Log (Ultrasonic Well Logging)	<i>Description:</i> Implement sonic attenuation and travel time to determine whether casing is cemented or free. The more cement which is bonded to casing, the greater will be the attenuation of sounds transmitted along the casing. Used to evaluate the integrity of the casing cement and assessing the possibility of flow outside of casing.
	<i>Benefits:</i> Evaluation of quality of engineered well system prior to leakage, allows for proactive remediation of engineered system. Indicates top of cement, free pipe, and gives an indication of well cemented pipe. Authorized as an MIT tool for the demonstration of external integrity of injection wells.
	<i>Challenges:</i> Good centralization is important for meaningful and repeatable cement bond logs. Cement bond logs should not be relied on for a quantitative evaluation of zonal isolation or hydraulic integrity. The cement should be allowed to cure for

	at least 72 hours before logging.
Gamma Ray Logging	<i>Description:</i> Use of natural gamma radiation to characterize the rock or sediment in a borehole.
	<i>Benefits:</i> Common and inexpensive measurement of the natural emission of gamma rays by a formation.
	<i>Challenges:</i> Subject to error when a large proportion of the gamma ray radioactivity originates from the sand-sized detrital fraction of the rock. Limited to site characterization phase.
Microseismic (Passive) Survey	<i>Description:</i> Provides real-time information on hydraulic and geomechanical processes taking place within the reservoir in the interwell region, remote from wellbores by implementing surface or subsurface geophones to monitor earth movement.
	<i>Benefits:</i> Technology with broad area of investigation that can provide provides high-quality, high resolution subsurface characterization data and can provide effects of subsurface injection on geologic processes.
	<i>Challenges:</i> Dependence on secondary reactions from CO ₂ injection, such as fracturing and faulting. Difficult to interpret low rate processes (e.g., dissolution/mineral trapping and slow leakage). Extensive data analysis required.
Crosswell Seismic Survey	<i>Description:</i> Seismic survey between two wellbores in which transmitters and receivers are placed in opposite wells. Enables subsurface characterization between those wells. Can be used for time-lapse studies.
	<i>Benefits:</i> Crosswell seismic profiling provides higher resolution than surface methods, but sample a smaller volume.
	<i>Challenges:</i> Mass-balance and dissolution/mineral trapping difficult to monitor.
Aqueous Geochemistry	<i>Description:</i> Chemical measurement of saline brine in storage reservoir.
	<i>Benefits:</i> Coupled with repeat analyses during and after CO ₂ injection can provide massbalance and dissolution/mineral trapping information.
	<i>Challenges:</i> Cannot image CO ₂ migration and leakage directly. Only near-well fluids are measured.
Resistivity Log	<i>Description:</i> Log of the resistivity of the formation, expressed in ohm-m, to characterize the fluids and rock or sediment in a borehole.
	<i>Benefits:</i> Used for characterization, also sensitive to changes in fluids.
	<i>Challenges:</i> Resistivity can only be measured in open hole or non-conductive casing.

Table 2.IX. Summary of possible monitoring methods and applicability; from EC (2011b).

Category	Method/Technique	Monitoring Application				Onshore/Offshore		Survey Category	Direct/Indirect
		Oper.	Plume	Path's	Env.	On	Off		
Operational measurement (Wellhead and Downhole)	Wellhead Pressure and Temperature Measurement							Wells	
	Wellhead flow metering & composition							Wells	Direct
	Downhole Pressure and Temperature Measurement							Wells	
Well Logging	Casing and Annulus Pressure							Wells	
	Injection Well Logging (Wireline Logging)							Wells	
	Sonic (Acoustic) Logging							Wells	
	Cement Bond Log (Ultrasonic Well Logging)							Wells	
	Pulsed Neutron Capture							Wells	
	Density Logging							Wells	
	Optical Logging							Wells	
	Gamma Ray Logging							Wells	
Well CO2 Sampling	Resistivity Log							Wells	
	Well sampling & chemical analysis							Wells	Direct
Seismic	Tracers							Wells	Direct
	2-D Seismic Survey							Surface	
	3-D Seismic Multi-component & Timelapse Survey							Surface	
	4-D Seismic Array							Surface	
	Vertical Seismic Profile (VSP)							Wells	
	Cross-Hole Seismic Survey							Wells	
	Microseismic Survey (Passive)							Wells	
Shallow High resolution geophysics	Sidescan sonar							Surface	
	Multibeam echo sounding							Surface	
	Shallow 2-D Seismic							Surface	
	Bubble stream detection (Sonar)							Surface	
	Boomer / sparker profiling							Surface	
	High resolution acoustic imaging							Surface	
Gravity Surveying	Ground penetrating radar							Surface	
	Time-lapse Gravity							Surface	
Electrical and Electromagnetic methods	Well gravimetry							Wells	
	Land electrical and electromagnetic methods						??	Surface	
	Induced Polarization							Surface	
	Spontaneous (Self) Potential							Surface	
	Airborne EM							Airborne	
	Magnetotelluric Sounding						??	Surface	
	Electromagnetic Resistivity							Surface	
	Seabottom electromagnetic (EM)							Surface	
	Permanent borehole Electromagnetic (EM)							Wells	
Cross-hole Electromagnetic (EM)							Wells		
Water Sampling & Geochemistry	Cross-hole Electrical Resistance tomography (ERT)							Wells	
	Seawater geochemistry							Seawater	Direct
	Ground-water Monitoring							Wells/water	Direct
	Downhole fluid chemistry							Wells/water	Direct
Soil/sediment sampling and Geochemistry	Long-term borehole monitoring of pH							Wells/water	Direct
	Seabed sampling & gas analysis							Surface	Direct
Vegetation imaging	Soil and Vadose Zone Gas Monitoring							Near surface	Direct
	Thermal Hyperspectral Imaging (Satellite)							Satellite	
	Thermal Hyperspectral Imaging (airborne)							Airborne	
Land surface deformation	Color Infrared (CIR) Transparency Films							Near surface	
	Satellite interferometry (InSAR)							Satellite	
Atmospheric CO2 Flux and Concentration Monitoring	Tiltmeter							Surface	
	CO2 Detectors							Surface	Direct
	Eddy Covariance							Surface	Direct
	Advanced Leak Detection System							Surface	Direct
	Laser Systems							Surface	Direct
	Tracers (Isotopes) in CO2 Samples							Surface	Direct
	Flux Accumulation Chamber							Surface	Direct
	Bubble stream chemistry							Surface	Direct
	Portable Infrared gas analysers							Surface	Direct
Other	Airborne Laser							Surface	Direct
	Ecosystems monitoring							Surface	

2.2.6.3. Evaluation of some techniques for use in coal series

Although a wide variety of monitoring techniques is available, the applicability of many techniques for CO₂ storage in coal layers is still a challenge. This is due mainly to the thin nature of coal seams, the low injectivity restricting the volume of injected CO₂ and hence the created density contrasts, the presence of CH₄ adsorbed on the coal surface which is replaced by CO₂ (again restricting the density contrast) and the small-scale heterogeneity of the coal sequences. The resolution of most techniques allows use for large-scale storage in saline aquifers or depleted gas fields only. Therefore, the use of some techniques in coal basins is discussed below.

2.2.6.3.1. Seismic techniques

Seismic surveys have become quasi standard for characterizing subsurface reservoirs and probably each CO₂ storage project will need seismic monitoring to verify the containment. Seismic monitoring has the advantage of providing a global overview of the storage site with reservoir, seal and overburden visualized. Repeat time-lapse surveys may display the distribution of the CO₂ plume and furnish information that helps updating reservoir models and monitoring plans. When compared with other geological settings, e.g. depleted oil and gas reservoirs and deep saline aquifers, coalbeds present special challenges and features to exploit in monitoring (Harris et al., 2007).

Coal has the following characteristics complicating the resolution of seismic data (Quan & Harris, 2006; Harris et al., 2007):

- ✓ thin layers
- ✓ low densities and low density change due to CO₂ – CH₄ replacement
- ✓ low seismic wave velocities, changing when gas being added
- ✓ high seismic attenuation (or low Q-values)
- ✓ large contrast vs. surrounding rocks → strong guided waves
- ✓ strong anisotropy (~40%) due to aligned fractures and micro layering

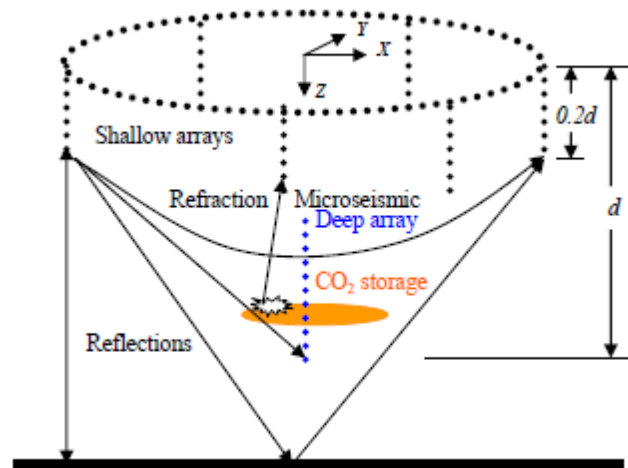


Figure 2.42: Optimal configuration for seismic imaging of shallow coal layers (Harris et al., 2007).

These particular characteristics ask for an appropriate design with an efficient configuration of seismic sources and detectors. Unfortunately, seismic acquisition has not been implemented in the CBM field development and the ECBM pilot test in the USA. In the RECOPOL – MOVECBM pilot in Poland application of seismic techniques showed inconclusive results (van Bergen et al., 2008). Several groups are still working on the optimization of seismic resolution for the ECBM case.

Harris et al. (2007) found that the maximum coverage and highest resolution for a same number of detectors can be achieved (at least for relatively shallow coals) by combining a circular array at surface with vertical arrays placed in boreholes (Figure 2.42). The latter technique where a (deep) vertical array of detectors is placed behind the well casing is called VSP (vertical seismic profiling; Figure 2.43). The optimum depth for the VSP array still needs to be determined and will be a trade-off between image resolution and cost efficiency. When seismic attenuation is measured between different wells it is called cross-well seismic profiling (XSP).

One of the difficulties associated with ECBM is that CO₂ replaces CH₄ in the coal matrix which results in only limited changes in density and hence only small acoustic velocity contrasts. As a result, only large volumes of CO₂ are detectable with time-lapse seismic surveys. The moving fluid front can be followed better in this case by passive seismic reflectivity imaging (monitoring of the microseismic events caused by CO₂ injection).

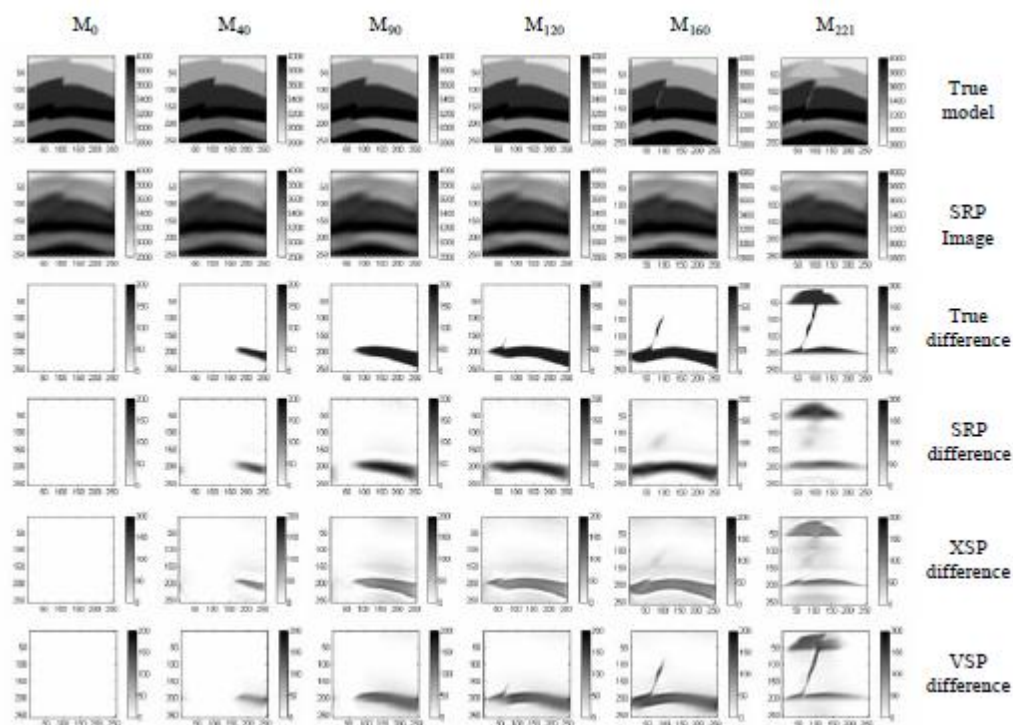


Figure 2.43. Filtered diffraction tomography for surface seismic reflection profiles (SRP), crosswell seismic profiles (XSP) and vertical seismic profiles (VSP) Harris et al. (2007).

As a comparison, the 3D time-lapse seismic monitoring at the Ketzin site (Lüth et al., 2010) showed conclusive results after approximately 25kton CO₂ had been injected (corresponding to about 11 – 21 kton CO₂ in place). Note, however, that this is a CO₂ storage in a saline aquifer at around 650m depth, which allows accumulation of free-phase CO₂ around the injection well increasing the density contrasts much faster than in the coal case. In addition, XSP and VSP were tested and yielded good results at the Ketzin site.

Other projects where seismic monitoring has been tested yield the following detection limits at reservoir depth (note that the resolution is depth-dependent): 10.000 ton CO₂ (Myer et al., 2002), 4.000 ton CO₂ (Sleipner; Arts et al., 2004), 2.500 ton (by 3D multi-component seismic reflection in Weyburn; White et al., 2004) and 1.600 ton CO₂ (by near-continuous VSP and XSP in the Frio Formation; Daley et al., 2005).

Practically, in a coal sequence it is expected that only stacking of CO₂ injection in multiple reservoir layers will give detectable changes.

2.2.6.3.2. Non-seismic well-logging

Gasperikova & Hoversten (2008) studied the spatial resolution and the detectability limits of two promising non-seismic geophysical well logging techniques for CO₂-monitoring in coalbeds:

- » electromagnetic resistivity (EMR): the decrease in brine saturation resulting from CO₂ injection should lead to a change in the EMR
- » gravity: CO₂ injection reduces the bulk density of the coal layer, causing a decrease in gravity response

The results from that study showed that EM and gravity measurements could, under certain circumstances (site-dependent), be used as a lower cost alternative to time-lapse seismic surveys. However, the reduction in cost should be balanced against the reduction in spatial resolution.

In coalbeds, adsorption of CO₂ on the coal matrix affects the bulk density eventually resulting in a density change that is smaller than predicted based on the CO₂ injection volume. For example, the electric field response from an EM survey would not detect 300 ton CO₂ injected into a single coal zone, but the response from injecting a total of 900 ton into three separate zones would be detectable.

In general, the composed signal of many coal zones together should be detectable (~ 1 kton CO₂) and better results are achieved by combining several techniques (e.g. inversion of gravity data combined with seismic monitoring). The analyzed techniques would produce measurable signals for industrial-scale injection.

2.2.6.3.3. Remote sensing techniques

Remote sensing techniques have the advantage of covering wide areas and when combined with local in-situ measurements can become cost-efficient monitoring tools. They eliminate the need of extensive ground-based monitoring infrastructure. The remote sensing methods can be subdivided in direct and indirect detection techniques and the source and/or sensor can be a satellite, an airborne or ground-based device. Direct measuring of CO₂ (and CH₄) in the air can be achieved by detecting the gas concentration between ground and sensor or by detecting the degree of absorption of natural light (light is partly absorbed and reflected through gases resulting in a different re-emitted spectrum). Indirect methods register secondary effects, such as vegetation stress due to increased gas concentrations or temperature differences.

So far the techniques are able to detect larger leaks (or gas pooling in topographically lower areas) only. Improvements are needed, but the potential is high.

Bateson et al. (2008) gives results from a remote sensing monitoring study above a natural analogue with gas vents in Italy. They used multi-/hyper-spectral data, LIDAR and digital imaging. Resolution on this site with the selected techniques can be estimated at a CO₂ flux of about 60 g / m² / d. The methods would work best in areas with low topographic contrasts and short, homogeneous or sparse vegetation.

Jacobson et al. (2007) tested direct CO₂ and CH₄ detection making use of airborne and satellite high resolution multi-spectral imaging. Here, a passive sensor screens for CO₂ and CH₄ absorption above artificially induced leaks.

Another interesting remote sensing study applicable to CO₂ storage in coalbeds can be found in Devleeschouwer et al. (2007; 2008). The authors used Radar interferometry to study ground movements above the abandoned Campine coal mines reflecting mining-induced subsidence and flooding-induced uplift.

2.2.6.3.4. Use of tracers

The use of tracers helps to detect leaks and to reconstruct the hydrogeological behavior of the reservoir. It is one of the best techniques to follow the CO₂ plume in coal beds which is a real challenge with other techniques. ECBM fields have a high density of wells that can be used as monitoring points to check the arrival of the tracer and CO₂.

The advantage of perfluorocarbon tracers (PFT) is that it is a non-toxic, chemically inert and colorless liquid. The SEQUIRE™ PFT tracer technology was developed by the Office of Fossil Energy's National Energy Technology Laboratory for tracking the movement of CO₂ in geological reservoirs and became the 2009 R&D 100 Award winner. Concentrations as small as parts-per-quadrillion can be detected. It was successfully tested in a San Juan Basin coalbed site in New Mexico.

Also in 2009, an ECBM pilot test was performed in the Central Appalachian Basin (Russell County, SECARB pilot) where the use of PFT was tested (Ripepi, 2009). During one month 1000 ton of CO₂ had been injected with addition of the tracer. The test has shown that there is an efficient hydrofracture network between the injection well and the producers. This resulted in the tracer travelling more than 1 km far (Figure 2.44) and early CO₂ breakthrough in closest wells, although this was not sustained. Since the PFC tracer is a larger molecule than CO₂ it has less tendency to adsorb on the coal surface and hence travels faster (mainly through cleats and fractures) through the coal than CO₂ does. Nevertheless, the PFC tracer indicates the direction of migration of the CO₂ front. After three months soaking, the test was evaluated by back-producing the CO₂. Only 2.5% was back-produced, making the project a success.

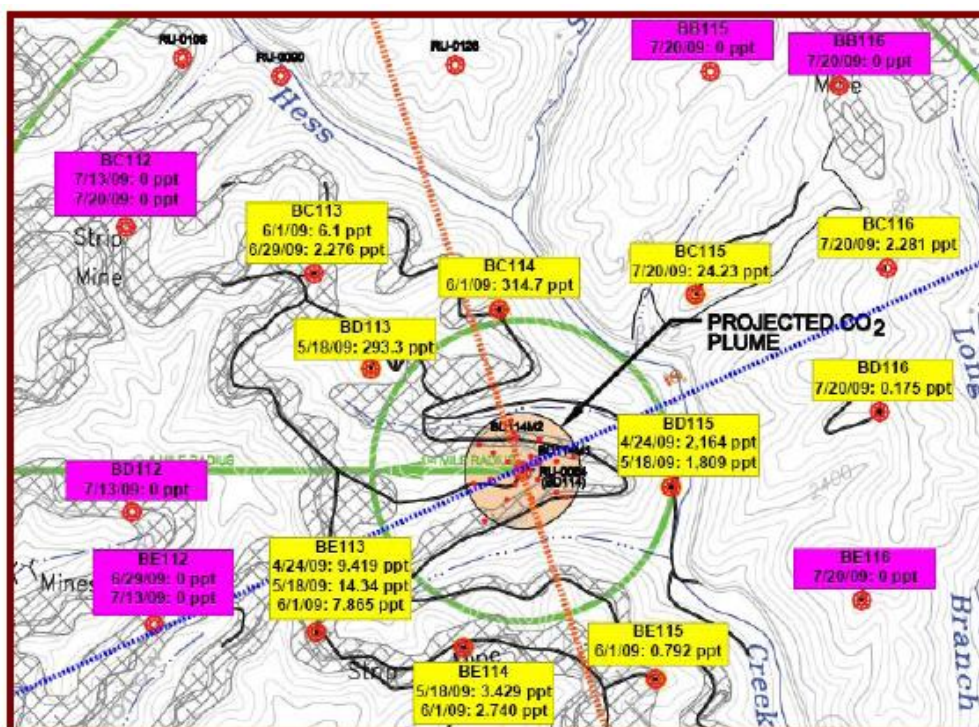


Figure 2.44. Tracer detection during the 2009 ECBM field test in Central Appalachian Basin. Indicated concentrations refer to tracer, not CO₂. From Ripepi (2009).

2.2.6.3.5. Presence of nearby abandoned mines

The presence of nearby mines is a concern since various migration pathways may have been induced by ancient mining activities (see above). However, if the storage reservoir is not in direct contact with the mined out area the presence of abandoned mine galleries could also be an opportunity for monitoring purposes. Would leakage from the reservoir occur, there is a good chance that CO₂ migrates towards the area with enlarged permeability and (when not completely flooded) under pressure depletion. This would imply that leaked CO₂ can accumulate in the (partly) flooded mine. Any changes in mine water chemistry (pH, EC, HCO₃⁻...) can be logged by drilling an entrance to the mine and placing a diver with measurement tools or by regularly analyzing water samples. Would the concentration of CO₂ become too high in the mine water so as to not longer safely hold CO₂ in dissolution, then remediation is possible because the CO₂ is contained within a limited space that can be easily accessed.

During the Recopol/MOVECBM project in Poland, a nearby mine was used for monitoring purposes. The injection site was located at 100m from an abandoned mine gallery (and about 700m above the injection depth) where devices for direct CO₂ measurements were placed. No elevated gas concentrations that could be linked to the injection were measured during and after the injection of 760 ton CO₂ (van Bergen et al., 2009).

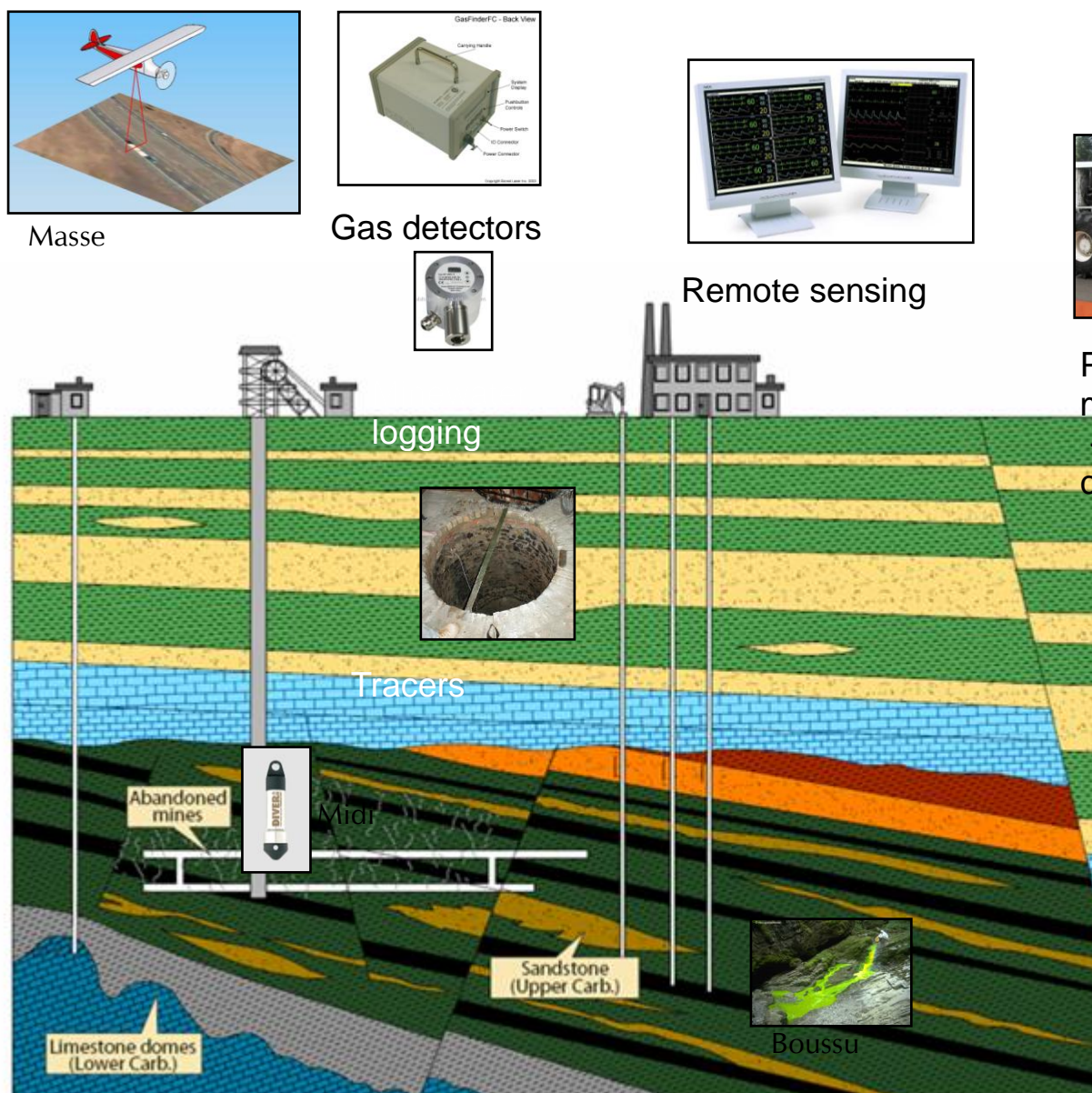


Figure 2.45. Sketch showing suitable monitoring techniques for CO₂ storage in coal series of the Campine Basin. The indicated wells represent different storage options in the Campine Basin (in the Dinantian limestones, in Westphalian coal seams or Triassic sandstones; see sink inventory made for PSS-CCS-phase I). Background figure modified after Lagrou (2002).

2.2.6.3.6. Conclusion

There is not one best monitoring solution for ECBM projects so far that answers all the monitoring needs. A combination of several suitable techniques would be the best option. Figure 2.45 gives an overview of suitable monitoring options, each with their own goals (plume tracing, leak detection...). These monitoring options include:

- On site gas detectors
- logging of well parameters (at head and down-hole)

- Tracers
- Seismic survey
- Minewater / groundwater analysis
- Tiltmeter
- Remote sensing

Seismic surveys are taken into account for monitoring protocols although the low injectivity rates in coal might be critical for conclusive detection.

A seismic survey is required anyway in the exploration phase in order to visualize the geometry of reservoir and seal. It is recommended that a seismic survey would be repeated after an injected volume of at least 1kton CO₂ and definitely at the end of the injection period. This is the only solution that allows a 3D overview of the distribution of CO₂ and the integrity of the reservoir and seals.

Tiltmeters or remote sensing techniques (e.g. permanent scatterers interferometric synthetic aperture radar (PS-InSAR) technique, Lidar) can be used to measure potential ground movements associated with CO₂ storage.

Non-seismic geophysical techniques such as gravimetry and electromagnetic resonance currently do not reach sufficiently high resolution to detect CO₂ accumulation in thin coal seams. The best results can be obtained when several techniques are combined.

2.2.7. Cost of monitoring and safety

2.2.7.1. Introduction

In order to estimate the costs associated with the monitoring program the boundary conditions need to be clear. These encompass:

- Space: How large should the monitoring area extend?
- Time: What is the obliged duration vs. project-specific requirements?
- Objectives: What do we need to measure (obligatory, required, optional)?

The first issue relating to space is clarified by EC (2011b):

The monitoring area should include the injection facilities, the storage complex (including where possible the CO₂ plume), and where appropriate the surrounding environment. The monitoring plan should be based on the geology of the storage complex and the geological framework of the surrounding environment. The site characterisation and modelling and risk assessment should be used to identify features, events and processes that could lead to leakage of CO₂ from the storage complex, and to model potential CO₂ migration and leakage routes and potential fluxes in the case of leakage.

Monitoring is obliged from the pre-injection stage up to the post-transfer stage, starting with a baseline survey for reference values and ending with a "light" version of long-term monitoring to further ensure the containment. In this view, EC (2011c) notes that *"the post-closure pre-transfer phase should be at least 20 years to ensure that the evidence for complete and permanent containment can be obtained, unless the competent authority is convinced that all available evidence indicates that the stored CO₂ will be completely and permanently contained (art. 18.1(a))"*.

The third constraint determining the cost of CO₂-monitoring relates to the objectives and protocols, and is discussed in the next paragraph.

2.2.7.2. Monitoring protocols

A wide variety of techniques is available that serve different purposes (e.g. tracing of the gas plume, proof of containment, well integrity...). Each technique has advantages and disadvantages within a certain context. An appropriate monitoring protocol should be composed for each site considering the best techniques available at that moment and the effectiveness of the methods in the given circumstances.

EC (2011b) states with respect to this matter that *"although specific experience with different methods for monitoring CO₂ storage is growing, overall there is limited experience, particularly in relation to the wide range of geological and site conditions and storage options across Europe. ... An integrated approach combining different methods and techniques is therefore recommended."*

EC (2011b) distinguishes three categories of monitoring: mandatory, required, and optional contingency monitoring. The mandatory parameters (for all sites) relate to operational monitoring. The required techniques are site-specific and relate to proof of containment and integrity. The optional techniques will only be used in case of irregularities.

Furthermore, baseline monitoring is obliged within the monitoring plan in order to have a standard for comparison with later results.

Also, EC (2011b) specifies that "the monitoring plan must in any case include continuous or intermittent monitoring of the following items which should therefore be considered mandatory:

- *Fugitive emissions of CO₂ at the injection facility;*
- *CO₂ volumetric flow at injection wellheads;*
- *CO₂ pressure and temperature at injection wellheads (to determine mass flow);*
- *Chemical analysis of the injected material;*
- *Reservoir temperature and pressure (to determine CO₂ phase behaviour and state)."*

Two examples of monitoring protocols have been worked out for both the aquifer and ECBM cases in Belgium (Figure 2.46 en Figure 2.47).

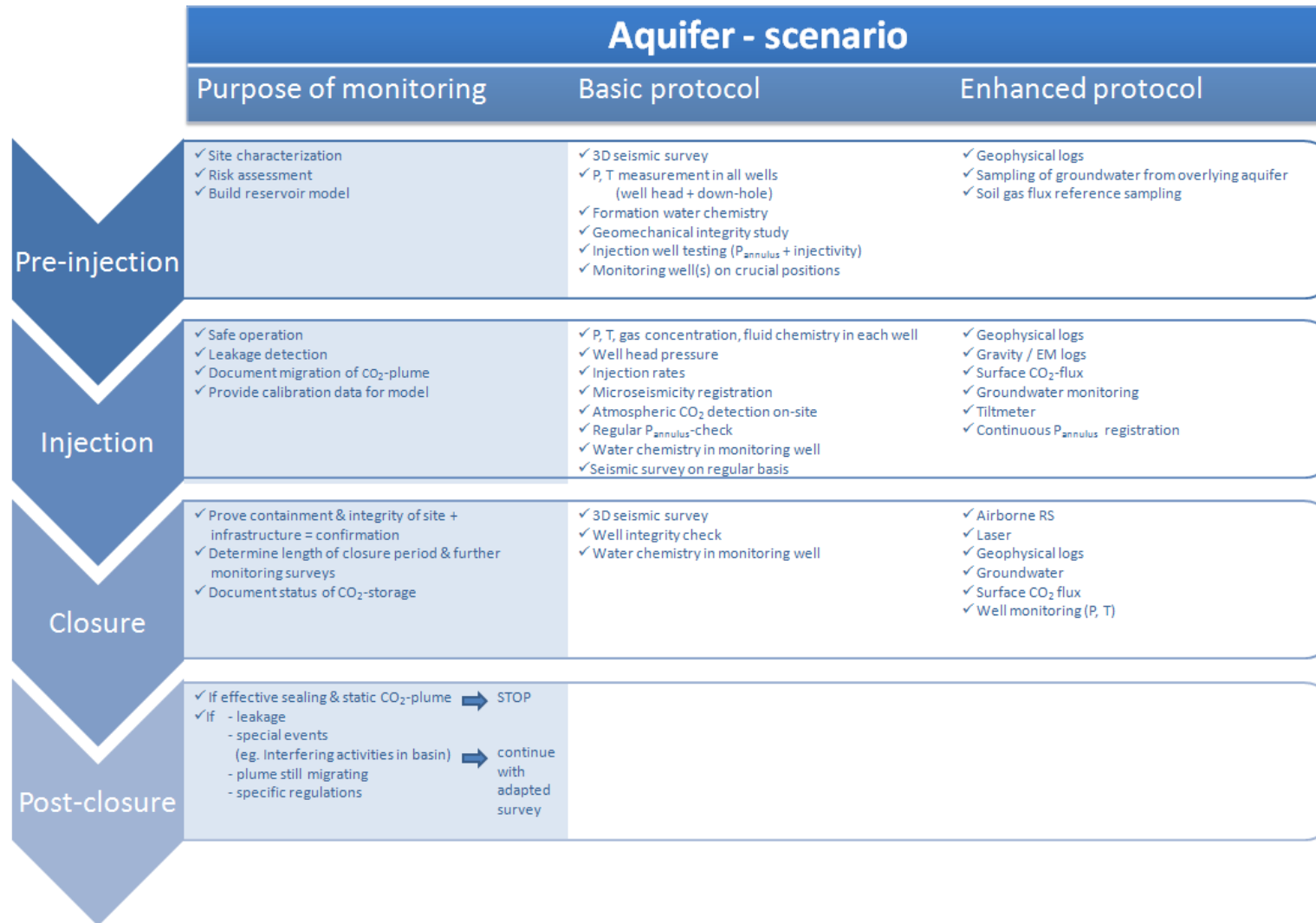


Figure 2.46. Example of a monitoring protocol for CO₂ storage in aquifers.

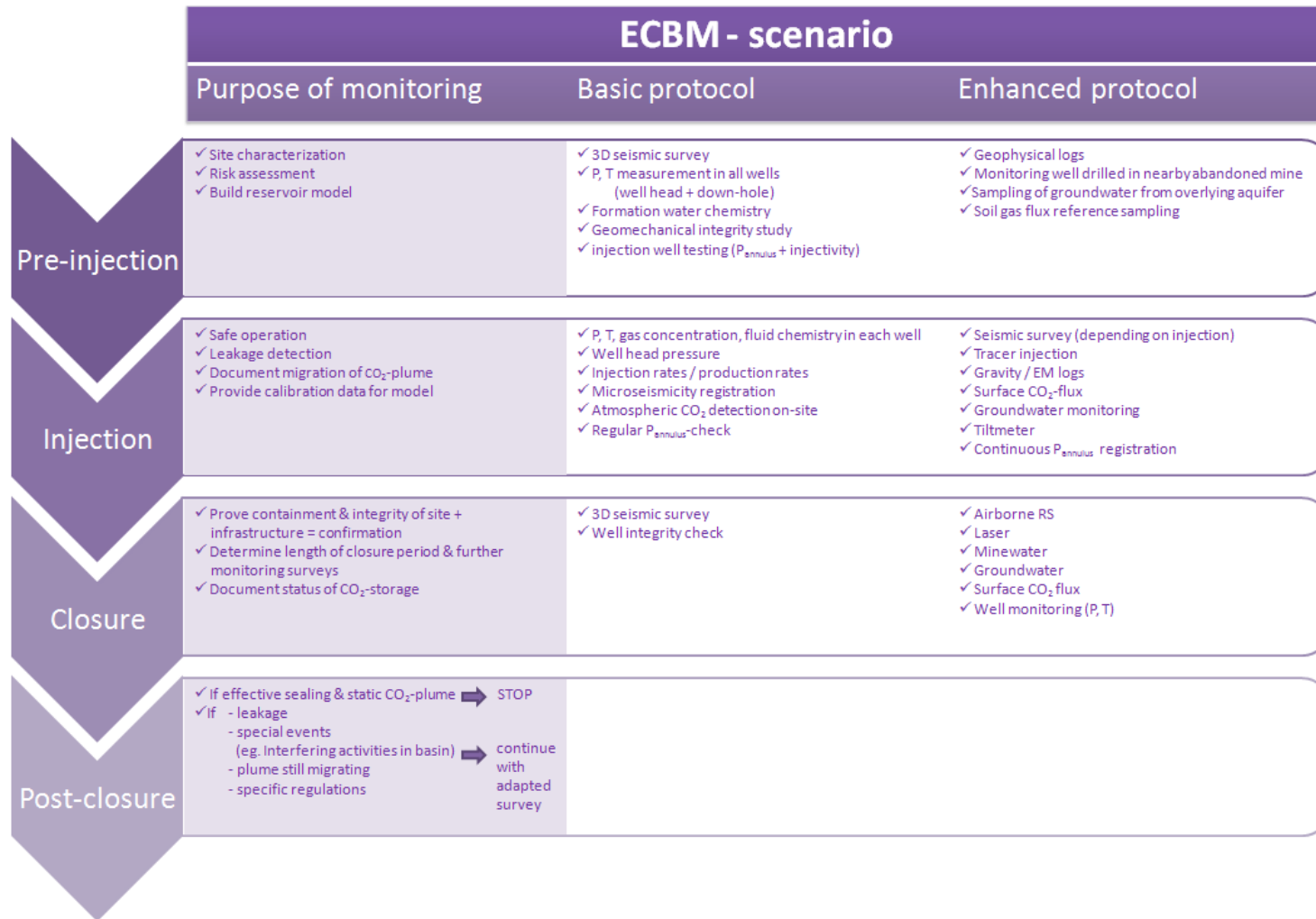


Figure 2.47. Example of a monitoring protocol for CO_2 storage in ECBM production.

2.2.7.3. Life-cycle monitoring costs estimates

Monitoring costs are often regarded as marginal cost on the CCS total. Most numbers reported in literature for commercial-scale projects stay well below 1€/ton CO₂ (e.g. Benson et al., 2005; Vidas et al., 2009). Nygaard & Lavoie (2009), on the contrary, calculated that monitoring costs for the large-scale Wabamun CO₂ sequestration project (WASP, Canada) amount up to 75% of the total project cost, considering an extensive monitoring protocol. Based on the cost breakdown numbers from Vidas et al. (2009) monitoring costs would account for 20 to 30% of the project cost (Figure 2.48). Very large projects require extensive and hence expensive monitoring programs, but nevertheless, the price per ton remains relatively low. Small pilot projects, however, are confronted with significant costs for their monitoring programs. Even with optimization of techniques and application of a minimal selection of monitoring tools the cost per ton CO₂ sequestered remains high. This is an intrinsic effect of the scale of the projects!

2.2.7.3.1. Type of costs

The cost structure of CO₂ storage monitoring encompasses a large number of cost elements and categories. First, an overview is given of the type of costs that need to be considered in order to estimate the price per ton CO₂ for the monitoring of a storage project.

- Research:
 - Composition of risk assessment (RA) plan, monitoring (MON) plan and corrective measures (CM) plan
 - Composition of numerical model of reservoir (static + dynamic)
 - Update of reservoir model when new data become available
 - Update of RA-MON-CM plans
- Work-over of old abandoned wells if necessary
- Baseline data
 - Pre-injection monitoring to obtain baseline reference values
- Monitoring program during different stages
 - Characterization
 - Site development
 - Operation
 - Closure
 - Post-transfer
- Monitoring of emissions on site:
 - Quantification of emissions (e.g. CBM flaring, combustion)
- Management:
 - Reporting to competent authority at least once a year
 - Review of storage permit/re-permitting when substantial changes
 - Inspections at least once a year
 - Communication with competent authority and public
 - Administration

- Updates of RA-MON-CM plans
- Preparation of transfer of responsibility
- Corrective measures:
 - Reserve RA budget for unforeseen costs related to corrective measures and the monitoring of their effectiveness in case of leakage or other irregularities during operation/closure
 - Reserve MON budget for intensified monitoring when needed
 - Reserve CM budget for additional costs at long-term when fault can be attributed to operator

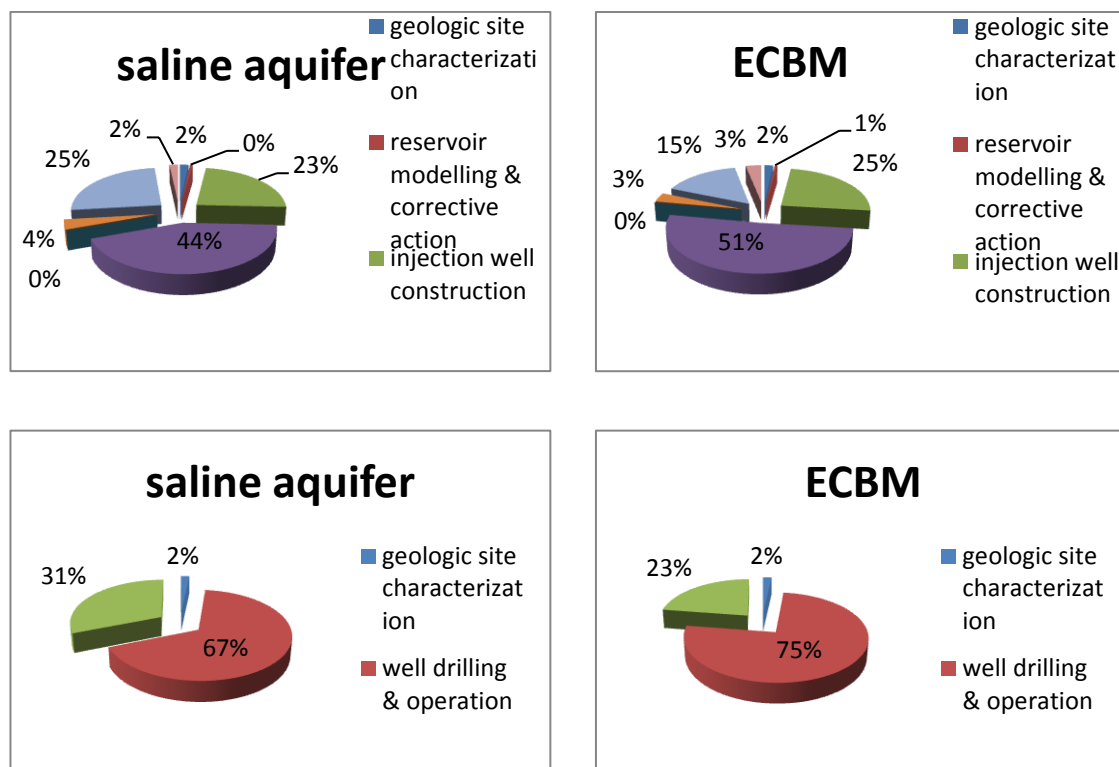


Figure 2.48. Cost breakdown for CO₂ storage projects based on data from Vidas et al. (2009). The presented figures refer to a commercial-scale project with sequestration of 1.8Mton CO₂ per year over 20 years. The upper two figures show cost breakdown for the categories distinguished in Vidas et al. (2009). The lower two figures group the same numbers into site characterization tasks, well construction and operation and monitoring issues. These figures clearly indicate that even in commercial projects monitoring costs can be substantial.

2.2.7.3.2. Cost-drivers

The main cost drivers are those associated with *drilling and operation of wells* and *periodic seismic surveys* (Figure 2.48 to Figure 2.50). Benson et al. (2005) indicate that repeated seismic surveys account for more than 50% of the total monitoring cost. Other monitoring techniques, as well as the coordination and management costs can be estimated as a fraction of the former costs. A crucial element in this perspective is the *total injection capacity and injectivity per well*, as this determines the number of wells needed in a project. This implies that monitoring costs can be very different depending on the storage option (saline aquifer, depleted gas field, ECBM...).

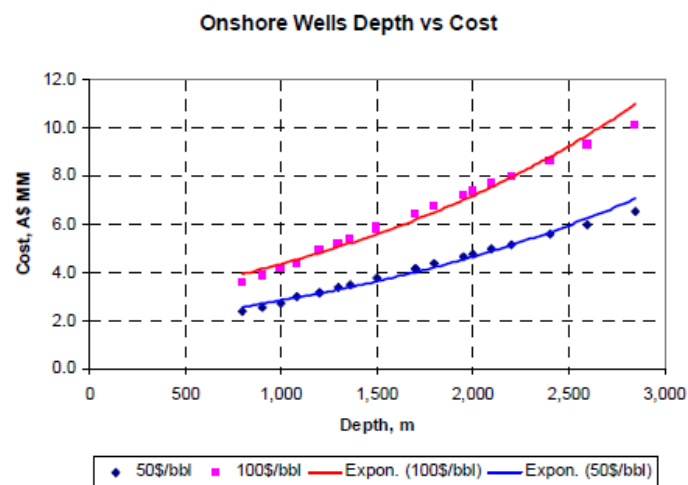


Figure 2.49. Cost versus depth curve for CO₂-injection wells (RISC, 2009).

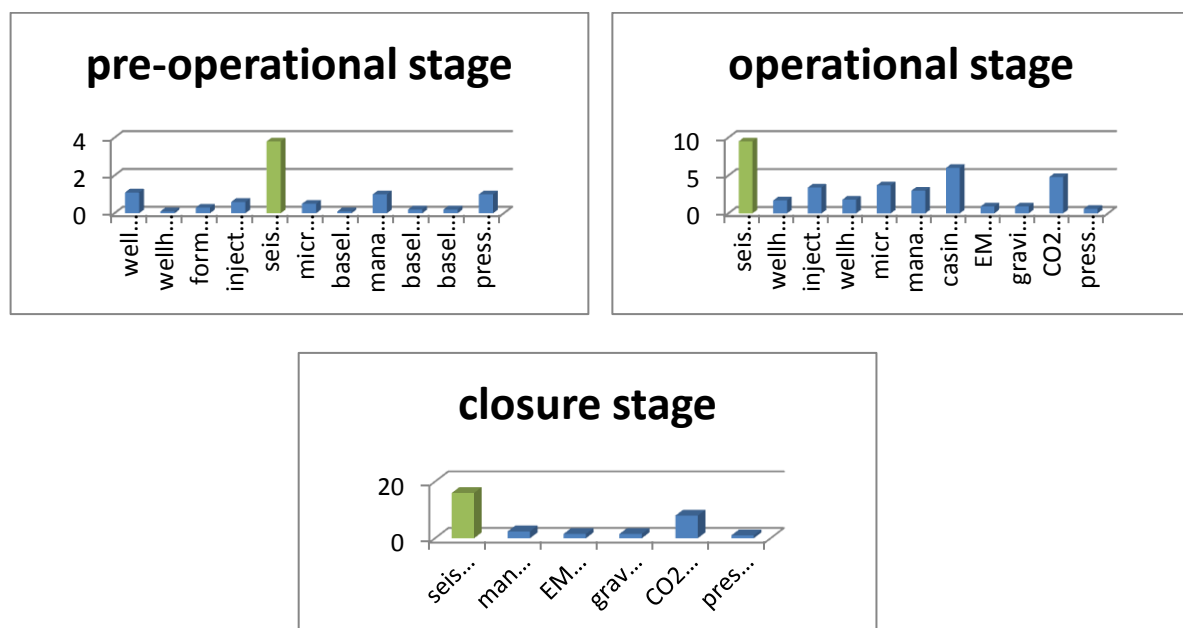


Figure 2.50. Costs per technique in an enhanced monitoring protocol for CO₂ storage in a saline aquifer. Based on Benson et al. (2005).

Other parameters that influence monitoring cost and which are site- and scenario-specific are:

- *Previous exploration efforts* → baseline data might be available already (eg CBM, oil,...), although this advantage competes with the disadvantage of old wells needing remediation
- Pilot projects in a similar context → lessons learnt could reduce the program
- *Mobility of plume* → influences the areal footprint and thus size of monitoring surveys
- *Reservoir size* → size of monitoring surveys
- Seal thickness & presence of faults → require specific monitoring
- *Number of wells needed* → increase of operation costs
- *Injected volume of CO₂* → competition between lower monitoring needs and higher unit price (per ton CO₂) for the monitoring program
- *Depth of storage* → direct impact on drilling costs
- *Duration of operation* → increase in monitoring cost
- Long-term monitoring program → increase in monitoring cost
- Relationship to overlying aquifers → require specific monitoring; NB: detect pressure changes rather than chemistry changes which are difficult to spot
- Special issues → site-specific risks (e.g. ground movement), local regulations,...

2.2.7.3.3. Examples in the Campine Basin

Two examples of monitoring costs have been worked out for known structures in the Campine Basin, the Poederlee dome and the fault-bounded Verloren Kamp structure.

The total volume of CO₂ that can be injected in the Carboniferous Poederlee dome has been estimated at 3 Mton CO₂. Table 2.X gives the costs for a basic monitoring protocol. When dividing the total monitoring cost by the total volume of CO₂ injected, a relative cost of 4.3 €/ ton CO₂ is calculated.

Table 2.X. Example of monitoring cost calculation for storage in the Poederlee dome.

Monitoring technique	Cost (M €)
3D seismic survey over 50km ² (frequency 5 times: before start, after 100kton, 1Mton, at end injection, before abandonement)	7,5
P-T & CO ₂ monitoring in injection well	0,04
surface CO ₂ detection on site	0,02
management & modelling	0,1
fluid chemistry	0,05
microseismicity	0,045
well logs	0,2
1 monitoring well	4
measurements in monitoring well	0,02
ground movements	0,5
mechanical integrity	0,1
post-closure	0,1
Reporting	0,05
TOTAL	12,725

The Verloren Kamp structure in the Buntsandstein Formation is a larger, fault-bounded antiformal structure with an estimated CO₂ storage capacity of about 20 Mton. Because of the presence of faults at both sides of the structures, at least two monitoring wells should be foreseen. Also the area of review is larger and the injection period longer than for the Poederlee dome, resulting in a more expensive monitoring program. Table 2.XI summarizes the monitoring costs accounted for. Total monitoring cost is 25 M€, but divided through the total volume of CO₂ injected, a relative cost of 1.25€ / ton CO₂ injected is calculated.

These two examples clearly show the effect of scale.

Table 2.XI. Example of monitoring cost calculation for storage in the Verloren Kamp structure.

Monitoring technique	Cost (M €)
3D seismic survey over 70km ² (frequency 7 times: before start, after 1Mton, 5Mton, 10Mton, 15Mton, at end injection, before abandonment)	15
P-T & CO ₂ monitoring in injection well	0,07
surface CO ₂ detection on site	0,025
management & modelling	0,2
fluid chemistry	0,1
Microseismicity	0,1
well logs	0,4
2 monitoring wells	8
measurements in monitoring well	0,04
ground movements	0,5
mechanical integrity	0,2
post-closure	0,15
Aquifer monitoring	0,15
reporting	0,075
TOTAL	25,01

In case of ECBM production, only part of the investment costs need to be accounted for as some infrastructure is present already and a lot of data are available already through the CBM assessment and production. Performing CO₂ injection without coeval methane extraction is not feasible in the low-permeable coals occurring in Belgium. Therefore, the potential of ECBM depends directly on CBM business, unless alternative injection schemes are applied whereby the coal series as a whole are targeted and injection is realized through the more permeable sandstone layers as was proposed for the Geleen project in the Netherlands (concept, VITO).

The monitoring cost per ton CO₂ in coal-cases directly depends on the injectivity (ton CO₂ / well / year) that can be reached. The better the injectivity, the larger the total volume of CO₂ injected and the lesser the number of injection wells needed and hence investment costs. As CBM business is still in a premature (prospection) phase, quantitative estimates on monitoring costs cannot be determined due to the many uncertainties.

2.3. Data collection for carbon capture in power and non-power sectors

2.3.1. Summary

This report discusses technological options for carbon capture in the power sector and in energy intensive non-power sectors. The report is data oriented because its main purpose is to assist model builders on input data for the project PSS-CCS II. The non-power sectors include the sectors of cement, iron and steel, hydrogen and ammonia, refineries and industrial boilers. For each of these sectors, the potential of CO₂ capturing technologies are discussed and economic data is presented.

The report starts with a general introduction (chapter 2.3.3. CO₂ Capturing technologies) on three broad categories of CO₂-capturing technologies: post-combustion, pre-combustion and oxy-fuel combustion. In the post-combustion process, CO₂ is removed from the flue gas, generated by the combustion of the primary fuel in air. In the pre-combustion process, the carbon is removed from the fuel prior to combustion. The fuel is transformed, typically forming CO₂ and hydrogen. The mixture is then separated and hydrogen is used for combustion. In the oxy-fuel combustion process, primary fuel is combusted with oxygen instead of air so that the flue gas mainly consists of H₂O and CO₂ which are easily separated by condensing the water. The major energy consumption is not in the flue gas treatment anymore but in the air separation unit (ASU) that produces the oxygen.

Chapter 2.3.4 (CO₂ capture in the power sector. presents the options for three main types of power plants: pulverized coal plants (PC), natural gas combined cycle (NGCC) and integrated gasification combined cycles (IGCC). For PC and NGCC, post-combustion capture as well as oxy-fuel combustion capture, are considered. For IGCC, pre-combustion would be more favourable. Economic data and technology performance are presented. The chapter further discusses capture technology options for a CCS ready plant that is intended to be retrofitted with CCS technology. Post-combustion capture as well as oxy-fuel combustion capture seem to be feasible options for retrofit. Performance and costs are presented for a SCPC plant. Modelling retrofit in TIMES is not a standard option and requires a specific approach. The chapter presents a structure that can be used for this purpose.

The cement industry is the largest industrial source of CO₂ emissions worldwide and is a major candidate for CCS deployment. In chapter 2.3.5 (CO₂ capture in the cement industry) the options for capturing CO₂ from cement plants are discussed. There are two sources of CO₂ emissions in the cement industry: the combustion of fuels and process emissions. This amounts in a very high CO₂-concentration in the process gas stream (25 – 35 %). This would make them a better candidate because CO₂ can theoretically be extracted easier. In this chapter technology performance and economic data is presented for three options of CO₂ capturing from the raw material related off-gas: 1.) post-combustion through chemical absorption, 2.) oxy-fuel combustion and 3.) chemical looping using calcium oxides which is a technology in early stage of development. Post-combustion is by far much more expensive than the other two options, mainly because of its high capital cost. Nevertheless, it is the technology emitting the lowest amount of CO₂. Oxy-fuel combustion can compete with conventional cement plant when ETS price is at 25 Eur/t CO₂ emitted.

CO₂ emissions from iron and steel making plants (chapter 2.3.6. capture in the iron and steel making industry) worldwide account for 27 % of the industrial emissions. This chapter focuses on the capturing of process CO₂ from the blast furnace, used in the iron making process, because this is the one with the highest direct potential for CCS. Technology performance and economic data for two options of CO₂ capturing from the blast furnace is presented: 1.) post-combustion using shift reaction and chemical absorption and 2.) oxy-fuel combustion.

Hydrogen production (chapter 2.3.7. CO₂ capture in the hydrogen industry) through reforming may be a good candidate for CCS. Hydrogen in industries is currently being produced on a large scale through reforming and electrolysis. Reforming of fossil fuels (or biomass) is the dominant hydrogen production processes, accounting for 96% of worldwide hydrogen production. During reforming, CO₂ is formed as a by-product and is separated from the hydrogen in order to produce hydrogen. Therefore, CO₂-capture is already carried out as part of the production process and consequently no additional capture installation is required. Since CO₂-purity is high at more than 99%, only compression (prior to transportation and storage) is required, making CO₂-capture a relatively low cost option. For modelling purposes, it is recommended to consider two levels of CO₂-capturing. Additional storage of CO₂-emissions from heat production is regarded at higher cost level. Here in principle, different capture options are feasible: 1) post combustion capturing using solvents when heat is produced by burning natural gas 2) pre-combustion capturing by burning an amount of the H₂ produced and 3) oxy-fuel burning. The latter solution seems to be less attractive as it requires additional equipment for O₂-separation.

The hydrogen produced can be used for ammonia production (chapter 2.3.8. CO₂ capture in the ammonia industry), as ammonia is synthesised from nitrogen and hydrogen. In Belgium, hydrogen producing units under the form of reforming plants are found in the ammonia production plants. The amount of CO₂ process emissions emitted directly to the air could be regarded as the direct potential for storage. Not all of the CO₂ process emissions are available for storage. Consequently, the amount of CO₂ that is re-used for other processes should be accounted for (e.g. soft drink industry).

The refinery sector (chapter 2.3.9. CO₂ capture in the refinery industry) is the third largest emitter among stationary CO₂ sources globally, after the power generation sector and the cement industry. The contribution of the refinery sector to global CO₂ emissions is around 4%. A refinery has multiple exhaust stacks that release CO₂. This chapter emphasizes on the following main CO₂ sources: the utilities/power plant, boilers and process heaters/furnaces, hydrogen plant and a Fluid Catalytic Cracking (FCC) Unit. Carbon Capture can be applied separately to these refinery units. For a combined stack of heaters and boilers, an overview of economic data of three studies are presented in this report, for post-combustion capture, for three options of pre-combustion capture and for two options of oxy-fuel combustion capture. For an existing FCC unit, economic data of one study is presented for post-combustion capture and two options of oxy-fuel combustion capture (two oxygen levels).

Chapter 2.3.10 (CO₂ capture from industrial boilers) emphasizes on the opportunities of CCS for boilers outside the electricity sector. The working principle of an industrial boiler is the same as a boiler in the power sector, but an important difference is in the scale of production. To overcome the issue of the relative small scale of industrial boilers, multiple small-scale units can be connected with each other in a ducting network in order to collect their flue gases in a centralized network. A single capture plant can provide the capturing of CO₂ for various industrial boilers. In this chapter, economic data is presented for two emerging capture designs (oxy-fuel combustion through oxygen transport membranes (OTM) and oxygen conducting membranes (OCM)) and post-combustion capture through amine absorption. The boilers with OTM and OCM offer a larger potential over air-fired boiler with chemical absorption. The chapter further discusses the feasibility of connecting dispersed CO₂ sources and routing the CO₂ to a centralized capture system.

2.3.2. Introduction

This report aims at describing capture technologies for power and non-power sector. The paper first describes the capture technologies for the power sector, including emerging technologies and gather data for each main type of techniques. A short discussion is made on performance and cost, on a comparative basis.

Industrial sectors should also be strongly concerned about CO₂ emission and the ways of reducing them. For some industrial processes it will be difficult to avoid completely the use of fossil fuels. Examples are the iron and steel industry for high-temperature heat demand and non-energetic use of coal, and the cement production process, resulting in considerable process related emission of CO₂ from the raw materials.

In 2005, 37% of the world's CO₂ emissions came from industrial processes. Iron and steel making plants, non-metallic minerals (mainly cement plants) and chemicals and petrochemicals were responsible for 72% of direct industrial CO₂ emissions (Source: IEA, 2008a).

In order not to duplicate what had been done in the previous project (PSS-CCS I), this paper does not re-explain topics such as transport, flue gas cleaning devices, etc. Instead, the emphasis will be on technology data, in a quite systematic way, for modelling purposes.

2.3.3. CO₂ Capturing technologies

Combusting of fuels in the energy sector, the industry, residential and tertiary sector and the transport sector is the major source of CO₂ emissions. Combustion of bio-fuels also releases CO₂, although they are not accounted for under the Kyoto protocol. Other sources of CO₂ emissions are industrial processes (production of steel, cement, ammonia, H₂). In this section we provide an overview of different capturing technologies in combustion processes and process emissions. In the following sections we handle the sector specific issues – why certain technologies are preferable or provide better perspectives in the near future.

There are three broad categories:

1. Post combustion technologies: typical the flue gas from combustion process contains a big fraction of N₂, smaller fractions of CO₂, H₂O, a minor fraction of O₂, and very small fractions of air pollutants such as N₂O, SO₂, and Particulate Matter (PM). Post combustion technologies separate CO₂ from the flue gasses without intervening in the combustion process itself.

2. Pre combustion technologies: this is based on a transformation of the fuel where all C is converted into CO₂ and removed from the fuel before the combustion process. The basic principle is that H₂ is produced which is then burned under normal conditions.
3. Oxy-fuel combustion: pure O₂ is used in the combustion process. This dramatically reduces the flue gas volume which now contains important fractions of CO₂ and H₂O. H₂O is easily removed by condensing. This process requires the separation of O₂ from the atmospheric air which typically contains 79 % N₂ and 21 % O₂.

2.3.3.1. Post-combustion technologies

2.3.3.1.1. Post-combustion technologies: description

In this section, a brief explanation of classical and emerging technologies is presented, followed by data estimations.

2.3.3.1.1.1. Post-combustion capture using monoethanol amines

The most known and mastered technique among post-combustion methods for capturing CO₂ is based on absorption-desorption cycle of the CO₂, using a solvent. The solvent called Mono-Ethanol-Amine (MEA) is a solvent used for a long time in the industrial sector. The major challenge is to scale up this technology to large scale power plants.

As shown on Figure 1, the flue gas coming from a classic fuel-fired power plant goes through an absorber column where CO₂ is absorbed by the solvent and separated from the other flue gas components. These are released to the atmosphere through the stack. The solvent, combined with CO₂, is directed to a second column called the stripper (or the desorber or the regenerator). The CO₂ is released by heating up the loaded solvent. The heat is commonly extracted from steam (the stripping steam). After desorption from the solvent, the carbon dioxide is sent to a CO₂ treatment unit whose role is to get the CO₂ ready for transport and eventually for downstream application. This unit covers different processes like compression, cooling, dehydration and deaeration. The solvent foreseen for large scale post-combustion capture plants is an amine. It is currently the most advanced and ready post-combustion technology.

Various pollutants like NO_x, SO_x, HCl, HF and particulate matters may react with the amine to produce stable salts which cannot be regenerated, thereby consuming the solvent. To mitigate this problem, amine-based capture requires additional unit operations to remove pollutants prior to CO₂ Capture. Oxygen also must be greatly removed from the gas since oxygen can impair the solvent performance and damage equipment by corrosion. Alternatively inhibitors can be applied to prevent corrosion.

The major drawback of the technology is the quantity of energy to supply for regeneration of the solvent after absorption. The heat input is estimated up to 3 – 4 GJ/t CO₂. Indeed, the compound amine-CO₂ needs to be warmed up to release CO₂. This technology is mature for industrial activities but the capture plant is not a full commercial size yet. Since a big penalty of carbon capture comes from the solvent regeneration energy, the choice of this solvent is a key point of the capture cost. There are currently different commercially available solvents and new solvents are expected to enter the market: MEA has been the commercial baseline in industrial applications, KS-1 has been developed by Mitsubishi Heavy Industries (MHI) and reduces the energy requirements for regeneration. Its low regeneration energy makes it highly valuable. Other promising developments are Fluor's Econamine FG PlusSM technology, Siemens PostCap, and many other.

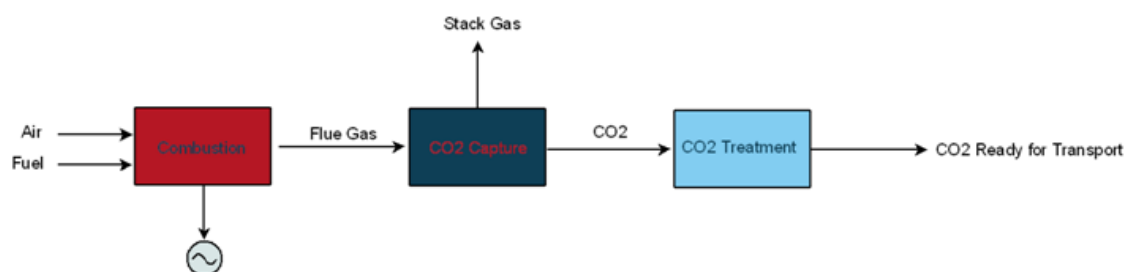


Figure 2.51. Post-combustion process

Commercially used solvents for CO₂ removal are listed in the table below. They are classified according to their chemical and physical properties. The chemical absorption process is affected by chemical reactions between CO₂ and the solvent. The physical absorption process depends on the solubility, pressure and temperature conditions. Pressure is the dominating factor. The higher the pressure, the easier the CO₂ will dissolve in the solvent.

Table 2.XII. Solvents for post combustion capturing (source IEA 2006).

	Solvent name	Solvent type	Process conditions
Physical solvents	Rectisol	Methanol	-10/-70°C, > 2 MPa
	Purisol	N-2-methyl-pyrrolidone	-20/+40°C, > 2 MPa
	Selexol	Dimethyl ethers of polyethyleneglycol	-40°C, 2-3 MPa
	Fluor solvent	Propylene carbonate	Below ambiante temperatures, 3.1-6.9 MPa
Chemical solvents	MEA	2,5-N-monoethanolamine and inhibitors	40°C, ambiante-intermediate pressures
	Amine guard	5-N- monoethanolamine and inhibitors	40°C, ambiante-intermediate pressures
	Econamine	6-N-diglycolamine	80-120°C, 6.3 MPa
	ADIP	2,4-N-diisopropanolamine, 2-N-methyldiethanolamine	35-40°C, > 0.1 MPa
	MDEA	2-N-methyldiethanolamine	
	Flexsorb, KS-1, KS-2, KS-3	Hindered amine	
	Benfield and versions	Potassium carbonate & catalysts, Lurgi & Catacarb processes with Arsenic-trioxide	70-120°C, 2.2-7 MPa
Physical/Chemical Solvents	Sulfinol-D, Slufinil-M	Mixture of DIPA or MDEA, water and tetrahydrothiopene (DIPAM) or diethylamine	> 0.5 MPa
	Amisol	Mixture of methanol and MEA, DEA, diisopropanolamine (DIPAM) or diethylamine	5/40°C, > 1 MPa

Expected trends:

This technology evolves permanently. The major challenges are:

- Reducing the heat requirement for regeneration
- Reducing the temperature level for regeneration
- Reducing auxiliary power for capture and compression consumption.
- Scale up and integration into a large scale fossil-fuelled power plant.
- Reduce costs.

Next figure presents IEA's view on future technical evolution of capture and treatment units (IEA, 2008a):

Table 2.XIII. Evolution of energy requirements for capture using chemical absorption.

Year	1995	2005	2015
Thermal energy	4.2 GJ/t CO ₂	3.2 GJ/t CO ₂	2.0 GJ/t CO ₂
Power equivalent factor used	0.292 kWh/kg CO ₂ (0.25)	0.178 kWh/kg CO ₂ (0.20)	0.083 kWh/kg CO ₂ (0.15)
Power for capture	0.040 kWh/kg CO ₂	0.020 kWh/kg CO ₂	0.010 kWh/kg CO ₂
CO ₂ compressor	0.114 kWh/kg CO ₂	0.108 kWh/kg CO ₂	0.103 kWh/kg CO ₂
Total	0.446 kWh/kg CO₂	0.306 kWh/kg CO₂	0.196 kWh/kg CO₂

Note: The Power equivalent factor used refers to the electric efficiency at which the thermal energy needed for capturing CO₂ could be used for power generation. There is considerable debate about these trends in the scientific community, and the trends shown here depend on some step-changes in the technology.

Source: Feron, 2006.

2.3.3.1.1.2. Chilled Ammonia

The post-combustion technology using chilled ammonia is in fact a classical absorption-desorption cycle and should therefore be included to the previous section. Nevertheless, since the chilled ammonia technique seems very promising, it is included in this overview.

One can see "chilled ammonia" as a new solvent that reduces the regeneration energy. Solvent and flue gas must be chilled down to present desired combination properties: 0-20°C, at ambient pressure. The captured CO₂ is then desorbed by increasing the temperature up to approximately 100°C at elevated pressure (20-40 bar).

The chilled ammonia related literature presents very optimistic statement: "For 1 kg of captured CO₂, the simulation yields a steam extraction of 0.59 kg, equivalent to a heat duty exceeding slightly 1.5. Assuming a cost of electricity of 7c€/kWh, the sole operation of the capture system totals 14 €/t CO₂."⁴ (Valenti et al, 2009)

Moreover, the corrosion issues encountered when using MEA are strongly mitigated when using chilled ammonia. The capture efficiency (> 90%), the purity of the CO₂ stream (99.9%), the modelled penalty (5.8 %) and the fact that the regeneration column works at high pressure thereby reducing the compressor work, are very encouraging characteristics.

⁴ 14 Eur/t CO₂ is quite small compared to the present goal of capture technologies: 25 Eur/t CO₂.

However, exact performance figures are not given by commercial parties, so it is important to keep in mind that such technology still must be proven. In addition, handling ammonia is not easy; NH₃ slip emissions are a possible concern. ALSTOM is currently working on various pilot and demonstration projects, e.g. in collaboration with EPRI in the United-States. Concerns about this technology include increased emission of ammonia into the atmosphere. However, mitigation options exist.

Appendix 7 presents assumption and results of a simulation of carbon capture using chilled ammonia, made by the department of energy of the poly-technique school of Milano. (Valenti et al, 2009).

2.3.3.1.1.3. Membranes

Membrane contactors are a promising innovation. They use solvents but membranes are used to enhance reaction and reduce solvent loss by unwanted reactions. Already used in commercial applications at high pressure and high CO₂ concentration, membranes are studied to be applied to flue gas. Nevertheless, the duty is hard since flue gas is characterized by low partial pressure of CO₂.

The compressor duty is the major energy expense of this process whose total duty is assessed in the best case at 2.5 GJ/t CO₂ avoided (GHGT9, CO₂ Capture by Hollow Fibre Carbon Membranes: Experiments and Process Simulations Xuezhong He, Jon Arvid Lie, Edel Sheridan, May-Britt Hägg; Department of Chemical Engineering, Norwegian University of Science and Technology, N-7491 Trondheim, Norway). The same study shows a CO₂ retention rate of 67% with a purity of 88%. The total capital cost has been calculated at 197 \$ per tonne CO₂ avoided.

The membrane technology presents an early stage of development and thus, also presents wide ranges of characteristics. The overall penalty on net plant efficiency should be between 8 and 15 % but the cost is very high. In addition, the technique faces troubles of membrane saturation and degradation of performance due to impurities and water.

Development of cheaper and more robust membranes is required, with great permeability and selectivity. They might reach the market around 2030, not before (ZEP, 2009).

Figure 2.52 shows the principle of membrane capture unit.

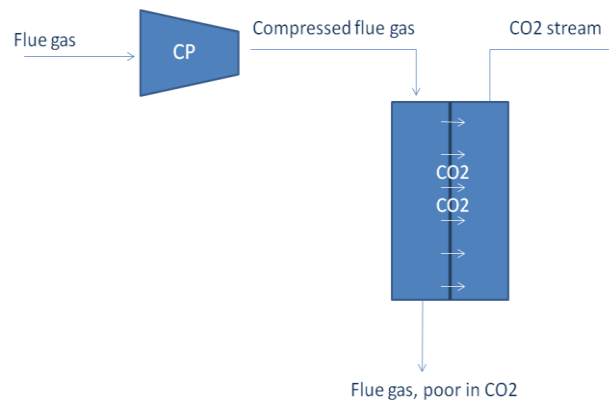


Figure 2.52.

A key characteristic of the process is the pressure ratio between feed and permeate of the membrane. A small pressure ratio increases the required area of the membrane (and so, a large capital cost). A higher pressure ratio reduces the required area but increases the compression costs. The optimal ratio depends from case by case and depends amongst other on the selectivity, permeability, CO₂ concentration in the flue gas and lay-out of the membrane section (He, 2009). Appendix 7 proposes results of a simulation.

2.3.3.1.1.4. Carbonate looping system

This technology separates CO₂ from the flue gas at high temperature (600 – 700 °C) using the reversible exothermic carbonation reaction of CaO. The CO₂ is released by the endothermic calcination of CaCO₃. This desorption produces a concentrated CO₂ stream suitable for purification, compression and storage (See Figure 2.53).

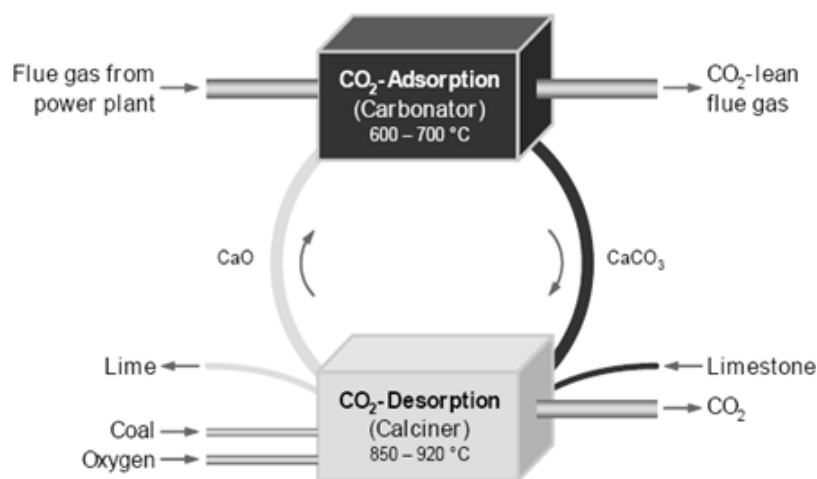


Figure 2.53. Principle of carbonate looping system (EnBW, PowerGen Europe 2009)

Some utilities are very interested in the technology such as EnBW in Germany. Nevertheless, it is hard to assess a commercialization time. Actually in the Caoling project, a 1 MW test plant, will be integrated in the 50 MW Hunosa coal fired plant in Northern Spain and facility is expected to start in the first quarter of 2011. Following ZEP statement (ZEP 2008), the technology is expected to be ready for commercialization from 2030 onwards.

Technology characteristics are quite promising: a penalty of 6.4 % points on a 1452 MW power plant; a retention rate of 82.8 % (EnBW, PowerGen Europe, 2009).

2.3.3.1.1.5. Bioconversion

This technology captures CO₂ thanks to photosynthesis in algae pond (or other). Algae can be further harvested and use as feedstock for biofuel. In this case, there is no storage and the CO₂ avoided comes from the fact that one carbon unit is used twice: the first one for power generation and the second one for engine powering.

Figure 2.54 presents a simple schematic of the basic principle:

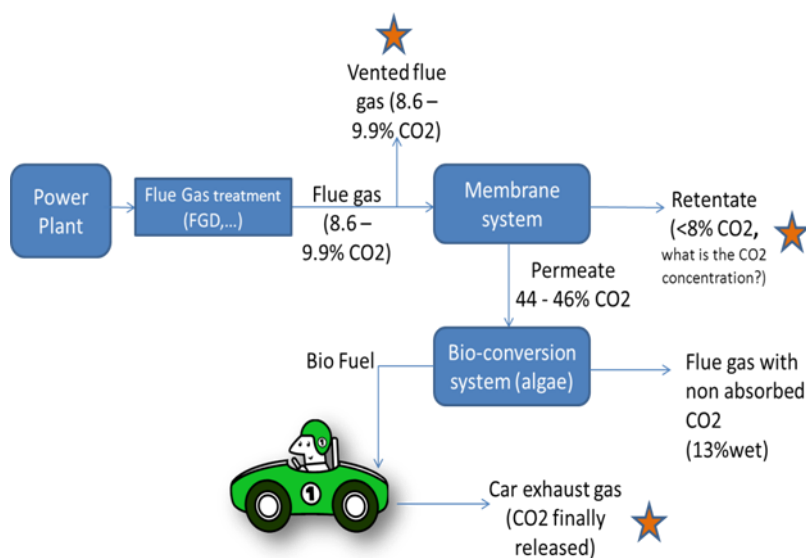


Figure 2.54. Basic principle of bioconversion

As it can be observed on the previous figure, a membrane system could be installed in order to increase CO₂ concentration of the flue gas going in the bioconversion system (pond or greenhouse), thereby improving the efficiency of the conversion process. It is possible not to increase the concentration, depending on the combustion type (coal,...) but in this case, performances stay quite low.

This technology is peculiar: it is not « capture-oriented » but has the main purpose to increase greenhouse/pond growth, in order to improve biofuel production.

Some countries are highly interested in the development of the technology such as Israel because of the high insulation and the agricultural potential. It is hard to forecast the deployment of the technology in Belgium and should not be considered in our study because there are too many uncertainties on the performance and it is very complex to implement in a model since it regards various sectors. Moreover, bioconversion technology requires a very large footprint which is not easy to get in a crowded country such as Belgium.

2.3.3.1.1.6. Anti-sublimation

Anti-sublimation states for the phase change from gas to solid CO₂. CO₂ is separated by frosting at about -100°C (depending on the concentration of CO₂) in evaporators using a refrigerant. The solid CO₂ is then liquefied by heating it up. There are 2 evaporators working alternatively in a frosting or defrosting mode so that the process can be continuous. Appendix 7 shows a flow diagram of the process (as well as estimate performance and costs).

Some laboratory experiment have been made by the "Center for Energy and Processes" (CEP) of Mines Paris-Tech, supported by EDF and have shown that good performance could be achieved: CO₂ purity of 99.3%, capture efficiency of 90%, penalty of 7.6 to 10%, incremental COE of 22.7 Eur/MWh and a cost of CO₂ avoided of 34.5 Eur/t CO₂ avoided (Powergen Europe 2009). This technology seems to be very interesting if waste cold is available, e.g. near a LNG terminal.

2.3.3.1.1.7. High pressure absorption processes

When pressure is high, there are other absorption processes or solvents that can be used: This is the case for the Selexol process (UOP), where CO₂ recovery is directly proportional to the partial pressure of CO₂ in the flue gas. Limitations with respect to the pressure are also the case for the less reactive solvents, including methyldiethanolamine (MDEA), diethanolamine (DEA), di-isopropanolamine (DIPA), triethanolamine (TEA). Other processes that are affected by CO₂ partial pressure include hot potassium carbonate, molecular-sieves membranes and cryogenic separation. For these processes, compression of the flue gas up to operating ranges will be expensive for economical CO₂ recovery. (IEA 2006)

2.3.3.1.1.8. Hot Potassium Carbonate

Hot Potassium carbonate solutions are also frequently used as chemical solvent in chemical absorption processes :

« Hot potassium carbonate (HPC) or "Hot Pot" is effectively used in ammonia, hydrogen, ethylene oxide and natural gas plants. To improve CO₂ absorption, mass transfer and to inhibit corrosion, activators and inhibitors are added. These systems are known as Activated Hot Potassium Carbonate (AHPC). The most widely licensed of these is the Benfield process, with over 675 units worldwide licensed by UOP (Figure below), and the Catacarb process, with over 100 units licensed as of 1992 by Eickmeyer & Associates. Other commercial processes are the Exxon Flexsorb HP process, which uses a hindered amine activator, and Giammarco-Vetrocoke's new process, which uses an organic activator. The full capacity of the "hot pot" family of processes requires a feed CO₂ partial pressure of about 700 kPa. The Benfield and Catacarb processes are commercially available for applications at a minimum CO₂ partial pressure of 210-345 kPag. » IEA (2006)

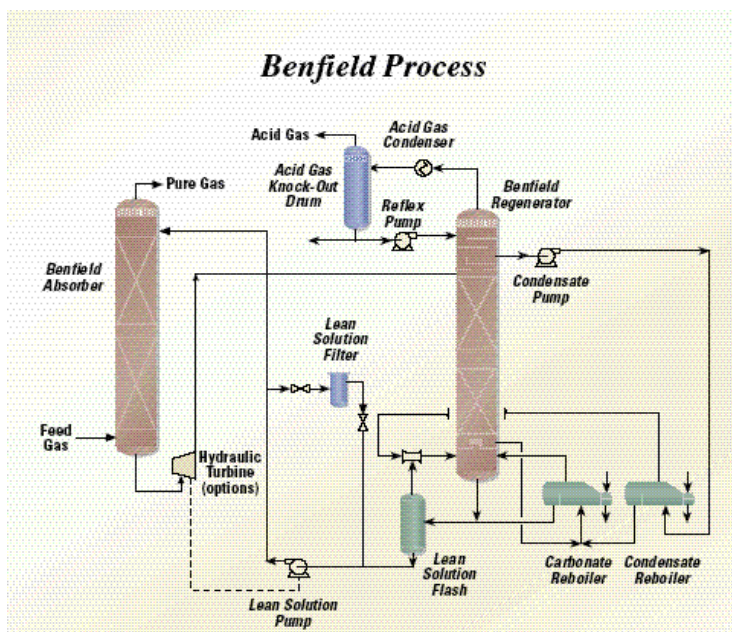


Figure 2.55. « The Benfield process » (Source : IEA, 2006)

2.3.3.1.1.9. Sterically hindered amines

« Kansai Electric Power Company (KEPCO) and Mitsubishi Heavy Industries have developed a proprietary process based on a sterically hindered amine, called KS-1 as a replacement for MEA in flue gas treatment (Figure below). KS-1 has lower circulation rate (due to its high lean to rich CO₂ loading differential), lower regeneration temperature (110°C), and 10-15% lower heat for its reaction with CO₂. It is non-corrosive to carbon steel (less than 25 µm/yr) at 130°C in the presence of oxygen. Another sterically hindered amine, AMP (2-amino-1-methyl-1-propanol) may have similar properties as KS-1 ».

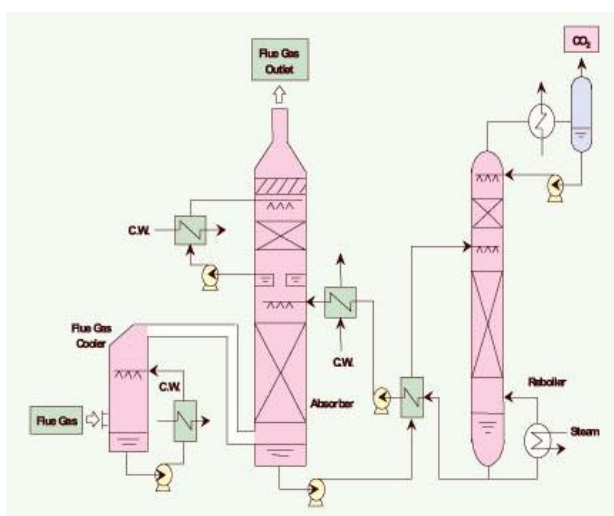
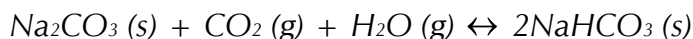


Figure 2.56. « The KEOCO/Mitsubishi KS-1 process » (IEA, 2006)

2.3.3.1.1.10. Low temperature gas-solid separation

« The removal of CO₂ from flue gas using solid Na₂CO₃ is based on the following reversible reaction:



The process is thought to be capable of capturing 25 to 50% of CO₂ without imposing significant energy penalty on the overall process. Increased CO₂-capture is possible but with a small energy penalty on the plant. A schematic diagram of the CO₂ capture process is shown in Figure 2.57 below. Flue gas and steam enter the carbonator reactor where CO₂ is captured by the solid sorbent. Next, CO₂ is released by providing recovered heat to the regenerator. The regenerated-sorbent flows continuously from the regenerator to the carbonator while the carbonated-sorbent flows continuously in the opposite direction. Dual circulating fluidised bed or transport reactors can be used to provide steady state operation ».

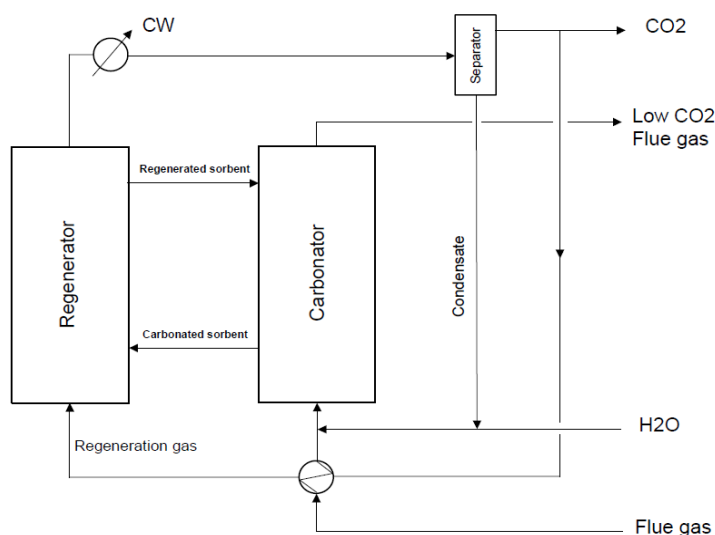


Figure 2.57. « Schematic diagram of the low temperature gas-solid CO₂ capture process » (IEA, 2006)

2.3.3.2. Pre-combustion technologies

2.3.3.2.1. Pre-combustion capture technologies: description

The main idea of pre-combustion is to remove the carbon from the fuel instead of removing from the flue gas.

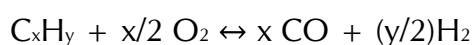
Description of a pre-combustion capture process:

Through a pre-combustion capture process, fuel is treated prior to combustion. Two basic chemical reactions form the basis of this technology. In steam reforming the fuel (mainly gas) reacts with steam to get a mixture of CO and H₂. In partial oxidation, the fuel reacts with oxygen to produce a mixture of CO and H₂. The latter process is called gasification.

Steam reforming (reaction with steam):

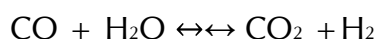


Gasification (reaction with oxygen):



The gasification requires oxygen that – in a traditional approach - must be produced from air in an "Air Separation Unit" (ASU) which is commonly highly energy consuming. After one of these reactions, the mix made of carbon monoxide and hydrogen, called "syngas", is sent to another reactor to undergo a "Shift Reaction" which converts CO into CO₂.⁵

Shift reaction(reaction with water):



CO₂ must be removed from shifted syngas in order to supply hydrogen to an application such as gas-fired combined cycle. The separation can be carried out by a chemical solvent similar to those used in a post-combustion capture, or by a physical solvent. A chemical solvent can be used when the partial pressure of CO₂ is below about 1.5 MPa and needs to be heated for the regeneration step. A physical solvent such as "Selexol" can absorb CO₂ at high partial or total pressure and be regenerated by a simple release of pressure making this process low energy consumer. This second option is preferred for IGCC because it is possible to bring the gas at high pressure from the gasifier.

New developments in pre-combustion are e.g. the integration of various step into one and the use of integrated membranes to provide the oxygen directly from air instead of using an ASU. These developments potentially reduce energy and investment costs.

⁵ It is important to remark that in the case of IGCC with no capture, the syngas is directly sent to a turbine for power generation. In this case, the turbine is designed to be fed with syngas.

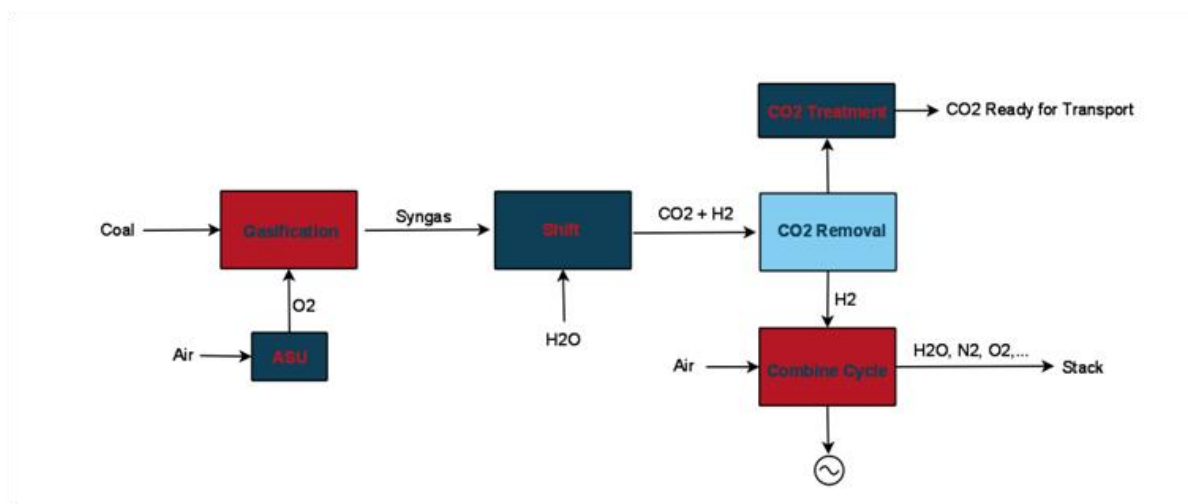


Figure 2.58. Pre-combustion process

2.3.3.3. Oxyfuel technologies

2.3.3.3.1. Technology description

The main idea of this technology is to replace air by oxygen in the combustion process. By doing so, the flue gas mainly consists of H₂O and CO₂ which are easily separated by condensing the water. The separation efficiency is quite close to 100%, despite the fact that a small amount of CO₂ is dissolved in water. The major energy consumption is not in the flue gas treatment anymore but in the air separation unit (ASU) that produces the oxygen.

A simple process flow diagram can be seen in Figure 2.59.

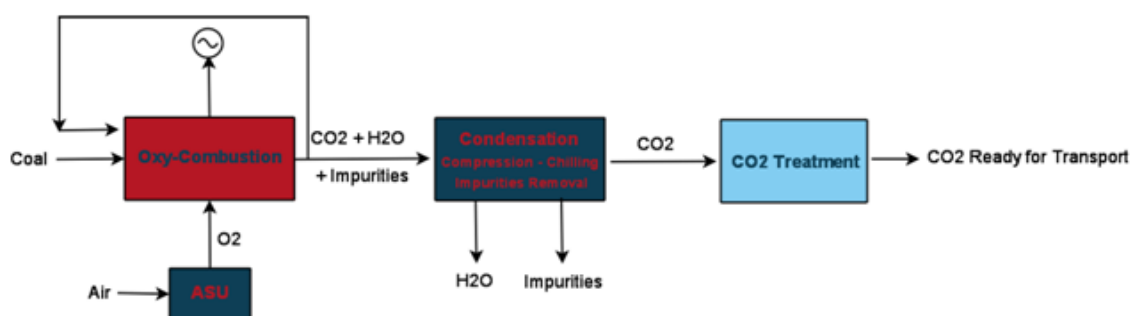


Figure 2.59. Oxyfuel process

As for post-combustion technologies, the oxyfuel sees a lot of recent developments in many fields that help improving the technology. There are currently pilot plants running in Germany and in Australia. Demonstration plants are foreseen for 2015 and a commercial deployment should be possible by 2020.

Nevertheless, the following items need to be addressed:

- Limit the air-ingress in the boiler.
- Fully understand the difference between air and oxy-fuel combustion.
- Handle the impurities deposit on equipment.
- Reduce the cost of oxygen production.
- Treat CO₂ stream to remove impurities (SO_x, NO_x, HCl, mercury,...) to make it suited for transport requirements. Oxy-fuelling introduces more O₂ in the CO₂ which could impair pipeline by corrosion. CO₂ may be diluted by air ingress and the use of less pure O₂ (95 % O₂ is the optimum for ASU)

The paper will later comprise a short description of the main emerging technology in oxyfuel.

2.3.4. CO₂ capture in the power sector.

The three capturing technologies are applicable in the power sector. In order to be pragmatic, this part of the paper presents three main types of power plants:

- Pulverized coal plants -PC-
- Integrated gasification combined cycles -IGCC-
- Natural gas combined cycle -NGCC-

Among the selected types of power plant, two of them are coal based (PC and IGCC) and the last one runs on natural gas (NGCC). It is reasonable to consider that capture will be implemented on highly efficient power stations⁶, therefore the best technology of each type of plant will be chosen as reference.

2.3.4.1. Post-combustion technologies: data

The previous section has presented the classical and emerging technologies of post-combustion carbon capture processes. For practical reasons, it is not interesting to implement each technology in the model. Indeed, there are too many technologies and in addition, they present quite high uncertainties. That is why it has been decided to gather these technologies under one single technology that is supposed to represent the average performance of the technology basket and their evolution.

⁶ As a rule of thumb, only power plant with an efficiency higher than 40 % are considered suitable for CCS.

As a general estimation, a large scale super-critical pulverized coal plant (net plant efficiency: 45%), using a capture station with a retention rate of 90 % and a solvent requiring 3 GJ/t CO₂ for regeneration will impact the net plant efficiency by 10 %points. Among these 10 points, 7 come from the fact that steam extraction must be performed at the turbine level, 2 points come from the compression work and the last 1 point is lost because of additional auxiliary power.

The following data have been identified in the literature (IEA, IEA GHG, scientific publications...) and have been checked in two ways: by a cross check of figures in related literature and by in-house calculations. These figures are as consistent as possible and realistic (not too conservative, not too optimistic).

Data gather costs, technical performance and their evolution through time by the use of TL (Technology Learning) coefficient. The currency has been chosen to be Euro-2010. The technical life time of the plants is given in years.

Two reference plants are considered: PC plant and NGCC. The choice of these plants will not necessarily influence the modelling outcomes. It is rather meant to illustrate how capturing will influence the relevant parameters for the plant. Characteristics for plants equipped with CCS have been derived from the corresponding reference plant, i.e. assuming same size of the boiler, turbines, generator and other equipment.

2.3.4.1.1. Reference plants

Coal plants: Supercritical pulverized coal plant

The reference plant must be the best available technology (BAT). Therefore, **the reference coal-fired plant is a highly efficient ultra supercritical pulverized coal plant**, fed with subbituminous coal (IEA, CCS 2009). The Rankine steam cycle reaches pressures up to 300 bars and temperatures up to over 600°C, approximately. Its efficiency reaches 47 % (LHV based).

Supercritical steam cycle present lower efficiency (43 – 45 %) and are taken as reference in various studies because they are the most deployed high efficient technology. It constitutes a conservative choice. Appendix 5 shows a simulation of a supercritical coal plant and its modification when CCS is applied. The calculated figures are confirmed by the IPCC report 2005 and, more recently by the "Energy Technology Perspective 2008 of IEA". Nevertheless, it is important to remember that the reference plant here is an ultra supercritical coal plant.

Table 2.XIV. Reference PC plant

Parameter ID	Value	Unit	Source
Investment (Inv0_dbl)	1564	Euro	IEA CCS 2009
		2010/kW	
Year of investment (Inv0RefY)	2010		IEA CCS 2009
VOM	2.52	Eur / GJ	Time Be CCS
FOM	29.52	Eur/kW	Time BE CCS
Production Capacity	510	MW	IEA ETP (2009) and Ph Mathieu, ULg
Availability	85.5	%	Kehlhofer R., Bachmann R., Nielson H., and Warner J. (1999).
Life Time	40	Years	
Net efficiency (ProdEff_sto)	47	%	IEA CCS 2009
Year of efficiency (ProdEffRefY)	2010		
Capture efficiency	---		
TL_Inv (TL_INV_sto)	-0.074		Calculation based on IEA CCS 2009
Inv ref year (TLRefY_INV_sto)	2005		
TL_Eff (TL_ProdEff_sto)	0.062814549		
Eff ref year (TLRefY_ProdEff_sto)	2005		

Gas plants: Combined cycle

The reference gas plant is a natural gas combined cycle power plant. The best commercially available technology average a net plant (LHV) efficiency of 57% (Energy Technology Perspective 2008, IEA). Some plant could even reach 60 %.

The gas reference is not a peak load gas turbine because these ones are characterized by a low efficiency, a high degree of variability (does not work at base load) and a few number of operating hours per year. That kind of plant is not a good candidate for CCS. Combined cycle plant is preferred.

Table 2.XV. Reference gas plant

Parameter ID	Value	Unit	Source
Investment (Inv0_dbl)	596	Euro	IEA CCS 2009
		2010/kW	
Year of investment (Inv0RefY)	2010		IEA CCS 2009
VOM	0.58	Eur / GJ	Time Be CCS
FOM	11.16	Eur/kW	Time BE CCS
Production Capacity	480	MW	ETP 2009, IEA and Ph Mathieu, ULg
Availability	89.5	%	"Combined-Cycle, gas and steam turbine power plants", 2nd edition, Rolf H. Kehlhofer, Judy Warner, Henrik Nielsen and Rolf Bachmann.
Life Time	30	years	
Net efficiency (ProdEff_sto)	57	%	IEA CS 2009
Year of efficiency (ProdEffRefY)	2010		
Capture efficiency	---		
TL_Inv (TL_INV_sto)	-		Calculation based on IEA CCS 2009
	0.101		
Inv ref year (TLRefY_INV_sto)	2005		
TL_Eff (TL_ProdEff_sto)	0.062		
Eff ref year (TLRefY_ProdEff_sto)	2005		

2.3.4.1.2. Plants with post-combustion capture

Coal plants:

As above mentioned, it has been chosen to gather the various post-combustion capture technologies into one single technology called "post-combustion capture", for each type of fuel. Compared to the reference coal plant, the efficiency is reduced by 9 % points.

Table 2.XVI. PC plant with post-combustion capture

Parameter ID	Value	Unit	Source
Year of commercialization	2020		
Investment (Inv0_dbl)	2304	Euro 2010/kW	IEA CCS 2009
Year of investment (Inv0RefY)	2010		IEA CCS 2009
VOM	2.77	Eur / GJ	Time Be CCS
FOM	34.49	Eur/kW	Time BE CCS
Production Capacity	427	MW	ETP 2009, IEA and Ph Mathieu, ULg
Availability	85.5	%	
Life Time	40	years	
Net efficiency (ProdEff_sto)	38	%	IEA CCS 2009
Year of efficiency (ProdEffRefY)	2010		
Capture efficiency	85	%	
TL_Inv (TL_INV_sto)	-0.138		Calculation based on IEA CCS 2009
Inv ref year (TLRefY_INV_sto)	2005		
TL_Eff (TL_ProdEff_sto)	0.091		
Eff ref year (TLRefY_ProdEff_sto)	2005		
CO ₂ pressure	137	bars	

Natural gas combined cycled plants:

The penalty compared to reference combined cycle is 8 % points. Capture efficiency is related to the energy penalty. When capture efficiency increases, then the energy penalty increases too.

Table 2.XVII. NGCC plant with post-combustion capture

Parameter ID	Value	Unit	Source
Year of commercialization	2030		
Investment (Inv0_dbl)	930	Euro 2010/kW	IEA CCS 2009
Year of investment (Inv0RefY)	2010		IEA CCS 2009
VOM	0.72	Eur / GJ	Time Be CCS
FOM	14.20	Eur/kW	Time BE CCS
Production Capacity	412	MW	ETP 2009, IEA and Ph Mathieu, ULg
Availability	89.5	%	
Life Time	30	years	
Net efficiency (ProdEff_sto)	49	%	IEA CS 2009
Year of efficiency (ProdEffRefY)	2010		
Capture efficiency	85	%	
TL_Inv (TL_INV_sto)	-0.126		Calculation based on IEA CCS 2009
Inv ref year (TLRefY_INV_sto)	2005		
TL_Eff (TL_ProdEff_sto)	0.083		
Eff ref year (TLRefY_ProdEff_sto)	2005		
CO ₂ pressure	137	bars	

2.3.4.2. Pre-combustion capture

In the power generation field, pre-combustion capture of CO₂ is often combined with Integrated Gasification Combined Cycle (IGCC): after CO₂ capture, the hydrogen is directed to an adapted gas turbine that can run on hydrogen rich fuel gas.

There are many advantages to use IGCC, even without capture because it may offer, in certain cases, a flexibility regarding the fuel (coal, mix of low quality coal and petcoke, biomass,...), it can produce H₂ as byproduct and be flexible regarding outputs (H₂ or electricity). In addition it has the potential to reduce emissions more than PC plants.

The pre-combustion capture technology development depends on the development of gasification, H₂ gas turbine, air separation, downstream processes, high temperature materials... So far, IGCC's do not capture CO₂. Small pilot tests are performed at the IGCCs in Buggenum, the Netherlands and Puertollano in Spain. There are still a lot of barriers such as H₂ gas turbine which hasn't been fully developed yet.

2.3.4.2.1. Reference plant

This reference is a plant without capture. Table 2.XVIII summarizes data for an IGCC with no capture. In this case, the syngas (CO + H₂) is directly burnt in a gas turbine and there is no shift and capture unit.

Table 2.XVIII. Reference IGCC

Parameter ID	Value	Unit	Source
Investment (Inv0_dbl)	1649	Euro 2010/kW	IEA CCS 2009
Year of investment (Inv0RefY)	2010		IEA CCS 2009
VOM	1.26	Eur / GJ	Time Be CCS
FOM	36.90	Eur/kW	Time BE CCS
Production Capacity	488	MW	ETP 2009, IEA and Ph Mathieu, ULg
Availability	85	%	
Life Time	30	years	
Net efficiency (ProdEff_sto)	44	%	IEA CCS 2009
Year of efficiency (ProdEffRefY)	2010		
Capture efficiency	---	%	
TL_Inv (TL_INV_sto)	-0.108		Calculation based on IEA CCS 2009
Inv ref year (TLRefY_INV_sto)	2005		
TL_Eff (TL_ProdEff_sto)	0.127		
Eff ref year (TLRefY_ProdEff_sto)	2005		

2.3.4.2.2. IGCC with capture

Once again, by adding capture, the overall performances decrease. The techniques used to separate CO₂ from H₂ are diverse⁷ and depend on the particular stream conditions. The capture process is not critical since there is another barrier to the technology emergence: the H₂ turbine. This latter still must be developed.

The penalty of the capture greatly depends on the type of gasifier, particularly the pressure at which the gasification occurs. A high pressure gasifier will lead to a small penalty when capturing by flashing (selexol) because a great pressure difference can be performed, thereby avoiding a high heat loss to recover CO₂.

Table 2.XIX presents data for IGCC plant equipped with carbon capture:

Table 2.XIX. IGCC with capture

Parameter ID	Value	Unit	Source
Year of commercialization	2020		
Investment (Inv0_dbl)	2156	Euro 2010/kW	IEA CCS 2009
Year of investment (Inv0RefY)	2010		IEA CCS 2009
VOM	1.38	Eur / GJ	Time Be CCS
FOM	43.11	Eur/kW	Time BE CCS
Production Capacity	436	MW	ETP 2009, IEA and Ph Mathieu, ULg
Availability	85	%	
Life Time	30	years	
Net efficiency (ProdEff_sto)	35	%	IEA CCS 2009
Year of efficiency (ProdEffRefY)	2010		
Capture efficiency	85	%	IEA CCS 2009
TL_Inv (TL_INV_sto)	-0.124		Calculation based on IEA CCS 2009
Inv ref year (TLRefY_INV_sto)	2005		
TL_Eff (TL_ProdEff_sto)	0.196		
Eff ref year (TLRefY_ProdEff_sto)	2005		
CO ₂ pressure	137	atm	

⁷ Physical absorption is preferred (Solexol, Rectisol...) but it is also possible to use chemical solvents, membranes, calcium oxides...

2.3.4.3. Oxyfuel technologies

2.3.4.3.1. Reference plants

As for the other technologies, the oxyfuel can run without capturing the CO₂. But as already mentioned, the capture station is not the most critical here. Indeed, the ASU consumption is the big change along with the new burner technology. Therefore, building an oxy-fuel plant that does not capture CO₂ does not make sense from an economical point of view. And should not then been chosen as reference.

For this reason, it has been decided that the reference plants of oxyfuel technology are:

- For coal plants: ultra supercritical PC plant (cf section 2.3.4.1.1 Reference plants)
- For gas plants: combined cycle (cf section 2.3.4.2.1 Reference plant)

2.3.4.3.2. Capture plants

This section presents the estimated performance and costs of oxy-fuel combustion technologies equipped with capture. It is important to note that the technology learning coefficients of the oxyfuel technology applied to a gas burner has been assumed to be the same than post-combustion capture on gas fired combined cycle power plant. Indeed, the lack of information on the oxy-gas development has led to this approximation.

Plant availabilities have been assumed to be the same as the reference plants. The penalties compared to the references are – 10 % point for oxy-coal plant and – 9 % point for oxy-gas plant. The capture rate for oxyfuel is better than for all other technologies: 90 % for oxy-coal plant and 95 % for oxy-gas (IEA CCS, 2009).

Coal plants:

Table 2.XX. Reference oxy-coal plant with capture

Parameter ID	Value	Unit	Source
Year of commercialization	2020		
Investment (Inv0_dbl)	2368	Euro 2010/kW	IEA CCS 2009
Year of investment (Inv0RefY)	2020		IEA CCS 2009
VOM	1.20	Eur / GJ	Time Be CCS
FOM	44.38	Eur/kW	Time BE CCS
Availability	85.5	%	
Life Time	30	years	
Net efficiency (ProdEff_sto)	37	%	IEA CCS 2009
Year of efficiency (ProdEffRefY)	2020		
Capture efficiency	90	%	
TL_Inv (TL_INV_sto)	[-.1 -.3]		Own estimation
Inv ref year (TLRefY_INV_sto)	2005		
TL_Eff (TL_ProdEff_sto)	0.339		
Eff ref year (TLRefY_ProdEff_sto)	2005		
CO ₂ pressure	137	bars	

Natural Gas Combined Cycle plants:

Table 2.XXI. Oxy-gas plant with capture

Parameter ID	Value	Unit	Source
Year of commercialization	2030		
Investment (Inv0_dbl)	1120	Euro 2010/kW	IEA CCS 2009
Year of investment (Inv0RefY)	2020		IEA CCS 2009
VOM	0.75	Eur / GJ	Time Be CCS
FOM	14.91	Eur/kW	Time BE CCS
Availability	89.5	%	
Life Time	30	years	
Net efficiency (ProdEff_sto)	48	%	IEA CCS 2009
Year of efficiency (ProdEffRefY)	2020		
Capture efficiency	95	%	
TL_Inv (TL_INV_sto)	-0.126		Calculation based on IEA CCS 2009
Inv ref year (TLRefY_INV_sto)	2005		
TL_Eff (TL_ProdEff_sto)	0.083		
Eff ref year (TLRefY_ProdEff_sto)	2005		
CO ₂ pressure	137	bars	

2.3.4.4. Electricity sector: discussion of costs and performance

Previous section provides the main figures of the various technologies. This section briefly aims at comparing these data in order to understand what is at stake.

2.3.4.4.1. Investment costs

Figure 2.60 compares the different investment costs of all the power plant that have been considered. Nevertheless, all these option seem currently attractive because of other parameters such as flexibility on fuel, flexibility of operation, cost of fuel, etc. In general, gas power plants are cheaper, per unit of installed power but gas is more expensive than coal and more volatile which make gas options more risky.

The gray bars represent coal plants while green are for gas plants.

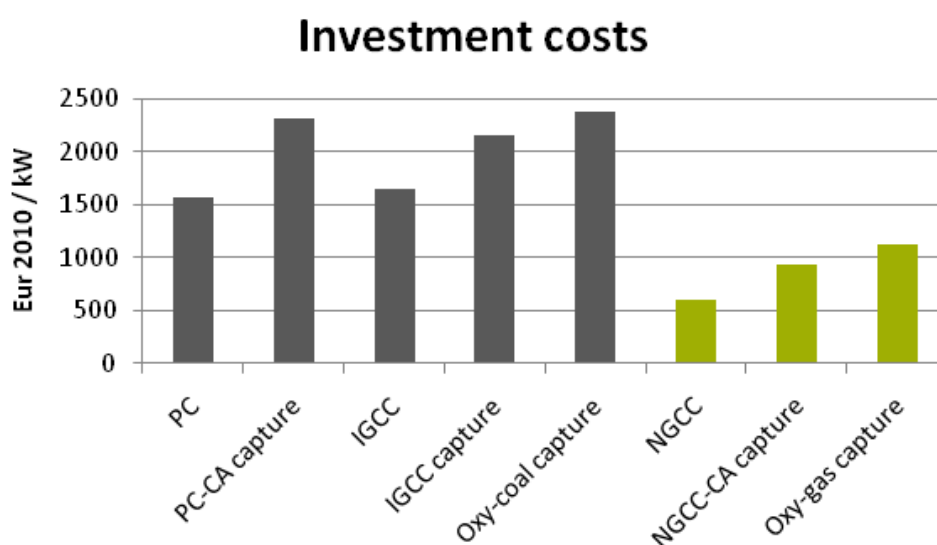


Figure 2.60. Investment costs. CA stands for chemical absorption

Investment costs for the three main coal based technologies equipped with capture, are quite competitive. Under these circumstances, the choice for a particular technology will be determined by other characteristics such as efficiency, reliability, variable operating costs. Actually it seems that oxy-fuel and post-combustion capture will be first developed, thereby leaving pre-combustion behind.

For gas plants, oxyfuel technology is assumed to be a little more expensive than post-combustion capture.

2.3.4.4.1.1. Effect of technology learning on investment costs

Since CCS refers to a bunch of emerging technologies, it has a great potential for improvement. In the future, costs will decrease while efficiency will increase. It is a difficult task to assess by how much these variables will change. That is why it is necessary to keep in mind that the results presented here are estimation calculated based on an IEA report (IEA, 2008a).

The following graph represents the reduction of investment over time, as a result of technology learning. Existing technologies have a small potential for improvement compared to emerging ones. In 2050, one can observe that the three coal technologies with capture present similar investment cost (about 1700 Eur/kW), in spite of much high cost for oxy-coal in 2020⁸.

Gas technologies with capture present similar cost in 2010 but oxy-gas appears to be the least cost option by 2050.

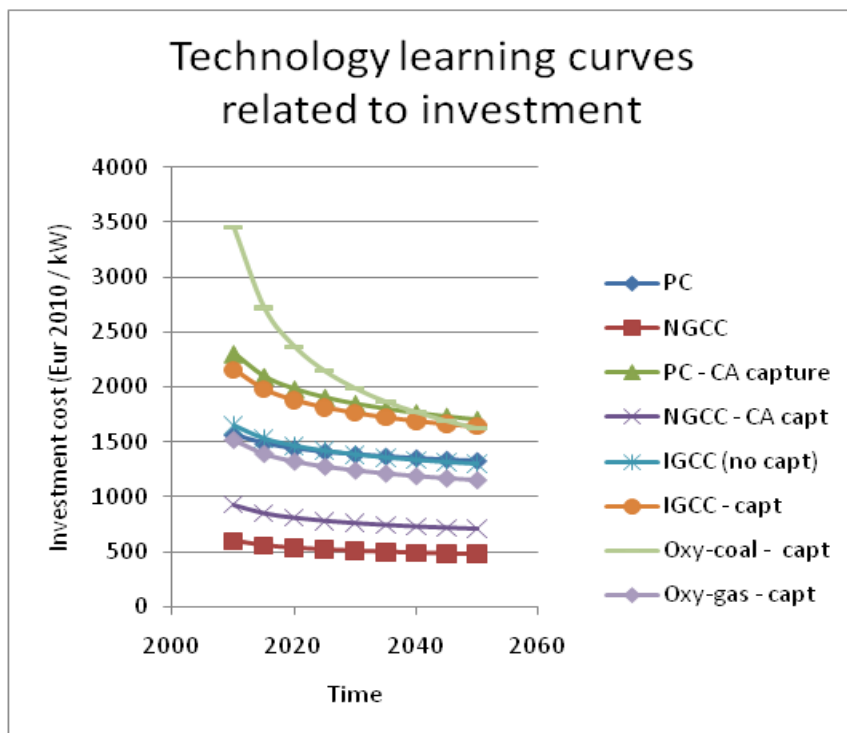


Figure 2.61. TL for investment

2.3.4.4.2. Efficiencies

Figure 2.62 represents the efficiencies of all analyzed technologies, making comparison easy. Basically, capturing CO₂ from a coal plant make the efficiency decrease by about 9 to 10 % points compared to the reference while gas plants present a slightly lower penalty (8 % points). In general, gas plants are more energy efficient than coal plant whether capture is installed or not.

⁸ A very high investment cost of oxy-coal in 2010 is due to the fact that calculation is based on data from 2020, not 2010.

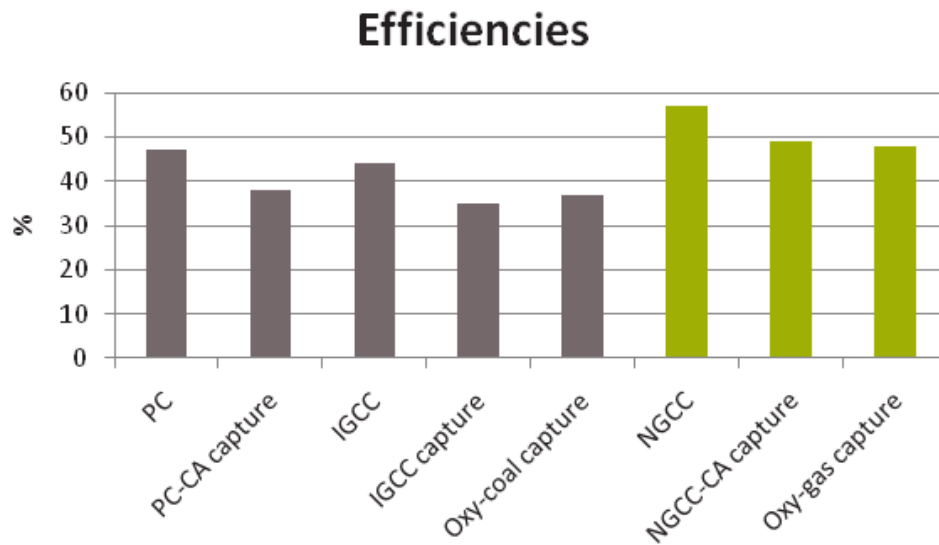


Figure 2.62. Efficiencies

2.3.4.4.2.1. Technology learning on efficiency

The evolution of the efficiency for each technology through time is represented in Figure 2.63:

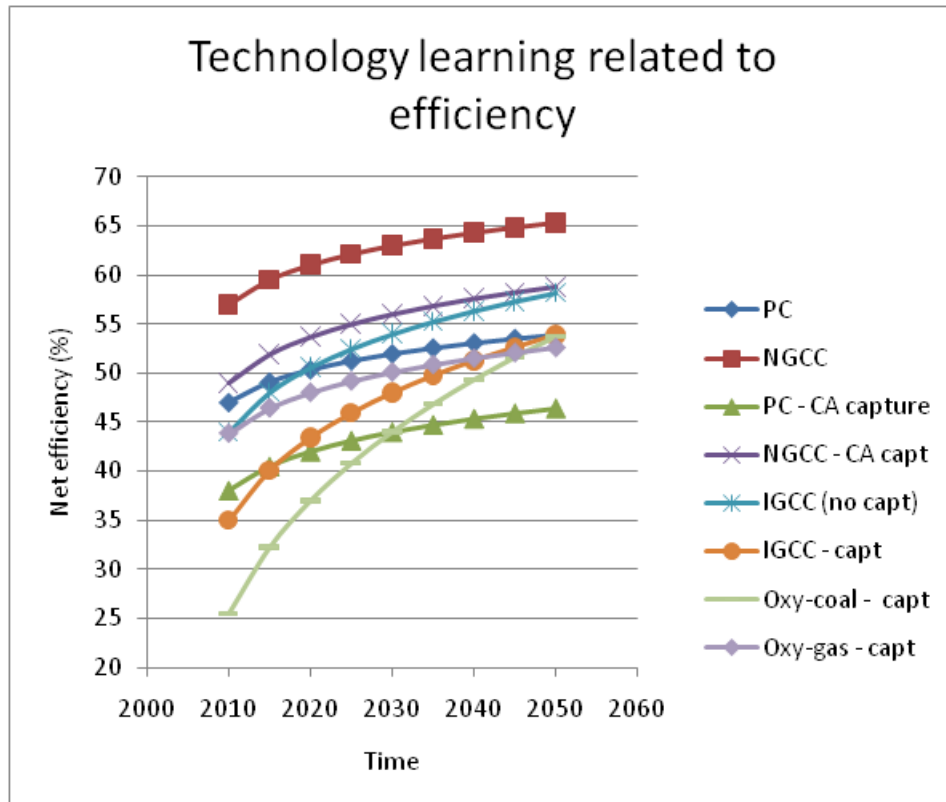


Figure 2.63. Evolution of efficiencies

Oxy-coal technology presents the greatest evolution while PC, although the best coal technology in the beginning, is gradually surpassed, first by IGCC-capture then by oxy-fuel. It is important to keep in mind the commercial availability of the various technologies: for example, IGCC-capture will improve from today until 2030 but will only appear in the market at that time (2030).

The concept of technology learning is easily accepted on theoretical grounds. However, when it comes to quantifying the speed and the sources of improvement (learning by doing, learning by research) then it is still an area of discussion. Often technologies improve a lot while others never reach the critical mass.

2.3.4.4.2.2. Cost of electricity and Emission Trading Scheme (ETS)

An important figure is the cost of electricity (COE). It encompasses the annuities due for investment, the O & M costs, the fuel cost, the transport and storage cost (in case of carbon capture) and the ETS cost (in case of trading system). Being added up, these costs represent the COE whose breakdown can be seen in Figure 2.64.

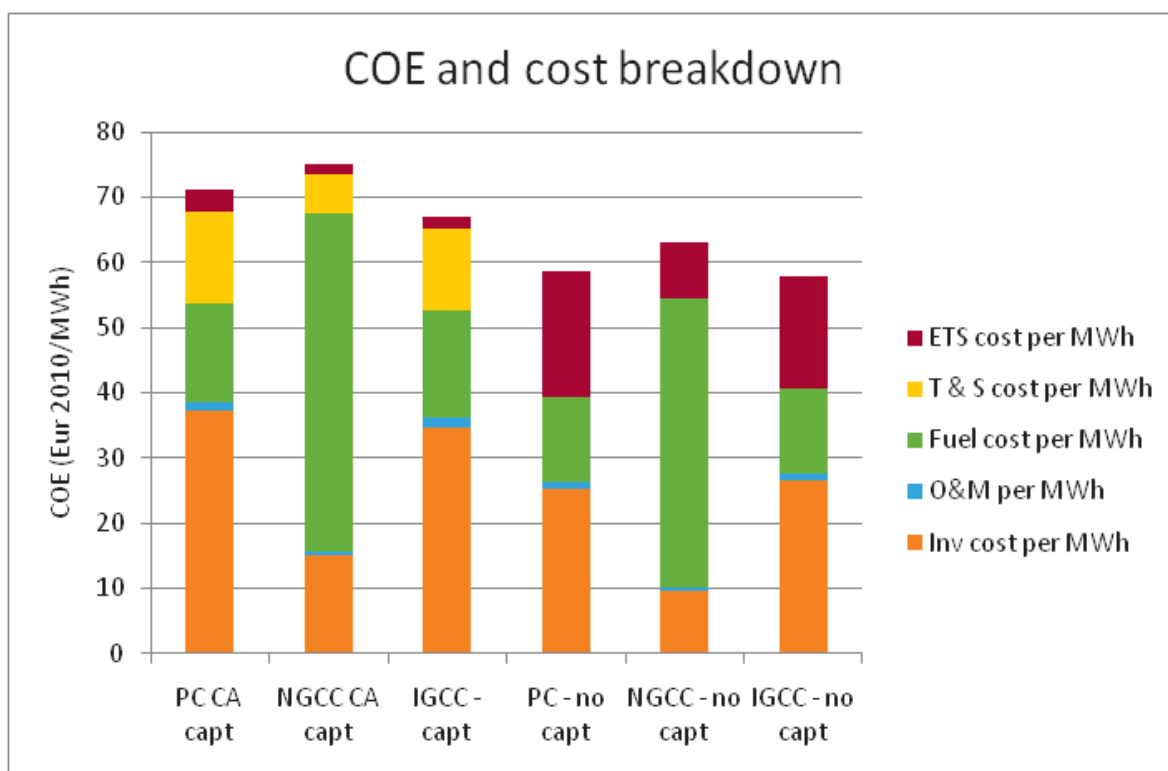


Figure 2.64. COE

In this figure, the ETS has been chosen at 25 Eur/t of CO₂. It is easy to observe that the emission trading system can act as a leverage for emerging technologies. Nevertheless, with the current technologies (2010 performance figures), even a 25 Eur/tCO₂ ETS price is not sufficient to make CCS competitive with common technologies. Indeed, for each technology, the COE remains smaller without CCS.

However, previous sections presented a large potential of technology improvement that will further reduce CCS cost. Combined with an increasing ETS price, CCS technologies could be cheaper in the future.

With the today's technology, the ETS price should be about 45 Eur/t CO₂ to make PC plant with CA CCS advantageous compared to PC plant, as observed on the next figure:

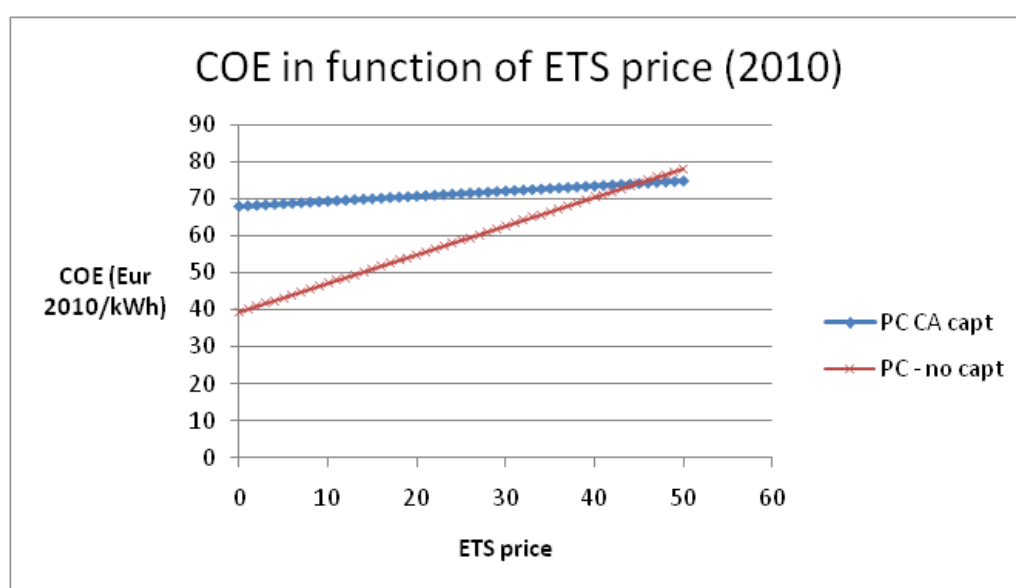


Figure 2.65. COE in function of ETS price for PC plant with and without CCS

It is very important to keep in mind that these figures are very depending on fuel price. Gas price is strongly volatile and therefore, it is hard to make assumption on such price. To avoid confusion, the assumptions used for calculation are presented here below.

Assumptions:

- Coal price: 1.59 Eur₂₀₁₀/GJ
- Gas price: 7.43 Eur₂₀₁₀/GJ
- Coal LHV: 28.3 MJ/kg
- Gas LHV: 48.2 MJ/kg
- Transport and storage cost: 17 Eur₂₀₁₀/t CO₂

2.3.4.5. CCS ready and retrofit options

2.3.4.5.1. Concept & Principles

A CCSR plant is intended to be retrofitted with CCS technology when the necessary regulatory and economic drivers are in place. Essential requirements for CCRS are:

- that a detailed engineering study demonstrates that the facility is technically and economically capable of being retrofitted with CCS capturing technology. This requires that the likely capturing technology is chosen;
- that the capture technology can be connected to the existing equipment without excessive outage period and that there will be sufficient space to construct and operate capture and compression facilities;
- that realistic pipeline routes for transport are identified;
- that potential storage sites have been appropriately assessed, suitable for safe storage of the project lifetime;

2.3.4.5.2. Capturing technology options

The choice of the technology has considerable consequences for the original design of the power plant. Whatever the choice, it seems that there is a penalty, either in terms of construction costs, either in terms of efficiency losses when a CCSR plant operates without retrofit.

Post combustion capturing technology requires huge amount of heat for the regeneration of the solvents. Estimates are in the range 2.7 and 3.3 GJ/t. For a PC plant this means that approximately 25 % of the heat produced in the boiler is required in the capturing process. This heat can be delivered at economic conditions if the plant is designed as a CHP plant, requiring specific dimensioning of the boiler and turbines. Another consideration relates to flue gas impurities. SO₂ and NO₂ degenerate the solvent and very low concentrations are desirable to avoid excessive losses of solvent.

Oxyfuel combustion capture also seems to be a feasible option for retrofit. Here considerations should be made about the boiler geometry and the recycling of CO₂. Flame temperature and heat capacity of gases to match fuel burning in air occurs when the feed gas used has a composition of approximately 35 % by volume of O₂ and 65 % (compared to 21 % in air) by volume of dry recycled CO₂ [2]

2.3.4.5.3. Performance and cost [3]

Different options for the design of a CCSR plant can be made with little or more additional costs. We consider a reference SCPC plant with a nominal capacity of 550 MW having a four steam turbine stages: one high, one intermediate, and two low-pressure stages.

	CCSR plant			CCS plant		
	\$000	MW	\$/kw	\$000	MW	\$/kw
NOT CCS ready	866	550	1575	1465	379	3865
Option 1	871	550	1584	1452	394	3682
Option 2	891	550	1620	1478	405	3651
Option 3	1110	550	2018	1568	546	2871

For Post combustion capturing the three options are:

- Option 1: This option considers only the front end engineering design. Once the CCS unit is installed, a throttle valve would be installed and used to extract the steam before the low –pressure steam turbine.
- Option 2: This option is more expensive but considers declutching the second low pressure steam turbine, which would improve heat rate performance
- Option 3: Considers over dimensioning of the steam boiler in order to avoid the loss in electricity generation. It is the most expensive option, but likely to be the most favourite one if the time lag for CCS investment is short.

	\$000	MW	\$/kw	\$000	MW	\$/kw
NOT CCS ready	866	550	1575	1248	420	2974
Option 1	870	550	1582	1247	420	2972
Option 2	873	550	1587	1257	431	2916
Option 3	881	550	1578	1266	443	2858

Oxy-fuel options are:

- Option 1: No additional equipment is purchased but provisions would be made in the front end engineering work for the recirculation of the flue gas back into the boiler and for the interconnection and integration of the air separation unit and the CO₂ compression plant.
- Option 2: Additionally includes the incorporation of an oversized turbo generator. In oxyfuel combustion approach some low grade heat becomes available from the flue gas recirculation, from the ASU and from the compression unit. This heat can be use to reheat condensate and feed water to improve the overall efficiency.
- Option 3: include additionally oversized gas turbine and cooling towers. In option two full recovery is constrained by steam turbine size and cooling capacity.

2.3.4.5.4. Retrofit model structure

Modelling retrofit in TIMES is not a standard option and requires a specific approach. The structure presented in Figure 2.66 can be used for this purpose. In this representation, investment of the CCSR plant is represented as a separate process, linking both to the CCSR plant and the CCS plant. The capacity loss due to the capturing is represented by using a higher capital input requirement for the plant with capturing. Additional investment costs for the CCS technology are defined inside the SCPC plant. This scheme has not been implemented in the TIMES simulations of PSS-CCS II. The option of building retrofittable power plants is embedded in the PSS II simulator, but is based on a different methodology.

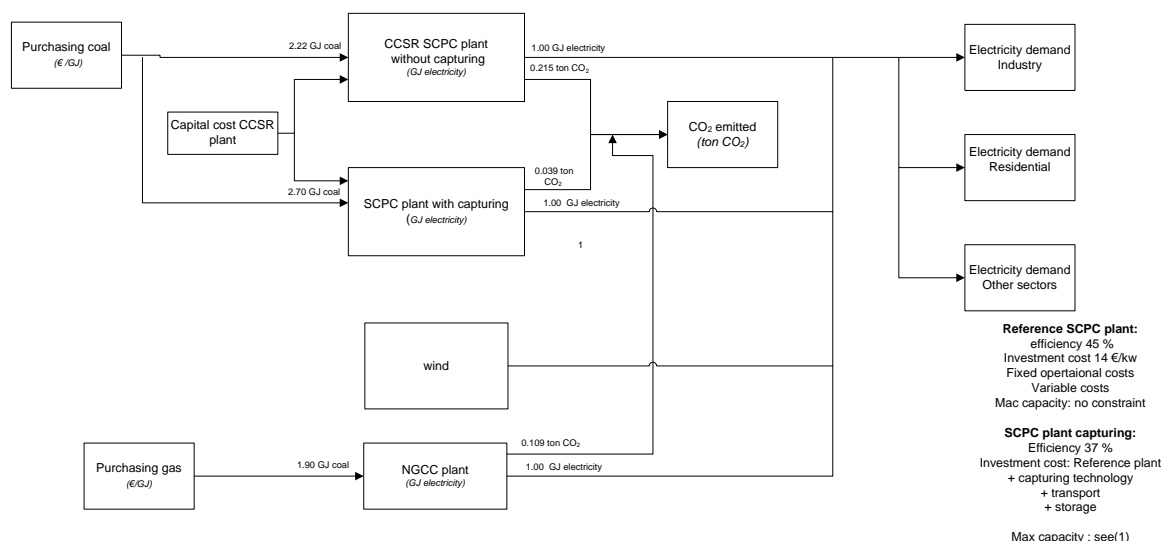


Figure 2.66. Model structure for retrofit option in TIMES

2.3.4.6. Conclusions

- A. Performance of the classical methods for capturing CO₂ has not been improved since their estimation by IPCC in 2005. Nevertheless, knowledge on these technologies has switched from the theory (models) into actual pilot scale units.
- B. A lot of emerging technologies have appeared and some present advantages compared to classical options. These technologies should play a role in a long term perspective.
- C. Nowadays, capture technologies on coal plants have similar penalties (9 – 10 % points) compared to gas plants (about 8 % points).
- D. Investment costs are about 66% higher for capture on a coal plant compared to the reference plant.
- E. Oxy-gas seems more interesting than CA on gas plant from an investment cost perspective.
- F. Technology learning can be predicted up to 2050 but introduces high uncertainties.

2.3.5. CO₂ capture in the cement industry

2.3.5.1. Introduction

Capturing CO₂ from a cement plant is an option that cannot be missed. Indeed, cement plants are very large sources of CO₂ emissions: 1.8 Gt/y in 2005 worldwide, which is 6 % of global emissions from the use of fossil fuel (Barker et al, 2009). At the same time, **the CO₂ concentration in the flue gas is higher** than in power plants (25 – 35 %). This would make them a better candidate because CO₂ can theoretically be extracted easier.

On the other hand, cement fabrication **involves multiple processes that release CO₂**. Depending on the type of fuel and the type of cement, about 30-50% of the CO₂ emitted comes from the fuel while 50-70% comes from the decomposition of carbonate mineral, i.e. the process. So, the CO₂ emissions are inherent to the process. Options for reducing CO₂ emissions are: increase the use of metal slack for clinker, use of biomass, improve the energy efficiency. However, energy efficiency has already been improved, leaving less opportunities for further improvement and the process emissions in clinker production are difficult to avoid. Consequently capturing CO₂ seems to be an interesting option to drastically reduce CO₂ emissions from cement plants.

Several capture technologies are currently being developed but none of them has had a commercial application so far. **This chapter aims at presenting the capture technologies, the performance of the plant with the capture process, the economics of such plant and the timeframe of technology development.** Other technologies for improving plant efficiency will also be briefly described.

2.3.5.2. Cement fabrication... how it works.

2.3.5.2.1. The cement

Cement is composed of calcium silicate, calcium aluminate and calcium aluminoferrite mineral. It is produced from a mixture of raw materials:

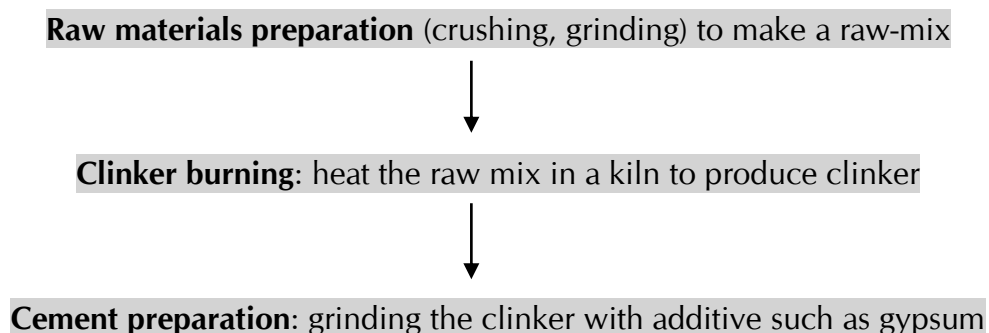
- Primary raw material is the calcium carbonate that will provide lime.
- Secondary materials are alumino-silicate clays and shales, silica sand, bauxite and iron ore.

The secondary materials will provide silica, alumina and iron oxide that will be combined with the lime, provided by the primary material.

The major characteristic of cement is its hydraulic binding properties. When the powder cement is mixed with appropriate amount of water, it becomes a hard paste which binds together sands and aggregates. The most common cement is the "Portland cement", whose composition is 95% clinker and 5% gypsum.

2.3.5.2.2. General process of cement production

There are four different ways of producing cement: the wet process, the semi-wet process, the semi-dry process and the dry process. The four of them involve the same process cascade:



In the second stage (clinker burning), several reaction will take place at different temperatures. These reactions are described here below, based on CEMBUREAU 1999 material:

Kiln temperature (°C)	Chemical reaction
20 – 900	Drying and preheating: the release of free and chemically bound water
850 – 950	Calcination: the release of CO ₂ from calcium carbonate (limestone) and initial reactions with formation of clinker minerals and intermediate phases
1250 – 1450	Sintering or clinkerisation: the formation of calcium silicates and partial melting
1350 – 1200	Kiln internal cooling: crystallisation of calcium aluminate and calcium ferrite from the partial melt

The main difference between the four processes is the moisture content of the feed going into the kiln. Along time, the cement production techniques have evolved from a wet process to a dry process because this latter requires less energy. The dry process is here below described.

2.3.5.2.3. Cement production using dry process:

A complete production scheme can be viewed in Figure 2.67 while a simple schematic is presented in Figure 2.68.

The cement production follows these stages:

- **Drying and grinding plant:** the raw material is first crushed then ground and dried in mills. The drying can be done by sweeping hot exhaust gas from the kiln.
- **Homogenizing and storage silos:** the raw mix is blended and homogenized using compress air.
- **Preheater:** the raw mix goes through several heat exchangers made of cyclones in series, in which the hot exhaust gas heats up the raw mix. Partial calcination can already take place in the preheater.
- **Precalciner:** a precalciner can be installed before the kiln to ensure complete calcinations of the mix prior to entering the kiln. Its installation improves energy consumption at the kiln level.
- **Kiln:** the clinker is produced by burning the mix entering the kiln.
- **Gypsum and additive components mixing:** After cooling, the clinker is mixed with gypsum and other additive in order to achieve desirable characteristics.
- **Transport.**

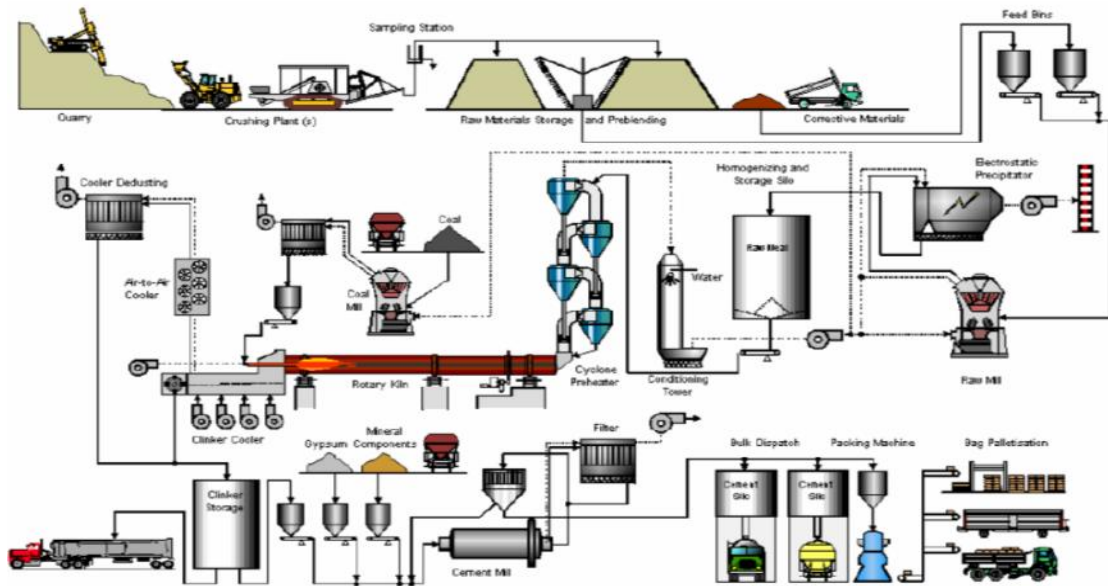


Figure 2.67. Cement production by dry process (detailed)

In the simplified Figure 2.68, the preheater, the precalciner and the rotary kiln are well separated. Nevertheless, in actual plants, they are in a row, close to each other. The precalciner is optional and leads to savings in fuel consumption. Indeed, it is possible to reduce the fuel consumption by 5 – 10 %. In case of precalciner, 60 – 70 % of the fuel is burnt in the latter while the remaining is burnt in the main burner of the rotary kiln.

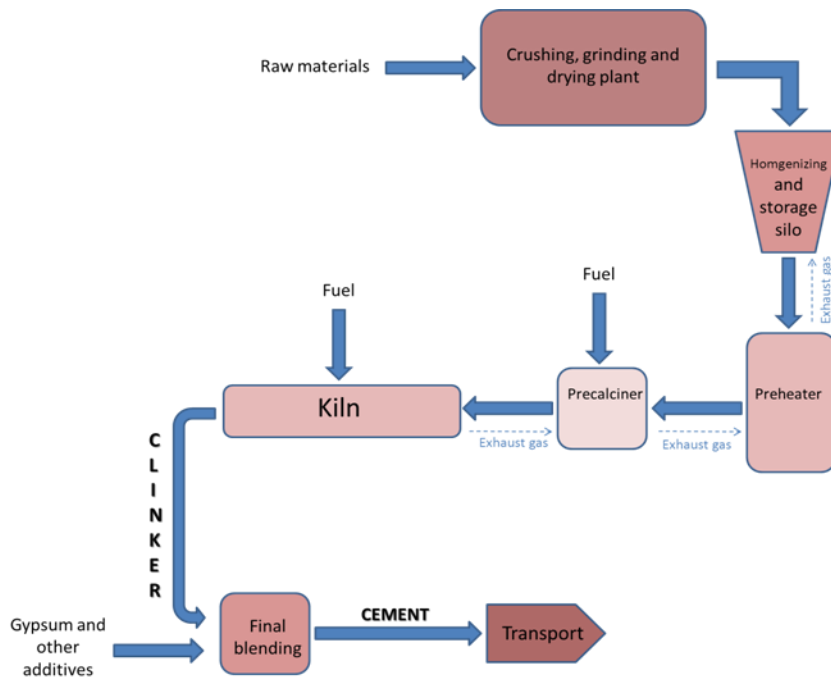


Figure 2.68. Cement production: schematic

Figure 2.69 helps to realize practically the arrangement of the preheater, precalciner and rotary kiln.

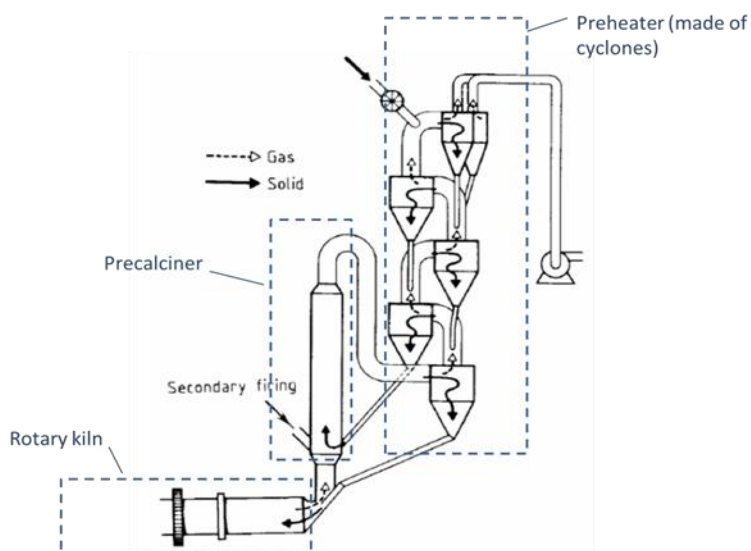


Figure 2.69. Preheater - Precalciner - Rotary kiln

2.3.5.2.4. Sources of CO₂ in a cement plant

There are three main sources of CO₂ in a cement plant: the calcinations, the fossil fuel combustion and the use of electricity.

A. Calcination:

The conversion of limestone to CaO necessarily releases CO₂, it is intrinsic to the cement making process:



The amount of CO₂ produced by this reaction represents the major part of CO₂ emissions (0.5 kgCO₂/kg Clinker).

B. Fossil fuel combustion:

Fuel is burnt at one end of the kiln and, possibly, in the precalciner. Combustion releases CO₂ and produces the desirable heat.

C. Electricity use:

A cement plant needs electricity at various levels to power machinery (mainly grinding).

2.3.5.3. Carbon capture from cement plants

There are many ways to reduce the CO₂ emissions from a cement plant. Before considering the installation of capture equipment, the plant should be checked for its environmental performance. Here are the various ways to reduce carbon intensity (Hendriks et al., 1998):

- Improvement of the energy efficiency of the process
- Shifting to a more energy efficient process (for example: semi-wet to semi-dry)
- Replacing high carbon fuels by low carbon fuels
- Replacing fossil fuels with alternative fuels
- Applying low clinker/cement ratio
- Removal of CO₂ from the flue gas

2.3.5.3.1. Capture technologies

Since a large amount of CO₂ originates from the non-fuel-related raw material, pre-combustion technologies will not be able to capture these emissions. For this reason, pre-combustion will not be envisaged for cement plants. Three main techniques are considered by the scientific community:

- ✓ Post-combustion capture using chemical absorption
- ✓ Oxy-combustion
- ✓ Chemical looping using calcium oxides

As for the electricity sector, there are many fields of research and development for each of these basic methodologies.

2.3.5.3.1.1. Post-combustion capture using chemical absorption

The post combustion process is similar to the one envisioned in the power sector: a chemical solvent absorbs CO₂ in a column (the absorber), the rich solvent, containing CO₂ is then directed to another column (the stripper) where the solvent releases CO₂ by supply of hot steam. The major energy requirement is the heat to produce the desired amount of steam. By choosing post-combustion capture, the core of the cement plant remains almost unchanged which is advantageous. The only difference is the addition of an SCR between the preheater and the raw mill which will reduce the temperature of the flue gas for drying the raw mill. If the SO₂ content is too high for amine based solvent, then an FGD should be placed after the drying.

Nowadays, an efficient kiln burning coal produces 800 kg of CO₂ per tonne of clinker. The capture rate can be up to 95 % when using chemical absorption nevertheless, the techno-economical optimum is lower. The regeneration energy is about 2.8 GJ/t clinker and the electricity required is about 0.2 GJ / t clinker (Barker et al, 2009).

Several configurations exist, depending on the plant type, the CO₂ streams to be captured... A model done by IEA has chosen a dry-type plant, with the configuration shown in Figure 2.70. Indeed, opposed to other configurations, this one allows to capture all of the CO₂ emitted from the cement plant, with minimal impact on standards process and easy potential retrofit.

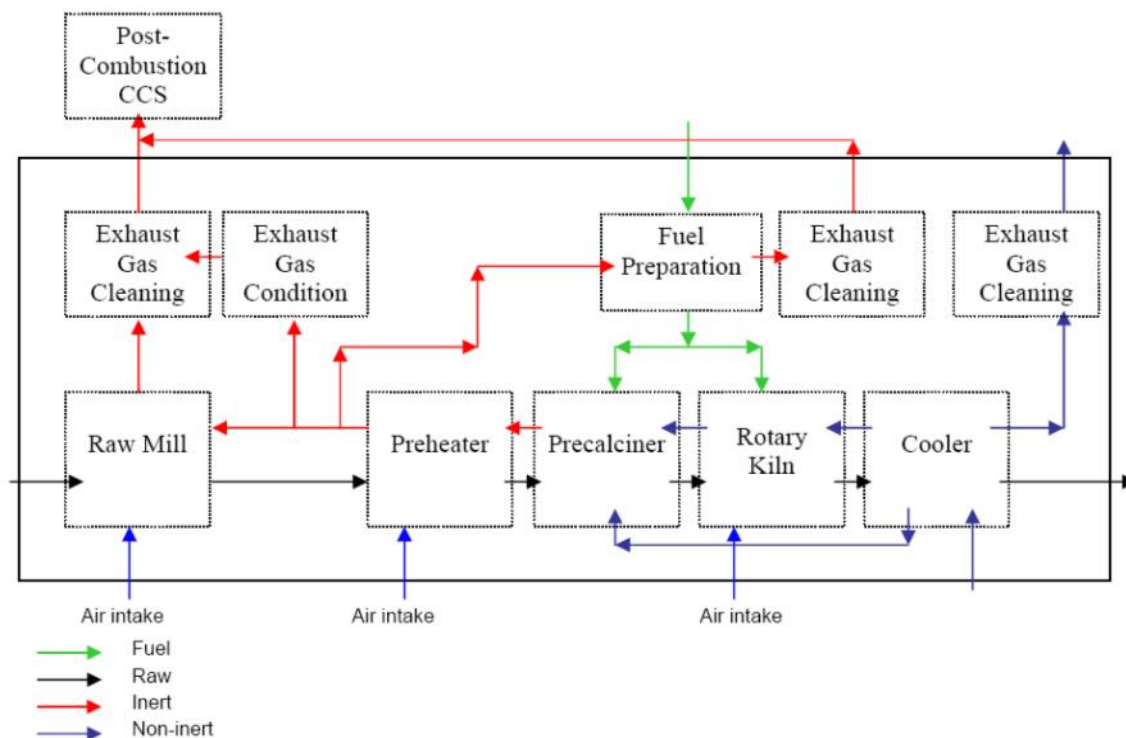


Figure 2.70. Post-combustion capture on cement plant

The major changes from conventional cement plant are (Barker et al, 2009) :

- An SCR is installed between the preheater and the raw mill for NO_x abatement.
- Regeneration heat is produced thanks to an auxiliary boiler or CHP plant who's CO₂ is also captured.
- An FGD is installed on the off-gas path.
- A CO₂ capture station based on chemical solvent is installed.
- A compression and dehydration unit is set up.

Post-combustion processes are currently strongly studied for coal power plant. The same technology should be suitable for cement plant, but the dimensioning of the absorbers and strippers should be based on a higher CO₂ content in the flue gasses.

2.3.5.3.1.2. Oxy-fuel technology applied to cement plants

Oxy-fuelling a cement plant is based on the same concept as oxy-fuelling a power plant. The oxidant is near pure oxygen, produced by cryogenic separation in an ASU. The combustion temperature is controlled thanks to a recirculation of the flue gas. The main constituent of the flue gas is CO₂ (about 80%mol, dry basis). This off-gas is purified to reach 95% CO₂ in a cryogenic separation unit during compression.

It has been decided to analyze the configuration with only the precalciner oxy-fuelled (Figure 2.71). In fact, this scheme avoids a CO₂ atmosphere inside the kiln that could impact the clinker production process; minimizes air ingress troubles in the kiln. Moreover, it seems the lowest risk option and the most cost-effective because it does not affect the plant but the precalciner. Nevertheless, oxy-fuel in both rotary kiln and precalciner should be investigated in further works.

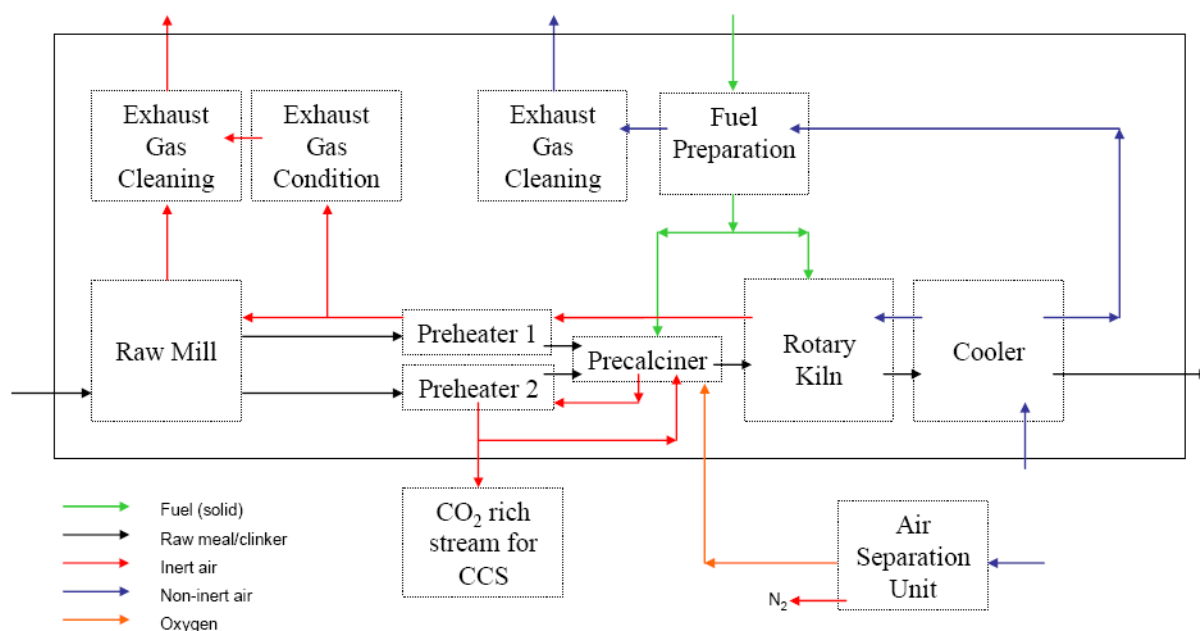


Figure 2.71. Cement plant with oxy-fuelled precalciner and CO₂ capture

In this configuration, there are two preheaters to allow a similar preheating capacity but to prevent mixing the two flue gas streams (Air atmosphere flue gas and CO₂ atmosphere flue gas).

2.3.5.3.1.3. Chemical looping using calcium oxide

This technology has been explained earlier among the post-combustion capture emerging technologies. Cement plants operators are used to handle materials such as CaCO₃ and CaO. That is why it would be suitable to capture CO₂ out of the flue gas by using CaO as carrier.

A major barrier to the deployment of this technology is the stability of CaO/CaCO₃ particles which can only withstand a limited number of cycles (IEA, 2008a). Since this technology is not known enough, it will not be considered for the cement industry

2.3.5.3.2. Carbon capture form cement plants: Data

2.3.5.3.2.1. Performance of a reference cement plant

Before analyzing a cement plant with capture, it is important to set a reference plant. The next tables gather parameters, inputs and outputs of a reference new-built cement plant. Values come from "CO₂ capture in the cement industry" (IEA, 2008a).

Table 2.XXII. Reference cement plant

	Parameter ID	Value	Unit	Source
Inputs	Coal	1.638	PJ	63 317 t/y with LHV coal = 25.87 MJ/kg) 32 876 t/y with LHVpet coke = 34.16 MJ/kg) 80 809 MWh Appendix A of IEA 2008/3
	Petroleum Coke	1.123	PJ	
	Electricity	0.291	PJ	
	Raw meal	1.535	Mt	
Outputs	Clinker	0.91	Mt	
	Cement	1	Mt	
	CO ₂ captured	0	Mt	
	CO ₂ emitted	728 422	t	
Performance	Capture efficiency	0	%	
	CO ₂ avoided	--		
	CO ₂ associated with power import-export	42	t	
	Overall net CO ₂ emissions	770 400	t	
Costs	CO ₂ emissions avoided including power import - export	--		
	Investment	263	MEur/MtCement/y	
	VOM	17	MEur	
	FOM	19	MEur/MtCement/y	
	Cost of avoidance	--	Eur/t CO ₂ avoided	
	Cost of cement production	65	Eur/t of cement	

2.3.5.3.2.2. Performance of post-combustion capture from cement plants

A study realized by IEA GHG (CO₂ capture in the cement industry, 2008/3) analyzed performance of a cement plant equipped with post-combustion capture using a common chemical solvent: MEA. This choice is quite conservative since. Nevertheless, it is a good analysis of the technology potential in 2010.

The analyzed plant is a normal size plant, producing 1 Mt/y of cement. The captured CO₂ stream is 99.9% pure and its pressure after compression is 11 MPa (110 bar). The capture rate of the overall equipment is 85 % which is also quite conservative but consistent with previously investigated power sector. Moreover, the stripping steam and electrical power are provided by an internal coal-fired CHP plant whose flue gas is also directed to the capture station.

The next table presents the performance of a cement plant equipped with post-combustion capture, using MEA process while the following table gathers details inputs and outputs in terms of submaterials. The technology learning on investment is assumed to be the same as PC plant with post-combustion capture. However, the choice of TL strategy is left to model builder provided no reliable data have been identified for assessing a potential learning.

Table 2.XXIII. Cement plant with post-combustion capture (MEA)

	Parameter ID	Value	Unit	Source
Inputs	Coal	7.54	PJ	291 633 t/y with LHV coal = 25.87 MJ/kg) 32 876 t/y with LHVpet coke = 34.16 MJ/kg) -22 734 MWh (CHP plant) Appendix A of IEA 2008/3
	Petroleum Coke	1.123	PJ	
	Electricity	-0.082	PJ	
	Raw meal	1.495	Mt	
Outputs	Clinker	0.91	Mt	
	Cement	1	Mt	
	CO ₂ captured	1 067 734	Ton	
	CO ₂ emitted	188 424	Ton	
Performance	Capture efficiency	85	%	
	CO ₂ avoided	540 000	Ton	
	CO ₂ associated with power import-export	- 11 822	Ton	
	Overall net CO ₂ emissions	176 600	Ton	
	CO ₂ emissions avoided including power import – export	593 841	Ton	
Costs	Investment	558	MEur/MtCement /y	
	VOM	31	MEur	
	FOM	35	MEur	
	Cost of avoidance	107.4	Eur/t CO ₂ avoided	
	Cost of cement production	129.4	Eur/t of cement	
Technology learning	TL_Inv (TL_INV_sto)	-0.138		
	Inv ref year (TLRefY_INV_sto)	2005		

Table 2.XXIV. Material and electricity in-outputs for cement plant with post-combustion capture

	Parameter ID	Value	Unit
Material inputs	Raw meal consumed	1 494 526	t/y
	Limestone for FGD	12 795	t/y
	Water for FGD	115 152	t/y
	Ammonia	1 855	t/y
	MEA make up	2 400	t/y
	Low pressure steam (3.5bar,141°C)	1 662 000	t/y
	Electricity consumption	333 666	MWh/y
Outputs	Clinker produced	910 000	t/y
	Cement produced	1 000 000	t/y
	Gypsum produced	16 374	t/y
	Net electricity exported	22 734	MWh/y
Technology learning	TL_Eff (TL_ProdEff_sto)	0.091	
	Eff ref year (TLRefY_ProdEff_sto)	2005	

The main barrier to post-combustion capture deployment in the cement industry is the cost. Indeed, without capture, a tonne of cement costs 65.6 Eur while the same tonne produced by a plant with post-combustion capture will cost 129.4 Eur, the double. This is due the need of hot LP steam and thus, the construction of a CHP plant. The amount of coal needed is by far larger than for the reference plant, also because of the CHP plant.

2.3.5.3.2.3. Performance of cement plant equipped with oxy-fuelled precalciner and CO₂ capture

Next tables present performance of a plant equipped with oxy-fuelled precalciner and CO₂ capture. The capture rate of the whole plant is 52 %. This low rate is due to the fact that only the CO₂ coming from the precalciner is the captured. The kiln is not oxy-fuelled so, its emissions are not captured. The technology learning related to investment is assumed to be the same than for a PC oxy-fuel plant

Table 2.XXV. Cement plant with oxy-combustion precalciner and CO₂ capture

	Parameter ID	Value	Unit	Source
Inputs	Coal	1.864	PJ	72 061 t/y with LHV coal = 25.87 MJ/kg)
	Petroleum Coke	0.925	PJ	27 091 t/y with LHVpet coke = 34.16 MJ/kg)
	Electricity	0.628	PJ	174 562 MWh
	Raw meal	1.508	Mt	Appendix A of IEA 2008/3
Outputs	Clinker	0.91	Mt	
	Cement	1	Mt	
	CO ₂ captured	465 014	Ton	
	CO ₂ emitted	282 853	Ton	
Performance	CO ₂ avoided	445 600	Ton	
	CO ₂ associated with power import-export	90 800	Ton	
	Overall net CO ₂ emissions	373 700	Ton	
	CO ₂ emissions avoided including power import - export	396 800	Ton	
Costs	Investment	327	MEur	
	VOM	22	MEur	
	FOM	23	MEur	
	Cost of avoidance	40.2	Eur/t CO ₂ avoided	
	Cost of cement production	81.6	Eur/t of cement	
Technology learning	TL_Inv (TL_INV_sto)	-0.343		
	Inv ref year (TLRefY_INV_sto)	2005		

Table 2.XXVI. Material and electricity in-outputs for oxy-combustion cement plant with CO₂ capture

	Parameter ID	Value	Unit
Material inputs	Raw meal consumed	1 508 424	t/y
	Oxygen (95%)	166 298	t/y
	Electricity consumption	174 562	MWh/y
Outputs	Clinker produced	910 000	t/y
	Cement produced	1 000 000	t/y
Technology learning	TL_Eff (TL_ProdEff_sto)	0.091	
	Eff ref year (TLRefY_ProdEff_sto)	2005	

2.3.5.3.3. Carbon capture from cement plants: Time frame

Research and development of CCS technologies applied to cement plant are currently done in theory and at lab scales. Pilot and demo plants are expected to be built and operated between 2015 and 2030. Commercialization should then get started from 2030 onwards.

Table 2.XXVII. Timeframe of CCS development for cement industry (Source: CO₂ capture and storage, a key abatement option; IEA 2008)

CCS	2008-2015	2015-2030	2030-2050
Technology stage	R&D	R&D demonstration	Demonstration commercial
Investment costs (USD/t CO ₂)	500	250-350	150-200
Emission reduction (%)	95	95	95
CO ₂ reduction (Gt CO ₂ /yr)	0	0-0.25	0.4-1.4

2.3.5.3.4. Carbon capture for cement plants: cost discussion

It is quite hard to compare the various technologies because there are very different. Post-combustion techniques require large amounts of steam and electricity. That is why a CHP on site has been preferred. Therefore, there is an export of energy (CHP generated electricity), as well as cement. This technology is very expensive and is not economically viable without any cut in the capital cost and increase of ETS price.

Figure 2.72 typically shows that post-combustion is by far much more expensive than the two other options, mainly because of its high capital cost. Nevertheless, it is the technology emitting the lowest amount of CO₂, thereby having the lowest ETS cost.

The ETS price has been set at 25 Eur/t CO₂ emitted. Under this assumption, oxy-fuel can compete with conventional cement plant. Even if oxy-fuel CO₂ carbon (only applied to the precalciner) has a low capture rate, it makes sense economically speaking and in order to do a first step towards carbon capture technologies.

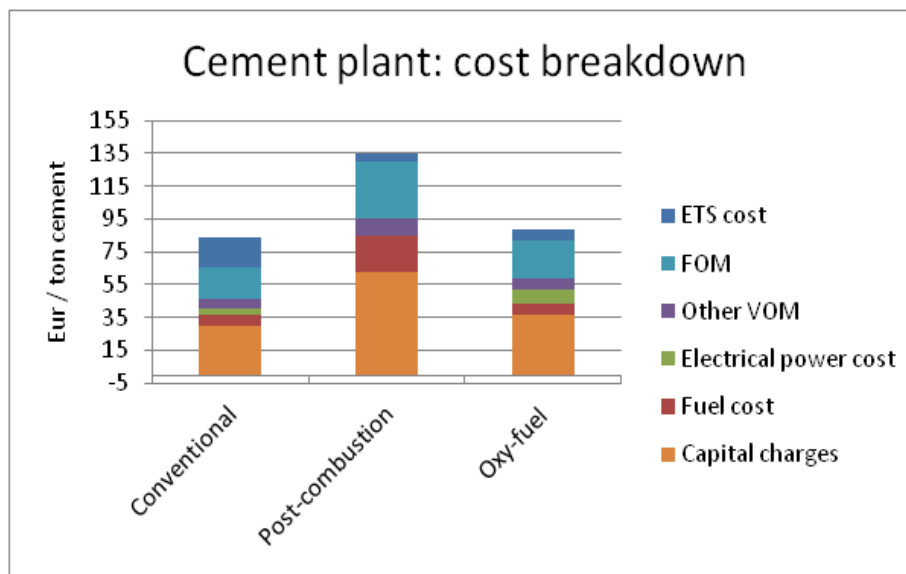


Figure 2.72. Cost breakdown of cement plant

2.3.6. capture in the iron and steel making industry

CO₂ emissions from iron and steel making plant worldwide account for 27 % of the industrial emissions. There are various processes involved in the steel factory of which the most important are: the coke making process (coke oven), the pellet or/and sinter production process, the iron making process (Blast furnace or other) and the steel making process (Basic oxygen furnace or electric arc furnace). After these processes, the crude steel undergoes other shaping and finishing processes such as casting, hot or cold forming, galvanizing, and so forth. These processes will not be studied further in this paper because they don't have a great CO₂ mitigation potential, directly.

Figure 2.73 presents a simple diagram of the whole iron and steel making chain, in a simple way:

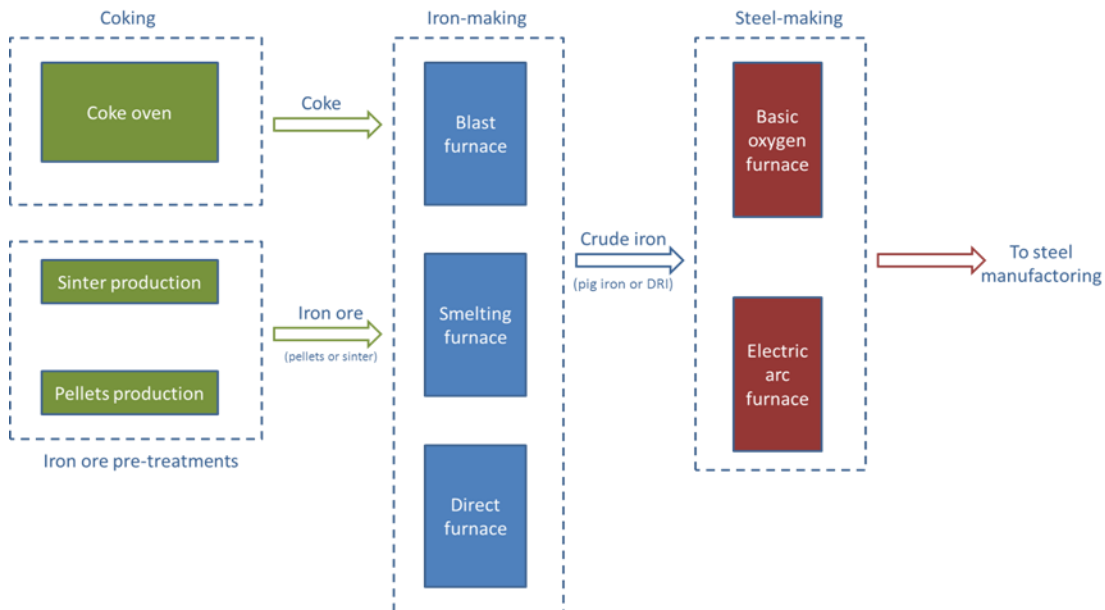


Figure 2.73. Iron and steel making process, simple diagram

Through this section, it is recommended to refer to Figure 2.74 that represents the fuel and materials (colored boxes) and the related processes (gray boxes).

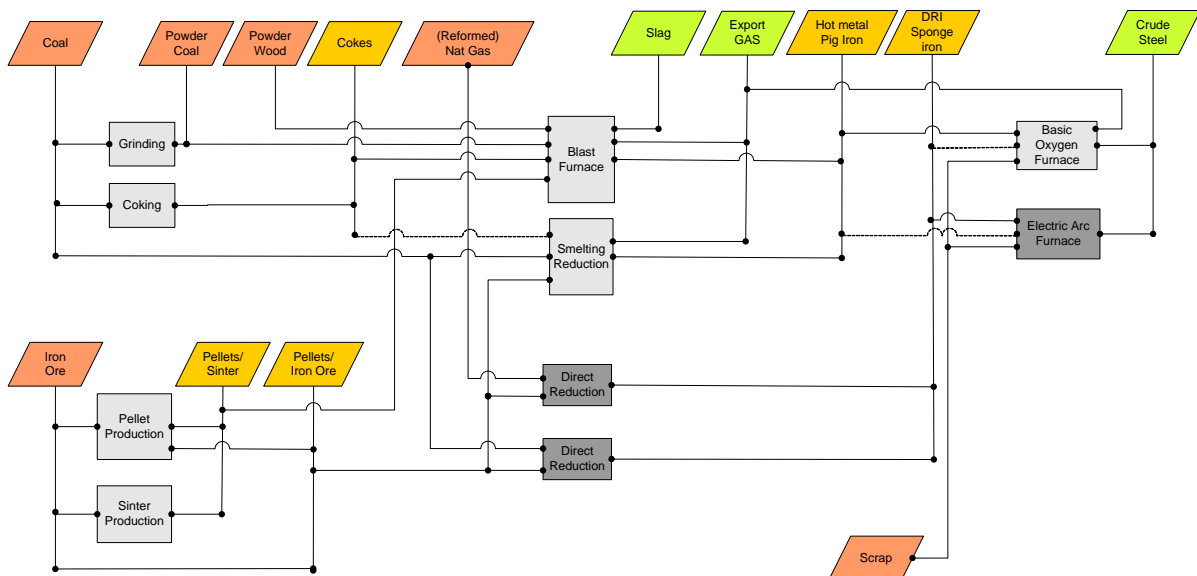


Figure 2.74. iron and steel making processes, detailed (Nijs et al, 2009)

2.3.6.1. Iron and steel making, conventional processes

Iron is the key element of iron and steel material. In nature, because of the presence of oxygen, iron is oxidized: Fe_2O_3 . Thus, to produce iron, it is needed to reduce the iron ore. This reduction can be done in various ways (Blast furnace, direct reduction, smelting reduction), using coal and, for blast furnace, coke. The product of this reduction is called "pig iron" and has a carbon content of about 4 – 5 % weight. To produce steel, whose carbon content varies between 0.2 and 2.1 % weight, the carbon content of the pig iron must be lowered. This is done in a steel making process such as "basic oxygen furnace" or "electric arc furnace".

2.3.6.1.1. Coke production

Iron making processes such as blast furnace (see here below) requires coke and coal as energy suppliers. To produce coke, coal must undergo a pyrolysis in an oxidation free atmosphere to prevent coal from ignition. The coal is heated up to 1000 – 1100 °C for about 16 – 40 hours. By heating, the coal releases volatile and undergoes subsequently a physical change (plastic paste before solidification). The coal fully carbonized and quenched is then called coke.

The flue gas of coking, called "coke oven gas" (COG), has a high energy content and should be further treated.

2.3.6.1.2. Sinter/pellet production

Sintering:

Sintering means "making object from powder". Applied to the metallurgy, the sintering process improves permeability and reducivity of the iron ore by changing its physical structure, from powder to agglomerates. Such a transformation is done by heating up the mix below its melting point, by ignition of coke in the right proportions.

Pelletisation:

Pelletisation is a process through which the iron ore is transformed into small balls (9 – 16 mm) while upgrading its iron content. The successive processes are: grinding and drying of the ore; green ball preparation in a balling drum; induration (drying, heating and cooling) which upgrades carbon content by transforming magnetite ore into hematite ore; screening and handling to recycle undersized and broken pellets.

2.3.6.1.3. Processes of iron making are:

Once one does have coal and/or coke and sinter and/or pellets, the pig iron is produced. This step is possible through various methods:

- Blast furnace produces liquid raw iron (pig iron) by melting pellets or sinter in a reducing environment. The process uses coke, coal, oxygen enriched air to heat up the bulk and reduce iron. There are three main outputs: raw iron, blast furnace gas and slag. The blast furnace gas is composed of CO (20 – 28 %) and H₂ (1 – 5 %) and inerts (CO₂, N₂), sulphur and dust. It has a calorific value (2.7 – 4 MJ/Nm³) and can consequently be used or sold.

Figure 2.75 depicts a blast furnace. The fuel and pellets or sinter are loaded from the top of the furnace and reducing reaction take place as the material moves downwards.

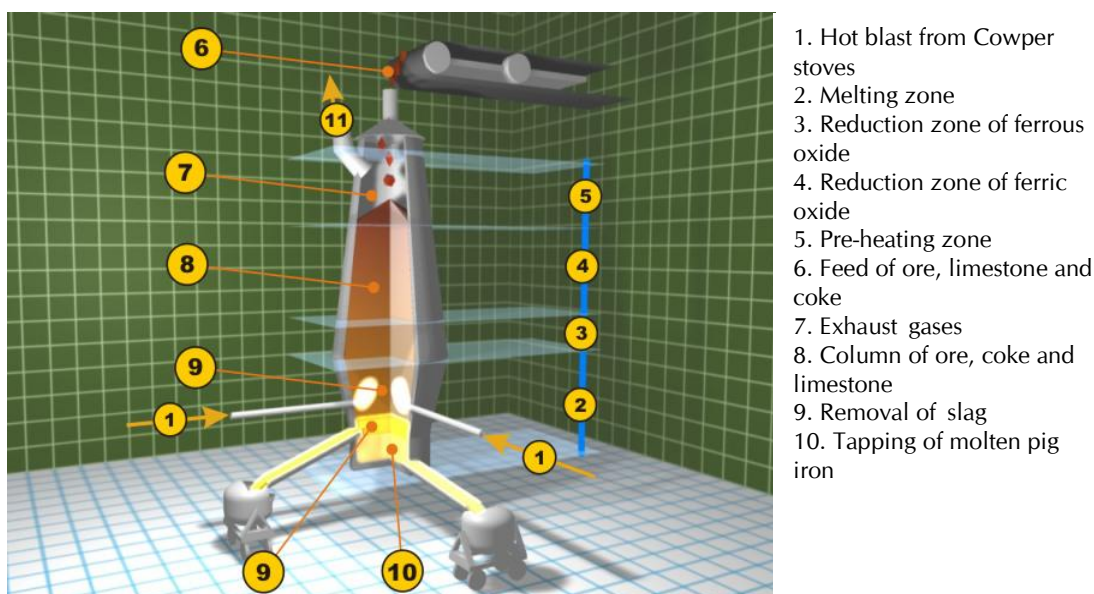


Figure 2.75. Blast furnace (Source : Wikipedia)

- Direct reduction (DR) refers to processes that reduce the iron ore at solid state, using various reducing agents such as natural gas. The iron product from DR is called direct reduction iron (DRI) or sponge iron. There are about 30 different processes of DR whose leading technology is the MIDREX process. The natural gas is reformed to carbon monoxide and hydrogen which act as reducing agent inside the shaft furnace.
- Smelting reduction is a process in which coal is gasified and reduces the iron ore. The principle is similar to the blast furnace but does not require coke.

The iron pellets are fed to the top of the pre-reduction shaft where a partial reduction in solid state occurs. The material is then directed to a "melter-gasifier" where it completes the reduction and melts while the coal is gasified. The hot gas from coal is directed to the pre-reduction zone as reducing agent.

Smelting reduction is the most recent option for iron production and the most deployed process is the COREX process.

2.3.6.1.4. Processes of steel making are:

- Basic oxygen furnace: In this process, the molten iron is further reduced to produce crude steel. Oxygen is blown on molten iron in order to lower carbon, silicon, manganese, and phosphorous content of the iron. Since the reaction is exothermic, the furnace needs to be cooled down. This is done by injecting scrap and iron ore in the mix. This addition acts as thermal ballast and allows recycling of steel scrap. The output is crude steel.
- Electric arc furnace (EAF) is primarily used for re-melting steel scrap but can also be filled with scrap iron, pig iron or direct reduced iron, in limited amount. The flue gas from the EAF preheats the scrap which is then directed to the core of the EAF. The electrodes are lowered to the scrap and an arc is struck, thereby melting the scrap. The product of EAF is crude steel.

2.3.6.2. Carbon capture processes in the iron and steel making industry

This chapter focuses on the capturing CO₂ from the iron making process because it is the one with the highest direct potential for carbon emissions mitigation. The chapter will also briefly present data on advanced technology for the other processes involved in the iron and steel chain with efficiency improvement and thereby CO₂ mitigation (but no capture).

2.3.6.2.1. Carbon capture from the blast furnace

There are basically two ways of capturing CO₂ from the blast furnace: by using a shift reaction and physical absorption capture or by using an oxy-fuelled blast furnace, recycling BFG and capturing the top gas.

2.3.6.2.1.1. Blast furnace with shift reactor and physical absorption capture

The principle of the process can be observed in the following figure:

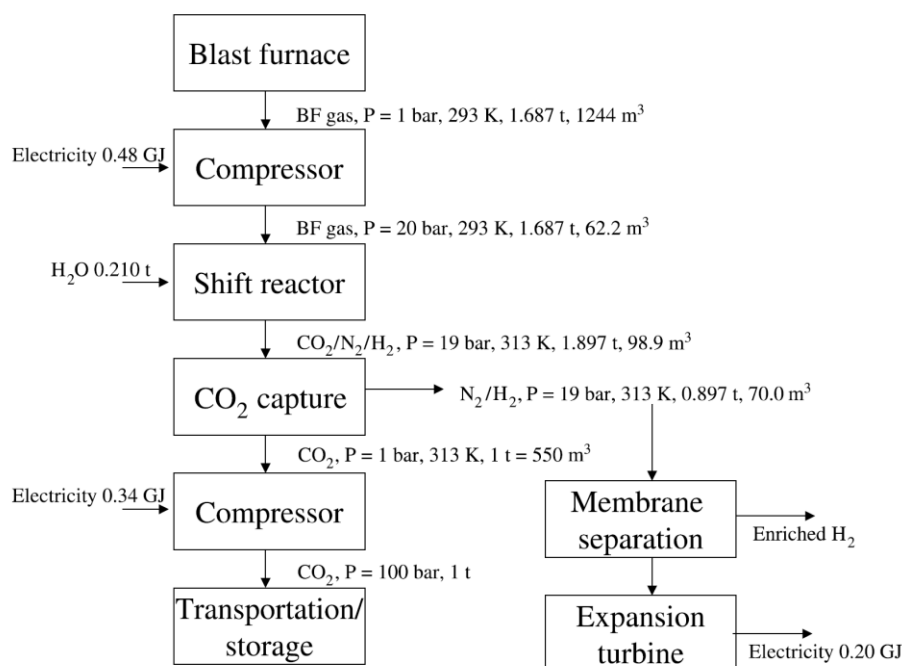


Figure 2.76. Shift reaction and physical absorption capture process.

Figure 2.76 envisions the case of producing electricity by using the hydrogen coming out of the capture station. Nevertheless, in order not to mix up iron and steel sector with power sector, the model will separate the iron and steel process from the power generation boxes. The stream composed of H₂ and N₂ will then be an output of the “iron and steel making process”.

In the process, the BFG at ambient temperature is first compressed up to 20 bar. Then, it undergoes a shift reaction ($\text{CO} + \text{H}_2\text{O} \rightarrow \text{CO}_2 + \text{H}_2$) thanks to steam provided. The CO₂ is separate from the two other major components: N₂ and H₂, by physical absorption (Pressure Swing Absorption, PSA). The CO₂ (at 1 bar now) is compressed up to 100 bar and is ready for transport and storage.

This process can be summarized as Figure 2.77:

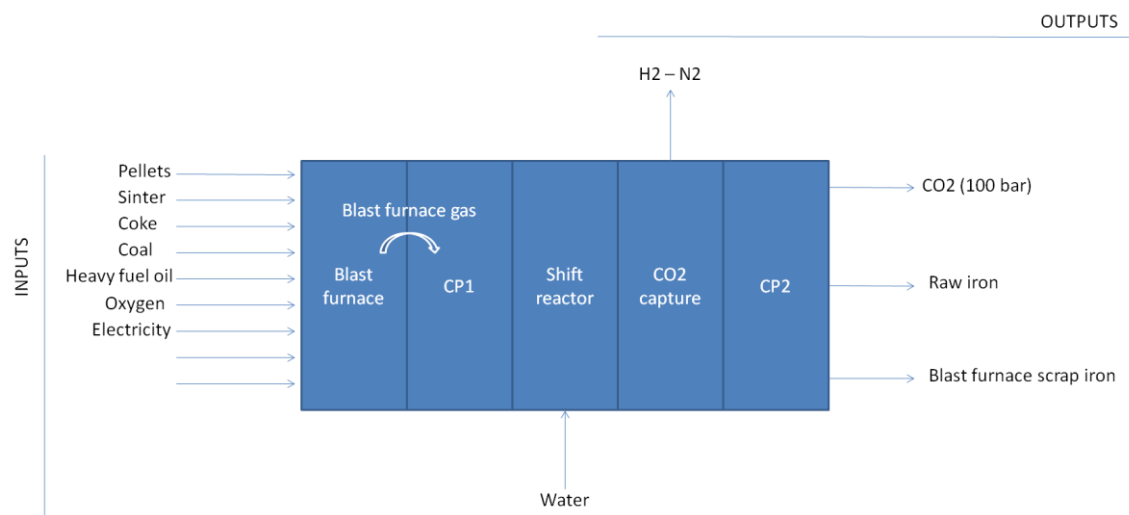


Figure 2.77. Inputs and outputs of blast furnace with physical absorption capture

2.3.6.2.1.2. Chemical absorption capture

The previous section describes processes and data of physical capture, after the blast furnace. This section focuses on chemical absorption capture. At the exhaust of the blast furnace, the BFG is directed to a boiler where it undergoes another partial combustion to heat up water that will be further used. The blast furnace gas is then sent to a capture station which mainly consists of an absorber and a desorber. The solvent chemically absorbs CO_2 and is directed to the desorber column where it desorbs CO_2 thanks to a heat supply given by the steam preliminary warmed up.

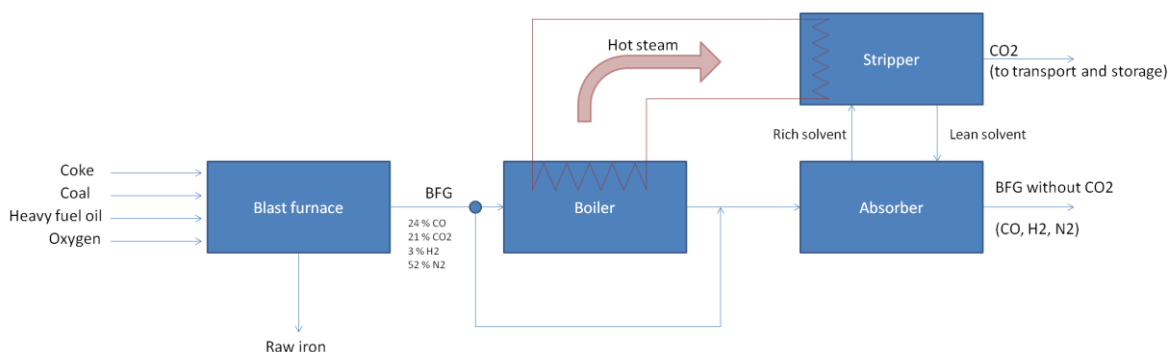


Figure 2.78.

However, even if the process looks good on the paper, it should not be considered regarding the whole carbon chain since the BFG going out of the absorber (without CO_2), still contains CO that will be further oxidized in CO_2 . If there is a subsequent CO_2 capture, it is environmentally good but economically poor because two consequent CO_2 capture are needed on a same stream. This option will then not be further analysed.

2.3.6.2.1.3. Oxy-fuelled BF with recycling

Oxy-fuelled without CCS:

Another option is to replace the air by oxygen. The blast furnace is then fed at the bottom by near pure oxygen. In order to control the temperature (higher when burning oxygen), part of the BFG must be recirculated. The recirculation also allows taking advantage of the calorific content of the top gas.

Blasting oxygen improves combustion reaction and more coal can be injected. The BFG contains higher concentration of combustibles because there is no nitrogen present, its calorific value is about two or three times higher than in conventional BF. This alternative already existed before talking about CCS because it increases process efficiency and reduces the amount of coke required and increases the hot metal productivity.

Indeed, since there is almost no nitrogen in the furnace, the reduction capability is increased. The blasted oxygen is at ambient temperature, in opposition to conventional BF that requires hot blast air, thereby reducing energy consumption.

A simple scheme of the process can be seen in Figure 2.79:

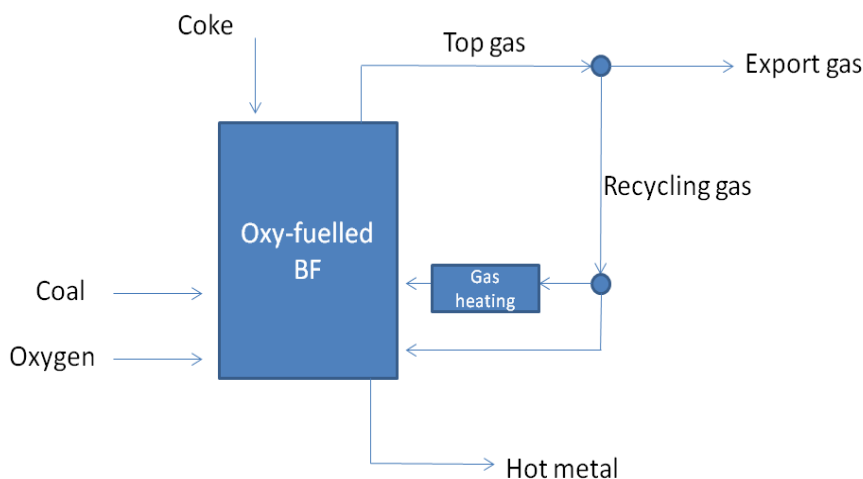


Figure 2.79. Oxy-fuelled BF, principle

Oxy-fuelled with CCS:

It is possible to capture CO₂ from the top gas and recirculate the top gas without CO₂. It gives more calorific value to the recycling gas and an environmentally friendly blast furnace if the CO₂ is stored downstream.

The principle can be observed in the next figure. It is possible to split the recycling stream in two different flows. One cold stream, injected at the bottom of the BF and a heated stream to be injected higher. It improves the process at the reaction level.

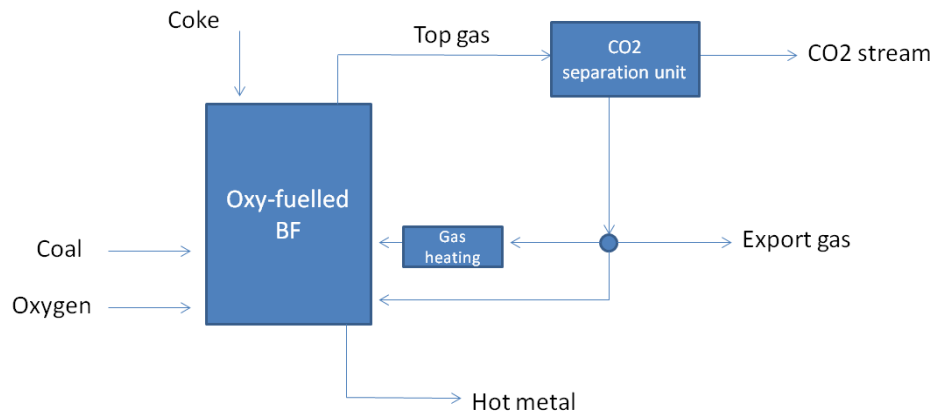


Figure 2.80. Oxy-fuelled BF with CCS, principle

2.3.6.3. Iron and steel processes, reference and CCS: Data

2.3.6.3.1. Blast furnace

2.3.6.3.1.1. Standard BF

Next table gathers inputs, outputs and costs of a standard BF that will be used as a reference case. This is done for a relative raw iron production. Indeed, the raw iron output is set at 1 MT⁹. The technology learning coefficient has been set at zero. The evolution through time has not been investigated in this paper.

⁹ The same methodology is used for CCS technologies.

Table 2.XXVIII.

Parameter ID	Value	Unit	Source
Investment cost	273.5	Euro 2010/tHM/y	ESTAP
O&M cost	118.2	MEuro 2010	ETSAP
FOM	10	Eur2010/tHM/y	Database PSS-CCS I (Markal)
VOM	2	Eur2010	Database PSS-CCS I (Markal)
INPUTS :			
Pellets (MISPLT)	0.04	MT	Database PSS-CCS I (Markal)
Sinter (MISSNT)	1.54	MT	Database PSS-CCS I (Markal)
Coke (MISCOK)	8.75	PJ	Database PSS-CCS I (Markal)
Coal	5.5	PJ	Database PSS-CCS I (Markal)
Heavy fuel oil	0	MT	Database PSS-CCS I (Markal)
Oxygen	0.05	MT	Database PSS-CCS I (Markal)
Electrical power	0.17	PJ	Calculation based on Dolf Gielen
Water	0	MT	
OUTPUTS:			
Raw iron (MISRIR)	1	MT	Database PSS-CCS I (Markal)
Blast furnace scrap iron (MISSCR)	0.25	MT	Database PSS-CCS I (Markal)
H2 – N2	0	PJ	Calculation based on Dolf Gielen
CO ₂ at 100 bar	0	kt	Calculation based on Dolf Gielen
Blast furnace gas	3.25	PJ	Database PSS-CCS I (Markal)
Availability	85	%	
Life Time	30	years	Database PSS-CCS I (Markal)
TL_Inv	0		No techn learning is considered
TL_Ref_Inv	0		No techn learning is considered
TL_Net efficiency	0		No techn learning is considered
TL_Ref_Net efficiency	0		No techn learning is considered

2.3.6.3.1.2. Standard BF with CCS by shift reaction and physical absorption

Next table presents the values of inputs and outputs data for a blast furnace followed by carbon capture unit using the shift reaction and physical absorption. The equipment needed for such process is similar than the one needed in IGCC with capture. Sizes and flow rate are similar. Adaptation will have to be made in order to fit with gas composition and particular requirement but in general, both installation (IGCC with capture and capture from blast furnace) require the same devices.

Table 2.XXIX. Carbon capture from blast furnace with physical absorption

Parameter ID	Value	Unit	Source
Year of commercialization	2030		Based on IGCC with capture
Investment cost	500	Euro 2010/tCO ₂ /y	Calculation based on Dolf Gielen
FOM	15	Eur2010/t hot metal/y	Database PSS-CCS I (Markal)
VOM	5	Eur2010	Database PSS-CCS I (Markal)
Pellets (MISPLT)	0.04	Mt	Database PSS-CCS I (Markal)
Sinter (MISSNT)	1.54	Mt	Database PSS-CCS I (Markal)
Coke (MISCOK)	8.75	PJ	
Coal	5.5	PJ	CO ₂ removal in the iron and steel industry, Dolf Gielen
Heavy fuel oil	0	Mt	Database PSS-CCS I (Markal)
Oxygen	0.05	Mt	Database PSS-CCS I (Markal)
Electrical power	0.782	PJ	Calculation based on Dolf Gielen
Water	0.157	Mt	Calculation based on Dolf Gielen
OUTPUTS:			
Raw iron (MISRIR)	1	Mt	Basis
Blast furnace scrap iron (MISSCR)	0.25	Mt	Database PSS-CCS I (Markal)
H ₂ – N ₂	3.014	PJ	Calculation based on Dolf Gielen
CO ₂ at 100 bar	746	Kt	Calculation based on Dolf Gielen
Availability	85	%	Database PSS-CCS I (Markal)
Life Time	30	years	Database PSS-CCS I (Markal)
TL_Inv	0.124		Based on IGCC
TL_Ref_Inv	2005		Based on IGCC
TL_Net efficiency	0		No tech learning on performance is considered
TL_Ref_Net efficiency	0		No tech learning on performance is considered
CO ₂ pressure	100	Bar	

2.3.6.3.1.3. Oxy-fuelled BF without CCS

Table 2.XXX.

Parameter ID	Value	Unit	Source
Commercialisation year	2020		
Investment cost	387	Euro 2010/tCHM/y	Average of St BF and oxy-BF with CCS
FOM	12.5	Eur2010/tHM/y	Average
VOM	3.5	Eur2010	Average
INPUTS :			
Pellets (MISPLT)	0.04	Mt	Database PSS-CCS I (Markal)
Sinter (MISSNT)	1.54	Mt	Database PSS-CCS I (Markal)
Coke (MISCOK)	5.916	PJ	
Coal	5.22	PJ	OBF-CC, Central I&S research, 2001
Heavy fuel oil	0	Mt	Database PSS-CCS I (Markal)
Oxygen	0.45		Calculation based on the oxygen needs for air-mode and reaction needs (source: Buchwalder et al (2004); Rosenqvist (2004))
Electrical power (ASU)	0.324	PJ	Calculation based on IEA and Vattenfall Europe Generation (2005), ASU consumption = 720 MJ/tO2
Electrical power (others)	0.17	PJ	Old database
Water	0	Mt	
OUTPUTS:			
Raw iron (MISRIR)	1	Mt	Database PSS-CCS I (Markal)
Blast furnace scrap iron (MISSCR)	0.25	Mt	Database PSS-CCS I (Markal)
H2 – N2	0	PJ	Calculation based on Dolf Gielen
CO ₂ at 100 bar	0	Kt	Calculation based on Dolf Gielen
Export gas	11.73	PJ	Calc based on OBF-CC, 2001
Availability	85	%	Database PSS-CCS I (Markal)
Life Time	30	years	Database PSS-CCS I (Markal)
TL_Inv	-		Based on oxy-fuel for power plants without CCS (coal)
	0.362		
TL_Ref_Inv	2005		
TL_Net efficiency	0		No learning on performance is considered
TL_Ref_Net efficiency	2005		

2.3.6.3.1.4. Oxy-fuelled BF with CCS

Table 2.XXXI.

Parameter ID	Value	Unit	Source
Investment cost	500	Euro	Calculation based on Dolf Gielen
FOM	15	2010/tHM/y	Time database
VOM	5	Eur2010	Time database
INPUTS :			
Pellets (MISPLT)	0.04	Mt	Database PSS-CCS I (Markal)
Sinter (MISSNT)	1.54	Mt	Database PSS-CCS I (Markal)
Coke (MISCOK)	5.916	PJ	Schmöle and Lungen (2004)
Coal	5.22	PJ	Schmöle and Lungen (2004)
Heavy fuel oil	0	Mt	Database PSS-CCS I (Markal)
Oxygen	0.45	Mt	Calculation based on the oxygen needs for air-mode and reaction needs (source: Development of injection of reduction gas into the blast furnace shaft, Joachim Buchwalder; book title: principle of extractive metallurgy, T. Rosenqvist)
Electrical power (ASU)	0.324 (OBF-CC based)	PJ	Calculation based on IEAGHG Oxy (Air Liquide), ASU consumption = 720 MJ/tO ₂
Electrical power of the capture station (only)	0.1	PJ	Total assumption!
Electrical power (others)	0.17	PJ	Old database
Water	0	Mt	
OUTPUTS:			
Raw iron (MISRIR)	1	Mt	Database PSS-CCS I (Markal)
Blast furnace scrap iron (MISSCR)	0.25	Mt	Database PSS-CCS I (Markal)
H ₂ – N ₂	0	PJ	Calculation based on Dolf Gielen
CO ₂ captured	833	Kt	Schmöle and Lungen (2004)
Export gas	0.7	PJ	Schmöle and Lungen (2004)
Availability	85	%	Database PSS-CCS I (Markal)
Life Time	30	years	Database PSS-CCS I (Markal)
TL_Inv	-0.343		Based on tech learning of oxy-fuel power plants with CCS (coal)
TL_Ref_Inv	2005		
TL_Net efficiency	0		No learning on performance is considered
TL_Ref_Net efficiency	2005		

Corex process:

Table 2.XXXII.

Parameter ID	Value	Unit	Source
Investment cost	200	Euro	(de Beer, 2009)
FOM	10	2010/tHM/y	Same value than standard BF (based on Google books)
VOM	2	Eur2010	
<u>INPUTS :</u>			
Pellets (MISPLT)	0.75	Mt	
Lump ore	0.75	Mt	
Coke (MISCOK)	3.1	PJ	
Coal	29	PJ	
Heavy fuel oil	0	Mt	
Oxygen	0.689	Mt	
Electrical power	0.55	PJ	
Water	0	Mt	
<u>OUTPUTS:</u>			
Raw iron (MISRIR)	1	Mt	
Blast furnace scrap iron (MISSCR)	0.35	Mt	
H2 – N2	0	PJ	
CO ₂ captured	0	Kt	
Export gas	10.9	PJ	
Availability	85	%	
Life Time	25	years	
TL_Inv	---		
TL_Ref_Inv	---		
TL_Net efficiency	---		
TL_Ref_Net efficiency	---		

2.3.6.3.1.5. Smelting reduction with CO₂ capture

Corex process with capture:

Table 2.XXXIII.

Parameter ID	Value	Unit	Sources
Investment cost	400	Euro 2010/tHM/y	Sum of Corex (200) + CCS station assumed to be 200
FOM	5	Eur 2010/tHM/y	Assumed to be the same than TGRBF with CCS
VOM	15	Eur 2010	Assumed to be the same than TGRBF with CCS
<u>INPUTS :</u>			
Pellets (MISPLT)	0.75	Mt	
Lump Ore	0.75	Mt	
Coke (MISCOK)	3.1	PJ	
Coal	27	PJ	
Heavy fuel oil	0	Mt	
Oxygen	0.689	Mt	
Electrical power	0.92	PJ	
Water	0	Mt	
<u>OUTPUTS:</u>			
Raw iron (MISRIR)	1	Mt	
Blast furnace scrap iron (MISSCR)	0.35	Mt	
H ₂ – N ₂	0	PJ	
CO ₂ captured	484	Kt	
Export gas	12.96	PJ	
Production Capacity	?		
Availability	85	%	
Life Time	25	years	
TL_Inv	---		
TL_Ref_Inv	---		
TL_Net efficiency	---		
TL_Ref_Net efficiency	---		
CO ₂ pressure	80	Bar	

2.3.7. CO₂ capture in the hydrogen industry

2.3.7.1. Introduction

There is a wide variety of hydrogen uses. Currently hydrogen is mostly used in the chemical and refinery industries. Globally, 50% of the hydrogen is used within the ammonia industry (Chapter 2.3.8. CO₂ capture in the ammonia industry) and 40% is used within the petrochemical industry (Chapter 2.3.9 CO₂ capture in the refinery industry). The remainder of 10% is used where a controlled atmosphere is necessary, as in glass production, the treatment of steel and the production of semiconductors. Hydrogen is also used in the food industry (as fat hardener) and in methanol manufacturing. While current uses of hydrogen are in industrial processes, future purposes include transport and utilities. Hydrogen can be used in transport for fuelling gas turbines and internal combustion engines in conjunction with fuel cells. Other future uses will be in decentralized power generation and space heating (Martens et al., 2006; IEA, 2008a; IEA, 2008b).

The use of hydrogen could yield an important benefit: no emissions of greenhouse gases are released at the time the hydrogen is consumed. However, on the production side of hydrogen, greenhouse gases are produced, and the emissions are dependent on the method of production that is considered. Hydrogen can either be produced from fossil fuels or electrolysis of water using electricity as energy source. If the electricity is produced from renewable or nuclear sources, no direct emissions of CO₂ are produced.

Large-scale hydrogen production has commercial applications for industrial uses, but not yet for uses in transport and utilities. In the current and near term, distributed reforming of natural gas and electrolysis of electricity can be used in the early stages of hydrogen as fuel for transport. In the medium to long term, large-scale centralized hydrogen production can be based on fossil fuels with CCS or biomass (with or without CCS)(IEA, 2006).

2.3.7.2. Hydrogen fabrication

Hydrogen hardly occurs in nature, therefore it has to be produced to meet the demand. There are many ways to produce hydrogen. The main processes are the following:

- Reforming of fossil fuels
- Electrolysis of water using electricity
- Biomass processes and water splitting processes by high-temperature (solar and nuclear) heat, photo-electrolysis and biological processes

The processes on solar and nuclear energy are currently being developed. None of them is close to have a commercial application so far (IEA, 2008b; IEA, 2006).

The reforming process and electrolysis are currently being used for large-scale hydrogen production in industries. Large-scale hydrogen production has commercial applications for industrial uses, but not yet for uses in transport and utilities. Indeed, this is important since hydrogen is an emerging fuel for transport and utilities. The figure below projects the main hydrogen pathways in the longer term according to the study of IEA (2006). In the near and current term, distributed hydrogen production would be based on electrolysis and the reforming of natural gas and coal. Electrolysis and reforming are proven technologies that can be used in the early stages of building a hydrogen infrastructure for transport. Small-scale natural gas reformers have only limited proven and commercial availability, therefore a number of units are being tested in demonstration projects. Only at a later stage, larger centralized hydrogen production would come through. In the medium to long term, large-scale hydrogen plants would be based on biomass and the reforming of fossil fuels, equipped with CCS (IEA, 2006).

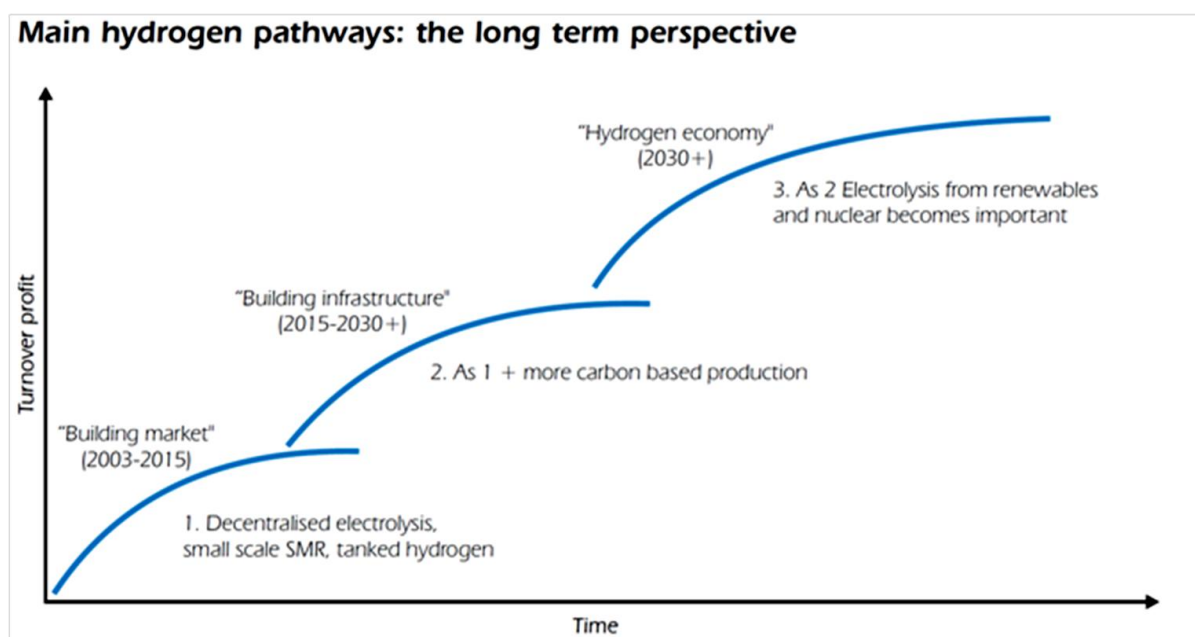


Figure 2.81. Pathways of hydrogen production in the short to long term (Source: IEA, 2006)

Today's hydrogen production is estimated at 65 Mt per year (IEA, 2008a). Reforming is the dominant hydrogen production technology. Around 96% of the hydrogen is produced by reforming and around 4% by water electrolysis (IPCC, 2005).

The most applied methods to produce hydrogen are discussed in the following paragraphs.

2.3.7.2.1. Reforming

The major part (96%) of hydrogen is produced via reforming. Reforming is a chemical process in which hydrogen-containing fuels in the presence of steam or oxygen are converted to a hydrogen rich mixture.

There are different reforming processes. Three types of processes are commercially used:

- Steam reforming of light hydrocarbons
(natural gas, naphtha, liquefied petroleum gas, refinery gas)
- Partial oxidation or gasification of heavy hydrocarbons:
 - Partial oxidation of gaseous and liquid fuels (heavy fuel oil, vacuum residue)
 - Gasification of solid fuels (coal, coke)
- Autothermal reforming, which combines steam reforming and partial oxidation.

More details about the reforming techniques are presented in the following sections, but first we give a brief outline below.

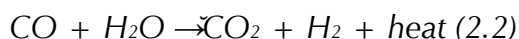
All the reforming processes firstly produce syngas, a mixture of hydrogen (H_2) and carbon monoxide (CO), from the primary hydrogen-containing fuel. The way in which they produce the syngas however varies with the type of process. Steam is added to the light hydrocarbon in the steam reforming process, whereas oxygen is added to the heavy hydrocarbon in the partial oxidation and gasification processes. The chemical reactions that deliver the syngas are found in equations (2.1), (2.2) and (2.3) in the following sections.

Syngas is a mixture of H_2 and CO. After the syngas is produced, CO is converted to CO_2 by the addition of steam in the water gas shift reaction. This results in a mixture of CO_2 and H_2 . The water gas shift reaction is common to the various process types. In the paragraphs below, this can be found in equation (2.2). The reaction allows to remove the CO_2 from the mixture of H_2 and CO_2 afterwards, in order to obtain the hydrogen.

Steam reforming of natural gas is the most applied reforming technique. Among the reforming processes, around 50% of global hydrogen is produced by steam reforming of natural gas, 31.3% by partial oxidation of oil, and 18.8% by gasification of coal (IPCC, 2005).

2.3.7.2.1.1. Steam reforming

Steam reforming involves the endothermic conversion of methane and water vapour into hydrogen and carbon monoxide (2.1). The heat is often supplied from the combustion of some of the methane feed-gas. The process typically occurs at temperatures of 700 to 850 °C and pressures of 3 to 25 bar. The product gas contains approximately 12 % CO, which can be further converted to CO₂ and H₂ through the water-gas shift reaction (2.2) (IEA 2006).



The figure below shows an overview of the steam reforming process of natural gas. The figure also shows that the hydrogen is purified using Pressure Swing Adsorption after the reforming process.

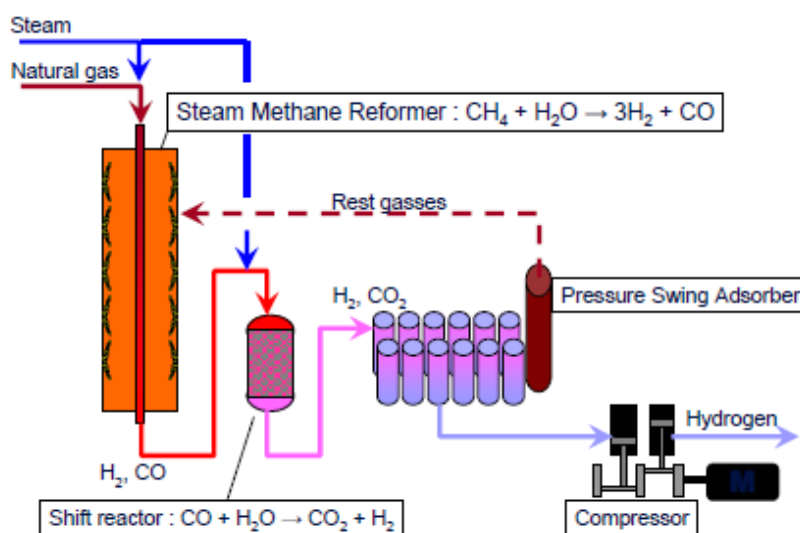


Figure 2.82. Steam reforming of natural gas (Source: Martens et al., 2006)

2.3.7.2.1.2. Partial oxidation

Partial oxidation of natural gas is the process whereby hydrogen is produced through the partial combustion of methane with oxygen gas to yield carbon monoxide and hydrogen (2.3). In this process, heat is produced in an exothermic reaction, and hence a more compact design is possible as there is no need for any external heating of the reactor. The CO produced is further converted to H₂ as described in equation (2.2) (IEA 2006).



2.3.7.2.1.3. Gasification of coal

Hydrogen can be produced from coal through a variety of gasification processes (e.g. fixed bed, fluidised bed or entrained flow). In practice, high-temperature entrained flow processes are favoured to maximise carbon conversion to gas, thus avoiding the formation of significant amounts of char, tars and phenols. A typical reaction for the process is given in equation (2.4), in which carbon is converted to carbon monoxide and hydrogen.



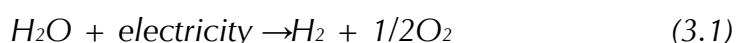
Since this reaction is endothermic, additional heat is required, as with methane reforming. The CO is further converted to CO₂ and H₂ through the water-gas shift reaction, described in equation (2.2). Hydrogen production from coal is commercially mature, but it is more complex than the production of hydrogen from natural gas. The cost of the resulting hydrogen is also higher. But since coal is plentiful in many parts of the world and will probably be used as an energy source regardless, it is worthwhile to explore the development of clean technologies for its use (IEA 2006).

2.3.7.2.1.4. Autothermal reforming

Autothermal reforming is a combination of both steam reforming (2.1) and partial oxidation (2.3). The total reaction is exothermic, and so it releases heat. The outlet temperature from the reactor is in the range of 950 to 1100 °C, and the gas pressure can be as high as 100 bar. Again, the CO produced is converted to H₂ through the water-gas shift reaction (2.2). The need to purify the output gases adds significantly to plant costs and reduces the total efficiency (IEA 2006). *Autothermal reforming (...) is used for small-scale units. No external heat is required in this case, what is an advantage for small systems* (Martens et al., 2006). This reaction results however in more by-products, lowering the efficiency. Partial oxidation, using only oxygen, is an exothermic reaction. So, heat is released at the expense of hydrogen formation. Also more by-products are formed. This pathway is used for higher carbonaceous fuels as gasoline, for which steam reforming is not possible.

2.3.7.2.2. Electrolysis

Water electrolysis is the process whereby water is split into hydrogen and oxygen through the application of electrical energy, as in equation (3.1). The total energy that is needed for water electrolysis is increasing slightly with temperature, while the required electrical energy decreases. A high-temperature electrolysis process might, therefore, be preferable when high-temperature heat is available as waste heat from other processes. This is especially important globally, as most of the electricity produced is based on fossil energy sources with relatively low efficiencies. The potential for future cost reduction for electrolytic hydrogen are significant (IEA, 2006).



There are two main types of electrolyzers: based on alkaline electrolyte and based on polymer electrolyte membrane (PEM). Alkaline electrolyte has some advantages over PEM.

At this moment Alkaline FC is the preferred technology, especially for large scale production. The technology is easily scaled up and easier to thermally manage. The alkaline electrolyser is a bit more efficient than the PEM electrolyser: about 60% on the lower heating value, which will increase to 70% (LHV) in the future (Martens et al., 2006).

Electrolysis does not involve direct CO₂ emissions.

2.3.7.2.3. Other technologies

Alternative technologies for H₂ production include:

- Biomass conversions processes
- Water splitting processes by photo-electrolysis or photo-biological production
- High-temperature decomposition

These technologies have no commercial applications and will not be considered further

2.3.7.3. Carbon capture from hydrogen plants

Hydrogen production through reforming of fossil fuels (or biomass) is a good candidate for CCS. Since CO₂ is separated from the hydrogen in order to produce hydrogen, the capture of CO₂ is already carried out as part of the production process. There are some opportunities for CCS in electrolysis as well.

2.3.7.3.1. Steam methane reforming with CCS

There are two options of CO₂ removal for steam methane reforming (SMR) fuel processor (IEA, 2005):

- CO₂ removal from the exhaust gas of the burner (after cooling); so that all the CO₂ is removed: from reforming, water gas shift, and burning of purged gas
- CO₂ capture at high pressure prior to the H₂-purification step; "the tail gas of the PSA (Pressure Swing Absorption) unit, which contains mainly methane, is recycled and used as feed in the process. However, (...) it does not reach 100% CO₂ removal unless part of the produced hydrogen is used as fuel for the reformer" (IEA, 2006).

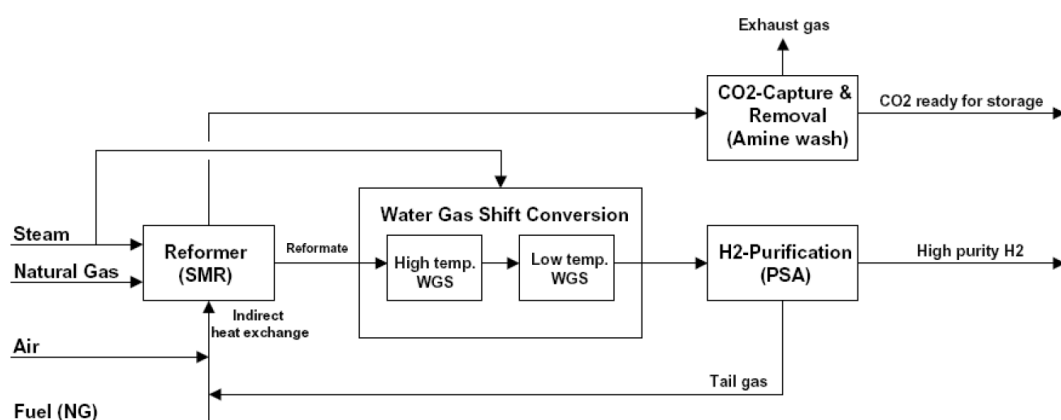


Figure 2.83. "Schematic drawing of an SMR fuel processor with CO₂-capture and removal" (IEA, 2006)

2.3.7.4. Carbon capture from hydrogen plants: data

The study of the IPCC (2005) brings together cost and performance estimates of different studies, as shown in the two tables below. We will refer to these studies and transform the data into useful data for our energy models (Markal/TIMES). As CO₂ capture is dependent on the actual production method, we classify the data according to the method of hydrogen production. It is important to note that we selected only those studies that consider costs of CCS for hydrogen production, and not for the combination of hydrogen and electricity production. The opportunities and costs of CCS for power production are discussed in the first chapter of the present study.

Table 2.XXXIV.

Study Assumptions and Results	Simbeck	NRC	NRC
	2005	2004	2004
<i>Reference Plant (without capture)</i>	*		
Plant products (primary/secondary)	H ₂	H ₂	H ₂
Production process or type	Steam reforming	Steam reforming	Texaco quench, CGCU
Feedstock	Natural gas	Natural gas	Coal
Feedstock cost, LHV (US\$ GJ ⁻¹)	5.26	4.73	1.20
Ref. plant input capacity, LHV (GJ h ⁻¹)	9848	7235	8861
Ref plant output capacity, LHV: Fuels (GJ h ⁻¹)	7504	5513	6004
Electricity (MW)	-44	-32	-121
Net plant efficiency, LHV (%)	74.6	74.6	62.9
Plant capacity factor (%)	90	90	90
CO ₂ emitted (MtCO ₂ yr ⁻¹)	4.693	3.339	7.399
Carbon exported in fuels (MtC yr ⁻¹)	0	0	0
Total carbon released (kg CO ₂ GJ ⁻¹ products)	81	78	168
Capture Plant Design			
CO ₂ capture/separation technology	Amine scrubber, SMR flue gas	MEA scrubber	Not reported
Capture plant input capacity, LHV (GJ h ⁻¹)	11495	8339	8861
Capture plant output capacity, LHV: Fuels (GJ h ⁻¹)	7504	6004	6004
Electricity (MW)	-129	-91	-187
Net plant efficiency, LHV (%)	61.2	68.1	60.2
CO ₂ capture efficiency (%)**	90	90	90
CO ₂ emitted (MtCO ₂ yr ⁻¹ ***)	1.280	0.604	1.181
Carbon exported in fuels (MtC yr ⁻¹)	0	0	0
Total carbon released (kgCO ₂ GJ ⁻¹ products)	23.0	13.5	28.1
CO ₂ captured (MtCO ₂ yr ⁻¹)	4.658	3.378	6.385
CO ₂ product pressure (MPa)	13.7	13.7	13.7
CCS energy requirement (% more input/GJ plant output)	21.8	9.5	4.5
CO₂ reduction per unit product (%)	72	83	83
Cost Results			
Cost year basis (constant dollars)	2003	2000	2000
Fixed charge rate (%)	20.0	16.0	16.0
Reference plant TCR (million US\$)****	668	469	1192
Capture plant TCR (million US\$)****	1029	646	1218
% increase in capital cost (%)	54.1	37.7	2.2
Ref. plant electricity price (US\$ MWh ⁻¹)	50.0	45.0	45.0
Capture plant electricity price (US\$ MWh ⁻¹)	50.0	45.0	45.0
% increase in assumed electricity price	0.0	0.0	0.0
Ref. plant fuel product cost, LHV (US\$ GJ⁻¹)	10.03	8.58	7.99
Capture plant fuel product cost, LHV (US\$ GJ⁻¹)	13.29	10.14	8.61
Increase in fuel product cost (US\$ GJ⁻¹)	3.26	1.56	0.62
% increase in fuel product cost	32.5	18.2	7.7
Cost of CO ₂ captured (US\$/tCO ₂)	38.9	20.7	4.1
Cost of CO ₂ avoided (US\$/tCO ₂)	56.3	24.1	4.4
Confidence level (see Table 3.6)	high		high

Notes: All costs in this table are for capture only and do not include the costs of CO₂ transport and storage.

* Reported HHV values converted to LHV assuming LHV/HHV = 0.96 for coal, 0.846 for hydrogen, and 0.93 for F-T liquids.

** CO₂ capture efficiency = (C in CO₂ captured) / (C in fossil fuel input to plant - C in carbonaceous fuel products of plant) x100; C associated with imported electricity is not included.

***Includes CO₂ emitted in the production of electricity imported by the plant.

****Reported total plant investment values increased by 3.5% to estimate total capital requirement.

Table 2.XXXV. Costs of CO₂ capture from hydrogen producing plants (Source: IPCC (2005))

Study Assumptions and Results	Simbeck	NRC	NRC
	2005	2004	2004
Capture Plant Design	*		
Plant products (primary/secondary)	H ₂	H ₂	H ₂
Production process or type	Autothermal reforming with O ₂ provided by ITM	78% efficient ATR/SMR, adv CO ₂ compressor	Gasifier LHV= 75-->80%, Adv ASU, membrane sep, adv CO ₂ compressor
Feedstock	Natural gas	Natural gas	Coal
Feedstock cost, LHV (US\$ GJ ⁻¹)	5.26	4.73	1.20
Plant capacity factor (%)	90	90	90
CO ₂ capture/separation technology	Oxy-fuel		
Capture plant input capacity, LHV (GJ h ⁻¹)	9527	7697	8121
Capture plant output capacity, LHV: Fuels (GJ h ⁻¹)	7504	6004	6004
Electricity (MW)	-13	-66	-88
Net plant efficiency, LHV (%)	78.3	74.9	70.0
CO ₂ capture efficiency (%)**	95	90	90
CO ₂ emitted (MtCO ₂ yr ⁻¹ ***)	0.086	0.505	0.873
Carbon exported in fuels (MtC yr ⁻¹)	0	0	0
Total carbon released (kgCO ₂ GJ ⁻¹ products)	1.46	11.10	19.45
CO ₂ captured (MtCO ₂ yr ⁻¹)	4.074	3.119	5.853
CO ₂ product pressure (MPa)	13.7	13.7	13.7
Cost Results			
Cost year basis (constant dollars)	2003	2000	2000
Fixed charge rate (%)	20	16	16
Capture plant TCR (million US\$)****	725	441	921
Capture plant electricity price (US\$ MWh ⁻¹)	50.0	45.0	45.0
Capture plant fuel product cost, LHV (US\$ GJ⁻¹)	9.84	8.53	6.39
Capture cost confidence level (see Table 3.6)	low	low	low

Notes: All costs in this table are for capture only and do not include the costs of CO₂ transport and storage.

* Reported HHV values converted to LHV assuming LHV/HHV = 0.96 for coal and 0.846 for hydrogen.

**CO₂ capture efficiency = (C in CO₂ captured)/(C in fossil fuel input to plant - C in carbonaceous fuel products of plant) x100; C associated with imported electricity is not included.

***Includes CO₂ emitted in the production of electricity imported by the plant.

****Reported total plant investment values increased by 3.5% to estimate total capital requirement.

2.3.7.4.1. Steam reforming of natural gas

For modelling purposes, it is recommended to consider two levels of CO₂ capturing, which can be done at different cost levels

1. Capturing CO₂ process emissions before the H₂ purification step. This involves little or no additional costs. After the separation stage, the gas stream with high CO₂ purity ($\geq 99\%$) only needs to be dried, compressed and transported for storage underground. The only additional costs thus arise from drying, compression, transportation and storage.
2. Additional capture of CO₂ emissions from heat production. Required process heat is produced by burning gas. Here in principle, different options are feasible: 1) post combustion capturing using solvents when heat is produced by burning natural gas 2) pre-combustion capturing by burning an amount of the H₂ produced and 3) oxy-fuel burning. The latter solution seems to be less attractive as it requires additional equipment for O₂ separation.

Cost and performance results of Simbeck (2005) and NRC (2004) are brought together by the IPCC (2005). Both NRC (2004) and Simbeck (2005) consider chemical absorption by means of the amine wash process as CO₂ separation technology. Simbeck (2005) uses an amine scrubber system on the steam methane reforming furnace flue gas, but it is not further defined which type of scrubbing solvent is used. NRC (2004) uses MEA scrubber, the mostly used scrubbing solvent.

Table 2.XXXVI, the energy balance of H₂ production by steam reforming of natural gas is presented. From 1 mol CH₄ and 2 mol H₂O, 1 mol CO₂ and 4 mol H₂ are produced. The combined process (steam reforming + water shift reaction) is endothermic and requires 168 kJ heat/mol CH₄ input (or 42 kJ mol H₂). Heat losses of 310 kJ reduces the overall efficiency to 75.8 %. Per Mol CH₄, 1 Mol of CO₂ process emissions is produced. These are available for capturing without any further processing. Emissions from heat production account for 26.8 gr.

Table 2.XXXVI. Energy balance of H₂ production by steam reforming of natural gas

Combined process	CH ₄ +	2H ₂ O +	= = heat >	CO ₂ +	4H 2
Atomair mass gr/mol	16			44	8
Heat value MJ /kg	50				121
kJ	800		168		968
Heat losses kJ			310		
Total heat requirement without capturing			478	26.8	
Efficiency of conversion process			0.75		8

2.3.7.4.1.1. Performance of a reference hydrogen plant

The values in the table below are derived from the results of Simbeck (2005) and NRC (2004) that are shown in the IPCC tables (Table 2.XXXIV & Table 2.XXXV). The heat requirement penalty is calculated on the heat requirements. This parameter amounts to 31% for Simbeck (2005) and only 16% for NRC. For comparison purposes, we remember that this parameter is about 25% for post combustion capturing in the electricity sector. Considering the difference in base year, Simbeck (2005) and NRC (2004) estimate the investment cost for a reference plant in the same order. However, the cost of a capture plant is more than 10% higher in Simbeck (2005) than in NRC (2004).

Table 2.XXXVII. Reference hydrogen plant (reformer of natural gas) according to Simbeck (2005) and NRC (2004)

	Simbeck 2005	NRC 2004	Average
CCS energy requirementst % more input /plant output	21.8	9.5	16
CCS heat requirements (mainly solvent regeneration)	211.0	92.0	151.5
Heat requirements including capturing	688.8	569.7	629.3
Heat requirement penalty	31%	16%	24%
CO ₂ captured	90%	90%	90%
Base year reference	2003	2000	
Exchange rate (EUR/USD)	0.884	1.0827	
investment cost reference plant (M\$ / MW)	0.32047	0.30626	
FOM (5% investment cost)	0.01602	0.01531	
investment cost capture plant (M\$ / MW)	0.49366	0.42184	
FOM (5% investment cost)	0.02468	0.02109	

2.3.7.4.2. Texaco quench, CGCU based on coal

NRC (2004) analysed the performance and economics of the gasification of coal with CGCU (cold gas clean-up) and quench, a way of syngas cooling. The results are shown in the tables of the IPCC (2005) (Table 2.XXXIV & Table 2.XXXV).

The tables below gather the parameters we derived from NRC (2004). Investment cost is based on a capacity of 1667 MW. Fixed O&M are assumed to be 5% of investment cost. Before analyzing a hydrogen production plant with CO₂ capture, it is important to set a reference plant.

2.3.7.4.2.1. Performance of a reference hydrogen plant

Table 2.XXXVIII. Reference hydrogen plant (CGCU of coal)

	Parameter ID	Value	Unit
Inputs	Coal	1,47	PJ
	Electricity	0,07	PJ
Outputs	H ₂	1	PJ
	CO ₂ emitted	1,18	Mt/year
Costs	Investment	0,7719	MEur2000/MW
	FOM	0,0386	MEur2000/MW (yearly)

2.3.7.4.2.2. Performance of a hydrogen plant with CCS

Table 2.XXXIX. Hydrogen plant (CGCU of coal) with CCS

	Parameter ID	Value	Unit
Inputs	Coal	1,47	PJ
	Electricity	0,11	PJ
Outputs	H ₂	1	PJ
Performance	CO ₂ captured	6,39	Mt/year
	CO ₂ capture efficiency	90	%
Costs	Investment	0,7887	MEur2000/MW
	FOM	0,0394	MEur2000/MW (yearly)

2.3.7.4.3. Autothermal reforming of natural gas

Simbeck (2005) analyzed autothermal reforming with oxygen provided by ITM (ion transport membranes). The results are shown in the tables of the IPCC (2005) (Table 2.XXXIV & Table 2.XXXV).

The table below gathers the parameters we derived for the hydrogen plant equipped with CCS. Performance and cost estimates of the reference plant are not given in IEA (2008a). Investment cost of the capture plant is based on a capacity of 2084 MW. Fixed O&M are assumed to be 5% of investment cost.

2.3.7.4.3.1. Performance of a hydrogen plant with CCS

Table 2.XL. Hydrogen plant (autothermal reforming of natural gas) with CCS

	Parameter ID	Value	Unit
Inputs	Natural gas	1,27	PJ
	Electricity	0,01	PJ
Outputs	H ₂	1	PJ
Performance	CO ₂ captured	4,07	Mt/year
	CO ₂ emitted	0,086	Mt/year
	CO ₂ capture efficiency	95	%
Costs	Investment	0,3537	MEur2000/MW
	FOM	0,0177	MEur2000/MW (yearly)

2.3.7.4.4. Autothermal/steam methane reforming of natural gas

NRC (2004) analyzed the performance and economics of a 78% efficient autothermal/steam methane reforming system, with an advanced CO₂ compressor. The results are shown in the tables of the IPCC (2005) (Table 2.XXXIV & Table 2.XXXV).

The table below gathers the parameters we derived for the hydrogen plant equipped with CCS. Performance and cost estimates of the reference plant are not given in IEA (2008a). Investment cost of the capture plant is based on a capacity of 1668 MW. Fixed O&M are assumed to be 5% of investment cost.

2.3.7.4.4.1. Performance of a hydrogen plant with CCS

Table 2.XLI. Hydrogen plant (autothermal/steam methane reforming of natural gas) with CCS

	Parameter ID	Value	Unit
Inputs	Natural gas	1,28	PJ
	Electricity	0,04	PJ
Outputs	H ₂	1	PJ
Performance	CO ₂ captured	3,12	Mt/year
	CO ₂ emitted	0,51	Mt/year
	CO ₂ capture efficiency	90	%
Costs	Investment	0,2856	MEur2000/MW
	FOM	0,0143	MEur2000/MW (yearly)

2.3.7.4.5. Gasification of coal

NRC (2004) analyzed the performance and economics of the gasification of coal with an advanced ASU (Air Separating Unit), membrane separator and advanced CO₂ compressor. The LHV¹⁰ efficiency is estimated to be at 75-80%.

The table below gathers the parameters we derived for the hydrogen plant equipped with CCS. Performance and cost estimates of the reference plant are not given in IEA (2008a). Investment cost of the capture plant is based on a capacity of 1667.78 MW. Fixed O&M are assumed to be 5% of investment cost.

2.3.7.4.5.1. Performance of a hydrogen plant with CCS

Table 2.XLII. Hydrogen plant (gasification of coal) with CCS

	Parameter ID	Value	Unit
Inputs	Coal	1,35	PJ
	Electricity	0,05	PJ
Outputs	H ₂	1	PJ
Performance	CO ₂ captured	5,85	Mt/year
	CO ₂ emitted	0,87	Mt/year
	CO ₂ capture efficiency	90	%
Costs	Investment	0,5964	MEur2000/MW
	FOM	0,0298	MEur2000/MW (yearly)

2.3.8. CO₂ capture in the ammonia industry

Anhydrous¹¹ ammonia is an important intermediate for the production of nitrogen-containing fertilizers. Ammonia is produced from a synthesis gas containing hydrogen and nitrogen. The nitrogen is retrieved from the air, whereas the hydrogen is retrieved from the hydrocarbons in the feedstock (mainly methane or methane-rich natural gas, but also naphtha and heavy hydrocarbons are candidate-fuels). The first phase in ammonia production is hydrogen production, where CO₂ is formed as a by-product. As hydrogen production requires the separation of H₂ from CO₂, the concentrated CO₂ gas stream is already captured as part of the ammonia production process. Therefore no additional capture installation is required. The separated CO₂ is used for production of fertilizers such as urea, or could also be used for transport and storage.

¹⁰ Lower heating value

¹¹ Anhydrous stresses the absence of water in ammonia

Not all of the CO₂ generated during ammonia production is available for storage. Worldwide about half of all produced and separated CO₂ is being used for urea manufacture. Ammonia plants are frequently integrated with urea plants (IEA, 2008a; IPCC, 2005). The ammonia plant serves the required feed (ammonia and carbon dioxide) to the urea plant (BREF, 2007). Urea, a popular type of nitrogen fertiliser, is formed from ammonia (NH₃) and CO₂ in a two step reaction¹²:



The amount of CO₂ that is required for urea manufacture is significant: 0.88 tonnes of CO₂ can be used to generate one tonne of urea (IEA, 2008a). Hence, urea plants are capable of using 70-90% of the CO₂ recovered from ammonia plants (IPCC, 2005).

Also in Belgium, not all of the CO₂ generated during ammonia production is available for storage. Indeed, part of the process CO₂ emissions is served to other plants. However, the use of the CO₂ in the Walloon region is not in urea plants, but in ammonium carbonate¹³ production, inert gas and food production. Nevertheless, this CO₂ is considered as emissions from ammonia plants in the emissions database of the UNFCCC, where it is assumed that the CO₂ will be vented to the atmosphere once (UNFCCC National Inventory rapport). The UNFCCC database reports that the amount of CO₂ emissions generated during Belgian ammonia production was at 1,38 tCO₂/tNH₃ in 2008. Hence, with a production of around 844,8 kt NH₃, around 1165,8 kt process CO₂ emissions were produced (NIR, 2010).

At BASF Antwerpen and Yara Tertre, two Belgian ammonia producers, respectively 85% and 68% of the process CO₂ were emitted directly to the air in 2010. Under the assumption that 90% of the CO₂ would be captured by the capture technology, potential for CO₂ storage would amount at about 932 kton CO₂ (which corresponds to around 16% of total CO₂-emissions in the chemical sector).

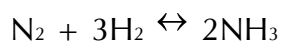
The IEA global CO₂ emissions database (IEA GHG, 2007) includes 194 ammonia plants with emissions larger than 0.1 Mt CO₂ per year. Together they produce 194 Mt CO₂ per year, or around 0.84% of total CO₂ emissions. The average annual emission per source would be 0.58 Mt CO₂.

¹² Reaction found in <http://nzic.org.nz/ChemProcesses/production/1A.pdf>

¹³ Ammonium carbonate ((NH₄)₂CO₃) is produced from a mixture of [ammonium chloride](#), or [ammonium sulfate](#) and [chalk](#), and is refined by sublimation in molecular proportions when it is obtained as a mixture of [ammonium bicarbonate](#) (NH₄HCO₃) and ammonium carbonate (NH₄)₂CO₃.

2.3.8.1. Ammonia fabrication

Ammonia is synthesised from nitrogen and hydrogen. Nitrogen is retrieved from the air and hydrogen from the hydrocarbons in the feed. The synthesis reaction that occurs during ammonia production is as follows:



Ammonia production can be divided into the following main steps:

- Hydrogen production
 - Purification of the feedstock
 - Reforming to produce syngas (mixture of CO and H₂O)
 - Shift conversion of CO and H₂O to CO₂ and H₂
 - Removal of CO₂
- Compression
- Ammonia synthesis

Reforming is already described in section 2.3.7.2 (Hydrogen fabrication).

Because of differences in reforming, there is not one single process of ammonia production but there are different processes of ammonia production. The processes can be described according to the reforming process. Although the processes vary in detail, they all comprise the same main steps, as listed above. It is important to know that most steps, such as shift conversion, CO₂ removal and ammonia synthesis, are independent of the type of ammonia production process.

A schematic overview of the ammonia production process by means of steam reforming and partial oxidation is shown in Figure 2.84 & Figure 2.85.

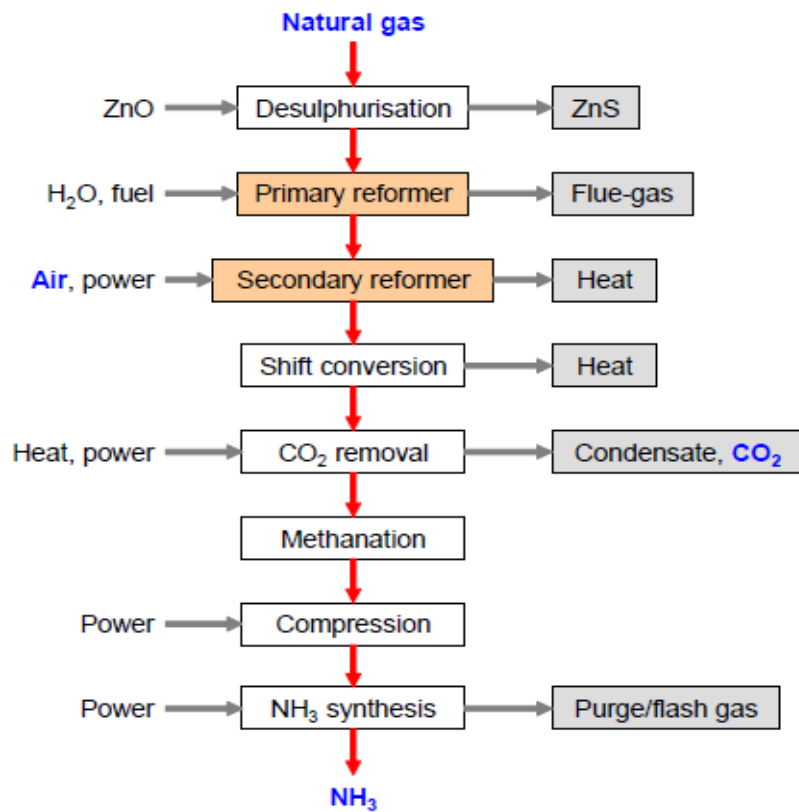


Figure 2.84. Ammonia manufacture by means of steam reforming of natural gas (Source: EFMA, 2000)

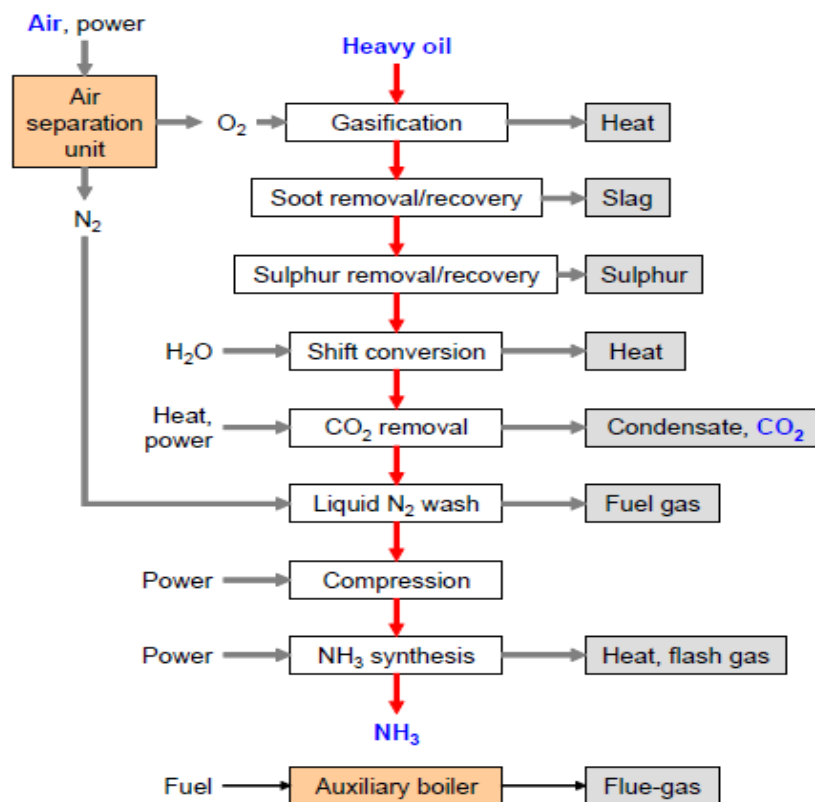


Figure 2.85. Ammonia manufacture by means of partial oxidation (Source: EFMA, 2000)

Worldwide about 83% of ammonia is produced by the steam reforming process. The remainder is produced by partial oxidation/gasification (16.5%) and water electrolysis (0.5%).

Table 2.XLIII. Share of world capacity (1990) for different processes and feedstocks (Source: BREF, 2007)

Feedstock	Process	% of world capacity
Natural gas	Steam reforming	77
Naphtha, LPG, refinery gas	Steam reforming	6
Heavy hydrocarbon fractions	Partial oxidation	3
Coke, coal	Partial oxidation	13.5
Water	Water electrolysis	0.5

Most plants use natural gas (methane) as feedstock for ammonia production. In Belgium, only steam methane reforming is applied (PSS-CCS I).

Concerning the future uses of processes, DFG Energy (2003) states that *"based on the known resources of fossil raw materials, it is likely that natural gas will dominate as feedstock for ammonia for the next 50 years at least. In the very long term, 50-200 years, one might expect coal to take over, based on world reserves and consumption rate. Heavy oil may be attractive under special environmental concerns, when natural gas is not available and the partial oxidation process could solve a waste problem (heavy residues, plastics recycle) [EFMA, 2000]"*

The CO₂ that is released during synthesis gas production varies with respect to the process type. BREF (2007) states that *"the carbon dioxide production in the steam/air reforming of natural gas is 1.15 – 1.40 kg/kg NH₃, dependent on the degree of air reforming (the figures do not include carbon dioxide in the combustion gases). A CO₂/NH₃ mole ratio of 0.5 (weight ratio 1.29), the stoichiometric ratio for urea production, is obtainable in the heat exchange reformer concepts. In partial oxidation of residual oils, CO₂ production is 2 – 2.6 kg/kg NH₃, dependent on the feedstock C/H ratio [1, EFMA, 2000]."*

Table 2.XLIV summarizes the CO₂ emissions from steam reforming and partial oxidation.

Table 2.XLIV. Process CO₂ emissions from ammonia synthesis gas production processes (Source: BREF, 2007)

Type of process	CO ₂ emissions	Unit
Steam reforming	1.65 – 1.9	kg CO ₂ /kg NH ₃
Partial oxidation	2.2 – 2.6	kg CO ₂ /kg NH ₃

The amount of CO₂ emitted from partial oxidation is higher than the amount of CO₂ emitted from steam reforming. CO₂ emission is dependent on the composition of the feedstock that is used in the process. Partial oxidation is based on heavy fossil fuels (oil, coal) with a relatively high C/H ratio. The typical feedstock for steam reforming, methane or methane-rich natural gas, contains relatively much hydrogen and less carbon.

Rafiqul et al. (2005) state that *"an emission factor of 1.56 t CO₂/t NH₃ produced is obtained, with a BAT energy consumption level of 28 GJ/t CO₂"*. Appelman et al. (2009) state that *"energy consumption ranges from 29 to 36 gigajoules per metric tonne (GJ/t)"*. These values are in the range of the Best Available Techniques (BAT) energy consumption level, that is concluded in BREF (2007): the total net energy consumption in the reforming BAT process ranges from 27.6 to 31.8 GJ (LHV)/t NH₃. The dominating group of BAT reforming processes for the present time and near future is considered to be the steam reforming processes of light hydrocarbons.

Capacity of a large ammonia plant is typically 1000-2000 tonnes per day. For new plants, capacities of up to 1800 tonnes per day are commonly reached (EFMA, 2000).

2.3.8.2. Carbon capture from ammonia plants

After shift reaction, CO₂ is generally removed through solvent absorption. The same CO₂ removal step is applied to both the steam reforming and partial oxidation process. This technique thus is independent of the type of process applied before CO₂ removal.

CO₂ is captured from the stream that is output from the reforming process, namely the process emissions. Flue gas stream from the burners (combustion emissions) are not captured, but vented to the atmosphere (PSS-CCS I).

The CO₂ can either be removed by a chemical or physical absorption processes. Some CO₂ removal processes nowadays used are listed in the table below. Solvent consumption in the absorption process should normally not exceed 0.02 – 0.04 kg solvent/t NH₃ (EFMA, 2000).

Table 2.XLV. Some CO₂ removal processes (Source: BREF, 2007)

Process name	Solvent/reagent + additives	CO ₂ in treated gas (ppm)
Physical absorption systems		
Purisol (NMP)	N-methyl-2-pyrrolidone	Less than 50
Rectisol	Methanol	Less than 10
Fluorsolv	Propylene carbonate	Function of pressure
Selexol	Polyethylene glycol dimethyl ether	Function of pressure
Processes with chemical reagents		
MEA	Water/monoethanolamine (20 %)	Less than 50
Promoted MEA	Water/MEA (25 – 30 %) + amine guard	Less than 50
Benfield	Water/K ₂ CO ₃ (25 – 30 %) + DEA, etc.	500 – 1000
Vetrocoke	Water/K ₂ CO ₃ + As ₂ O ₃ + glycine	500 – 1000
Catacarb	Water/K ₂ CO ₃ (25 – 30 %) + additives	500 – 1000
Lurgi	Water/K ₂ CO ₃ (25 – 30 %) + additives	500 – 1000
Carsol	Water/K ₂ CO ₃ + additives	500 – 1000
Flexsorb HP	Water/K ₂ CO ₃ amine promoted	500 – 1000
Alkazid	Water/K ₂ -methylaminopropionate	To suit
DGA	Water/diglycolamine (60 %)	Less than 100
MDEA	Water/methyl diethanolamine (40 %) + additives	100 – 500
Hybrid systems		
Sulfinol	Triethanolamine/monoethanolamine	Less than 100
TEA-MEA	water/sulpholane/MDEA	Less than 50

Residual content of CO₂ is usually in the range of 50-3000 ppmv. The residual CO₂ content is depending on the process that is applied:

- for the MEA solvent, CO₂ content < 50 ppm,
- for other chemical processes, CO₂ content is 500-1000 ppm, except for
 - MDEA, with 100-500 ppm,
 - DGA, with < 100 ppm,
 - alkazid: to suit

Solvent absorption for ammonia production is the same technology as the solvent absorption for hydrogen production.

CO₂ can also be removed by Pressure Swing Adsorption (PSA). This technique should be considered as BAT in some new plants (EFMA, 2000). Modern plants use a pressure swing adsorber to recover a relatively pure H₂ gas stream: "(...) other gases than H₂ are adsorbed in a set of switching beds containing layers of solid absorbent such as activated carbon, alumina and zeolites. The CO₂ is contained in a stream, from the regeneration cycle, which contains some methane and H₂ » (IPCC, 2005). However, as « PSA does not selectively separate CO₂ from the other waste gases and so for an SMR application the CO₂ concentration in the waste gas would be 40-50%, further upgrading to produce pure CO₂ for storage is required» (IPCC, 2005).

Some data concerning properties of the captured CO₂ can be retrieved from the demonstration project for CO₂ capture in ammonia production executed by DSM Agro/GTI in the Netherlands.

During ammonia production, the CO₂ is removed from the gas stream in an absorption process. The pressure of the CO₂ that is output of the absorption process is low at 1.4 to 1.6 bar. Temperature is between 10 and 35°C.

CO₂ purity is high at more than 99%. Impurities in the separated gas stream are limited. An overview of the quality of the captured CO₂ stream is given in the table below.

Table 2.XLVI. Quality of the captured CO₂ stream

(Source: Storage of CO₂ in Limburg coal and sandstone layers project, oral communication)

Contaminant	Share
CO ₂	≥ 99 %
H ₂	0,30 %
N ₂	0,00 %
Hydrocarbons	30 – 600 ppm(v)
Methanol	50 – 500 ppm(v)
CO	6 – 50 ppm(v)
O ₂	< 1 ppm(v)
NH ₃	< 1 ppm(v)
H ₂ O	7 – 25 g/Nm ³

The quality of the CO₂ stream is sufficient for injection. Therefore the CO₂ is directly usable for injection. Only compression is necessary, in order to raise the pressure of the CO₂ stream from 1.4-1.6 bar to the required level (110 - 200 bar) for transport. After capture and compression, the CO₂ stream is ready for transportation and storage. CCS from ammonia plants therefore represents a relatively low-cost CCS option.

2.3.8.3. Carbon capture from ammonia plants: data

Costs and performance of CO₂ capture from ammonia production have already been analyzed. Input parameters for the energy MARKAL-TIMES model were gathered. These input parameters are already implemented in the MARKAL-TIMES model.

Cost estimates of ammonia production are given for standard ammonia production (without CO₂ capture), advanced ammonia production (without CO₂ capture) and advanced ammonia production (with CO₂ capture).

In each of the cases, a continuation is assumed without much improvement. All parameters are kept constant until 2050.

2.3.8.3.1. Standard ammonia production without CCS

Table 2.XLVII. Costs of standard ammonia production without CCS

	Parameter ID	Value	Unit
Parameter	Lifetime	25	years
	Capacity	1	Mt
	Availability	90	%
Inputs	Gas	34,5	PJ
	Power	0,5	PJ
Outputs	NH ₃	1	Mt
Costs	Investment	285	MEur2000/Mt
	VOM	---	MEur2000/Mt
	FOM	8,5	MEur2000/Mt

2.3.8.3.2. Advanced ammonia production without CCS

The difference in advanced and standard production is in gas consumption.

Table 2.XLVIII. Advanced ammonia production without CCS

	Parameter ID	Value	Unit
Parameter	Lifetime	25	years
	Capacity	1	Mt
	Availability	90	%
Inputs	Gas	29,3	PJ
	Power	0,5	PJ
Outputs	NH ₃	1	Mt
Costs	Investment	285	MEur2000/Mt
	VOM	---	MEur2000/Mt
	FOM	8,5	MEur2000/Mt

2.3.8.3.3. Advanced ammonia production with CCS

CO₂ capture would increase the investment cost.

Table 2.XLIX. Advanced ammonia production with CCS

	Parameter ID	Value	Unit
Parameter	Lifetime	25	years
	Capacity	1	Mt
	Availability	90	%
Inputs	Gas	29,3	PJ
	Power	0,5	PJ
Outputs	NH ₃	1	Mt
Performance	CO ₂ captured	1,65	MEur2000/Mt
	CO ₂ capture efficiency	90	%
Costs	Investment	330	MEur2000/Mt
	VOM	---	MEur2000/Mt
	FOM	8,5	MEur2000/Mt

2.3.8.4. Differences in capturing from hydrogen or ammonia processes and from large combustion processes

Small-scale pilot projects have been developed for the CO₂ capture from industrial and power applications, however there have been no demonstration projects at large-scale power plants of several hundred megawatts. The same technology used in ammonia manufacture, i.e. solvent absorption, would be used for one of the methods of post-combustion capture from power plants. **Although the same technique is applied, differences between the solvent absorption for ammonia production and for power generation exist.** In the following paragraph, we will briefly discuss these differences and their impact on the possibilities to transfer solvent absorption from ammonia plants to other processes.

Differences between the solvent absorption from ammonia plants and post-combustion capture are explained by the process conditions under which it must operate. The gas flows from which the CO₂ is captured are different mainly according to the following key variables:

- CO₂ concentration
- CO₂ partial pressure
- (flue)gas composition

Ammonia plants generate more highly concentrated CO₂ than power plants. The flue gases that are inputted in the solvent absorption from ammonia plants contain typically 18% CO₂, whereas the flue gases that could be inputted in post-combustion capture have a low CO₂-concentration (no more than 15%). For post-combustion capture from power plants there is a variety of carbon dioxide levels according to the type of fuel used and the excess air level used for optimal combustion conditions: the lowest and highest concentrations are commonly known in natural gas turbines (3%) and in coal fired boilers and Integrated gasification combined cycle (IGCC) (14%).

Table 2.L. CO₂ concentration and pressure of the gas stream inputted to a capture process (Source: IPCC, 2005)

Source	CO ₂ concentration (% vol)	Pressure of gas stream (MPa)	CO ₂ partial pressure (MPa)
Natural gas fired boilers	7-10	0,1	0,007 - 0,010
Gas turbines	3-4	0,1	0,003 – 0,004
Oil fired boilers	11-13	0,1	0,011 – 0,013
Coal fired boilers	12-14	0,1	0,012 – 0,014
IGCCb: after combustion	12-14	0,1	0,012 – 0,014
Ammonia production	18	2,8	0,5
Hydrogen production	15-20	2,2 - 2,7	0,3 – 0,5

CO₂ partial pressure is another key property that is different according to the flue gases from ammonia plants and power stations. CO₂ partial pressure is determined by the pressure of the gas stream and the CO₂ mole fraction. This property has an important impact on the conditions of the capture process. IPCC (2005) states that “the lower the CO₂ partial pressure of a gas stream, the more stringent the conditions for the separation process”. IPCC (2005) further states that “where emissions sources with high partial pressure are generated, for example in ammonia or hydrogen production, these sources require only dehydration and some compression, and therefore have lower capture costs”.

Carbon capture has already been applied to hydrogen and ammonia production for several decades, generally by the means of solvent absorption with either chemical or physical solvents. As the capture of CO₂ is already a part of the current production process, hydrogen and ammonia production facilities could provide the early learning needed for CCS for other combustion processes, e.g. heat and electricity generation.

2.3.9. CO₂ capture in the refinery industry

Another large source of CO₂ emissions is a refinery. A typical world-scale complex refinery handling 300,000 barrels of oil per day emits 0.8 to 4.2 Mt of CO₂ per year (Van Straelen et al., 2009). From European refineries the amount of CO₂ emitted varies from 0.15 to 5.5 million tonne per year, depending on the type of refinery and heat integration (BREF, 2010). The refinery sector is the third largest emitter of CO₂ among stationary CO₂ sources globally, after the power generation sector and the cement industry. The contribution of the refinery sector to global CO₂ emissions is around 4% (Van Straelen et al., 2009). This corresponds to about 800 Mt CO₂ per year, which is counted from 638 refineries that are included in the IEA GHG global CO₂ emissions database. The database only contains refineries with emissions larger than 0,1 Mt per year (IEA GHG, 2007).

In Belgium, about 4636 kt CO₂ was emitted from petroleum refining in 2008. The amount of petroleum refined related to these emissions amounts to 1582 PJ (CRF tables UNFCCC, 2010).

Capturing the CO₂ seems to be the only route to drastically reduce CO₂ emissions from refineries. In addition to the option of carbon capture, other process improvements can be implemented. The most interesting route from an economical point of view is energy conservation. Van Straelen et al., (2009) state that *"a number of examples of successful energy reduction schemes such as through the construction of cogeneration plants, the reduction of flaring and the use of alternative energy sources have been published (IPIECA, 2007). However, the nature of refinery processes imply that even a refinery which is highly energy efficient will continue to consume considerable amounts of energy, and therefore produce considerable amounts of CO₂. A way to further reduce these emissions is through CO₂ capture and storage."*

There are opportunities for the use of carbon capture within refining. A refinery has multiple exhaust stacks that release CO₂. The main sources of CO₂ are power plants, furnaces and boilers, flares, process vent emissions and hydrogen production (PSS-CCS I). Carbon capture can be applied separately to these refinery assets. For some of the main CO₂ sources, as for boilers in power plants and hydrogen production units, capture technologies are already being developed. For furnaces, feasibility of capture is also being investigated (as we will describe in the paragraphs below).

2.3.9.1. Refinery processes

BREF (2010) states the following:

"The purpose of refining is to convert natural raw materials such as crude oil and natural gas into useful saleable products. Crude oil and natural gas are naturally occurring hydrocarbons found in many areas of the world in varying quantities and compositions. In refineries, they are transformed into different products as:

- *fuels for cars, trucks, aeroplanes, ships and other forms of transport*
- *combustion fuels for the generation of heat and power for industry and households*
- *raw materials for the petrochemical and chemical industries*
- *specialty products such as lubricating oils, paraffins/waxes and bitumen*
- *energy as a by-product in the form of heat (steam) and power (electricity).*

In order to manufacture these products, these raw materials are handled and processed in a number of different refining facilities, alone or as a mixture with agrofuels. The combination of these processing units to convert crude oil and natural gas into products, including its supporting units and facilities, is called a refinery. The market demand for the type of products, the available crude quality and certain requirements set by authorities influence the size, configuration and complexity of a refinery. As these factors vary from location to location no two refineries are identical ».

BREF (2010) further states that*"(...) the combination and sequence of processes are usually very specific to the characteristics of the raw materials (crude oil) and the products to be produced. In a refinery, portions of the outputs from some processes are fed back into the same process, fed to new processes, fed back to a previous process or blended with other outputs to form finished products. (...) all refineries are different regarding their configuration, process integration, feedstock, feedstock flexibility, products, product mix, unit size and design and control systems. In addition, differences in owner strategy, market situation, location and age of the refinery, historic development, available infrastructure and environmental regulation are amongst other reasons for the wide variety in refinery concepts, designs and modes of operation. The environmental performance can also vary from refinery to refinery.*

The production of a large number of fuels is by far the most important function of refineries and will generally determine the overall configuration and operation. Nevertheless some refineries can produce valuable non-fuel products such as feedstocks for the chemical and petrochemical industries. Examples are mixed naphtha feed for a steam cracker, recovered propylene, butylene for polymer applications and aromatics manufacture covered under the Large Volume Organic Chemical Industry BREF. Other speciality products from a refinery include bitumen, lubricating oils, waxes and coke. In recent years the electricity boards in many countries have been liberalised allowing refineries to feed surplus electricity generated into the public grid ».

2.3.9.2. Carbon capture from refineries

Refineries have multiple exhaust stacks that release CO₂.

According to the BREF (2010) the key sources of CO₂ are the generation of energy. The main sources of CO₂ are the process furnaces and boilers, gas turbines, fluid catalytic cracking (FCC) units, flare systems and incinerators (table below).

Table 2.II. Main sources of CO₂ in a typical complex refinery (Source: BREF (2010))

Main air pollutants	Main sources
Carbon dioxide	Process furnaces, boilers, gas turbines Fluidised catalytic cracking regenerators CO boilers Flare systems Incinerators

Key point

Process heaters account for half of the CO₂ emissions from oil refining.

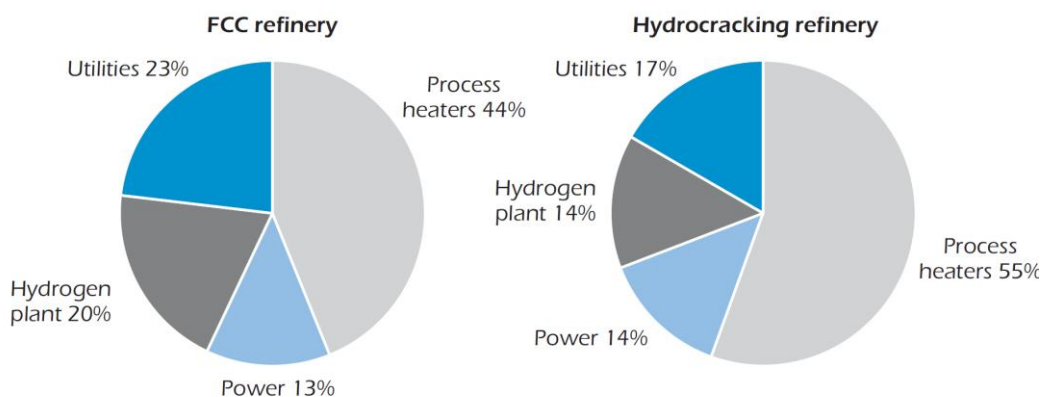


Figure 2.86. CO₂ emissions from two types of oil refineries (Source: IEA (2008a))

The study of IEA (2008a) shows the sources of CO₂ emissions according to two types of refineries (figure below). It is remarked there that process heaters are responsible for 50% of total CO₂ emissions from oil refining. According to the IEA (2008a), “reformers, FCC and possibly vacuum distillation units could be equipped with high temperature CHP units with CO₂ capture”.

Van Straelen et al. (2009) described the main sources of CO₂ emissions as listed in the table below.

Table 2.III. Overview main sources of CO₂ from a typical complex refinery (Source: Van Straelen et al., (2009))

CO ₂ emitter	Description	% of total refinery emissions
Furnaces and boilers	Heat required for the separation of liquid feed and to provide heat of reaction to refinery processes such as reforming and cracking	30–60%
Utilities	CO ₂ from the production of electricity and steam at a refinery	20–50%
Fluid catalytic cracker	Process used to upgrade a low hydrogen feed to more valuable products	20–35%
Hydrogen manufacturing	For numerous processes, refineries require hydrogen. Most refineries produce this hydrogen on-site, for example via steam methane reforming or with a gasifier	5–20%

In this chapter, we will emphasize on carbon capture from the following refinery assets:

- Boilers and process heaters/furnaces
- Utilities/power plant
- Fluid catalytic cracking (FCC) unit
- Hydrogen plant

2.3.9.2.1. Heaters and boilers

A major source of CO₂ emissions from a refinery are heaters and boilers. They are responsible for 30 to 60% of total CO₂ emitted by a refinery (Van Straelen et al., 2009). CO₂ concentration ranges from 7 to 10% for boilers burning natural gas, 11 to 13% for boilers burning oil and 12 to 14% for boilers burning coal. CO₂ concentration is around 8% for heaters (IPCC, 2005).

Normally production of heat is distributed across the refinery infrastructure. This involves a challenge for CCS as it is most applicable to centralized production. For this reason flue gases of wide-spread heaters and boilers are connected in a ducting network and routed to one centralized point for CO₂ capture.

2.3.9.2.2. Utility plant

Another key source of CO₂ emissions is the plant that provides power and steam for the refinery. CO₂ emissions from the utilities plant account for 20 to 50% of the refinery complex. There is a variety of possible production methods for utilities, e.g. gas turbines, cogeneration units, integrated gasification combined cycle (IGCC). Carbon capture technologies for these energy technologies are already being developed.

2.3.9.2.3. Fluid catalytic cracker (FCC) unit

CO₂ emissions from fluid catalytic cracking (FCC) ranges from 20 to 35% of total CO₂ emissions from a refinery (Van Straelen et al., 2009).

Mello et al., (2009) state the following:

« The conventional catalytic cracking process converts heavy oil fractions to lighter products such as liquid petroleum gas (LPG) and gasoline with the use of a cracking catalyst. During the reaction step, coke is also formed and deposited on the surface of the catalyst, which is then deactivated. To reestablish catalyst activity, coke is burned in the regenerator with the use of air, thus forming CO₂, which is present in the flue-gas at typical concentrations of 10 – 20% vol. (full combustion). »

« Based on the characteristics of the FCC process, two possible ways to capture CO₂ from FCC include post-combustion technologies, such as CO₂ absorption, as well as oxyfiring, with the substitution of air by pure O₂ in the regeneration step. In this later configuration, some of the captured CO₂ is recycled back to the regenerator mainly to prevent temperature runaways during the combustion reaction. In this way the excess N₂ injected with air in the conventional mode is avoided and the separation of N₂ from produced CO₂ is not required. However an air separation unit (ASU) is required to produce the oxygen. The oxyfiring concept has been previously described in literature for coal gasification as well as for FCC processes. »

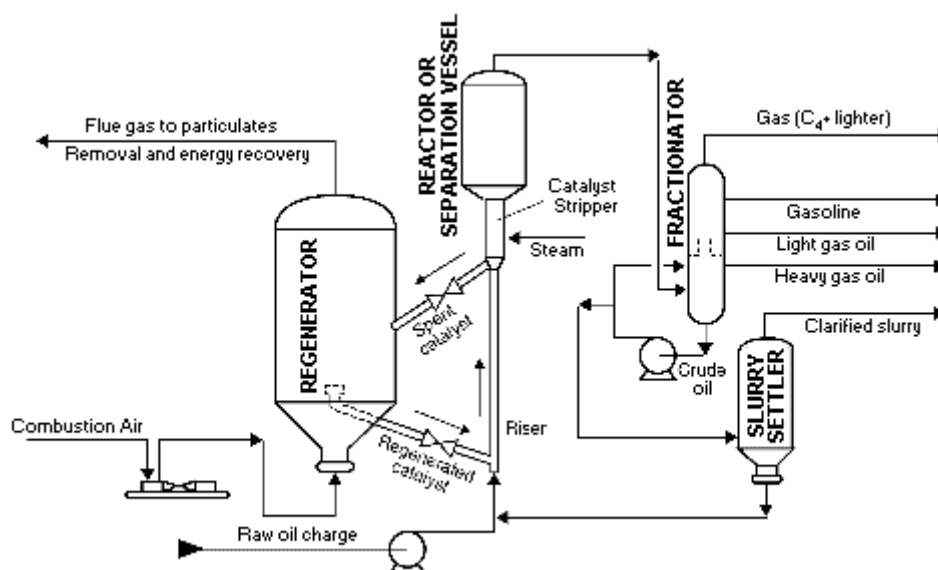


Figure 2.87. Fluid Catalytic cracking (FCC) (Source: <http://www.hghouston.com>)

The CO₂ Capture Project (CCP) has started an oxy-combustion capture trial on a pilot-scale Fluid Catalytic Cracking (FCC) unit. The test is expected to bring closer a more cost-effective technology capable of capturing up to 95% of FCC CO₂ emissions, potentially equating to some 20-30% of emissions from a typical refinery. The demonstration is taking place at a full burn FCC unit at a Petrobras research complex in Parana state, Brazil, with testing scheduled for completion at the end of May 2011. It is expected to confirm the technical and economic viability of retrofitting an FCC unit to enable CO₂ capture through oxy-combustion. The project will test start-up and shut-down procedures and different operational conditions and process configurations – allowing the CCP partners to gain reliable data for scale-up.

2.3.9.2.4. Hydrogen production

Hydrogen is consumed at refineries in the hydrocracking and hydrotreating processes. A refinery may have a lot of these hydrogen-consuming processes. Most refineries produce the hydrogen on-site. The hydrogen is provided by the reforming units of the refinery, which produce sufficient quantities when configuration of the refinery is the simplest. However, as refineries nowadays are complex plants with extensive hydrocracking and hydrotreating processes, huge amounts of hydrogen are required. When hydrogen consumption is larger than the quantity the catalytic reforming unit is able to produce, extra hydrogen will be established either from steam reforming or partial oxidation/gasification.

The choice of type of process (steam reforming or partial oxidation/gasification) for additional hydrogen production is depending on the following criteria:

- The nature of excess hydrocarbon streams which are available
 - Steam reforming of light hydrocarbons
 - Partial oxidation/gasification of heavy hydrocarbons
- The quantity of hydrogen that needs to be provided

The quantity of hydrogen that is required has an impact on the choice of process type. Gasification utilizes the heavier hydrocarbon streams with low H/C ratio (the heavier the feedstock, the lower the H/C ratio). If not enough hydrogen is present in the heavy hydrocarbons to produce the required quantity of hydrogen, extra hydrogen will be supplied through steam reforming of light hydrocarbons.

2.3.9.3. Carbon capture from refineries: data

In this chapter, we first describe the CCS possibilities for the heaters and boilers and then describe the CCS possibilities for the FCC units. CCS data of carbon capture from utility plants are not described in this chapter since it was already estimated for other sectors in the PSS-CCS I project. Data of carbon capture from hydrogen production is not described since it is part of chapter 2.3.7 (CO₂ capture in the hydrogen industry). The data in this chapter are all given for the capture system only. Reason for this is that the studies do not report the data for the reference process and the process with CCS, but for the capturing only.

It is technically feasible to apply post-combustion capture at a world-large scale complex refinery. This is concluded by Van Straelen et al. (2009). The authors investigated post-combustion capture, by the means of amine absorption, for a complex refinery with a capacity of 0.4-0.5 million barrels of oil per day. The CO₂ emissions profile of these existing refinery assets corresponds to that of a typical refinery, therefore representative for a large world-scale complex refinery.

The analyzed refinery involves a gasifier for hydrogen manufacture, a stand-alone cogeneration plant, a fluid catalytic cracker (FCC) and multiple smaller unit operations spread out over the plant infrastructure. The three largest emission point sources of the group of refinery assets are the cogeneration plant, the gasifier and a large combined stack, all emitting close to 1.2 Mt CO₂ per year. The large combined stack gathers flue gases from a number of large flue gas sources, for example furnaces and gas turbines.

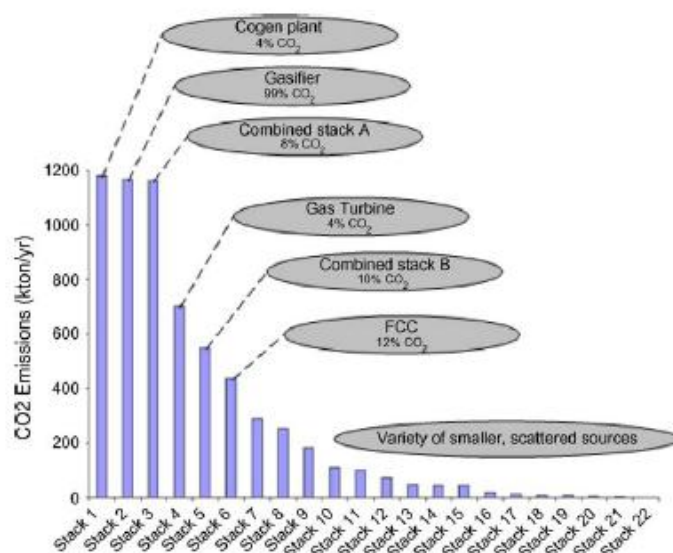


Figure 2.88. CO₂ emission profile of a refinery representative for a world-large scale complex refinery (Source: Van Straelen et al., 2009).

Van Straelen et al. (2009) derived the costs of capture as a function of CO₂ concentration in the gas stream and as a function of the flue gas volume (Figure 2.89 and Figure 2.90). By combining the two functions, the authors estimated the CO₂ avoided costs from all the point sources (Figure 2.91).

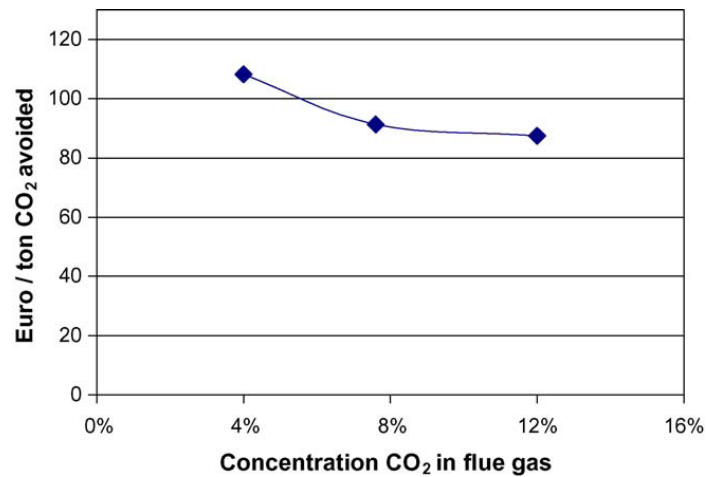


Figure 2.89. Capture costs as a function of CO₂ concentration in the exhaust gas. Costs are based on the capture 1 Mt CO₂ per year, CO₂ recovery has been optimised per case to between 85% and 90% (Source : Van Straelen et al. (2009)).

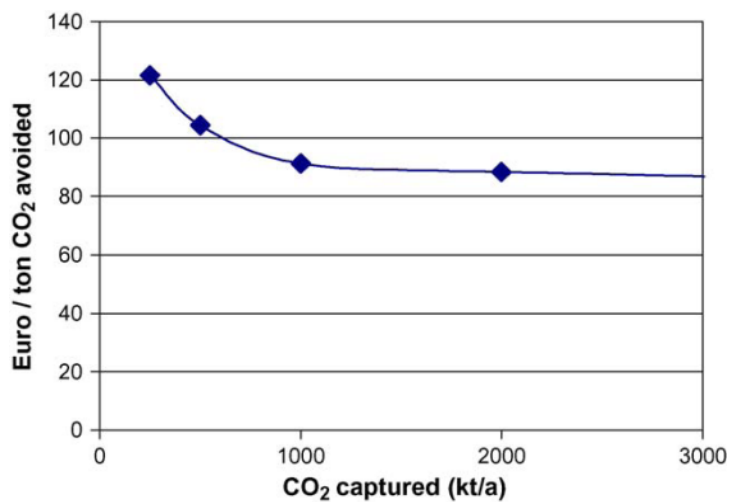


Figure 2.90. Capture costs as a function of flue gas volume for a flue gas containing 8% CO₂ (Source : Van Straelen et al. (2009)).

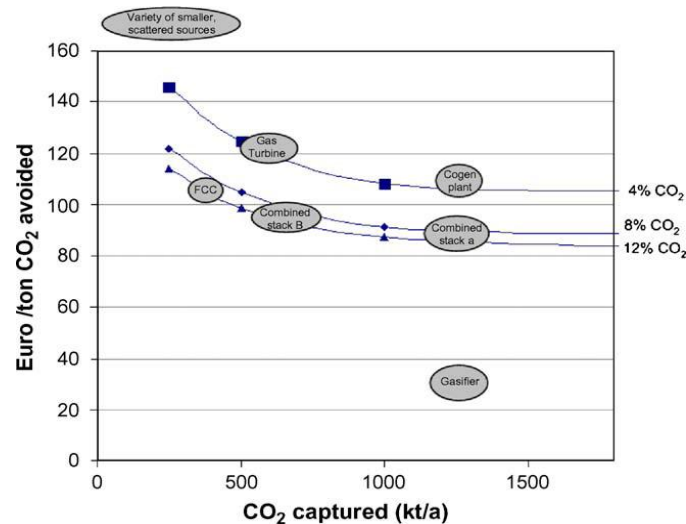


Figure 2.91. Overview of costs per tonne CO₂ avoided with MEA from emission point sources at a typical refinery (Source : Van Straelen et al. (2009)).

They also presented the CO₂ capture costs in a marginal abatement curve, where only sources of more than 400 kt per year are included.

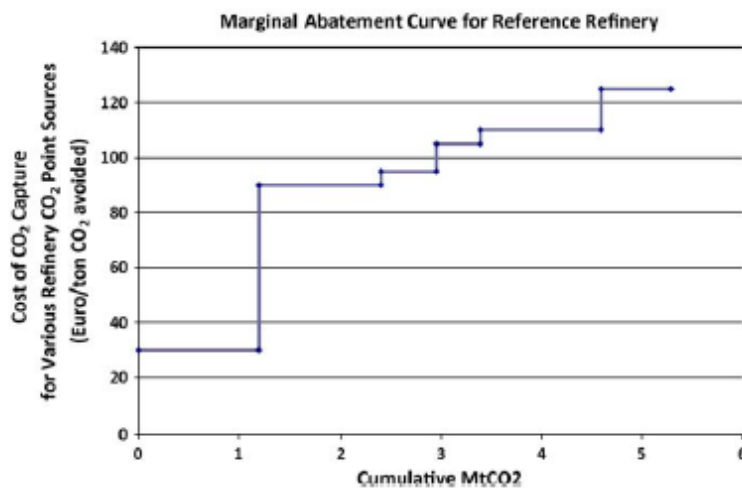


Figure 2.92. Marginal abatement curve CO₂ capture with MEA from CO₂ emission point sources at a typical refinery. Only sources of more than 400 kt per year are included (Source : Van Straelen et al. (2009)).

Carbon capture from the gasifier is found to be the cheapest, as the gas stream is already highly concentrated and CO₂ separation is already part of the hydrogen manufacture process. Furthermore, the most suited candidate for post-combustion capture is found to be the large combined stack, as it has the highest CO₂ concentration (8%) from the sources requiring chemical absorption and emitting 1.2 Mt CO₂/year. The next section investigates the performance of capture from the large combined stack into more detail.

2.3.9.3.1. Combined stack of heaters and boilers: incremental capture costs

The next paragraphs bring performance and cost estimates together from three different studies. All these studies investigate carbon capture from a common stack of refinery heaters and boilers, distributed across a refinery complex. The studies do not report a reference situation/process. The economics reported in these studies only reflect **the incremental costs of the capture system**, which comprise the cost of the additional capture system. One could interpret these costs as the difference between activity with CCS and activity without CCS. All the studies have a cogeneration unit to fulfil the utility needs for capturing the carbon dioxide.

The next table gives an overview of the investment costs we derived from the three studies. Note that the same scenario of heaters and boilers is considered in the studies of Simmonds et al., (2003) and Melien (2005). Simmonds et al., (2003) only consider post-combustion, whereas Melien (2005) also includes pre-combustion and oxy-fuel combustion. Because Simmonds et al., (2003) give more detailed data about energy consumption, we still include the results of Simmonds et al., (2003) in the present study. The lifetime of heaters and boilers is not given in each of these studies. We assumed lifetime to be 20 years in the calculation of costs per tonne CO₂ captured.

Table 2.LIII. Overview results of three studies

Study	Capture technology	CO ₂ separation technology	Investment (MEur2010/Mt captured/year)	cost CO ₂
Van Straelen et al (2009)	Post-combustion	Amine MEA ¹	235	
Simmonds et al (2003)	Post-combustion	Amine MEA ¹	158	
Melien (2005)	Post-combustion	Amine MEA ¹	158	
Melien (2005)	Pre-combustion	MWGS-DOE ²	227	
		MWGS-DOE/GRACE ³	103	
		Pd – MWGS/Grace ⁴	121	
		FG-Rec ASU ⁵	194	
Melien (2005)	Oxy-fuel combustion	FG-Rec ITM ⁶	293	

Notes : (1) monoethanolamine ;

(2) Membrane water gas shift w/DOE-membrane (MWGS/DOE) ;

(3) Membrane water gas shift GRACE&DOE-membrane (MWGS-DOE/GRACE) ;

(4) Membrane water gas shift GRACE & Pd-membrane (Pd – MWGS/Grace) ;

(5) Heaters and boilers with flue gas recycle and ASU : FG-Rec ASU

(6) Heaters and boilers with flue gas recycle and ionic transport membrane : FG-Rec ITM

2.3.9.3.1.1. Van Straelen et al. (2009)

About 1.11 Mt CO₂ per year is emitted by the combined stack. However, the output capacity of the combined stack is not given in Van Straelen et al., (2009). To capture the CO₂ from the combined stack, a capture plant was designed. The plant capacity factor is 95%. The capture efficiency of the overall equipment amounts to 90% (1 Mt CO₂ per year is captured). The energy and utility needs of the capture plant are supplied through a new stand-alone utility plant (the high energy demands couldn't be provided by existing utility assets of the refinery). The next table lists the required power and steam amount to be served to the capture plant.

Table 2.LV. «Overview utilities for capture plant » (Source: Van Straelen et al. (2009))

Net power output	16.4MW
LP process steam	128MW
Combined heat and power efficiency	93.5%
Fuel gas consumption	157mW
CO ₂ produced	270 kt/a

Based on the results of Van Straelen et al., (2009), we compile the data that can be readily inputted to the energy MARKAL-TIMES model. These parameters are presented in Table 2.LXII.

Table 2.LV. Combined stack with post-combustion CO₂ capture (incremental costs and utilities)

	Parameter ID	Value	Unit	
Inputs	LP process steam	3,84	PJ	
	Power	0,4913	PJ	
Performance	CO ₂ captured	1	Mt/year	
	CO ₂ avoided	0,73	Mt/year	
	CO ₂ capture efficiency	90	%	
Costs	Investment	235	MEur2010/Mt	CO ₂ captured/year
		18,9	MEur2010/year ¹⁴	
	VOM	---		
	FOM	---		

¹⁴ Based on lifetime of 20 years, annuity with discount rate 5%

The investment cost could be simulated, as total yearly cost is formed by the yearly cost of gas consumption together with the annuity of investment cost. We tried out which investment cost would give us the CO₂ avoided cost, after we had calculated the yearly cost of gas consumption. The CO₂ avoided cost for the large combined stack is estimated at 90 Eur/t CO₂ avoided (results of Van Straelen et al., 2009, Figure 2.91). The yearly cost of gas consumption is calculated using fuel gas consumption, plant capacity factor of 95% and assuming fuel gas price amounts to 10 Eur/GJ. The next table gives an overview of the input parameters we filtered out of Van Straelen et al., (2009) and our own assumptions.

Table 2.LVI. Parameters inputted to the simulation of the investment cost from table 1

Parameter ID	Value	Unit	Source
Fuel gas consumption	157	MW	Van Straelen et al., (2009)
Plant load	8322	hours	Van Straelen et al., (2009) : availability = 95%
Fuel gas price	10	Eur/GJ	Own assumption
Lifetime	20	years	Own assumption
Discount rate	5	%	Own assumption
CO ₂ avoided cost	90	Eur/t avoided	CO ₂ Van Straelen et al., (2009)
CO ₂ captured cost	66	Eur/t captured	CO ₂ Own calculation

2.3.9.3.1.2. Simmonds et al., (2003); CO₂ capture project (CCP)

It is technically feasible to apply **post-combustion CO₂ capture** to process heaters and boilers across a refinery and petrochemical complex. This is concluded by Simmonds et al., (2003). The authors examine results found in the CO₂ capture project (CCP) for an actual based site, the BP Grangemouth refinery and petrochemical complex situated in the United Kingdom.

Post-combustion capture, by the means of amine absorption, is applied to refinery fired heaters (burning low sulphur fuel oil and natural gas), power plant boilers (burning low sulphur fuel oil) and chemical plant reaction furnaces (burning sulphur free natural gas). As these refinery assets are distributed across the plant infrastructure, the flue gases are connected in a collection network comprising about 2 km of ducting. To push the flue gases through this ducting network, 15 MW is required to serve the blower power demand. To overcome the pressure drop imposed by the packed column absorbers, 10 MW of power is served to additional blowers.

The capture system can collect 2 Mt CO₂ per year (or 6000 t CO₂ per day). Because of this very large scale capture, the high energy and utility demands of the capture plant need to be supplied through a new stand-alone utility plant (as it can't be provided by the existing utility capacity of the refinery). A combined heat and power (CHP) plant is chosen to serve the utilities to the capture system. An overview of the energy and utilities requirements of the capture plant, as given by Simmonds et al., (2003), is shown in Table 2.LVII.

Table 2.LVII. Utility requirements of the CO₂ capture plant (Source: Simmonds et al., 2003)

Utility	Quantity	Units	Plant Description
Steam	480	tonnes per hour	CHP plant (back pressure turbine)
Power	72	megawatts	CHP plant (72 MW generator)
Cooling Water	18,139	cubic metres per hour	Two cooling towers (10,000 m ³ /h each)
Natural Gas	396	megawatts	Direct import for CHP firing
Water	1,025	tonnes per hour	Direct import for system makeup

Though the purpose of the capture plant is to reduce environmental emissions, activity of the capture system is related to waste streams and emissions as well. The amount of CO₂ emissions from the utility plant boiler is around 0.5 Mt CO₂ per year. Other pollutants are emitted as well (as NO_x and SO₂, therefore pre-treatment is required).

A breakdown of total capital costs of the CO₂ capture plant is summarized in Table 2.LVIII.

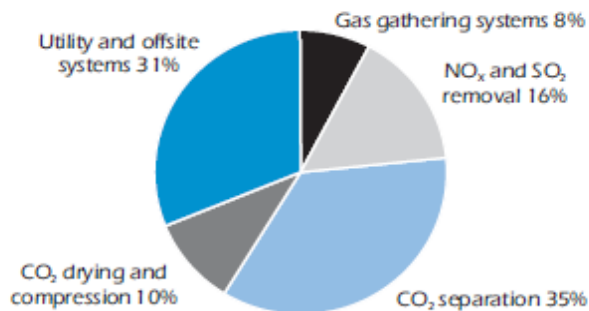
Table 2.LVIII. Total capital cost breakdown of the CO₂ capture plant (Source: Simmonds et al., 2003)

Capture Plant Unit	Millions US\$
Gas gathering systems	39
NO _x and SO _x removal	74
Econamine FGSM	166
CO ₂ drying and compression	48
Utility and offsite systems	149
TOTAL	476

The study of IEA (2008) is based on the same paper (Simmonds et al, 2003) and gives a breakdown of these investment costs (figure 52). It is remarked that CO₂ separation and compression accounts for less than half of the incremental investment costs.

Key point

CO₂ separation and compression is responsible for less than half of the capture investment costs for oil refining.



Source: Simmonds, et al., 2003.

Figure 2.93. Investment cost structure for the CO₂ capture plant (Source: IEA, 2008a)

A full operational cost structure for the CO₂ capture plant was unavailable at the time the study of Simmonds et al. (2003) was published. Preliminary results suggest that operational costs are to a large extent established from the price of natural gas.

The unit CO₂ capture costs are estimated at 47-57 Eur2010 (indicative values). These costs will be dominated by future swings in gas price (Simmonds et al., 2003).

Based on the results of Simmonds et al. (2003), we compile the data that can be readily inputted to the energy MARKAL –TIMES model. These parameters are presented in the next table.

Table 2.LIX. Incremental costs of post-combustion capture for common stack of refinery heaters and boilers

	Parameter ID	Value	Unit	
Inputs	Steam	6,65	PJ	
PJ	Power	2,05	PJ	
Performance	CO ₂ avoided	1,5	Mt/year	
	CO ₂ captured	2	Mt/year	
	Capture efficiency	85	%	
Costs	Investment	158	MEur2010/Mt	CO ₂ captured/year
			MEur2010/year ¹⁵	
	VOM	---		
	FOM	---		

¹⁵ Based on lifetime of 20 years, annuity with discount rate 5%

We derived investment cost from the breakdown of total capital costs, but the cost of utility and offsite systems is left out. The cost of utility should not be included in the data of the energy MARKAL - TIMES model as this cost is already in the model via the standard energy production methods. Therefore we have estimated the part of the CHP capital cost in the cost of utility and offsite systems. We calculated that CHP delivers 218 MWe to serve the capture plant, thereby assuming that electric efficiency equals 55% (as in a standard power plant without heat production). Assuming an investment price of 500 euro₂₀₁₀/kW (as in a standard gas-fired power plant), the fired duty would cost 108.9 Meuro₂₀₁₀. This cost is underestimated because we assumed CHP to be a simple power plant. This leads us to the conclusion that the cost of utility and offsite systems (143 Meuro₂₀₁₀) could be entirely accounted for the cost for producing heat and electricity.

2.3.9.3.1.3. Melien (2005); CO₂ capture project (CCP)

Costs and performance data of several capture technologies for refinery heaters and boilers are found in the CO₂ capture project (CCP), and these are summarized by Melien (2005). Costs and performance of a range of capture technologies are evaluated: **post-combustion, pre-combustion and oxyfuel combustion**. The technology cases are developed for an actual site, the BP Grangemouth refinery and petrochemical complex located in the UK. This complex refinery is provided by a fixed amount of heat and steam coming from heaters and boilers. The common capacity of the heaters and boilers selected for capture is 1351 MW. Uncontrolled CO₂-emissions from this range of heaters and boilers amount to 2.6 Mt CO₂/year.

Because of the very large scale emissions from the target heaters and boilers, the high energy and utility demands of the capture systems cannot entirely be supplied through existing utility capacity of the refinery. Therefore demands are partly generated on-site, partly provided by imports from external sources. Some of the capture technologies require a new stand-alone utility plant in order to deliver power to the capture system. In these cases, investment cost includes the building of the new on-site power plant. The cost estimates comprise the following cost components:

- Full cost (capital and operational costs) of the new on-site built power plant
- Fuel gas and excess power export streams
- Primary capture processing facilities
- Systems collecting CO₂ from distributed emissions sources

The incremental costs are furthermore estimated at generic and local (regional: UK) price levels. The unit costs and rates for utilities, energy and labour supplies are based on current market data in case of the generic prices, whereas they are site-specific in case of the local prices. Generic prices are partly established from current market data, nevertheless one should interpret these as long-term (10-25 years horizon) expected price levels.

In the following paragraphs, we gather economics and performance estimates at both generic and local prices. On the one hand, price levels for energy supplies are not of interest for this study, as energy and production methods should not be included in the energy MARKAL model. On the other hand, price levels for capital costs and O&M are of interest for this study. Therefore it is still useful to report incremental capital and O&M costs at both generic and local prices.

In Melien (2005), price and unit cost assumptions are only mentioned for energy supplies. Price and unit cost assumptions for labor cost/productivities are not given. Because energy price levels will have an impact on the value of CO₂ avoided costs (see Figures 2.94 and 2.95), we still list these in the next table.

Table 2.LX. Generic and local (UK) prices used in CO₂ avoided costs (Source: Melien (2005))

Technology	Generic	Local (UK)	Unit
Post-combustion			
Natural gas	2,72	2,72	Eur2010/GJ
Electricity	32,55	32,55	Eur2010/MWh
Pre-combustion			
Natural gas	2,72	2,72	Eur2010/GJ
Electricity	32,55	32,55	Eur2010/MWh
Oxyfuel combustion			
Natural gas	2,72	2,91	Eur2010/GJ
Electricity	32,55	28,81	Eur2010/MWh

In the following, we firstly report incremental cost estimates at generic prices, after which we continue in reporting cost estimates at local prices.

1. Generic prices

Table 2.LXI, Table 2.LXII & Table 2.LXIII summarize the **incremental cost** estimates of the post-combustion, pre-combustion and oxyfuel combustion capture systems at generic price levels.

For each capture technology, total O&M (excl. energy) is known from Melien (2005). Fixed O&M and variable O&M however are not known. For this reason, we established fixed O&M and variable O&M from total O&M. We split up total O&M by assuming that fixed O&M is responsible for 4% of total O&M. We also accounted for the onstream factor of 90.4% for variable O&M.

- **Post-combustion baseline (BL) amine MEA**

Post-combustion capture for the UK scenario was already discussed in section 10.3.1.2. Indeed, cost estimates of post-combustion capture from heaters and boilers of the UK BP Grangemouth site are examined both in the study of Simmonds et al., (2003) and Melien (2005). Though the same scenario is described, the two study's have a different method in reporting the results.

Melien (2005) only reports the net result of the import and export power streams of the utility plant. The author does not mention separately the amount of power that is generated with the amount of fuel gas consumed, or the amount of steam/power that needs to be provided to the capture system. The advantage of the results of Simmonds et al. (2003) is that heat integration was not considered.

But in contrast with Simmonds et al. (2003), Melien (2005) also reports costs concerning O&M. In Simmonds et al. (2003), capital costs are the only costs estimated (Figure 2.93, and summarized in Table 2.LIX) because the economic analysis was not yet completed at the time their paper was published.

According to the economics reported in Melien (2005), we retake the results for the UK scenario. Table 2.LIV reports the parameters we gathered.

Table 2.LXI. Incremental costs of post-combustion capture for common stack of refinery heaters and boilers

<i>Post-combustion</i>	Parameter ID	Value	Unit
Inputs	Heat	11,29	PJ
Outputs	Electricity/steam	0	PJ
Performance	CO ₂ captured	2,19	Mt/year
	CO ₂ avoided	1,55	Mt/year
Costs	Capture efficiency	85	%
	Investment	158	MEur2010/Mt CO ₂ captured/year
	Fixed O&M	13,86	MEur2010
	Variable O&M	7,50	MEur2010/Mt CO ₂ captured/year

• **Pre-combustion**

In the CCP program, three pre-combustion technologies are evaluated:

- Membrane water gas shift w/DOE-membrane (MWGS/DOE) : MWGS-DOE
- Membrane water gas shift GRACE&DOE-membrane (MWGS/DOE) : MWGS-DOE/GRACE
- Membrane water gas shift GRACE & Pd-membrane (MWGS/Grace) : Pd – MWGS/Grace

We gather costs and performance data for each of the technology cases (Table 2.LV). Both fixed and variable O&M exclude energy supplies.

Table 2.LXII. Incremental costs of pre-combustion capture for common stack of refinery heaters and boilers

<i>Pre-combustion</i>	Parameter ID	MWGS-DOE	MWGS-DOE/GRACE	Pd – Grace	Unit
Inputs	Heat	13,83	8,58	8,58	PJ
Outputs	Electricity/steam	1,20	0	0	PJ
Performance	CO ₂ captured	2,19	1,99	1,99	Mt/year
	CO ₂ avoided	1,54	1,5	1,5	Mt/year
Costs	Capture efficiency	85	77	77	%
	Investment	227	103	121	MEur2010/Mt CO ₂ capt/year
	Fixed O&M	19,91	8,19	9,61	MEur2010
	Variable O&M	1,06	1,83	2,11	MEur2010/Mt CO ₂ capt/year

- **Oxyfuel combustion**

In the CCP program, two oxyfuel combustion technologies are evaluated:

- Heaters and boilers with flue gas recycle and ASU : FG-Rec ASU
- Heaters and boilers with flue gas recycle and ionic transport membrane : FG-Rec ITM

We gather costs and performance data for each of the technology cases (Table 2.LVI). Both fixed and variable O&M exclude energy supplies.

One should notice that the amount of electricity exported from the utility plant is especially high in the case of oxyfuel combustion with flue gas recycle and ionic transport membrane. The power export stream corresponds to 45% of the imported heat demand, which is enormous.

Table 2.LXIII. Incremental costs of oxyfuel combustion capture for common stack of refinery heaters and boilers

<i>Oxyfuel combustion</i>	Parameter ID	FG-Rec ASU	FG-Rec ITM	Unit	
Inputs	Heat	4,28	28,05	PJ	
Outputs	Electricity/steam	0,31	12,71	PJ	
Performance	CO ₂ captured	2,08	2,09	Mt/year	
	CO ₂ avoided	1,87	1,95	Mt/year	
Costs	Capture efficiency	80,93	81,32	%	
	Investment	194	293	MEur2010/Mt CO ₂ captured/year	
	Fixed O&M	16,16	24,47	MEur2010	
	Variable O&M	2,10	1,23	MEur2010/Mt CO ₂ captured/year	

The breakdown of the CO₂ avoided costs at generic prices is shown in figure 53.

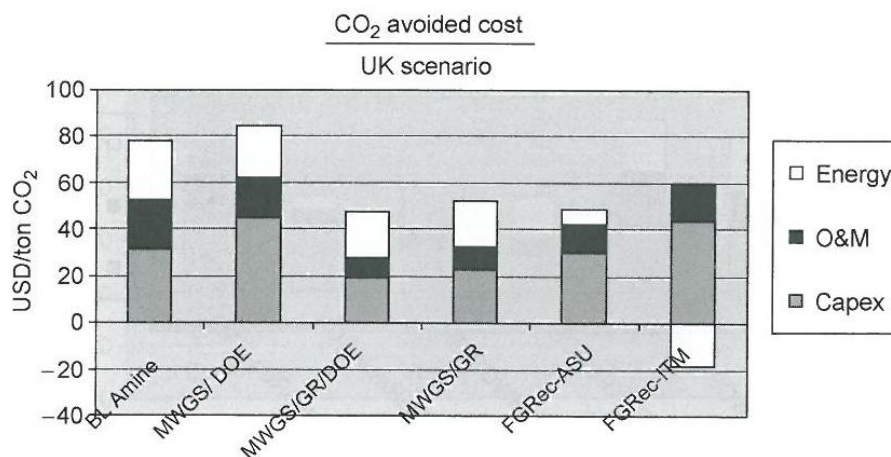


Figure 2.94. CO₂ avoided cost breakdown at generic prices (Source: Melien, 2005)

2. Local or regional prices

Table 2.LXIV lists the incremental investment and O&M costs at generic prices.

Table 2.LXIV. Incremental costs of capture systems at generic and prices for refinery heaters and boilers

<i>Technology</i>	<i>Investment cost (MEur2010/Mt CO₂ captured/year)</i>	<i>Fixed O&M (MEur2010)</i>	<i>Variable O&M (MEur2010/Mt CO₂ captured/year)</i>
(Post) Amine MEA	158	13,86	16,43
(Pre) Pd-MWGS/GRACE	227	19,91	2,33
(Pre) MWGS-DOE/GRACE	103	8,19	3,64
(Pre) MWGS-DOE	102	9,61	4,19
(Oxy) FG-Rec ASU	193	16,16	4,36
(Oxy) FG-Rec ITM	293	24,47	2,58

The values of variable O&M for post-combustion are high in comparison to the values of variable O&M for the other capture technologies.. The investment cost of post-combustion is lower than the investment cost of pre-combustion (by the means of Pd-MWGS/GRACE) and oxyfuel combustion.

The breakdown of the CO₂ avoided costs at local prices is shown in Figure 2.95.

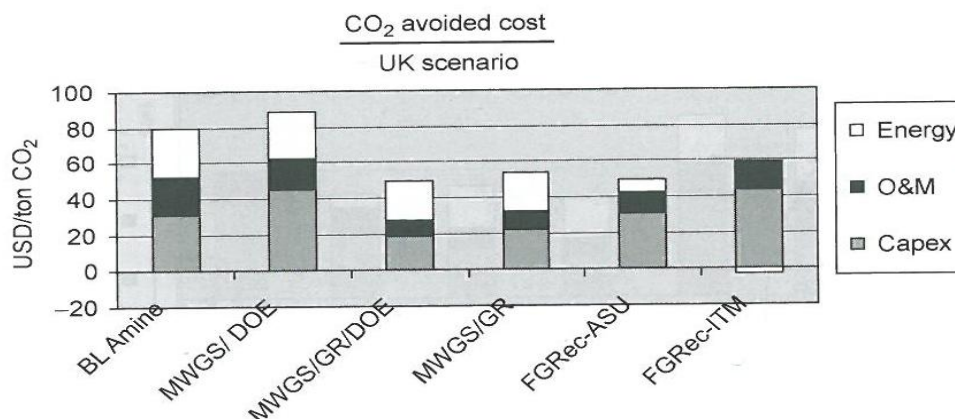


Figure 2.95. CO₂ avoided cost breakdown at local prices (Source: Melien, 2005)

2.3.9.3.2. Utility plant

CCS data of carbon capture from utility plants are not described in this chapter since it was already estimated for other sectors in the PSS-CCS I project.

2.3.9.3.3. FCC units

2.3.9.3.3.1. Van Straelen et al., (2009)

Results of Van Straelen et al., (2009) are previously discussed in section 2.3.9.3.1.1 (Van Straelen et al. (2009)). The authors investigated post-combustion capture for a number of refinery assets in a typical complex refinery. Only capture from a large combined stack was worked out with incremental costs and performance estimates. The other refinery assets, including the FCC unit, were not further completed with costs and performance estimates.

Nevertheless, some important variables (CO₂ concentration and flue gas volume) that determine costs of carbon capture were shown for all refinery assets (Figure 2.91). This allows as to extrapolate costs estimates for the FCC unit, as costs of capture are derived as a function of these variables (Figure 2.92).

We know that the CO₂ concentration of the FCC unit (12%) is higher than the CO₂ concentration of the combined stack (8%) in the reference case. The higher the CO₂ concentration, the lower the capture costs. According to Figure 2.91, costs corresponding to 12% CO₂ concentration are however nearly the same as costs corresponding to 8% CO₂ concentration. This means that the higher value of CO₂ concentration does not lead to a significant difference in the CO₂ avoided costs.

The other variable determining costs is the volume of the flue gas. The volume of CO₂ to be captured is lower for the FCC unit (0.4 Mt CO₂ per year) than for the combined stack (1 Mt CO₂ per year). According to Figure 2.91, differences between these two volumes have a significant impact on costs. Therefore, capture from the FCC unit is more expensive than capture from the large combined stack.

Because of the smaller scale of capture, the CO₂ avoided costs of the FCC unit (105 Eur/t CO₂ avoided) is around 17% higher than the CO₂ avoided costs of the large combined stack (90 Eur/t CO₂ avoided) (Figure 2.89). Therefore we assume that the parameters we gathered for the large combined stack will be 17% lower than the parameters for capture from the FCC unit. So we derive cost estimates for the FCC unit that are 17% higher than those of the large combined stack. Thereby we assume that the rise in costs is distributed evenly between gas consumption costs and investment costs, and that energy prices remain the same.

Table 2.LXV gathers parameters based on Table 2.LX and our own assumptions.

Table 2.LXV. Incremental costs of post-combustion capture system for an FCC unit of a typical complex refinery

<i>Post-combustion</i>	Parameter ID	Value	Unit
Inputs	LP process steam	4,46	PJ
	Power	0,5692	PJ
Performance	CO ₂ captured	0,4	Mt/year
	CO ₂ capture efficiency	90	%
Costs	Investment	274	MEur2010
	VOM	---	
	FOM	---	

2.3.9.3.3.2. Mello et al., (2008)

Mello et al., (2008) have evaluated the economical and technological performance of two capture technologies for an existing FCC unit: post-combustion capture (by means of chemical absorption) and oxy-fuel combustion capture. The chemical absorption technology was chosen to be the base case of the study (since it is the most advanced, commercially proven process). The oxy-firing technology considered two oxygen purity levels: 99.5% and 95%. These two technologies required changes in FCC operation. "For the study, a 10000 m³/d resid FCC unit was set as reference".

The flue gas composition for the base case and the two oxyfuel-cases are listed in Table 2.LXVI.

Table 2.LXVI. Flue gas composition for chemical absorption (base case) and oxy-fuel combustion with 99.5% O₂ and 95% O₂ (Source: Mello et al. (2008)).

	Base case	Oxyfiring	
		99.5% O ₂	95% O ₂
Total flow-rate (t/h)		765 666	755 170
O ₂ (%mol)	2.7	2.8	2.8
CO ₂ (%mol)	13.5	89.4	84.3
H ₂ O (%mol)	10.0	6.95	6.98
N ₂ (%mol)	72.90	0.17	1.71
Ar (%mol)	0.85	0.40	3.99
CO (ppm)	9.0	9.0	9.0
SO _x (ppm)	378	2383	2246
NO _x (ppm)	81	536	505

The value of CO₂ concentration is 13.5% when post-combustion is applied, whereas values are significantly higher (89.4% and 84.3%) in the two oxyfuel-cases.

The CO₂ in the gas stream needs to be purified before being captured. Results of the CO₂ purification process are as listed in Table 2.LXVII:

Table 2.LXVII. CO₂ purity and CO₂ recovery rate for chemical absorption (base case) and oxy-fuel combustion with 99,5% O₂ and 95% O₂ (Source: Mello et al. (2008)).

	Units	Base Case	99.5%O ₂	95%O ₂
CO ₂ Purity	vol%	99.95	96.07	95.24
CO ₂ Recovery	%	90.42	99.99	90.52
Product CO ₂	ton/h	101.7	112.3	101.6

After purification, the level of CO₂ purity is high at 99.95% for amine absorption and 96.07% and 95.24% for the two oxyfuel-cases. Note that also the CO₂ recovery rate is shown in Table 2.LXVII.

Chemical requirements and costs as listed in Mello et al. (2009) are shown in the table below.

Table 2.LXVIII. "Chemical requirements and costs" (Source: CCP (2009))

	Cost (\$/kg)*	Annual chemical requirement (t/year)		
		Chemical requirements and costs		
		Base Case	99.5%O ₂	95%O ₂
MEA (100%)	2.76	632	-	-
Corrosion inhibitor	6.61	49	-	-
Filter aid	2.76	67	-	-
Activated carbon	3.86	67	-	-
Sodium carbonate	0.56	556	-	-
Disposal	0.077	10,116	-	-
Molsieve	3.86	48	5.4	5.9
Limestone (100%)	0.0195	5,364	5,364	5,364
Final cost (MM\$/y)	-	3.73	0.86	0.86

*based on prices in the USA (2007)

Utility requirements as listed in Mello et al. (2008) are shown in table 61.

Table 2.LXIX. "Utility requirements" (Source: Mello et al. (2008))

	Units	Base case	99.5%O ₂	95%O ₂
Water makeup	m ³ /h	67.5	59.8	59.8
Water blowdowns	m ³ /h	15.1	18.3	18.3
Cooling tower water	m ³ /d	572.2	288.3	314.1
STEAM CONSUMED	t/h	140.3	0.3	0.4
HP	t/h	0	2.3	2.4
MP	t/h	216.5	0	0
LP	t/h	78.7	103.6	102.2
STEAM PRODUCED (WHSG)	MW	15.8	74	71.2
HP	m ³ /h	67.5	59.8	59.8
Electrical power		15.1	18.3	18.3

Heat integration was not considered in the study. The steam inputted to the capture process is assumed to be supplied through the refinery. The high-pressure steam exported back to the refinery is produced from the stream heat generator (WHSG). The duty of the WHSG is to purify the CO₂. While the hot flue gases are passing through the WHSG, high-pressure steam is produced.

The structure of the installed costs is shown in Table 2.LXX.

Table 2.LXX. Structure of the installed costs (Source: Mello et al. (2008))

	Relative contribution to total capital cost (% of total)		
	Base Case	99.5%O ₂	95%O ₂
WHSG	11.4	8.4	8.2
SO _x Removal	17.8	12.3	12.0
Amine plant	44.9	-	-
ASU	-	43.0	39.9
Recycle compression	-	10.8	13.0
CO ₂ compression	9.5	8.7	7.2
Dehydration	3.2	0.9	1.0
Propane refrigeration	-	-	1.8
Balance of plant	6.9	5.1	5.4
Home office engineering	3.5	6.7	7.0
Insurance	0.3	0.4	0.5
Profit	2.6	3.6	4.0
		% change relative to base case	
Total cost	-	+45	+48

The base case (amine absorption) seems to have lower capital costs than both the oxy-firing cases: installed costs are 45% lower for oxyfuel with 99.5% O₂ and 48% lower for oxyfuel with 95% O₂.

The table above only shows relative cost estimates. Absolute values of capital costs are listed in the table below. As these values are not found in Mello et al (2008), we obtained them from Mello et al. (2009).

Table 2.LXXI. Absolute installed costs (Source: Mello et al., 2009)

	Capital cost estimation (MM\$)		
	Base Case	99.5%O ₂	95%O ₂
WHSG	152	16.2	16.2
SO ₂ Scrubber	237	23.7	23.7
Amine plant	598	-	-
ASU	-	83.1	78.8
Recycle compression	-	20.9	25.7
CO ₂ compression	126	16.9	14.3
Dehydration	4.2	1.8	2.0
Propane refrigeration	-	-	3.5
Balance of plant	9.2	9.9	10.7
Home office engineering, insurance and profit	8.4	20.8	22.6
Plant total	344	70.3	78.8
Total	133.1	193.3	197.5

Also obtained from Mello et al. (2009) are data about CO₂ emissions from the FCC unit, CO₂ captured and CO₂ avoided. Note that for both oxy-combustion cases there is a net steam production rather than consumption.

Table 2.LXXII. Total CO₂ emissions from FCC, CO₂ captured and CO₂ avoided (Source : Mello et al., 2009)

	Unit	Values		
		Base case	99.5% O ₂	95% O ₂
Total CO ₂ from FCC	t/h	112.46	112.27	112.27
Product CO ₂ (captured)	t/h	101.69	112.26	101.63
Net steam consumption	t/h	277.8	-101	-99.4
Steam-related CO ₂ emission	t/h	33.3	-12.1	-11.9
Net power consumption	MW	15.8	740	71.2
Power-related CO ₂ emission	t/h	585	2738	2634
Avoided CO ₂	t/h	62.5	970	87.2

CO₂ capture and as given in Mello et al. (2008) are listed in table 65.

Table 2.LXXIII. CO₂ capture costs (Source: Mello et al., 2008)

	Relative contribution to total cost (% of total)		
	Base Case	99.5% O ₂	95% O ₂
CAPEX	18	41	42
OPEX	82	59	58
Total cost		% change relative to base case	
Capture	-	-44	-38
Avoided	-	-61	-56

Post-combustion (base case) has lower capital expenditures (Capex) than the two oxyfuel cases but also has higher operational expenditures (Opex). This can be clearly seen in Figure 2.96.

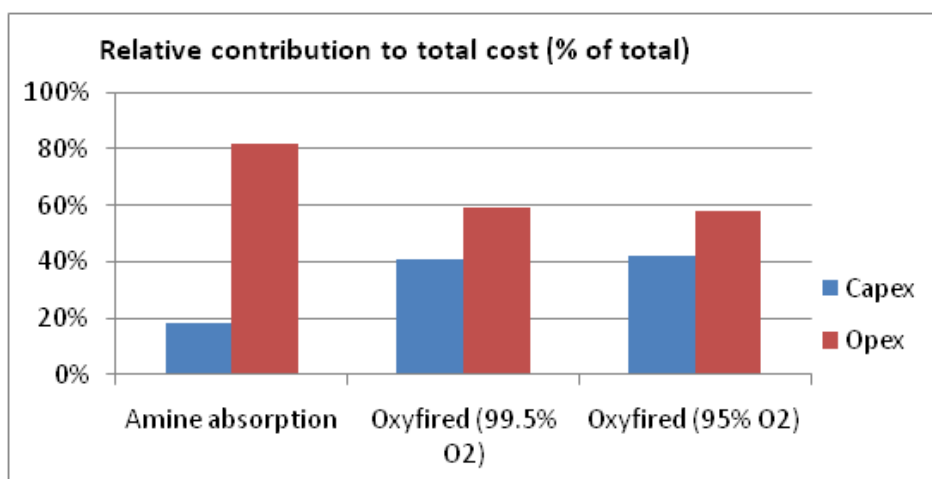


Figure 2.96. Relative contribution of capex (capital expenditures) and opex (operational expenditures) to total cost

At the end, the profit of lower Opex outweighs the extra costs of higher Capex. The two oxy-fuel cases "showed an approximate 45% to 60% reduction in capture and avoided costs, respectively".

Based on the results of Mello et al. (2008) and Mello et al. (2009), we compile the data that can be readily inputted to the energy MARKAL-TIMES model. These parameters are presented in the next tables. Note that they are only given for the capture system only.

For each of the cases, we assumed that capacity factor is 90% (corresponding to 7884 hours). O&M are 4% of the investment costs, as mentioned in Mello et al. (2008).

- **Post-combustion CO₂ capture**

Table 2.LXXIV. Incremental costs, inputs and outputs of post-combustion capture from an FCC unit

	Parameter ID	Value	Unit
Inputs	HP steam	1,78	PJ
	MP steam	0	PJ
	LP steam	2,32	PJ
	Power	0,27	PJ
Outputs	HP steam	1	PJ
Performance	CO ₂ captured	0,89	Mt/year
	CO ₂ avoided	0,55	Mt/year
	CO ₂ capture efficiency	90,42	%
Costs	Investment	1,68	MEur2010/MW
	O&M	0,0672	MEur2010/MW

- **Oxy-fuel combustion capture with 99.5% O₂**

Table 2.LXXV. Incremental costs, inputs and outputs of oxyfuel combustion (99,5% O₂) from an FCC unit

	Parameter ID	Value	Unit
Inputs	HP steam	0,003	PJ
	MP steam	0,020	PJ
	LP steam	0	PJ
	Power	0,805	PJ
Outputs	HP steam	1	PJ
Performance	CO ₂ captured	0,98	Mt/year
	CO ₂ avoided	0,85	Mt/year
	CO ₂ capture efficiency	99,99	%
Costs	Investment	1,68	MEur2010/MW
	O&M	0,0743	MEur2010/MW

- **Oxy-fuel combustion capture with 95% O₂**

Table 2.LXXVI. Incremental costs, inputs and outputs of oxyfuel combustion (95% O₂) from an FCC unit

	Parameter ID	Value	Unit
Inputs	HP steam	0,004	PJ
	MP steam	0,022	PJ
	LP steam	0	PJ
	Power	0,783	PJ
Outputs	HP steam	1	PJ
Performance	CO ₂ captured	0,89	Mt/year
	CO ₂ avoided	0,76	Mt/year
	CO ₂ capture efficiency	90,52	%
Costs	Investment	1,92	MEur2010/MW
	O&M	0,0769	MEur2010/MW

2.3.9.3.4. Hydrogen production

Cost estimates of carbon capture from hydrogen manufacture are already discussed in a previous chapter of this study. This data can be transferred to carbon capture from hydrogen production in the refinery sector.

2.3.10. CO₂ capture from industrial boilers

2.3.10.1. Introduction

Little data about CO₂ emissions from medium-scale sources like boilers exist. The study of IEA GHG (2007) estimates that coal-fired boilers are responsible for 6% of worldwide emissions and natural gas-fired boilers for 3% of worldwide emissions. Capture technologies are currently being developed for boilers in power plants. However, there exists little research about capture technologies for boilers outside the electricity industry. Reason for this is that CCS is most applicable to central production and to large-scale point sources. Nevertheless, there are opportunities for medium-scale installations like industrial boilers as well.

Opportunities for CCS are further discussed in this chapter. The chapter aims at presenting the possibilities of CO₂ capture for industrial boilers and the performance and economics of these boilers with the capture process.

2.3.10.2. CO₂ capture from industrial boilers

This chapter emphasizes on the opportunities of CCS for boilers outside the electricity sector. Many similarities between boilers found in a power plant and elsewhere (commercial, residential and industrial sectors) exist. The working principle of the boiler is always the same. Only temperature of combustion gases at the outlet are different for boilers in power plants and industrial boilers. Besides that, an important difference is in the scale of production. The scale of the point source is an important factor because energy consumption and costs both depend on them. Larger CO₂ sources have lower energy consumption and costs due to the economy of scale. To overcome the issue of the relative small scale of industrial boilers, multiple small-scale units can be connected with each other in a ducting network in order to collect their flue gases in a centralized network. A single capture plant can provide the capturing of CO₂ for various industrial boilers. Where industrial boilers are scattered sources that are not located close to each other, the challenge to route the gas streams to the centralized capture system is big.

In the following, we will first emphasize on the possibilities of CO₂ capture of a single industrial boiler. Then, we will consider the possibilities of connecting multiple small-scale boilers with each other to form a network of CO₂ capturing.

2.3.10.2.1. CO₂ capture from a single boiler

Air is used for combustion in conventional boilers. Where air is used as the oxidant stream in combustion processes, partial pressure of the CO₂ in the exhaust gas is low (less than 10%). The low partial pressure makes CO₂ separation techniques difficult and expensive. However, by increasing CO₂ partial pressure (and decreasing that of diluents like N₂ and O₂) CO₂ can be more easily separated. One effective method to generate a gas stream with high CO₂ concentration is to fire on oxygen rather than air. Oxy-fired boilers may be better candidates for CO₂ separation than air-fired boilers (Switzer et al., 2005).

In the following, we will present the design of a conventional air-fired boiler and two designs of oxy-fired boilers. The oxy-fuel fired boilers differ in the way the oxygen for combustion is supplied. Thereafter we will present performance and economics of these selected boiler types.

2.3.10.2.1.1. Conventional air-fired boiler (natural gas)

Switzer et al. (2005) present the conceptual layout of a conventional air-fired boiler burning natural gas (Figure 2.97). The CO₂ concentration of the air-fired system is low at 8%. Because of this, chemical absorption is required to separate the CO₂ from the other components of the exhaust gas.

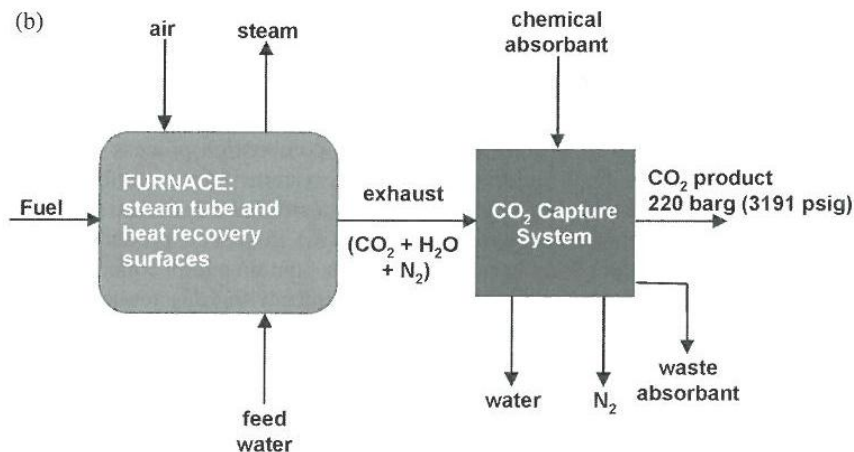


Figure 2.97. Conventional air-fired boiler with CO₂ capture by means of chemical absorption (Source: Switzer et al., 2005)

2.3.10.2.1.2. Natural gas-fired boiler with oxygen transport membranes (OTM)

Switzer et al. (2005) also present an oxy-fired boiler design in which the oxygen is supplied by oxygen transport membranes (OTM) surfaces integrated with the boiler system. The boiler with OTM is based on the advanced boiler concept to produce product steam under development by Praxair, Inc. OTM is a technology that is expected to significantly reduce the cost of oxygen production. OTM selectively moves O₂ across a ceramic membrane.

The OTM boiler can be equipped with a CO₂ capture system. The CO₂ capture system comprises compressors and equipment for heat exchange and drying.

Switzer et al. (2005) state that *"The overall design of the advanced boiler and CO₂ capture system consists of three basic parts: a furnace section, a heat recovery system, and an exhaust compression system. (...) The furnace section combusts the fuel and produces steam as a product. This part of the unit contains the ceramic membranes and steam tubes. A portion of the unused heat from the furnace section is recuperated in the heat recovery system. In this section, the hot exhaust and N₂-rich OTM offgas from the furnace section are utilized to preheat the incoming air and feed water streams. Finally, in the exhaust compression system, a series of compressors and heat exchangers are used to remove the water from the exhaust and compress the remaining CO₂ into a supercritical product. »*

The layout of the boiler design with OTM is presented schematically in the figure below.

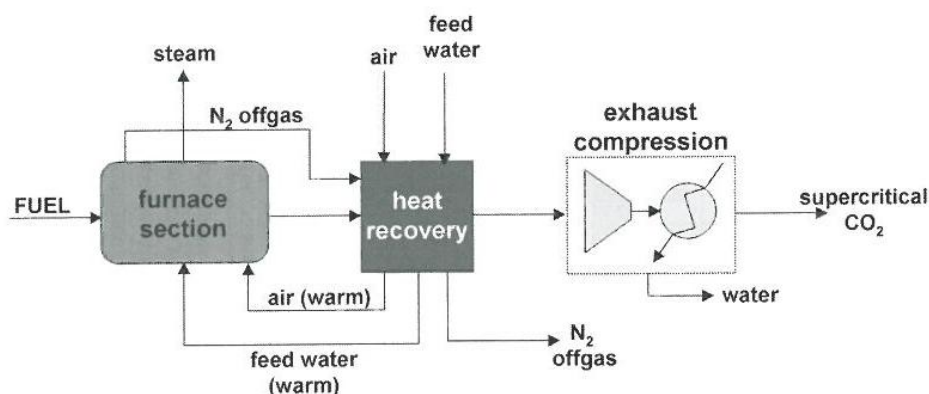


Figure 2.98. Boiler with oxy-fuel combustion via oxygen transport membranes (OTM's) (Source: Switzer et al., 2005)

2.3.10.2.1.3. Coal-fired boiler with oxygen conducting membranes (OCM)

IEA GHG (2007) presents an oxy-fired boiler in which the oxygen is combusted together with coal. The oxygen is supplied by oxygen conducting membranes (OCM) surfaces integrated with the boiler system. The OCM technology, however, is still in development and full-scale application cannot be expected within the next 10 to 15 years. The selected boiler type is a circulating fluidized bed boiler utilized to produce low pressure steam (10 bar, 20°C).

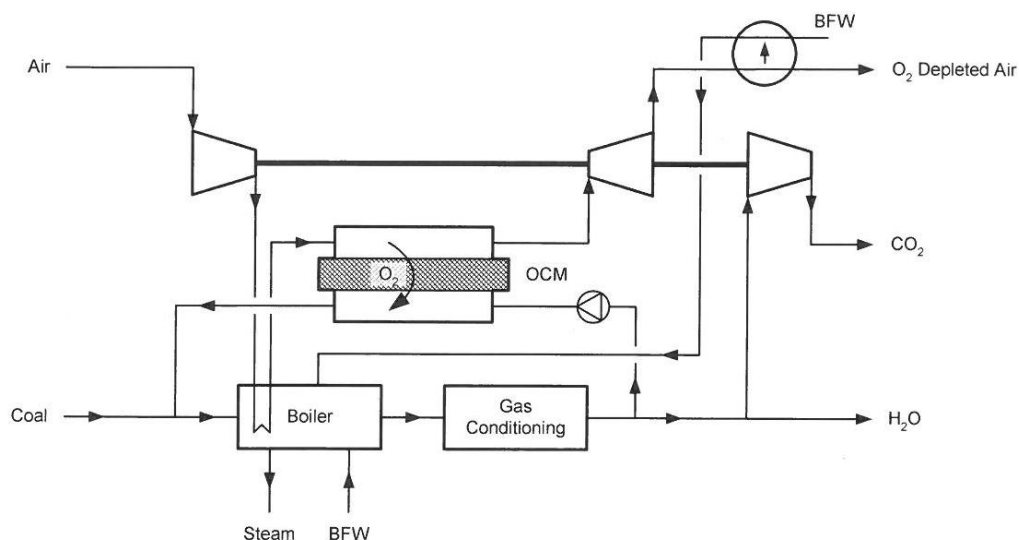


Figure 2.99. Conceptual layout of a coal-fired boiler with oxy-fuel combustion via oxygen conduction membranes (OCM) (Source: IEA GHG, 2007)

Three approaches of CO₂ capturing for the coal-fired boiler with OCM are presented by the IEA GHG (2007):

Case 1: natural gas is combusted in order to preheat the air fed to the OCM. This means that not only coal is an input but natural gas as well.

Case 2: a heat exchanger is mounted inside the boiler in order to preheat the air fed to the OCM. Coal is the only feedstock.

Case 3: CO₂ capture is not accomplished by oxy-fuel firing but by air-firing. Post-combustion by means of the MEA solvent is considered.

2.3.10.2.1.4. Natural gas-fired boiler with oxygen conducting membranes (OCM)

IEA GHG (2007) also presents an oxy-fired boiler in which the oxygen is combusted together with natural gas. The oxygen is supplied by oxygen conducting membranes (OCM) surfaces integrated with the boiler system.

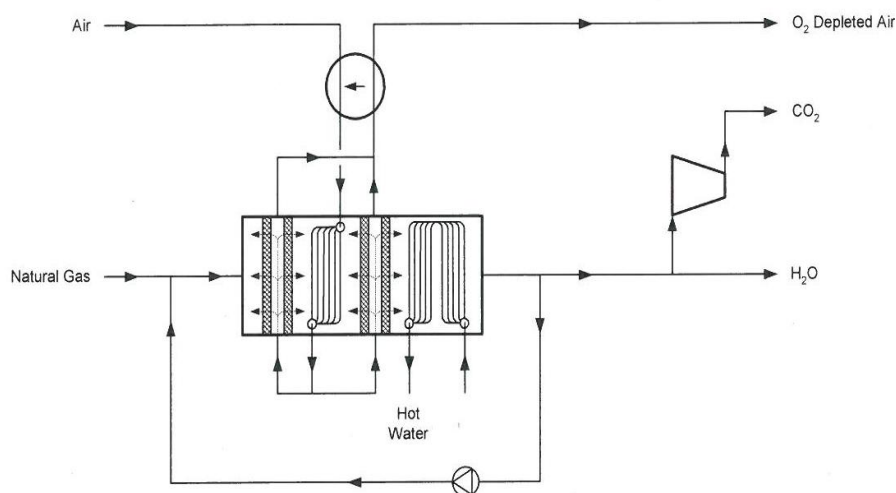


Figure 2.100. Conceptual layout of a natural gas fired boiler with oxy-fuel combustion via oxygen conducting membranes (OCM) (Source: IEA GHG, 2007)

2.3.10.2.2. CO₂ capture from multiple scattered boilers

2.3.10.2.2.1. Van Straelen et al. (2009)

Due to high capital costs and power requirements, Van Straelen et al. (2009) state that it does not appear to be a feasible opportunity to connect a number of widespread small sources of CO₂ to one capture point:

« *The opportunity to combine a number of smaller sources and route all these emission sources to one CO₂ capture plant was also evaluated. These smaller distributed sources would correspond to (...)a large variety of operations such as small boilers, small furnaces and perhaps the emissions from an on-site chemicals plant. Such sources would total to about 1000 kt/a CO₂ in the refinery (...).* » *The widespread sources account for 50% of total refinery emissions. « However, the dimension of a large complex refinery may be over 5 km², and CO₂ emissions point sources are scattered around the site. Therefore, many kilometers of additional ducting is required to collect the CO₂. **Both the capital costs, as well as the required blower duty will be of such a magnitude that this does not appear to be a feasible opportunity. Furthermore, finding space for the large diameter ducts in an already cramped refinery will be a challenge** ».*

We know that this involves a typical large-scale refinery complex and that the refinery infrastructure covers an area over 5 km². Unfortunately, Van Straelen et al. (2009) do not mention the output capacities of the various boilers and other refinery assets.

2.3.10.2.2. Allam et al. (2005)

For a refinery infrastructure covering over 3 km², Allam et al. (2005) have investigated oxy-fuel technology for a total of 7 boilers and 13 process heaters of various types. In contrast to Van Straelen et al. (2009), Allam et al. (2005) conclude that it is feasible to apply oxy-fuel combustion capture to the wide-spread boilers and heaters. The aim was to avoid approximately 2 Mt of CO₂ emissions (or around 50% of total emissions from the refinery).

All heaters and boilers are converted to use oxygen rather than air for combustion. There are 7 boilers, 13 process heaters and one hydrogen producing steam/natural gas reformer burning fuel gas :

- 5 Simon Carves boilers fired by refinery fuel gas (40%) and fuel oil (60%). The 5 boilers are linked to 2 stacks. Each boiler has a capacity of around 83 kW.
- 2 Babcock steam boilers fired by refinery fuel gas (40%) and fuel oil (60%). The two boilers are linked to 1 stack. Each boiler has a capacity of around 214 MW.
- 13 process heaters of which duty varies from 10,3 to 112,3 MW. These are either fired on gas alone or on a combination of gas and fuel oil.

All boilers and heaters are converted to oxy-fuel firing. The oxygen is supplied through two ASU's (Air Separation Units) which require power from the system. The oxygen is distributed to each CO₂ point source. The CO₂ is collected from the point sources according to five zones. Each of the zones will dry and compress the CO₂. Afterwards the CO₂ flue gases are collected and pushed through a ducting network to a central location for final purification and compression.

Figure 2.100 is a figure that illustrates the layout of the whole system in the refinery. Allam et al. (2005) give an overall description of the process steps:

« Oxygen generation

Boilers and heaters normally firing on air are converted to oxyfuel firing by replacing the air feed with oxygen and recycling part of the hot flue gases. Therefore, a large ASU is required in order to generate sufficient quantities of oxygen. Here, we consider two trains of 3700 tonnes/day cryogenic ASUs. These are very large plants. Currently, the largest plants operating are around 3000 tonnes/day; however, 3500 tonnes/day plants are in construction.

Oxygen distribution

The units to be converted and the area of the site which could locate the extra equipment cover an area of around 600 m by 700 m. The oxygen must be distributed around this site to each unit. An economic study has shown that oxygen distribution at low pressure (0.7 barg feed pressure) is the most favourable. In order to be able to use carbon steel piping it is essential to ensure that the velocity within the pipework is kept below a maximum so as to avoid the risk of fire caused by impingement of foreign objects within the piping against the pipe walls. In addition, the configuration of the piping should be such as to avoid situations in which impingement would be worse. Therefore, only long radius bends are used and T-junctions can only be used when flow goes from the main into the branch.(...)

Heater and boiler conversion

Each heater and boiler considered within the study must be converted to fire on oxygen rather than air, with air firing maintained as a backup. Foster Wheeler have considered the conversion of the heaters and Mitsui Babcock the boilers. Each unit produces a hot wet CO₂ stream that must be cooled, dried, purified and compressed.

Local CO₂ collection and drying

Due to the widely spread out nature of the site, the units to be converted are considered to be within one of five zones. Each of these zones takes the hot, wet CO₂ from the converted heaters or boilers, cools this stream and removes water by direct contact with cooling water. The crude CO₂ gas is then compressed and further dried down to a dew point of - 60°C.

CO₂ collection

The compressed dry CO₂ is transported at a pressure of 30 barg from each of the five local zones, by a carbon steel piping network, to a central zone for further purification and compression. The layout of this pipeline was also considered and where possible routed with the oxygen piping.

CO₂ purification and compression

The central CO₂ purification and compression system takes the dried CO₂ from the distribution pipeline and removes inerts from this stream by cooling down to close to the triple point of CO₂ and separating out the uncondensed inerts. The purified gas is then further compressed to the delivery CO₂ pressure of 220 barg and transported by pipeline to the EOR site for disposal. »

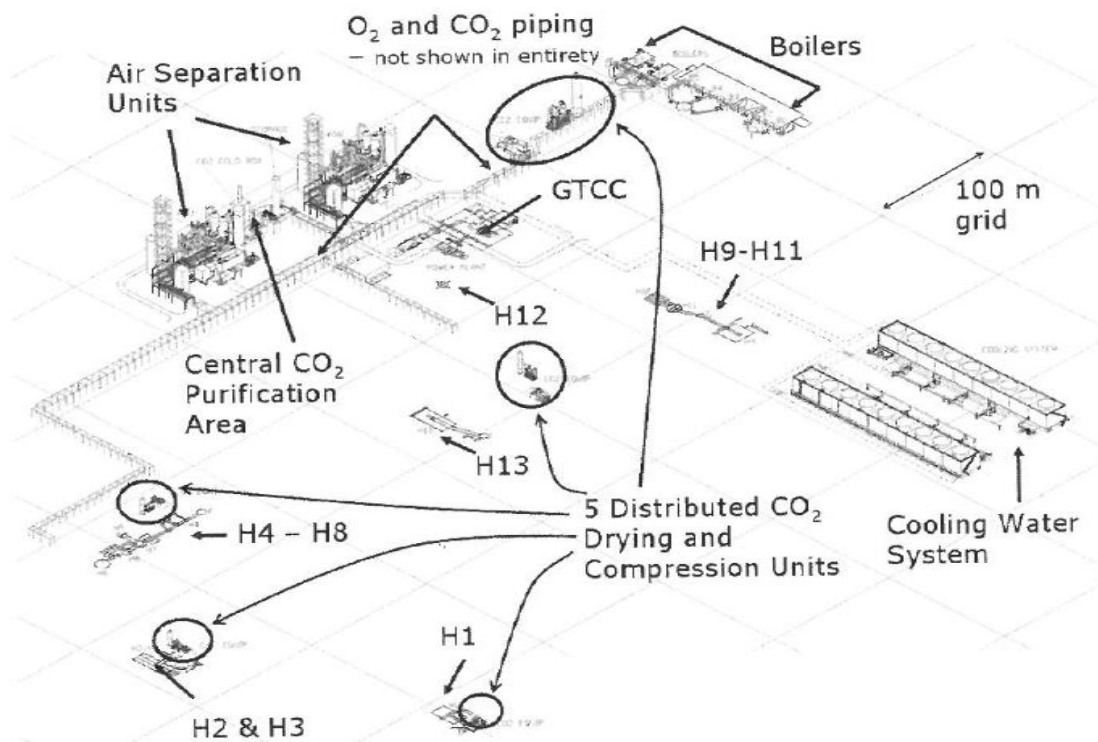


Figure 2.101. Conceptual layout of the entire oxy-fuel system with the location of the boilers and heaters, the air separation units the cooling towers and the oxygen piping network (Source: Allam et al., 2005)

Three approaches of generating the electrical energy required for the ASU compressors and the CO₂ compressors are presented by Allam et al. (2005):

Case 1: A GE 6FA gas turbine combined cycle system is used to generate power.

Case 2: A GE 7EA gas turbine plus heat recovery steam generator (HRSG) is used. Steam produced in the HRSG is used to replace part of the steam production of the existing boilers.

Case 3: "A similar GE 7EA gas turbine plus HRSG is used, but in this case the fuel is hydrogen produced from an oxygen autothermal reformer with product steam generation and CO₂ removed using a methyl diethanolamine (MDEA) system¹⁶" (Allam et al. (2005)).

¹⁶ See 2.3.3.1.1.7 or 2.3.8.2 for more information about MDEA

2.3.10.3. CO₂ capture from industrial boilers: data

- **CO₂ capture at the level of an individual boiler**

An overview of the results of the two studies is given in the next table. Results are for new-build boilers (and different boilers types).

- **CO₂ capture from multiple scattered boilers**

Allam et al. (2005) conclude that it is technically feasible to apply CO₂ capture to multiple wide-spread boilers (and heaters) of the BP Grangemouth refinery complex located in Scotland. The boilers and heaters are connected to one centralized capture system. The boilers and heaters must be converted to oxy-fuel firing. Costs involve the conversion of the boilers and heaters and the supply of the entire oxy-fuel system with installation and start-up and all required utilities. Three approaches of generating the electrical energy required for the ASU compressors and the CO₂ compressors are presented.

2.3.10.3.1. CO₂ capture at the level of an individual boiler

2.3.10.3.1.1. Conventional air-fired boiler (natural gas)

We assumed that capacity factor is 90% (corresponding to 7884 hours) and that O&M costs are 4% of investment costs. We assumed that all O&M costs are fixed O&M costs.

- **Air-fired boiler without CCS**

Table 2.LXXVII. Conventional air-fired boiler without CCS

	Parameter ID	Value	Unit
Inputs	Fuel	1,18	PJ
	Power	0,0008	PJ
Outputs	Steam	1	PJ
Costs	Investment	0,250	Meur2010/MW
	Fixed O&M	0,0011	MEuro2010/MW (yearly)

- **Air-fired boiler with CCS**

CO₂ captured is not mentioned in Melien (2005). Only for the boiler design with oxygen transport membranes (OTM) we know that CO₂ out is 9.1 kg/s (or 0,287 Mt/year). As Melien (2005) compares energy requirements and performance of the air-fired boiler with the boiler with OTM, we assume that potential of CO₂ capture of both boilers is equal. Therefore, we estimate CO₂ captured to be 0,287 Mt per year.

Table 2.LXXVIII. Air-fired boiler with chemical absorption (post-combustion capture)

	Parameter ID	Value	Unit
Inputs	Fuel	1,18	PJ
	Power	0,05	PJ
	Steam	0,26	PJ
Outputs	Steam	1	PJ
Performance	CO ₂ captured	0,287	Mt/year
	CO ₂ capture efficiency	100	%
Costs	Investment	0,400	Meur2010/MW
	Fixed O&M	0,0068	MEuro2010/MW (yearly)
	O&M chemical consumption	0,0067	MEuro2010/MW (yearly)

2.3.10.3.1.2. Natural gas-fired boiler with oxygen transport membranes (OTM)

We assumed that capacity factor is 90% (corresponding to 7884 hours) and that O&M costs are 4% of investment costs.

- **Boiler with oxygen transport membranes (OTM)**

Table 2.LXXIX. Boiler with oxygen transport membranes (OTM) without CO₂ capture system

	Parameter ID	Value	Unit
Inputs	Fuel	1,10	PJ
	Power	0,03	PJ
Outputs	Steam	1	PJ
Costs	Investment	0,2625	Meur2010/MW
	Fixed O&M	0,0015	MEuro2010/MW (yearly)

- **Boiler with oxy-fuel combustion via oxygen transport membranes (OTM)**

CO₂ captured is not mentioned in Melien (2005). Only for the boiler design with oxygen transport membranes (OTM) we know that CO₂ out is 9.1 kg/s (or 0.287 Mt/year). We assume that this amount corresponds to the amount of CO₂ captured from the boiler design with OTM.

Table 2.LXXX. Boiler with oxy-fuel combustion via oxygen transport membranes (OTM)

	Parameter ID	Value	Unit	
Inputs	Fuel	1,10	PJ	
	Power	0,05	PJ	
Outputs	Steam	1	PJ	
	Performance	CO ₂ captured	0,287	Mt/year
Costs		CO ₂ capture efficiency	100	%
		Investment	0.2925	Meur2010/MW
		Fixed O&M	0.0026	MEuro2010/MW (yearly)

2.3.10.3.1.3. Coal-fired boiler with oxygen conducting membranes (OCM)

As mentioned in IEA GHG (2007), operation time is 7500 hours per year and O&M costs are 4% of total investment costs.

- **Coal-fired boiler with oxygen conducting membranes (OCM)**

Table 2.LXXXI. Boiler with oxygen conducting membranes (OTM) without CO₂ capture system

	Parameter ID	Value	Unit
Inputs	Heat	1,15	PJ
	Power	0,02	PJ
Outputs	Steam	1	PJ
Costs	Investment	0,3964	Meur2010/MWth
	O&M	0,0159	Meur2010/MWth

- **Coal-fired boiler with oxygen conducting membranes (OCM) and CO₂ capture**

The next table shows that the coal-fired boilers with oxy-fuel combustion via OCM offer lower avoidance costs than the coal-fired boiler with capture by means of MEA.

Table 2.LXXXII. CO₂ avoidance costs for the coal-fired boiler with OCM (IEA GHG, 2007)

Coal-fired boiler with OCM	CO ₂ avoidance costs (Eur/t CO ₂ avoided)
Case 1 (coal & natural gas to preheat air to OCM)	22,22
Case 2 (coal only)	21,46
Case 3 (MEA post-combustion)	70,31

The next table lists performance and cost estimates for case 1 (coal-fired boiler with oxy-fuel via OCM and the air fed to the OCM is preheated by combustion of natural gas).

Table 2.LXXXIII. Coal-fired boiler with oxy-fuel combustion via OCM and the air fed to the OCM is preheated by combustion of natural gas

	Parameter ID	Value	Unit	
Inputs	Heat	1,14	PJ	
	Power	0,0697	PJ	
Outputs	Steam	1	PJ	
	Performance	CO ₂ captured	0,1357	Mt/year
		CO ₂ avoided	0,1293	Mt/year
		CO ₂ capture efficiency	95	%
Costs	Investment	0,5360	Meur2010/MWth	
		15,84	MEur2010/year ¹⁷	
	O&M	0,0214	Meur2010/MWth	

The next table lists performance and cost estimates for case 2 (coal-fired boiler with oxy-fuel via OCM and the air fed to the OCM is preheated by mounting a heat exchanger inside the boiler).

Table 2.LXXXIV. Coal-fired boiler with oxy-fuel combustion via OCM and the air fed to the OCM is preheated by mounting a heat exchanger inside the boiler

	Parameter ID	Value	Unit	
Inputs	Heat	1,15	PJ	
	Power	0,0805	PJ	
Outputs	Steam	1	PJ	
	Performance	CO ₂ captured	0,1610	Mt/year
		CO ₂ avoided	0,1455	Mt/year
		CO ₂ capture efficiency	95	%
Costs	Investment	0,6529	Meur2010/MWth	
		16,28	MEur2010/year ¹⁸	
	O&M	0,0261	Meur2010/MWth	

The next table lists performance and cost estimates for case 3 (coal-fired boiler with OCM and CO₂ capture by means of MEA, post-combustion)

¹⁷ Based on lifetime of 20 years, annuity with discount rate 5%

¹⁸ Based on lifetime of 20 years, annuity with discount rate 5%

Table 2.LXXXV. Coal-fired boiler with OCM and CO₂ capture by means of MEA (post-combustion)

	Parameter ID	Value	Unit	
Inputs	Heat	1,58	PJ	
	Power	0,1805	PJ	
Outputs	Steam	1	PJ	
	Performance	CO ₂ captured	0,1906	Mt/year
		CO ₂ avoided	0,1083	Mt/year
		CO ₂ capture efficiency	95	%
Costs	Investment	0,9569	Meur2010/MWth	
		20,15	MEur2010/year ¹⁹	
	O&M	0,0383	Meur2010/MWth	

¹⁹ Based on lifetime of 20 years, annuity with discount rate 5%

3. POLICY SUPPORT

3.1. Results of the PSS II simulator

3.1.1. Power sector

The power sector is the first and most obvious candidate for the commercial deployment of CCS, being the most CO₂-intensive industry in Belgium. Several improved power production technologies (next generation) are and will become available, with or without CCS. A restriction was set on biomass energy production because in reality a restriction exists on fuel supply: only one power plant was given the possibility to choose biomass fuel.

Three stages of CCS ready for PC SC Steam Turbine were added to the possible technologies. These CCS ready technologies, together with the non-CCS-ready technology, can be retrofitted for CCS. Building a CCS ready plant has a slightly higher investment cost and lower efficiency, depending on the level of "capture readiness". Switching to actual capture will however become cheaper and more efficient if up-front CCS ready investments are higher.

3.1.1.1. Technology portfolio

To make comparison of different technologies easier, these were grouped in 8 categories (Table 3.I).

Table 3.I. Technology grouping for ease of presenting the technology portfolio results.

Category	Production technology
Coal	IGCC
	PC SC Steam Turbine
	SC Steam Turbine HFO
	Subcritical Steam Turbine
Gas	NGCC
	FuelCell MCFC
	FuelCell SOFC
Bio	Biomass
CoalCCS	IGCC CCS
	PC SC Steam Turbine CCS
GasCCS	NGCC CCS
BioCCS	BiomassCCS
CCSReady	PC SC Steam Turbine 3 stages of CCS ready
Retrofit	PC SC Steam Turbine 3 retrofits for CCSReady, 1 for regular PC SC Steam Turbine

To get an overview of the chosen technology portfolio, total production numbers for these technology groups are averaged for all Monte-Carlo calculations for each scenario. Converting these into relative numbers we can see how the power production technology portfolio is divided through time. These numbers represent the newly installed production.

In scenario 1 (Figure 3.1) most new production is based on coal. Some gas and biomass technologies are installed, and almost no CCS is applied because of the constant low CO₂ price of 20 €/tonne (it should be noted that the *outlook value* of this CO₂ price *will* change when looking to the future; 2.1.6.2 Stochastic outlook parameters). Remarkable is that more than half of the coal-fired production is built as CCS ready, which makes CCS retrofitting cheaper but has a slightly higher cost itself. Here the effect of real options is becoming clear: having more possibilities in the future is regarded as an advantage, thus CCS ready is preferred over non-CCS technology. Because CO₂ prices stay low these CCS-ready plants almost never switch to a CCS retrofit. Some gas, biomass with and without CCS, and a very small amount of coal with CCS are chosen. Together with the small amount of retrofitting this is caused by stochastic parameters and the simulator's urge to create a technology portfolio.

In scenario 2, when CO₂ price rises and the nuclear phase-out is maintained, a totally different portfolio emerges (Figure 3.2). Coal without CCS is far less frequently chosen, while gas-fired technologies are a more obvious choice. More CCS-ready plants are retrofitted and from 2020 onward the share of biomass energy production is significant. Also from 2020 on, CCS becomes commercially available and is chosen regularly. In 2050 more than 50% of the energy production uses CCS technology. The share of gas technologies shrinks towards 2050, probably reflecting the effect of rising gas prices.

If nuclear energy production is available (scenario 5), energy demand from fossil fuels and biomass mostly stays below 20000 GWh/y and CO₂ price is a bit lower compared to the previous scenario (Figure 2.13 & Figure 2.14c). A first look at the technology portfolio gives a completely different outline than the other scenarios (Figure 3.3). At first mostly gas technologies without CCS are chosen. Towards 2050 some CCS ready plants are converted into CCS retrofits, and from 2040 coal and gas with CCS, and biomass are chosen.

This prediction is apparently difficult to explain and in conflict with the results from the former scenario, but when converted into absolute average total production figures (Figure 3.4) and with the demand graph in mind (Figure 2.14c) it makes more sense (bear in mind that total production figures do not represent actual average production, since production numbers are only averaged if a technology occurs). Given this context, the choices made by PSS II are now more straightforward. With some additional production needed in the first years, and an outlook towards a high CO₂ price but no CCS technologies available yet or still with a low efficiency, gas is chosen as the best option. Up to 2040 demand drops (due to the increasing capacity of nuclear power), so no new production is needed and the energy portfolio remains the same. From 2035 to 2040, most newly installed production capacity has aged because the 25 years lifetime of gas technology has passed. New, although still limited, capacity is needed and because of the high CO₂ price CCS technology and biomass is preferentially installed. A constant base load of coal-fired energy production is installed from 2012 and lasts up to 2050 because of the long lifetime of 40 years.

This artifact is partly caused by a the limitation of the PSS II Simulator to bridge shortfalls in demand. If demand is low, new production will be installed, even if demand will drop steeply in the following years. During the next years, this excess of production will be exported.

In scenario 7, with low total electricity demand, the technology portfolio looks somewhat like the scenario 2 portfolio, although there are some differences (Figure 3.5). At first mostly coal and some gas technologies are chosen since CO₂ emissions are free of charge (price of CO₂ is 0€/t). From 2020 the CO₂ price starts to rise and remarkably a significant amount of biomass with CCS is chosen, probably because of its ability to create negative emissions (and costs). From 2025 onwards a continuously growing share of biomass, coal with CCS and gas with CCS is installed.

From the scenario's technology portfolios we can conclude that a high CO₂ price is needed to implement CCS as an economic activity. Biomass energy production also creates the opportunity to drastically reduce CO₂ emissions. Comparing scenarios 2 and 7 regarding the implementation of biomass (with or without CCS) technology, biomass with CCS seems to be beneficial in case of very low CO₂ prices if the future outlook prices are high. In general the share of gas is diminishing towards the future because of very high rising fuel prices. CO₂ price, and the timing of its increase, is reflected in the technology portfolio. The success of CCS technology is greatly depending on this parameter.

Two questions still remain unanswered in this study. Firstly the largest share of newly built CCS ready plants is not retrofitted to CCS operational, even at, or with outlook to, a very high CO₂ price of up to 800 €/tonne. Preliminary results seem to indicate that the time window to economically retrofit CCS-ready installations is actually very limited. A paper on this topic and its implications is being prepared for the 11th International Conference on Greenhouse Gas Control Technologies (GHGT-11) in November 2012. Secondly, in scenario 2 a significant share of biomass is chosen while in scenario 7, with a quite similar portfolio, mostly biomass with CCS is chosen instead. This is probably a competition between the higher costs of biomass with CCS versus higher profit due to negative emissions. These issues need to be addressed in further research, as well as the fact that it may be more likely that biomass is co-fired with coal, rather than being used as a pure source of fuel.

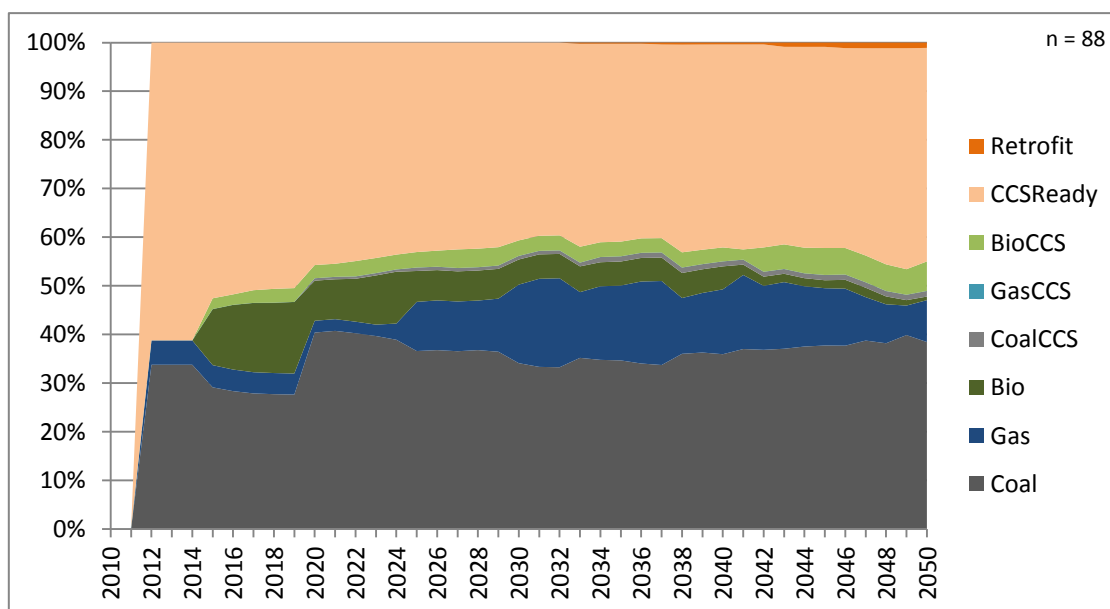


Figure 3.1. Relative technology portfolio for scenario 1. Mainly coal technologies are chosen because of a low CO₂ price of 20 €/tonne. A large percentage of the total capacity is built as CCS ready because of real options, but is never upgraded to CCS operational again because of a low CO₂ price. Some gas, biomass with and without CCS and coal with CCS is installed.

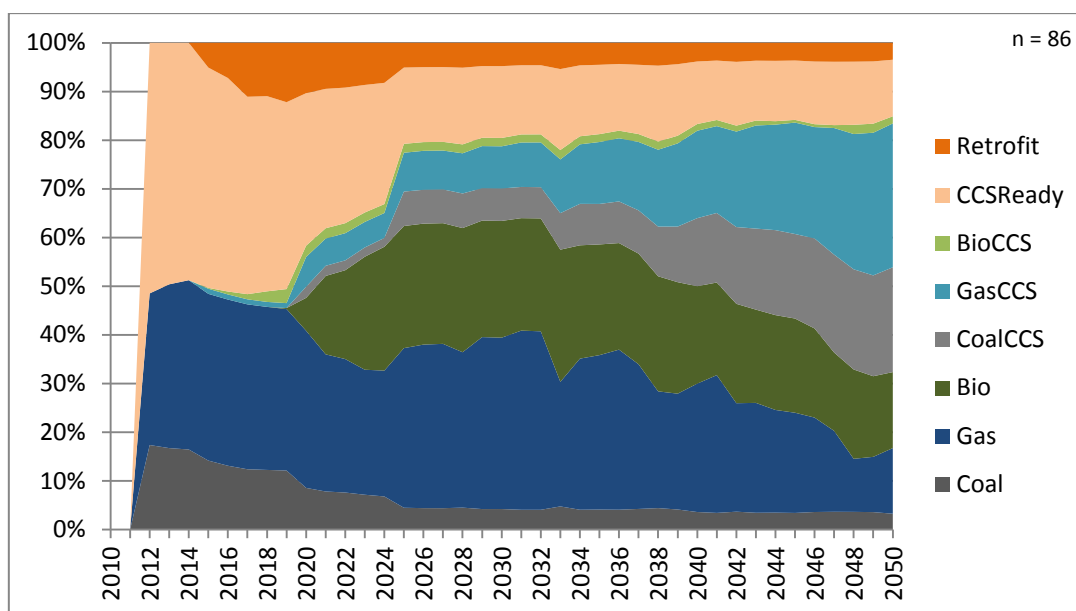


Figure 3.2. Relative technology portfolio for scenario 2. If stringent climate targets are set and nuclear will phase-out (scenario 2), a clear change is made in the energy portfolio choices. At first, when CO₂ prices are still moderate, CCS ready coal technology is built and some are retrofitted. CCS is not yet available and gas technology is activated with the outlook of a high CO₂ price. From 2020 on, when CCS becomes commercially available, a switch is made towards CCS technologies and biomass. Despite the very high CO₂ price, not all CCS ready capacity is retrofitted. In 2050 more than 50% of the energy production uses CCS technology.

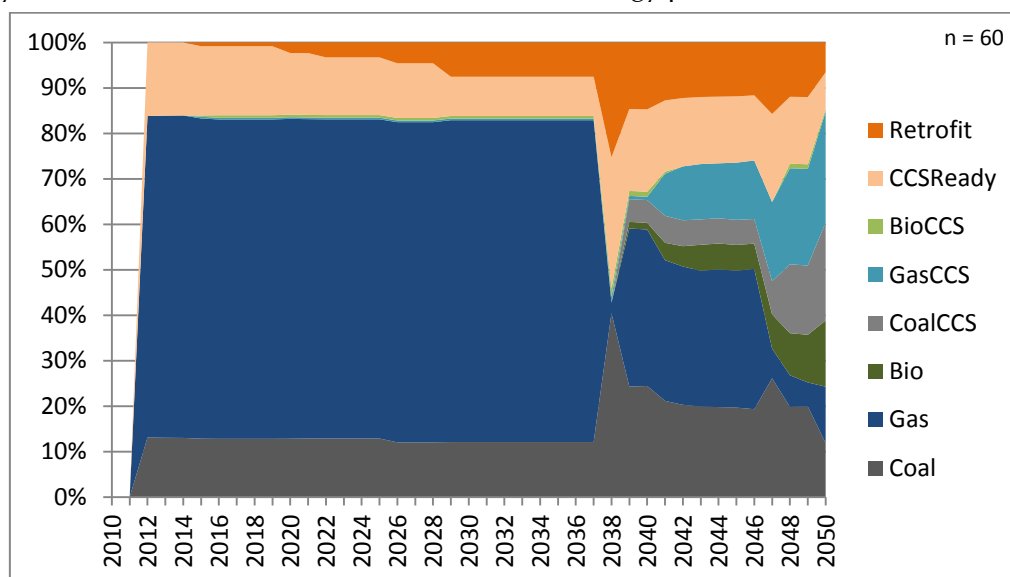


Figure 3.3. Relative technology portfolio for scenario 5. If nuclear energy production is allowed, energy production from fossil fuels is much lower (scenario 5). With an outlook towards a rising CO₂ price, but no CCS technology available yet, mostly gas technology is installed at first. Since PSS II has a demand outlook of just one year, the lowering in demand is not anticipated, and the installed gas-fired capacity is maintained; overcapacity will be exported. After the decommissioning of these installations, around 2035, CO₂ price is high and CCS technology is installed. This numbers is transformed into the absolute average production (Figure 3.4) to enable a more accurate interpretation.

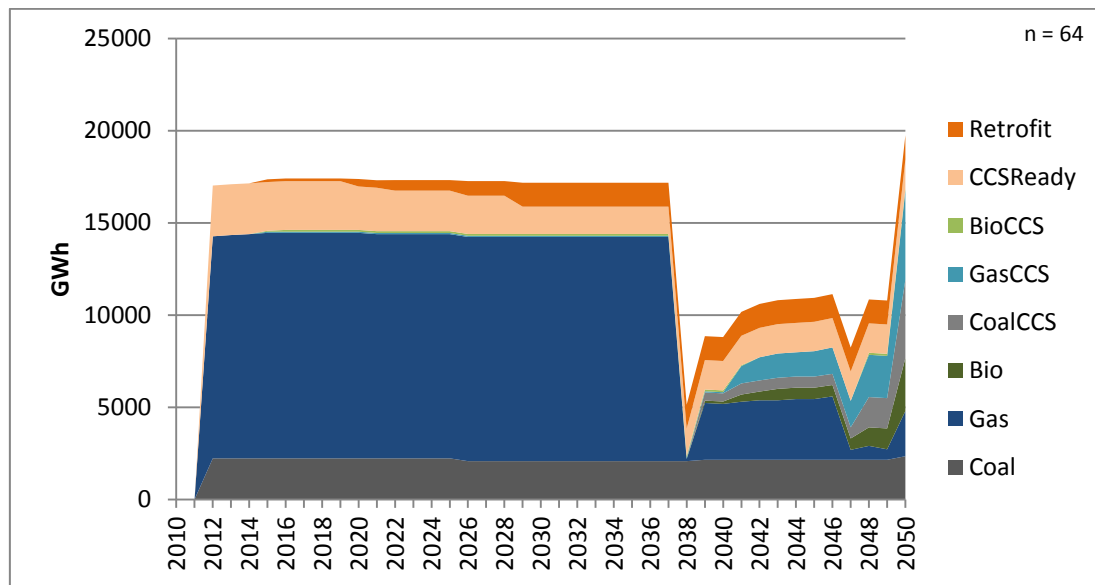


Figure 3.4. The production portfolio and production numbers for scenario 5 are presented here as absolute numbers, opposed to Figure 3.3. When comparing with the demand graph (Figure 2.14c) one can see the installed production in 2011, mainly gas technology, will generate overproduction up to around 2035. The gas-fired power plants are decommissioned after 25 years and new production is needed. With high CO₂ prices CCS is chosen, and the existing coal-fires production is not decommissioned yet and keeps existing.

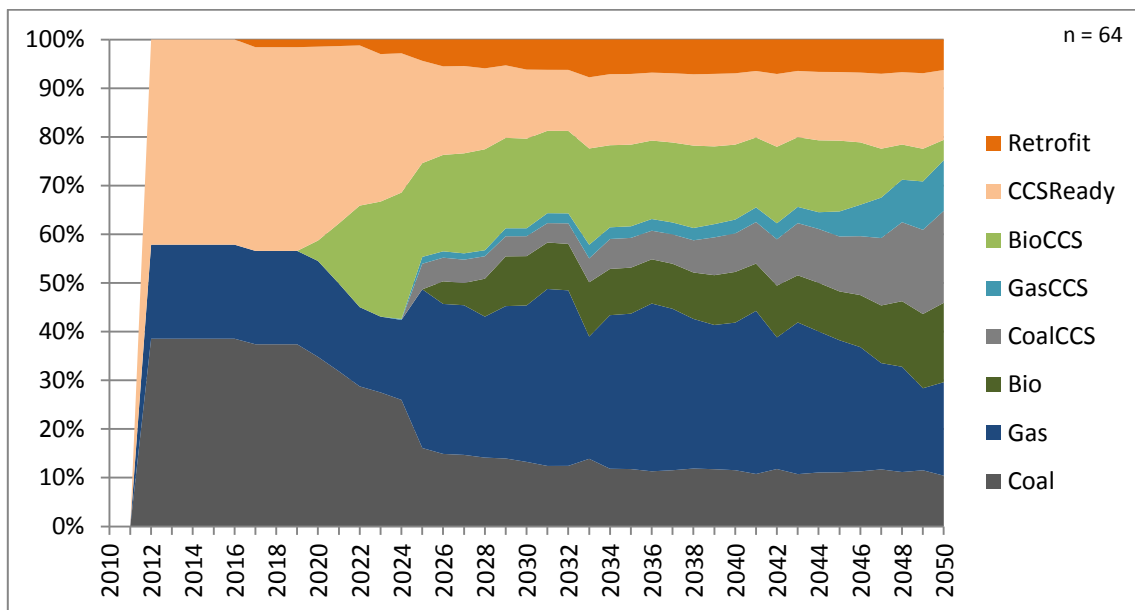


Figure 3.5. Relative technology portfolio for scenario 7. With lower general demand the technology portfolio is somewhat comparable to scenario 2 although with a few differences. CO₂ price starts at 0 €/tonne in 2010 and rises later compared to scenario 2 and 5. This results in a larger share in coal technology and a smaller part being retrofitted. CCS technology in general has a smaller share compared to scenario 2, although the biomass with CCS appears with a significant share in an early stage, diminishing towards 2050.

3.1.1.2. Decision production cost

The most important decision parameter for the PSS II Simulator is the production cost. Some remarks need to be made to correctly understand the numbers presented here.

1. Production costs here are given for each separate technology, not the technology groups as in chapter 3.1.1.1 (Technology portfolio), because e.g. two coal technologies can have a very different production cost.
2. The production costs given here are the production costs used for making project decisions, not the actual production costs. In the inner Monte-Carlo loop (chapter 2.1.2.2 Structure) production cost is calculated for decision making using the outlook parameters. After portfolio evaluation, the selected projects are activated using the standard set of parameters.
3. Production costs in PSS II are calculated accounting for future changes in CO₂ price, fuel price etc. and discounted (chapter 2.1.3.2 Cost calculation for capture). Only one value is obtained, which is stored for all years. If a technology is not frequently chosen this can result in a production cost staying constant (because it is not updated) through time or making sudden jumps.
4. Production cost is given only for years that projects using this technology are active. Even using results of several Monte-Carlo runs this means some years (or even an entire scenario) may not display a production cost for certain technologies.
5. Biomass with and without CCS is not displayed due to an output problem. In general these costs would plot at the top-end of the average values, with an increase towards 2050 due to rising fuel prices. In scenarios with high CO₂ price costs are low or even below 0 for negative emissions.

In scenario 1 (Figure 3.6) production costs for most technologies are around 0.07 €/kWh in 2010 up to 0.08 €/kWh in 2050. NGCC cost rises just above 0.10 €/kWh after 2040 due to high gas prices. A few technologies are more expensive. Both gas fuel cell technologies and the retrofit technologies cost between 0.11 and 0.14 €/kWh.

The effect of a rising CO₂ price is immediately visible in the production cost. Results for scenario 2 and 7 are similar (Figure 3.7 & Figure 3.9). Here however the effect of remark nr. 3 in the introduction becomes clear. Scenario 2 has a faster rising CO₂ price compared to scenario 7. Hence, production costs of at least all non-CCS technologies should become more expensive towards the future. The gas fuel cell technologies become much more expensive compared to other technologies when comparing scenario 2 and 7. These gas fuel cell technologies have a lifetime of 7 years, which means a new production cost is calculated regularly, and reflects better the instantaneous cost. Other technologies have a lifetime of 25 to 40 years and therefore have a more stable production cost that is calculated using the CO₂ price of a longer time span.

Most other technologies start with a production cost of about 0.08 €/kWh. CCS ready and non-CCS technologies cost rise just a little over time. CCS technology costs rise up to 0.15 €/kWh and CCS retrofit costs remain stable around 0.15 €/kWh.

In scenario 5 not much production capacity is needed, distorting the graph as mentioned in the introduction (remark nr. 4, Figure 3.8). Gas fuel cell technologies are again the most expensive. CCS ready technologies replace NGCC as the cheapest technology by 2040. CCS and CCS retrofit technologies cost about 0.15 €/kWh in 2050.

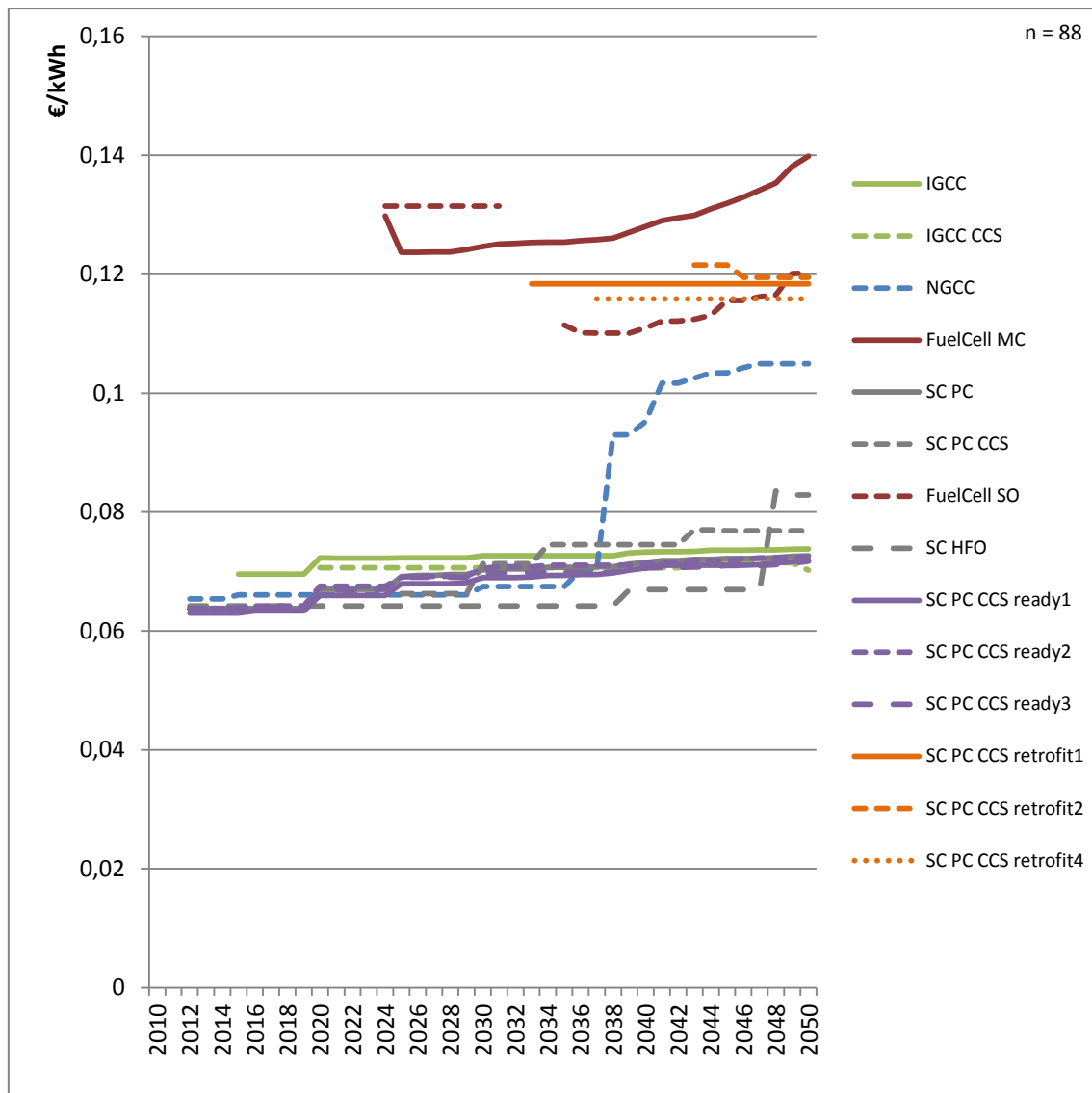


Figure 3.6. Average production costs for different technologies for scenario 1. A low CO₂ price causes only a small increase in production cost towards 2050 for most technologies. Gas fuel cell and retrofit technologies are expensive at between 0.11 and 0.14 €/kWh, and NGCC production cost increases around 2040 because of high gas prices.

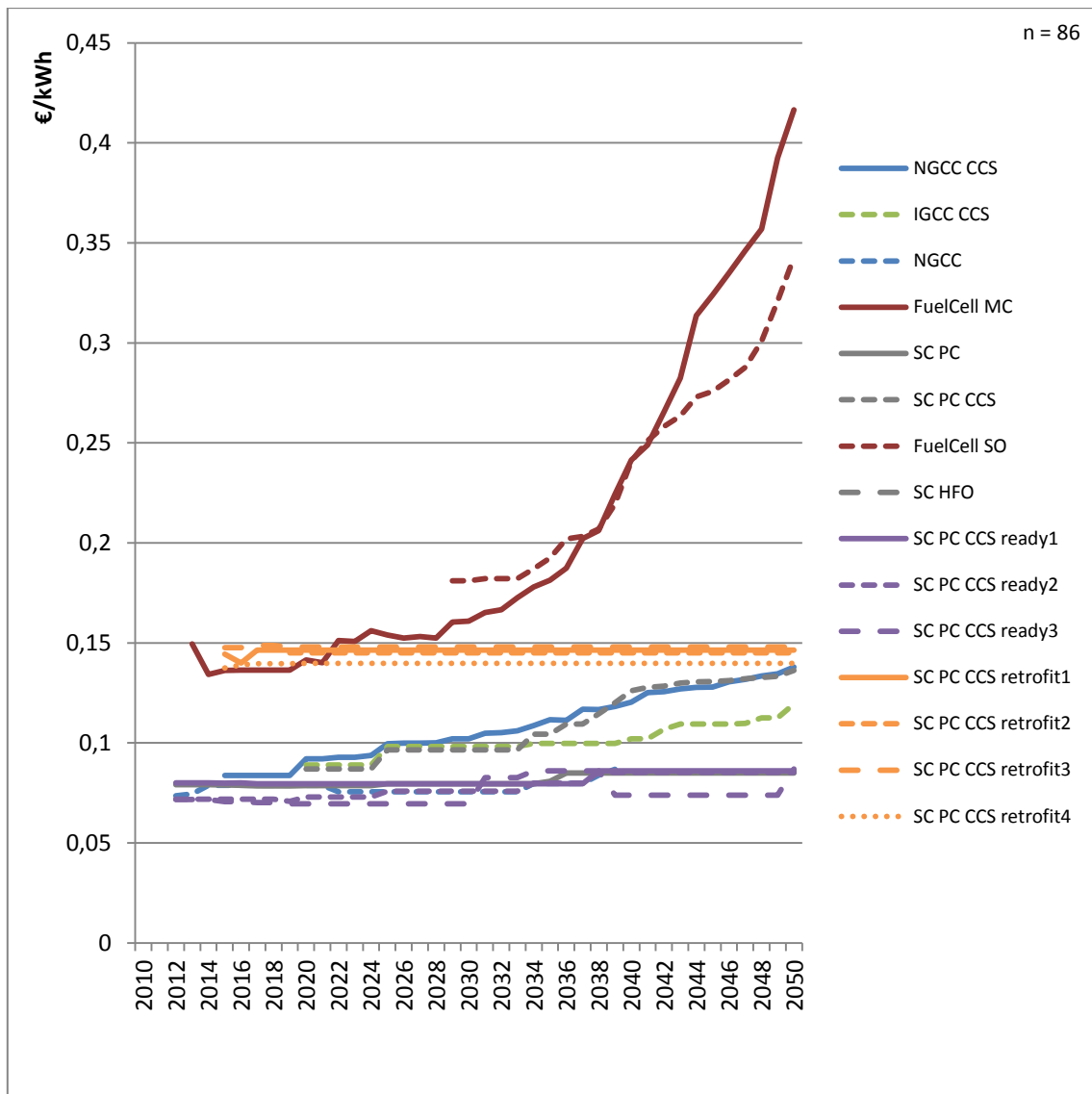


Figure 3.7. Average production costs for different technologies for scenario 2. A high CO₂ price has a dramatic effect on the fuel cell technologies. Retrofit technology prices keep steady around 0.15 €/kWh, while all other technologies start from 0.08 €/kWh up to 0.14 in 2050. The CCS ready technologies are the cheapest and prices stay there up to 2050.

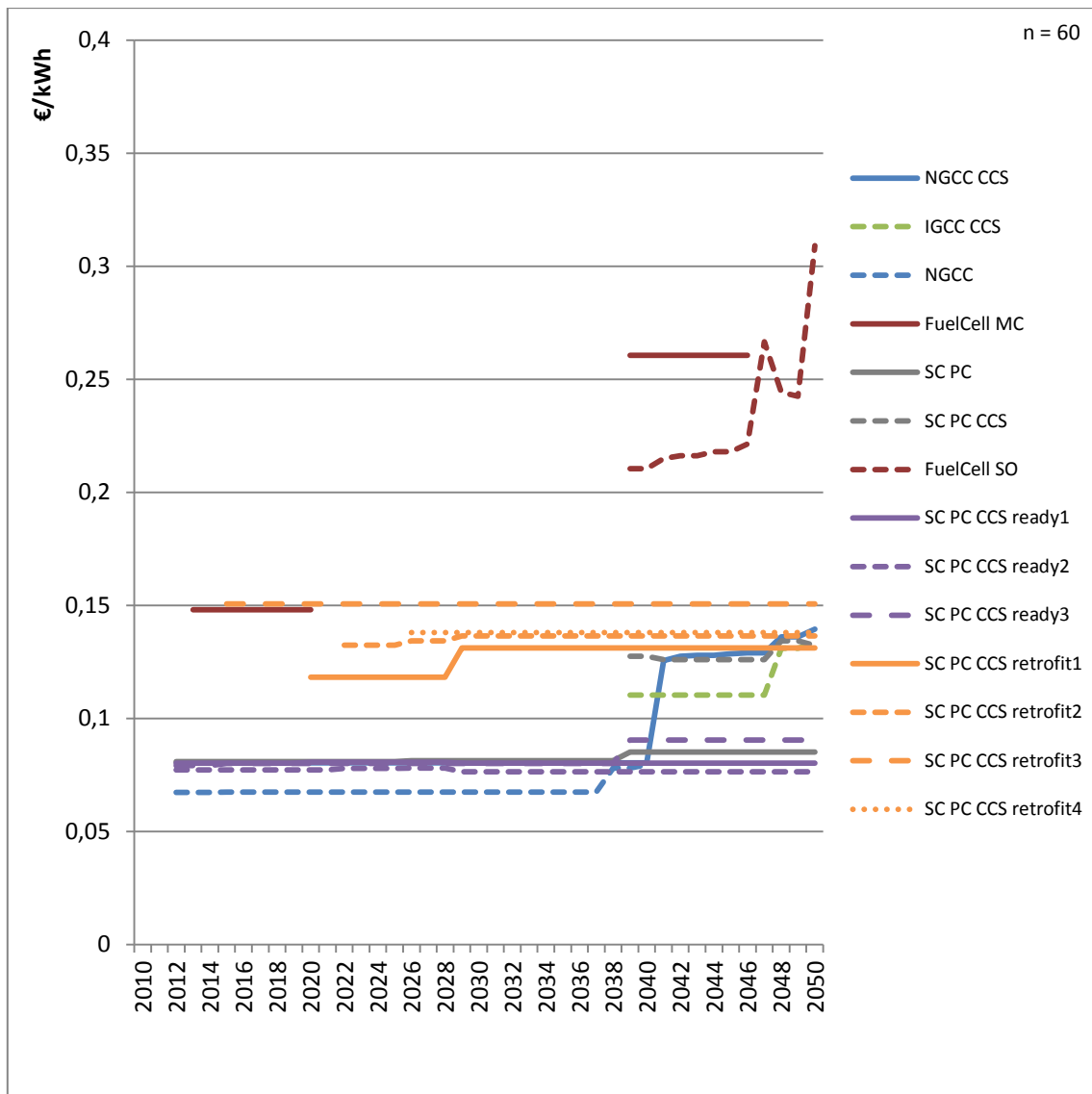


Figure 3.8. Average production costs for different technologies for scenario 5. Not much production capacity needed, thus distorting the graph producing mostly straight lines as mentioned in the introduction. Again gas fuel cell technologies are the most expensive. NGCC starts as the cheapest technology, being replaced by the CCS ready technologies around 2040.

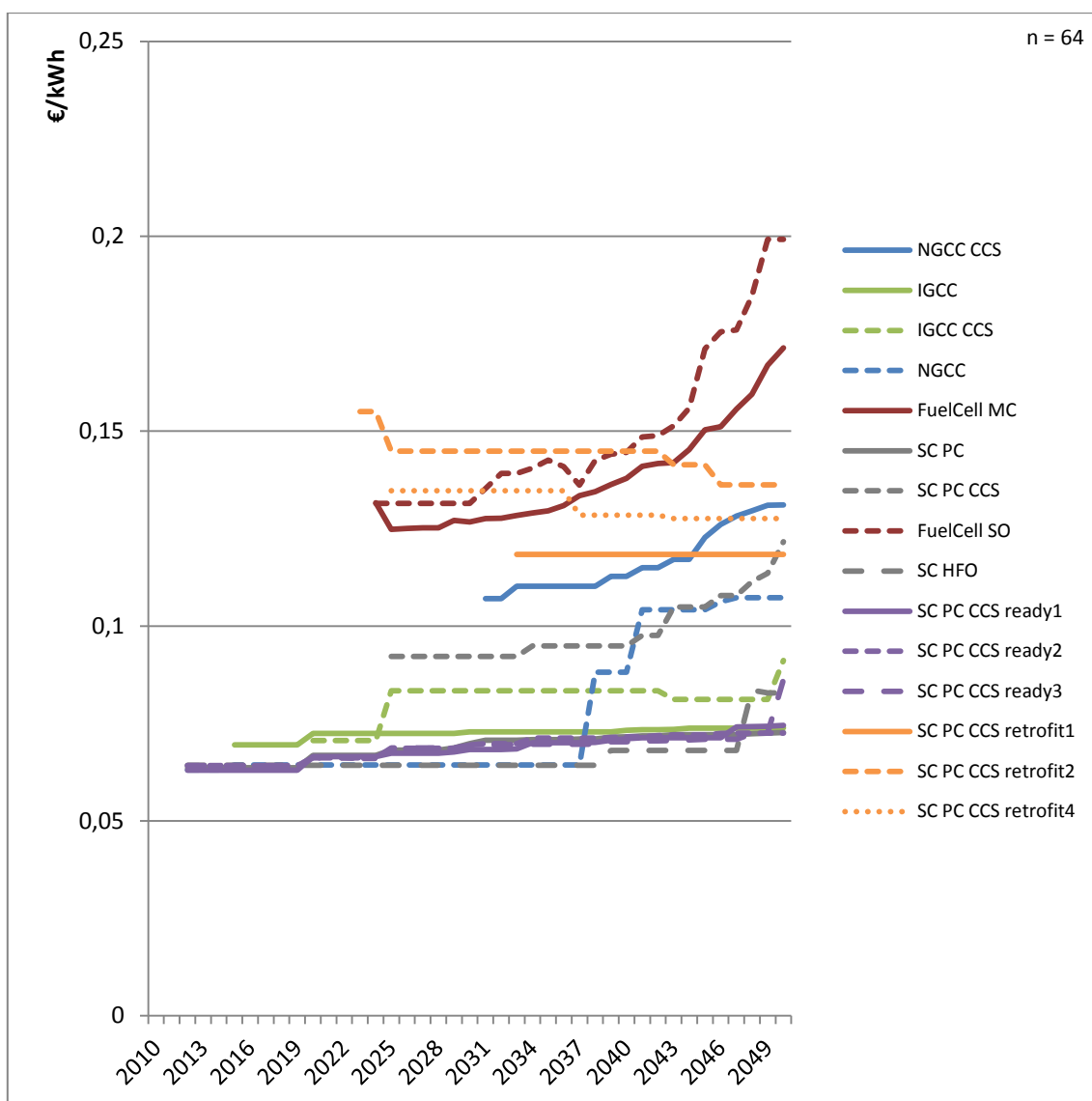


Figure 3.9. Average production costs for different technologies for scenario 7. Gas fuel cell technology costs are lower because of a delayed rise in CO₂ price. CCS ready technologies are still the cheapest at around 0.07 €/kWh up to 0.09 €/kWh in 2050. NGCC starts out at the same price point but rises from 2037 on because of rising gas and CO₂ prices. CCS retrofits are at the highest end of the range, slowly dropping towards 2050.

3.1.1.3. Actual production cost

The production cost presented here is the actual production cost for electricity for an active power plant. These values may differ from the production cost used for decision making in the previous chapter because of outlook uncertainties. Again some remarks need to be made to correctly interpret the graphs.

1. Production costs here are given for each separate technology, not the technology groups as in chapter 3.1.1.1 (Technology portfolio), because e.g. two coal technologies can have a very different production cost.

2. The actual production costs presented here are calculated using a discounted and annualised investment cost. All costs are those of the year of activation; no future changes in CO₂ price, fuel price etc. are accounted for. Investment costs, fixed and variable operation and maintenance costs and fuel costs are added resulting in the production & capture cost. Transport, storage and emission cost are added separately.
3. For a certain project, a value is only calculated for the year of activation. Because not all technologies are each year activated, even when using results of several Monte-Carlo calculations, production costs for several years and technologies are not available. Therefore decadal averages are made. Even with this methodology, some decades will not display a production cost.
4. Only supercritical pulverised coal, IGCC and NGCC with and without CCS are displayed here since these are and will likely be the main technology types for fossil fuel power production. This selection is necessary because it is impossible to include all technologies in the graphs used.

Figure 3.10 displays the production costs of scenario 1 for time periods 2010-2020, 2020-2030, 2030-2040 and 2040-2050. The largest part of the total costs are production costs (including capture costs for CCS technologies). Because CO₂ price remains constant, in general production costs only slightly increase through time and non-CCS technologies remain cheaper on average than CCS technologies. Transport, storage and emission costs are relatively small; only the SC PC CCS in 2020-2030 has a higher average storage cost. This storage cost is based on just one value, being an expensive coal seam storage project. NGCC with CCS was never chosen in this scenario and was therefore never economic.

In the first decade of scenario 2 production costs (Figure 3.11) are comparable to those in scenario 1, around 80 €/MWh. CCS technology is still more expensive because of higher costs and low CO₂ prices. In the next decades the CO₂ price rises and non-CCS becomes more expensive than CCS, with SC PC having an average production cost of 130 €/MWh in 2020-2030 and 200 €/MWh in 2030-2040. In 2040-2050 only CCS technologies are activated, having an average production cost between 130 and 170 €/MWh, about twice the cost compared to the 2010-2020 period. In this scenario IGCC without CCS is never chosen.

In scenario 5 again production cost lies around 80 €/MWh between 2010 and 2020 (Figure 3.12). Because of the decreasing demand (Figure 2.14c), no new SC PC, IGCC or NGCC plants are built between 2020 and 2030. After 2030 new production is built and high CO₂ prices lead to high production costs for SC PC without CCS. After 2040 only CCS is installed, having an average production cost of around 130 €/MWh.

SC PC and NGCC are installed between 2010 and 2020 in scenario 7, without emission cost because there is no CO₂ price (Figure 3.13). Hereafter the numbers are comparable to those of scenario 2 with a rising emission cost towards 2050. Comparing these two scenarios the effect of a delayed rise in CO₂ price is visible: emission costs remain relatively low until 2040. This is most noticeable for SC PC without CCS between 2030 and 2040.

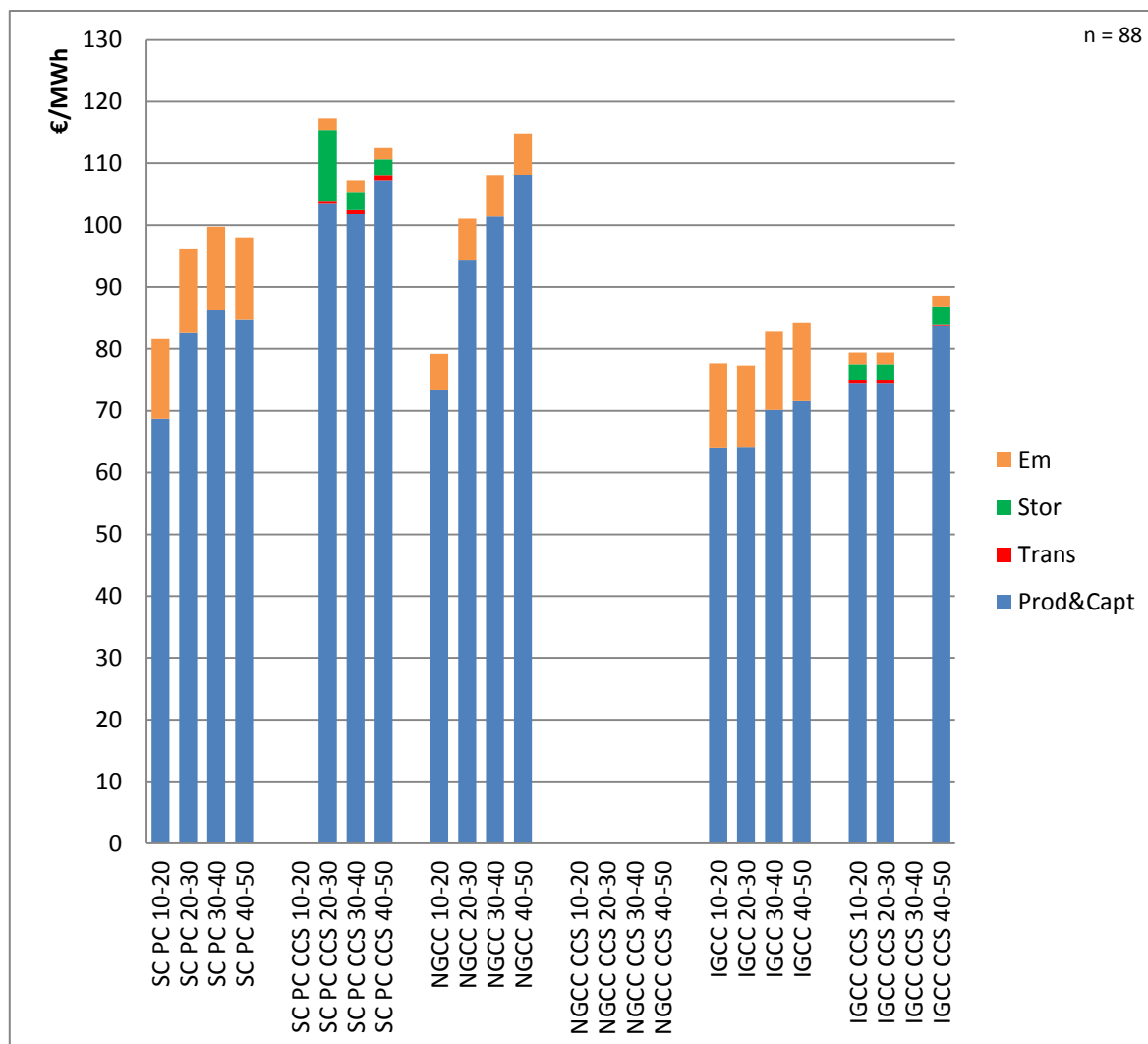


Figure 3.10. Production cost breakdown for SC PC, NGCC and IGCC, each with and without CCS for scenario 1, averaged for 2010-2020, 2020-2030, 2030-2040 and 2040-2050. Production and capture costs rise slightly because of rising fuel prices. Emission costs are stable through time since CO₂ price remains 20 €/t. NGCC with CCS is never chosen in this scenario.

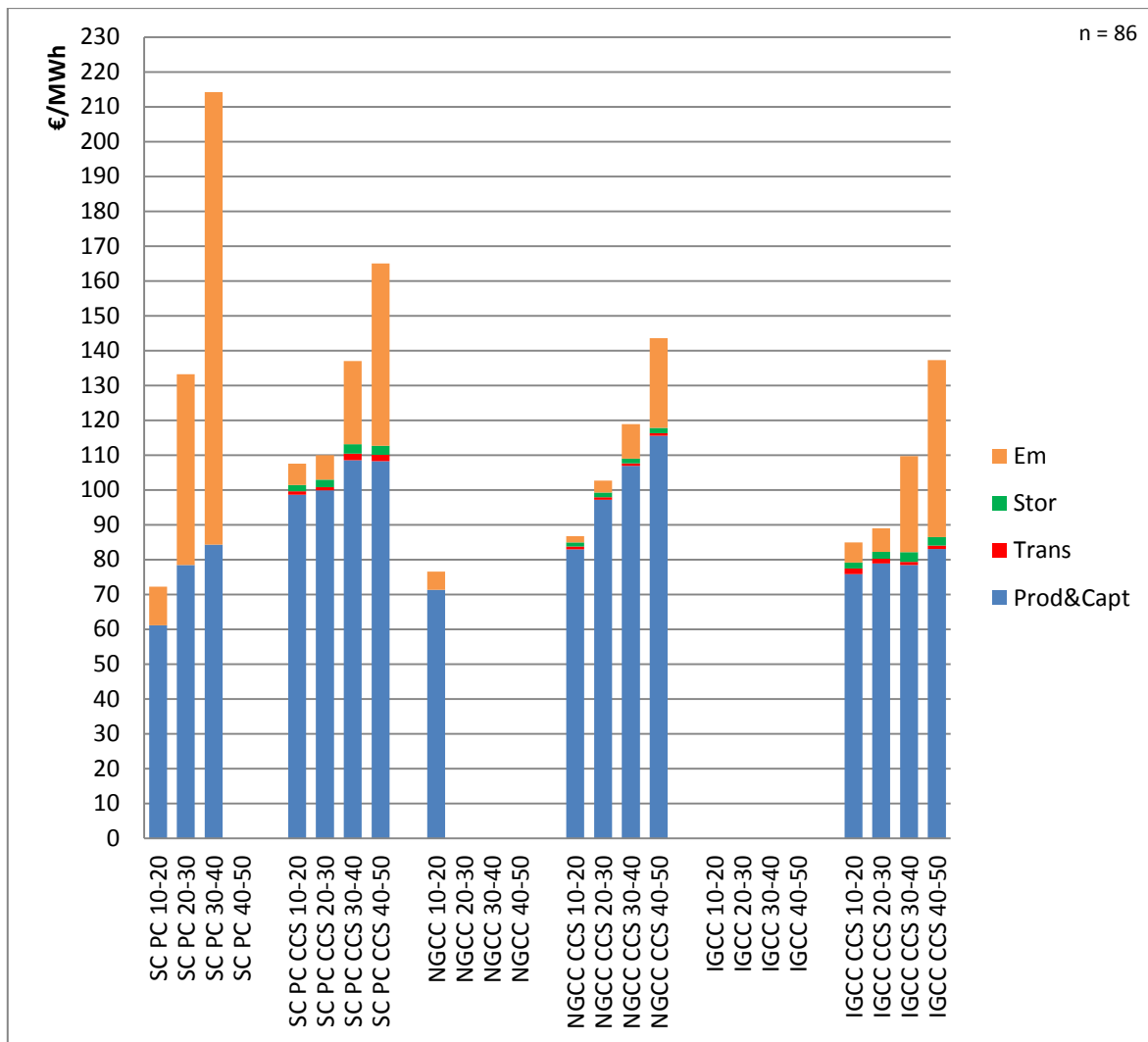


Figure 3.11. Production cost breakdown NGCC, SC PC and IGCC with and without CCS for scenario 2, averaged for 2010-2020, 2020-2030, 2030-2040 and 2040-2050. Emission costs are rising high because of the rising CO₂ price. CCS technologies quickly become cheaper than the non-CCS equivalents. After 2040 only CCS technologies are activated. IGCC without CCS is never chosen in this scenario.

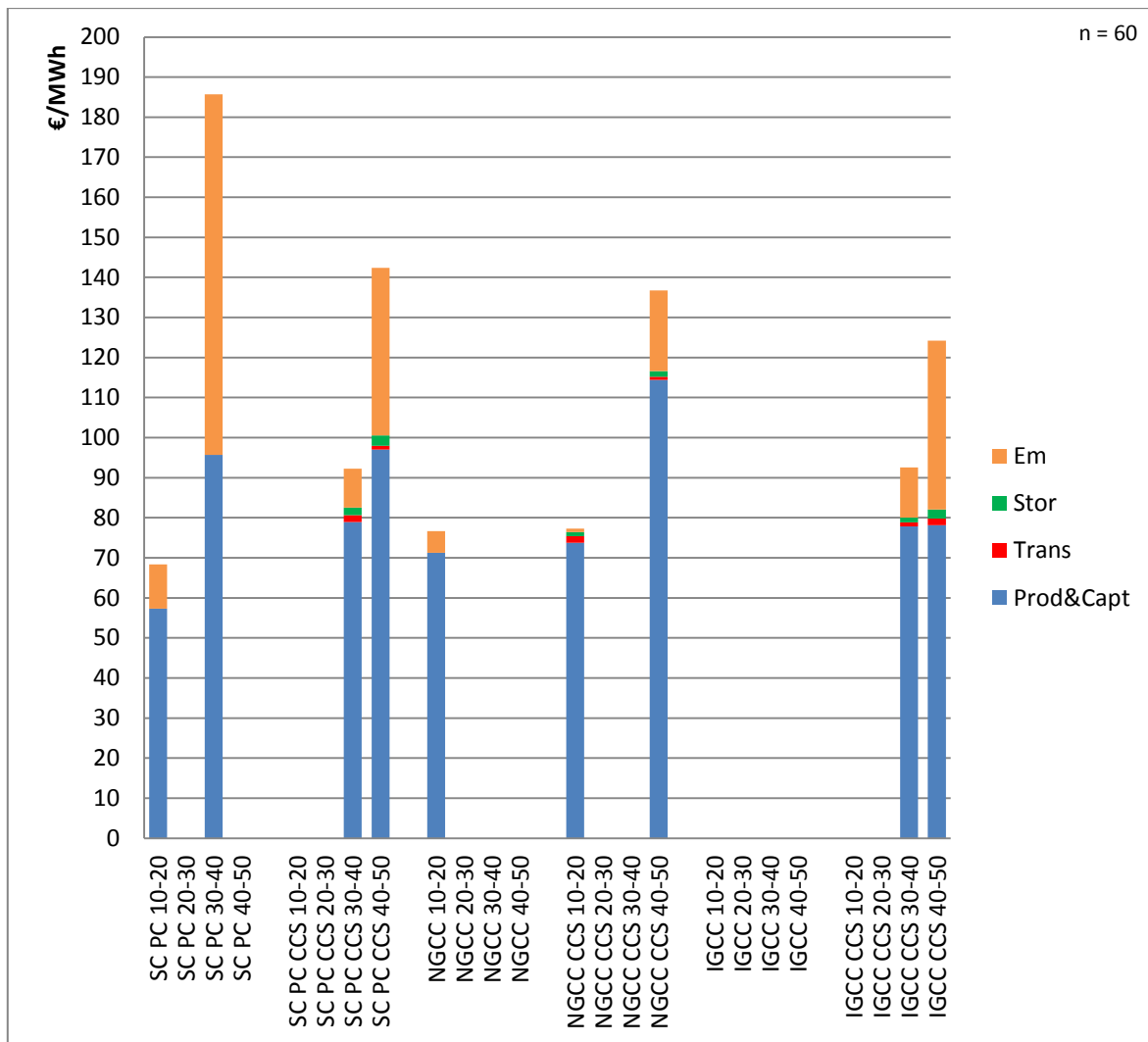


Figure 3.12. Production cost breakdown NGCC, SC PC and IGCC with and without CCS for scenario 5, averaged for 2010-2020, 2020-2030, 2030-2040 and 2040-2050. Demand drops in this scenario and no new production is added in 2020-2030. After 2030 CO₂ price has risen high and CCS technologies become cheaper compared to non-CCS. SC PC becomes the most expensive CCS technology of these three after 2040.

Supercritical pulverised coal production cost for both non-CCS and CCS is calculated higher within the PSS projects compared to the ZEP report. This difference can be explained looking into detail to the individual cost factors. Capital, operational and coal fuel costs are all higher in PSS II than used by ZEP. IGCC with CCS is considered to be slightly less costly in PSS II than in the ZEP study, even using the same high hard coal price. The difference is mainly in the low investment cost. Assumptions regarding the natural gas prices are comparable between this report and ZEP's, resulting in a very comparable production cost for NGCC technology. NGCC with CCS production costs are again lower than those reported by ZEP because of a difference in investment cost.

Table 3.II. Comparison between production and capture cost of the ZEP capture report and costs presented here. Differences can mainly be explained by a difference in investment, operational and fuel costs between both studies.

Technology	Unit	Production cost ZEP	Production cost PSS II
PC SC	€/MWh	52.7	61.2-82.6
PC SC CCS	€/MWh	75.9	98.5-103
IGCC CCS	€/MWh	80.2	74.4-78.9
NGCC	€/MWh	91.4	71.3-94.4
NGCC CCS	€/MWh	122.1	83.0-97.1

3.1.1.4. Net CO₂ emissions

Net emissions are regarded as the total emissions from fossil fuels that reach the atmosphere. These net emissions include emissions from the source, from transport and from reservoir operation (but excluding leakage). The main goal of CCS is to quickly reduce these emissions thus making this the main environmental parameter. Because of the addition of power production using biomass, possibly combined with CCS, zero or even negative emissions can be obtained since CO₂ is effectively removed from the atmosphere by growing biomass. When burned and emitted into the atmosphere no net emissions are generated. When captured and stored, negative emissions are generated. The negative costs are also subtracted from the production cost. Negative emissions can be observed in the following graphs in case a significant amount of biomass energy production with CCS is installed.

In scenario 1 a large spread of possible future emissions is observed (Figure 3.14). In the most likely scenario, net emissions from the power sector will rise from about 18 Mt/y in 2020 to about 50 Mt/y in 2030. From 2030 onwards emissions don't change much. In 2050 these emissions represent almost the total CO₂ produced by the power sector (almost no CO₂ is captured and stored). Most remarkable is the large spread of these results, with between 2020 and 2030 even possible negative emissions from biomass power production with CCS. These are however unlikely scenarios. This uneven spread can be directly linked to the high demand and low CO₂ price: CCS technologies are not likely to be chosen, causing the high probability for high emissions. However because of high demand and the portfolio choices, a diverse energy portfolio is still possible.

In the second scenario, in total most power production will come from fossil fuels and biomass (Figure 2.14b). Due to a very high price for CO₂ emissions CCS becomes an economic option from 2020 onwards as seen in Figure 3.2 (technology portfolio). Emissions will first most likely steadily rise until 2025, because of increasing demand for fossil fuel power production (Figure 3.15). From 2025 onwards emissions slowly fall from about 20 Mt/y to 15 Mt/y or lower. Demand will stop increasing, and coal fired power plants are being replaced by biomass and CCS. In this scenario also negative emission are possible from 2025 onwards, with a relatively low probability.

Remarkable for the results of scenario 5 is the very high certainty (Figure 3.16). All Monte-Carlo runs produce an almost identical emission future with a very low spread of possible futures. Keeping nuclear energy production combined with a high CO₂ price seems a secure option to keep emissions very low. Until 2035 this is because of very low demand for fossil fuel and biomass power production. From 2035 on a high CO₂ price induces the installation of CCS and biomass technology.

Results for scenario 7 are similar to the second scenario, although with a larger spread both positive and negative (Figure 3.17). Most probable are net emissions of about 10 Mt/y in 2050.

Comparing all four scenarios we can conclude that a high rising CO₂ price is needed for drastic reductions of CO₂. Even if CO₂ prices are very low, or even 0 at this moment (scenario 7), a future outlook to a high price will mitigate emissions significantly. If nuclear remains a future option next to CCS, then there is a high probability that CO₂ emissions from the power sector will steadily decrease to approach 0 in 2050.

Earlier results from PSS I (Piessens et al., 2009) are confirmed when comparing the results of scenario 2 and 5 of PSS II with the friendly scenario of PSS I (all with nuclear phase-out and CCS technology available): a net emission of 10 to 20 Mt CO₂ in 2050 is obtained. This demonstrates the robustness of the simulator.

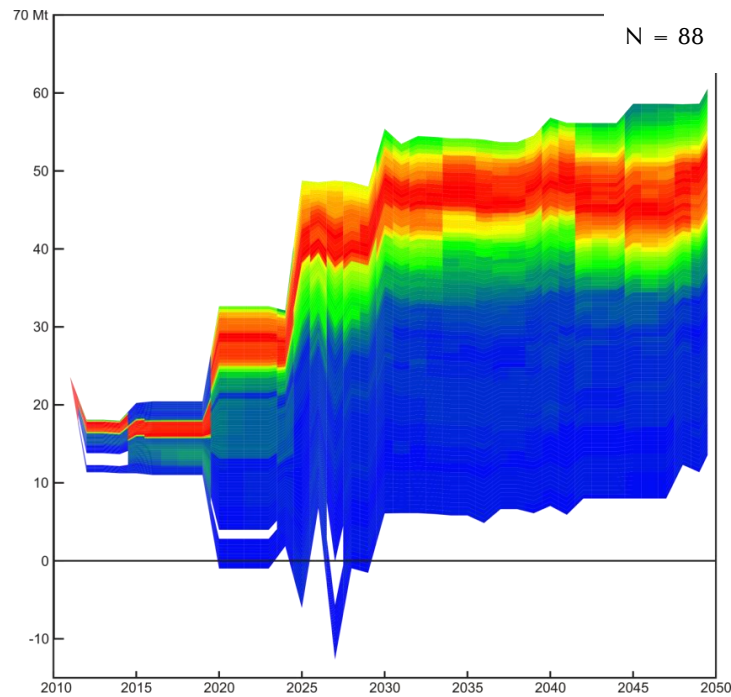


Figure 3.14. Net CO₂ emissions for the power sector for scenario 1 for the existing and newly built installations. With a low CO₂ price almost all CO₂ is emitted into the atmosphere. In the most likely scenario about 50Mt/y is emitted. In very rare cases negative emissions are possible around 2025 using biomass with CCS. The large spread of results is caused by the high demand and therefrom arising portfolio possibilities.

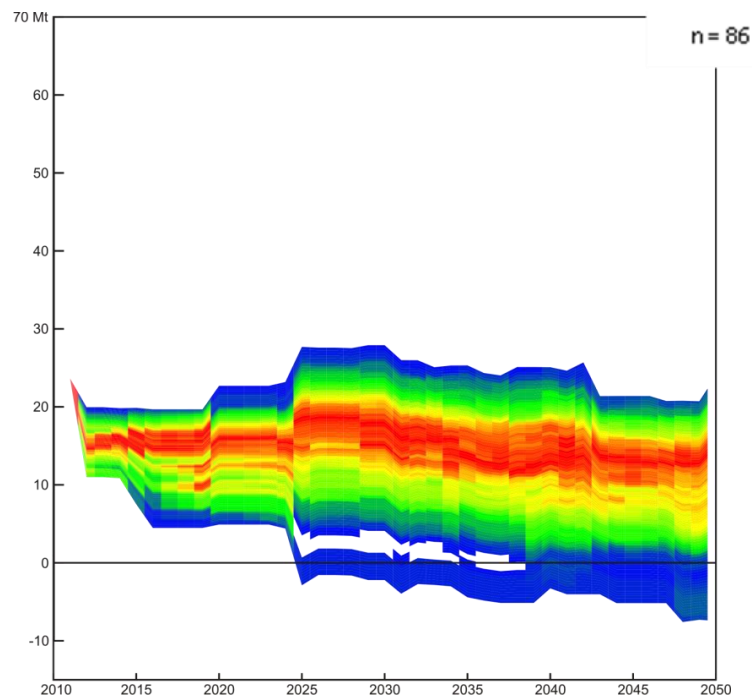


Figure 3.15. Net CO₂ emissions for the power sector for scenario 2 for the existing and newly built installations. The high CO₂ price triggers CCS and biomass technology to be installed. CO₂ emissions will rise just a bit until 2025. From 2030 until 2050 emissions will fall, most likely from 20 to 15 Mt/y. Negative emissions are possible from 2025 on with a low probability.

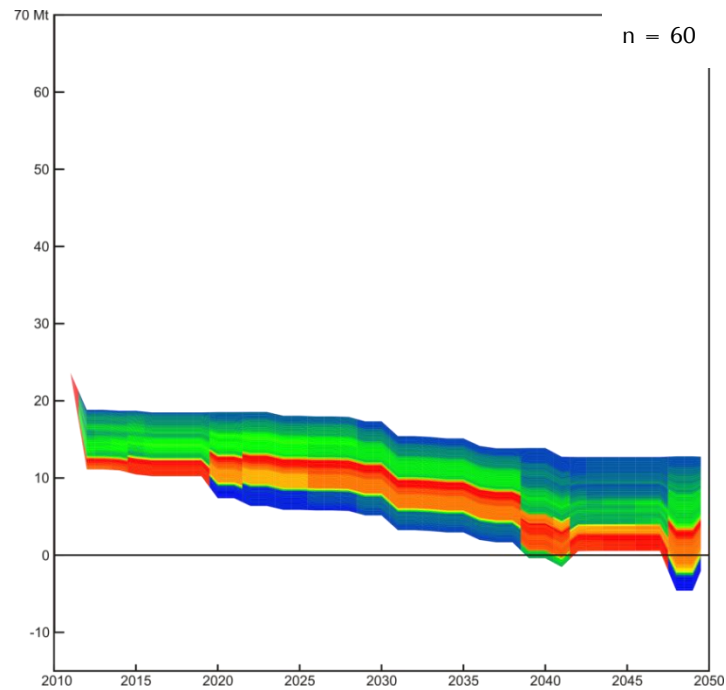


Figure 3.16. Net CO₂ emissions for the power sector for scenario 5 for the existing and newly built installations. All Monte-Carlo calculations produced an almost identical result. Keeping nuclear energy production, causing a low demand for fossil fuel and biomass energy production, generates a very secure scenario for lowering CO₂ emissions from 10-20 Mt/y in 2010 to around 0 in 2050.

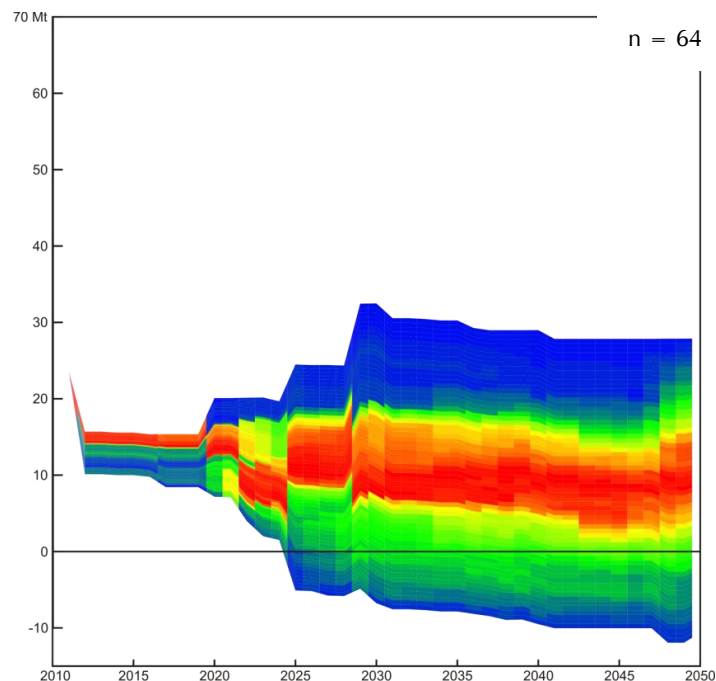


Figure 3.17. Net CO₂ emissions for the power sector for scenario 7 for the existing and newly built installations. Results are similar to those of scenario 2, although with a larger spread. A high CO₂ price will force emissions to stay low. Highest probability for net emissions is about 10 Mt/y in 2050. Negative emissions are possible from 2025 on, with a low probability.

3.1.1.5. Captured CO₂ emissions

Opposed to the net emissions are the amounts of CO₂ that are captured and stored in geological reservoirs. The yearly amounts that are captured are given here for the power sector.

The yearly amount of CO₂ captured and stored in scenario 1 is on average close to 0, with a large spread from 0 to 25 Mt/y (Figure 3.18). The probability of reaching amounts over 10 Mt/y are very low (15% probability). Only after 2040 captured CO₂ amounts rise because of the continuously rising demand and production efficiencies of capture technologies.

The effect of a high CO₂ price becomes immediately clear, with a (low) possibility of over 10Mt/y in 2015 already (Figure 3.19). Between 2025 and 2035 the highest probability rises up towards this 10 Mt/y, and 15-20 Mt/y in 2050. Large emission cuts seem to be triggered when CO₂ price rises over 200 €/tonne. This may mean that above this price level, non-CCS technologies are no longer economic, not even when considering a portfolio for energy production.

In scenario 5 not much CO₂ is captured (Figure 3.20). In all cases the amount of captured CO₂ remains below 10 Mt/y, despite higher CO₂ prices. Because of low demand, not much new installations are needed. Around 2040 the share of gas-fired power plants has aged and is replaced partially by plants with CCS, induced by the high CO₂ price and causing the slight increase in captured CO₂.

In scenario 7 uncertainty increases. Most pathways between 0 and 30 Mt/y have a similar probability, coloured green in Figure 3.21. Two main pathways are chosen, one with about 4 Mt/y of captured and stored CO₂ and one with double that amount. The relatively high level of uncertainty was already observed in the net emission Figure 3.17 versus Figure 3.15 and Figure 3.16.

As was already observed in the net CO₂ emissions, a high CO₂ price is needed for large amounts to be captured.

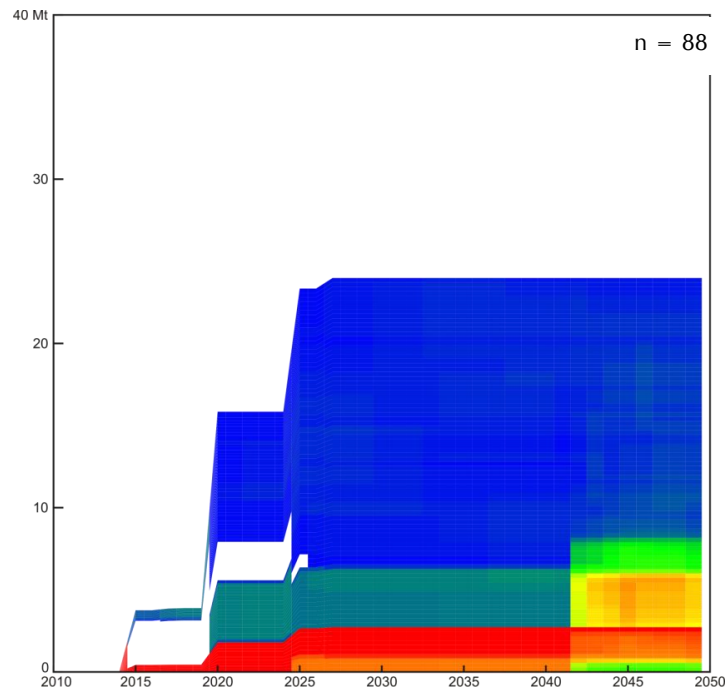


Figure 3.18. CO₂ emissions captured for the power sector in scenario 1 are generally very low, with a very low probability of more than 10Mt/y. From 2041 onwards captured CO₂ might be a little higher because of the continuously high demand and rising efficiencies of CCS technologies, lowering production costs.

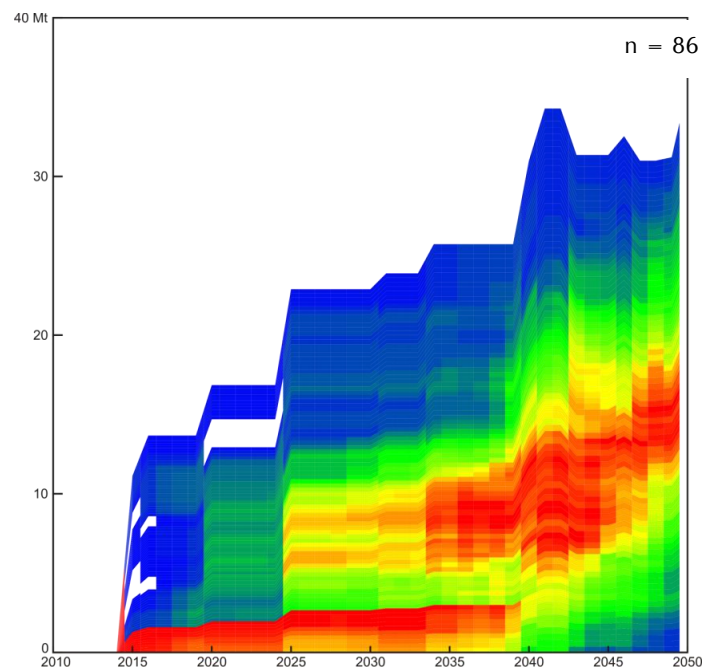


Figure 3.19. CO₂ emissions captured for the power sector in the second scenario are somewhat higher from the start. Until 2025 the probability of high storage numbers, over 5 Mt/y, remains low. From 2035 onwards, together with a steep rise in CO₂ price, capture is increasing up to a highest probability value of about 15 Mt/y with a range of 0-30 Mt/y. Noticeable in this graph is that a large cut in CO₂ emissions is in many cases delayed until the moment the CO₂ price rises over 200 €/tonne.

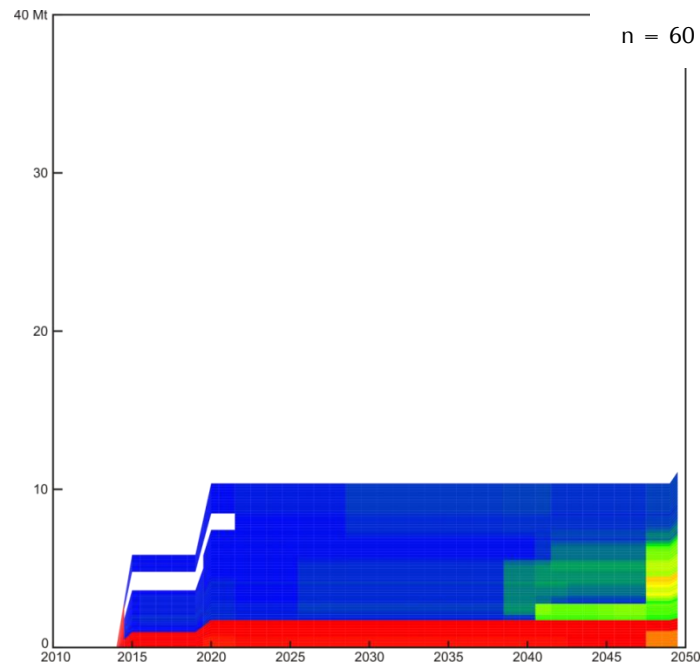


Figure 3.20. CO₂ captured for the power sector in scenario 5. In this scenario not much CO₂ is captured. In all cases the amount of captured CO₂ remains below 10 Mt/y, despite high CO₂ price. As has been explained in chapter 3.1.1.1 (Technology portfolio) electricity production from gas is chosen first to meet demand, since CCS technologies are not available yet. Thereafter demand drops which prevents new project activations with CCS technology. Around 2040 old installations are replaced and some CCS is installed, although not much because of relatively low demand.

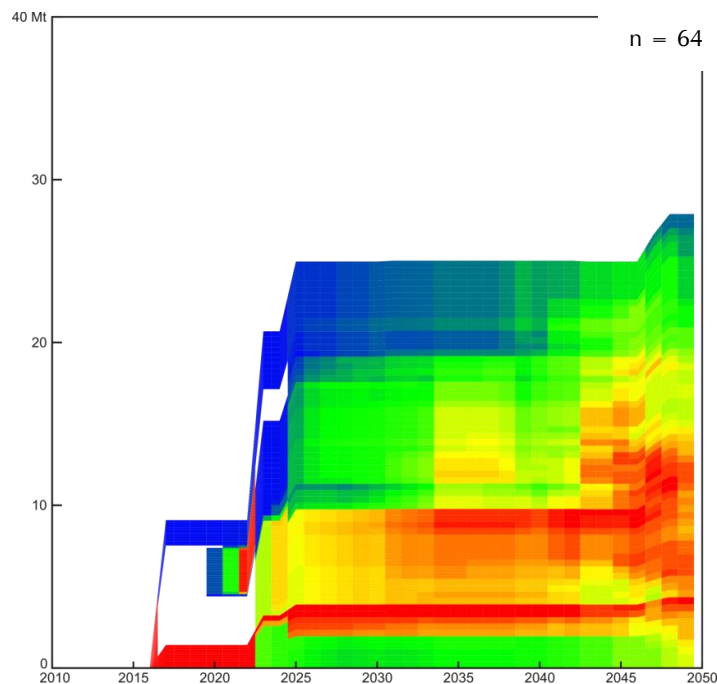


Figure 3.21. In scenario 7 a more erratic pattern emerges. Two main pathways are chosen, one with about 4 Mt/y of storage and one with double that amount. These two pathways can however not be observed in the net emissions graph (Figure 3.17).

3.1.2. Iron & steel sector

3.1.2.1. Technology portfolio

For iron production, five production technologies are available: blast-furnace with pulverised coal injection, oxy-fuelled blast furnace, oxy-fuelled blast-furnace with CCS (physical absorption), COREX and COREX with CCS. Existing production capacity is reduced between 2020 and 2040 in three steps. Demand for the iron & steel sector is equal for all scenarios (at 10 000 kt/y). Therefore the changes observed between the four scenarios are caused only by a difference in CO₂ price.

The results are presented on a relative scale, and it is therefore important to recall that new production capacity is built from 2020 or 2030 onwards, gradually increasing over time. Only from 2040 on the entire production comes from newly built facilities.

The COREX process, with or without CCS, is never chosen because of its high cost. While blast-furnace with CCS becomes available from 2020, it gets chosen for all scenarios only from 2030 on. Even in scenario 1, 50 to 70% of the portfolio becomes filled with CCS technology (Figure 3.22). In the other scenarios almost 100% of the portfolio consists of CCS technology by 2050 (Figure 3.23, Figure 3.24 & Figure 3.25). Only in the 2nd and 7th scenario some oxy-fuelled blast-furnace without CCS is activated in the mid 2040's. These results indicate that CCS in the iron & steel sector is a very viable option, even if the price of CO₂ stays relatively low.

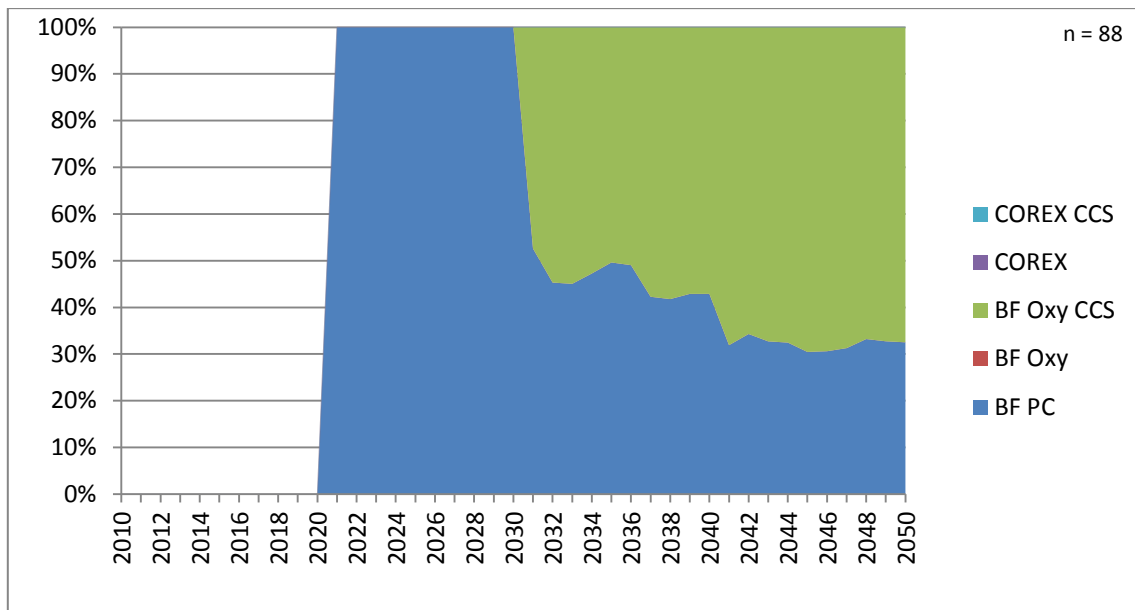


Figure 3.22. Technology portfolio of the newly installed production for iron production for scenario 1. From 2020 on new production is installed. Even at low CO₂ prices up to 70% of the production technology portfolio is converted to CCS from 2030 on. Only blast-furnace with pulverised coal and oxy-fuelled blast-furnace with CCS are chosen, COREX technologies are too expensive.

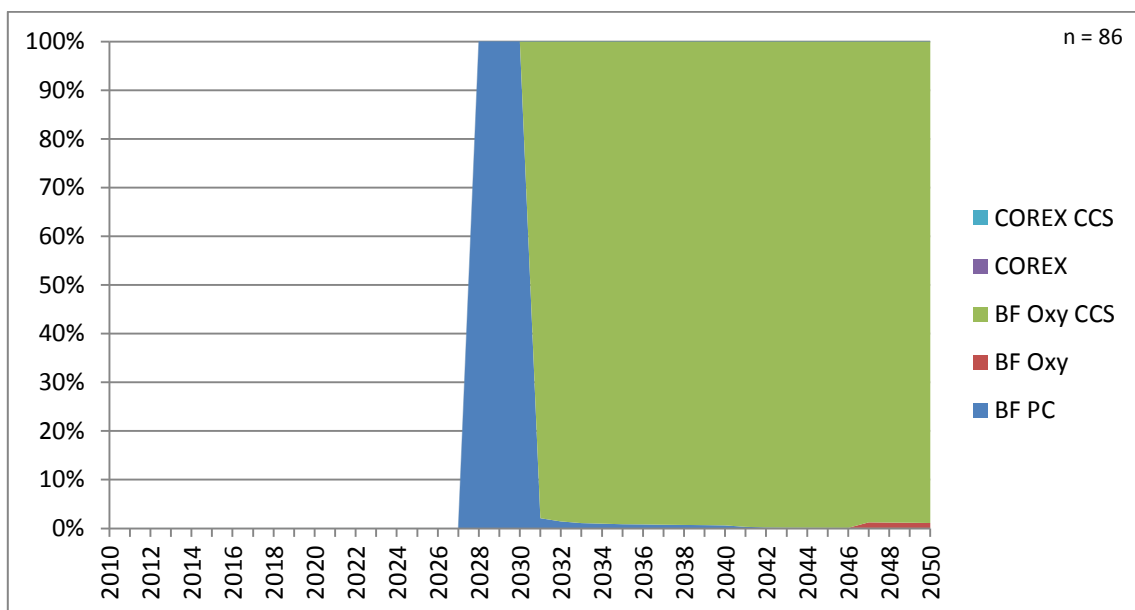


Figure 3.23. Technology portfolio of the newly installed production for iron production for scenario 2. From 2027 on new production is installed. With a high CO₂ price, almost the whole technology portfolio is converted from blast-furnace with pulverised coal to oxy-fuelled blast-furnace with CCS in 2030. Only from 2047 on, a negligible amount of oxy-fuelled blast-furnace without CCS is installed, probably due to portfolio decisions.

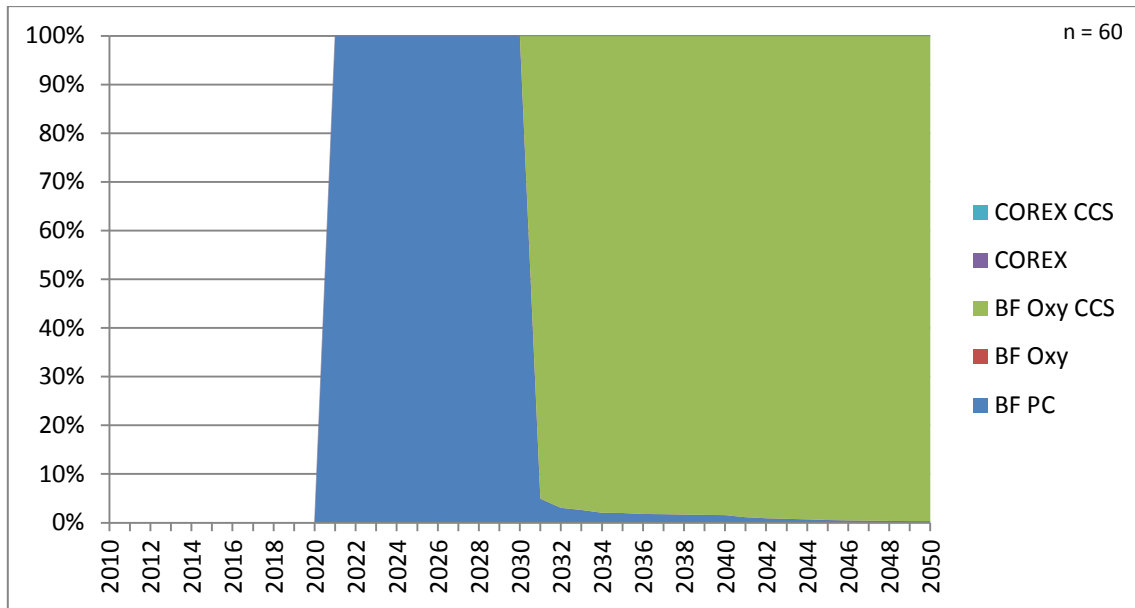


Figure 3.24. Technology portfolio of the newly installed production for iron production for scenario 5. From 2020 on new production is installed. The high CO₂ price triggers the conversion of nearly all production capacity from blast-furnace with pulverised coal to oxy-fuelled blast-furnace with CCS in 2030. Other technologies are not chosen because of higher cost.

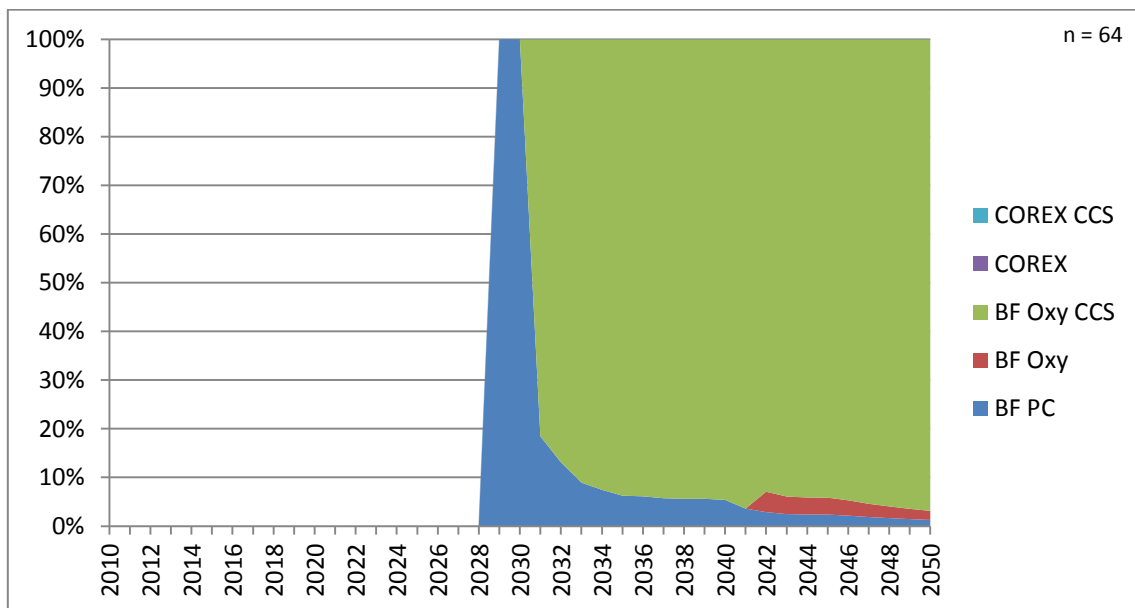


Figure 3.25. Technology portfolio of the newly installed production for iron production for scenario 7. From 2029 on new production is installed. The high CO₂ price triggers the conversion of nearly all production capacity from blast-furnace with pulverised coal to oxy-fuelled blast-furnace with CCS. As in scenario 2, a small amount of oxy-fuelled blast-furnace without CCS is installed in the 2040's due to portfolio decisions.

3.1.2.2. Captured CO₂ emissions

In the four scenarios CCS technology is installed and CO₂ is captured. The amounts captured for the iron & steel sector from the different Monte-Carlo calculations are plotted in rainbow graphs (Figure 3.26, Figure 3.27, Figure 3.28 & Figure 3.29). The four graphs have a similar look with what appears to be a split in possible futures at 2030. This is true up to some degree but part from it is also due to a graphical artefact. In reality around 2045 the highest probability pathways rise from around 1 to 7 Mt/y, as is indicated by the black dotted line.

Existing production is phased-out in different steps until 2040 to make place for new installations. Starting in 2030 CCS installation are built with a first rise in captured emissions in 2035. The timing of the second and most important rise appears to be related to the timing of the rise in CO₂ price (Figure 2.13): in all scenarios except scenario 1 the about 8 Mt CO₂ will most likely be captured in 2050. In scenario 2 this amount will be reached before 2044 while in scenario 7 this will only be reached by 2049.

In scenario 1 less CO₂ is captured which is also reflected in the technology portfolio (Figure 3.22) with 30% of non-CCS production still remaining in 2050.

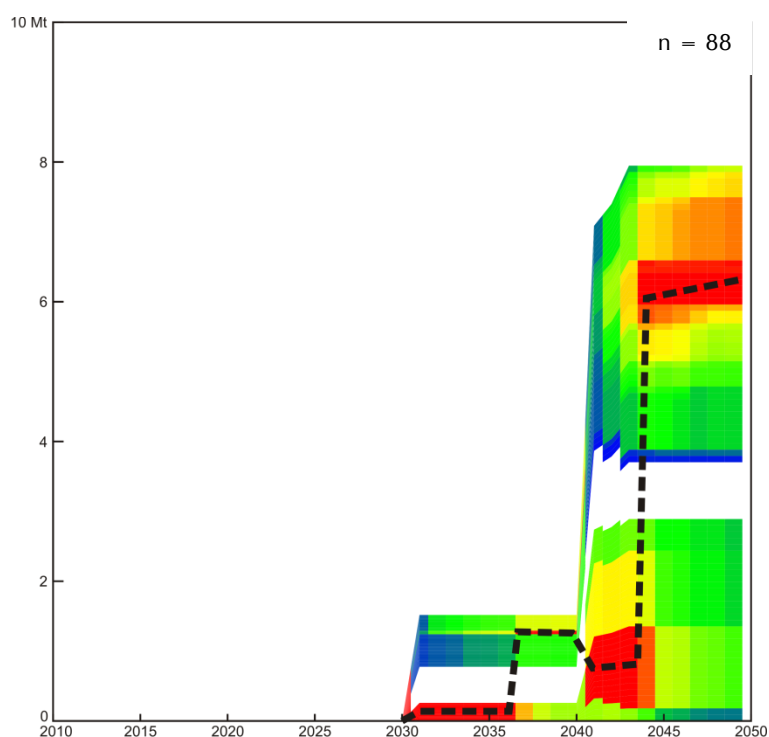


Figure 3.26. CO₂ captured from iron production in scenario 1. The most likely scenario is indicated with a black dotted line because the two-split graph may not give a correct first impression of the chosen pathways. Capture starts from 2030 with low amounts. From 2044 the CO₂ captured will be around 6 Mt/y.

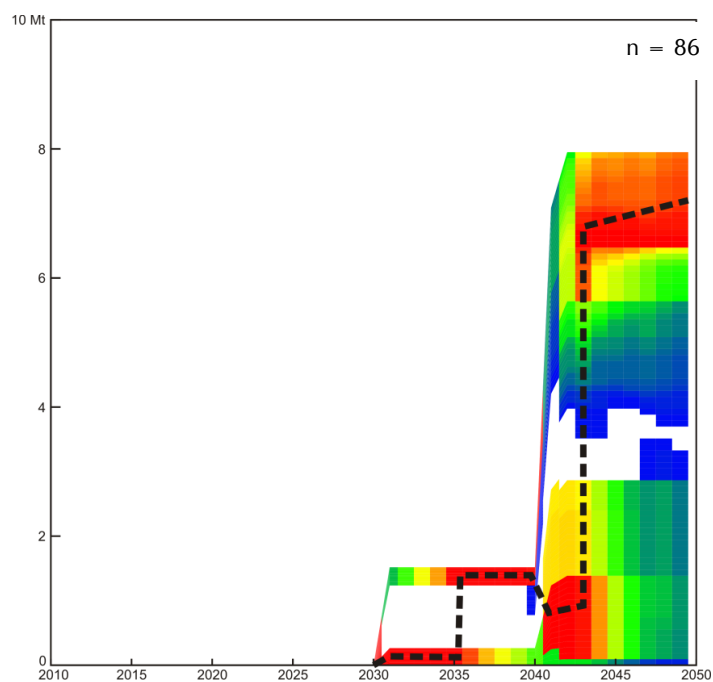


Figure 3.27. CO₂ captured from iron production in scenario 2. The most likely scenario is indicated with a black dotted line because the two-split graph may not give a correct first impression of the pathways. Capture starts from 2030 with low amounts, although probabilities for larger amounts are a little higher compared to scenario 1 because of high CO₂ price. Again, only from 2043-2044 larger amounts are captured with highest probabilities for 7 to 8 Mt/y.

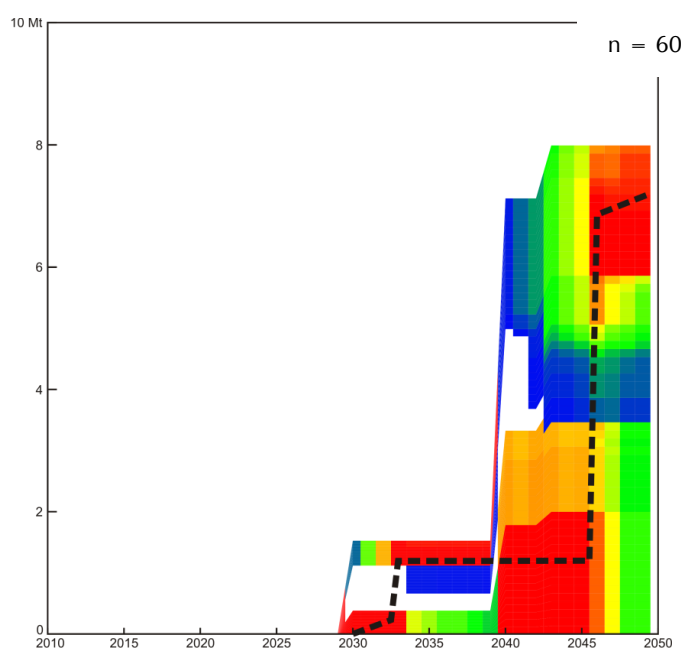


Figure 3.28. CO₂ captured from iron production in scenario 5. The most likely scenario is indicated with a black dotted line because the two-split graph may not give a correct first impression of the pathways. Capture starts from 2030 with low amounts, comparable to those of scenario 2. The moment CO₂ captured rises to 7-8 Mt/y is delayed until 2046 since CO₂ price rises later in time (Figure 2.13).

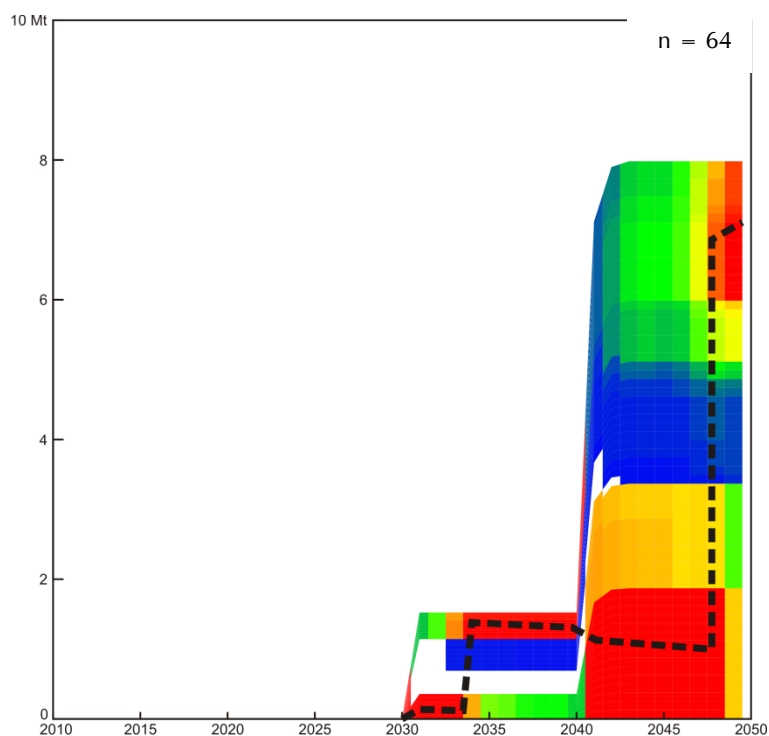


Figure 3.29. CO₂ captured from iron production in scenario 7. The most likely scenario is indicated with a black dotted line because the two-split graph may not give a correct first impression of the pathways. The same image appears for this scenario as for scenario 2 and 7, yet the rise up to 7-8 Mt/y of captured CO₂ is delayed until 2049 because of the late rise of CO₂ price (Figure 2.13).

3.1.3. Transport

For producing the results presented here the multiple time step network calculation method (chapter 2.1.4.5 Pipeline networks) was enabled. Figure 3.30 shows an approximation of the major existing pipelines in Belgium. These trajectories were entered in PSS II as pipeline corridors (chapter 2.1.4.4 Pipeline corridors).

Pipeline trajectory nodes are always attached to a grid cell in PSS II, although each trajectory may bridge up to three cells. For each Monte-Carlo calculation a map is drawn using the grid cells. If one or more pipelines are crossing the cell, one count is added for that cell. Stacking these maps results in a probability map of where pipelines may be constructed (Figure 3.31). Red colours indicate the grid cell is crossed by one or more pipelines in (almost) all MC calculations. Blue colours are for low probabilities. No colour means no pipelines ever crossed this grid cell. The pipeline cost grids were kept the same for all scenarios; therefore all scenarios are plotted onto one map.

For interpretation, the pipeline corridors, source locations and reservoir injection locations are superimposed on this figure (Figure 3.32). Pipelines generally tend to follow the imposed corridors, but deviate where this is cost effective. In most cases, pipelines are constructed from the source locations towards the nearest border, for export. The pipelines in the north-eastern part of the country are somewhat scattered between the different MC calculations. Main reason is the relatively higher density of injection locations in this area, resulting in many possible pipeline trajectories depending on which injection site is selected.

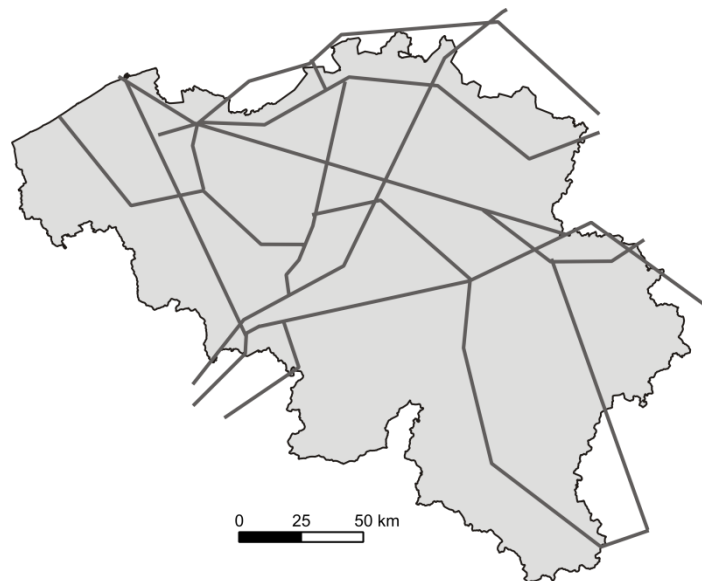


Figure 3.30. Approximation of the major existing pipeline trajectories in Belgium, regarded as pipeline corridors. The according grid cells are given a lower cost for routing, although the real cost stays the same. This way pipelines are forced into the corridors.

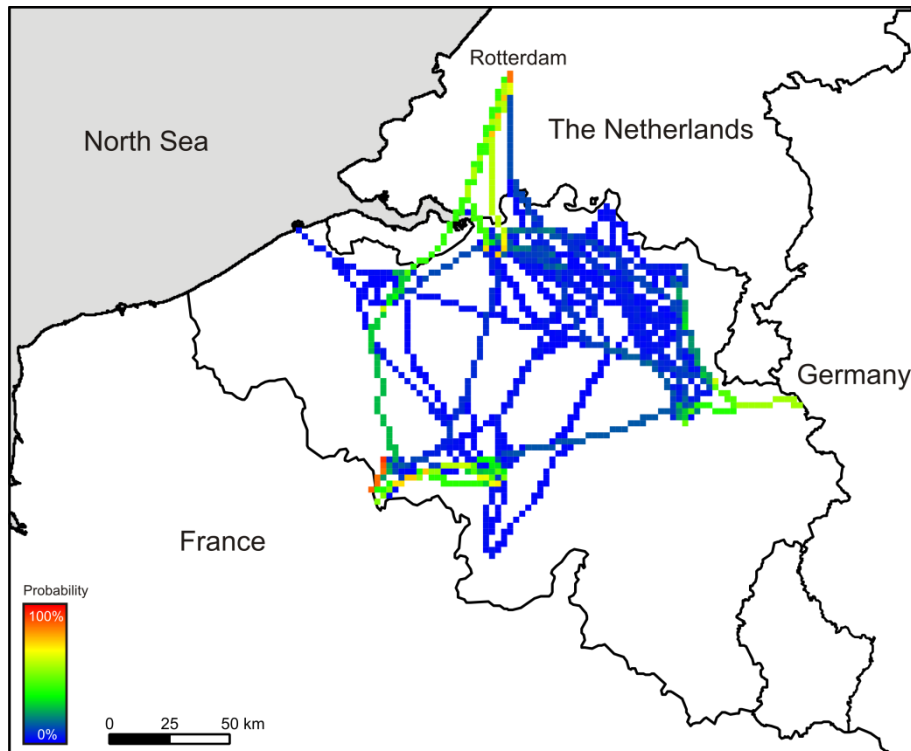


Figure 3.31. The probability one or more pipelines cross a raster cell for all scenarios and Monte-Carlo calculations is plotted on the map of Belgium and surrounding countries. Red colour indicates the cell is crossed by one or more pipelines in almost all Monte-Carlo calculations. The connections to France, Germany and the North Sea are cut off at the border. Towards the Netherlands, the raster grid continues to Rotterdam from where the CO₂ is distributed towards the individual regions and reservoirs. The pipeline connections towards the neighbouring countries are often chosen on the same trajectory. Pipelines in the north-eastern part of Belgium have a less fixed trajectory over the calculations.

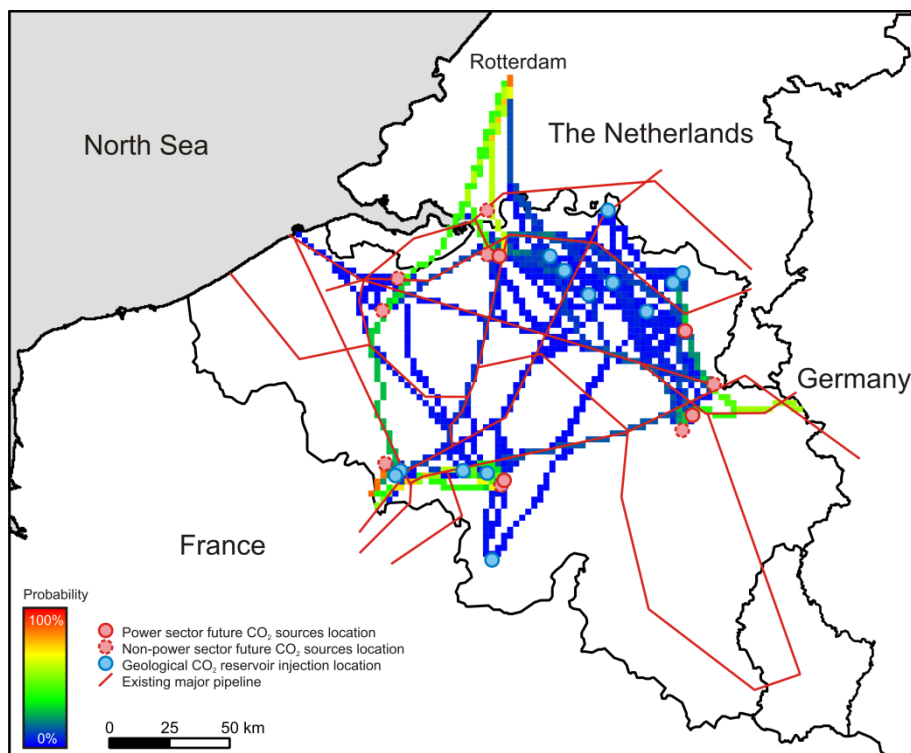


Figure 3.32. Plotting other information on top of Figure 3.31, a clearer image of the pipeline trajectories is shown. Pipelines tend to follow the predetermined pipeline corridors (red lines), although in the north-eastern part pipeline trajectories are scattered throughout the Monte-Carlo's. Pipelines clearly start at sources and end at injection sites (e.g. most southern trajectories) or borders (e.g. Germany in the east).

3.1.4. CO₂ storage

Economic decisions, technology portfolios and net emissions for different sectors are calculated independently from each other by PSS II. Storage of these emissions however happens in the same reservoirs, and therefore emissions for all sectors currently present in PSS are presented here as a whole. The sectors considered are power, iron & steel, cement, ammonia and hydrogen. The largest emissions will come from the power sector, being the most CO₂-intensive industry in Belgium.

For scenario 5 and 7 additional simulations were made compared to the results presented in previous chapters, because the results for the reservoirs were presumed not to be stable yet. Final results for scenario 5 and 7, as presented here, are generated using about twice as much Monte-Carlo calculations as for results in previous chapters. When comparing the final results these did change, although not dramatically, indicating the extra simulations were useful.

3.1.4.1. International storage

It is likely that once CCS becomes a widespread economic activity, CO₂ will be transported cross-border for storage in the optimal geological reservoir. As discussed in chapter 0 (

Dutch reservoirs), the storage data of the Netherlands was updated and detailed compared to PSS I, while data on the other neighbouring countries was not altered. The latest developments in CO₂ storage related policy in the Netherlands and Germany are not yet reflected in these results. From PSS II results the probability that Belgian emissions will be stored in a certain country can be calculated (Table 3.III). Here, the probability in % is given that, if CCS is applied, storage will happen in a certain country.

If CCS is applied, there is for all scenarios more than 50% chance that some amount will be stored in Belgium. Storage probabilities for Belgium are higher if the CO₂ price is higher (and more CO₂ is stored in total). This effect is also very well visible for export to Germany since export prices for relatively small amounts of CO₂ are more expensive than for the Netherlands or France. These two countries both have high storage probabilities for all scenarios.

Table 3.III. Probability that if CCS is applied, storage will be in a country or region, for the different scenarios and averaged for all Monte-Carlo calculations In all scenarios storage is happening in Belgium with a probability of over 50%.

Scenario	Belgium	Netherlands	France	Germany	North Sea
1	54	75	84	16	0
2	66	95	98	90	7
5	67	85	88	74	0
7	70	93	87	72	1
Average	64	87	89	63	2

3.1.4.2. Belgian reservoirs

The innovative part of the PSS II Simulator on the geological side is its ability to generate results using reservoir capacity estimates with a very large uncertainty distribution. Using the PSS Explorer (chapter 2.1.5 Storage) the practical capacity (Bachu et al., 2007) can be calculated as a cost versus probability versus capacity distribution. An important question to be answered is: what is the matched capacity of a reservoir. In other words, what is the amount of CO₂ stored in a reservoir if chosen for CCS. Both yearly injection rates (yearly capacity) and total capacity are given as an average of all MC runs per scenario. A second result for the storage reservoirs is the probability that a reservoir will be developed in the future. Values were calculated as in (Piessens & Welkenhuysen, 2010) (similar to Table 3.III): the number of MC calculations in which a certain reservoir is used (this can be for one or more CCS projects and years) is counted and divided by the total number of Monte-Carlo calculations.

In general, considering all scenarios, two groups of reservoirs can be made, based mainly on probability. The Neeroeteren, Buntsandstein and Dinantian reservoirs are chosen more frequently and have on average a higher capacity than the Cretaceous, Devonian and coal reservoirs (Figure 3.33, Figure 3.34, Figure 3.35 & Figure 3.36).

Some exceptions are the Buntsandstein in scenario 1, the karstified Dinantian in the Walloon region in scenario 5, and the Devonian in the Flemish region in scenario 7, with the highest total capacity but low probability. This combination of high capacity and low probability can happen if a reservoir possibly has a large capacity but is not well known or technical difficulties exist (see the coal seam reservoirs in Piessens & Welkenhuysen, 2010). This will pose a high risk on developing a reservoir. If successfully developed however, a large capacity is available.

In general the amounts stored in Belgium are relatively low, comparing the matched capacity presented here with other capacity estimations (Piessens & Welkenhuysen, 2010), with almost no reservoir having a total capacity of over 10 Mt. Storage cost is the limiting factor here: exporting emissions to neighbouring countries is in many cases cheaper and more secure, considering available data.

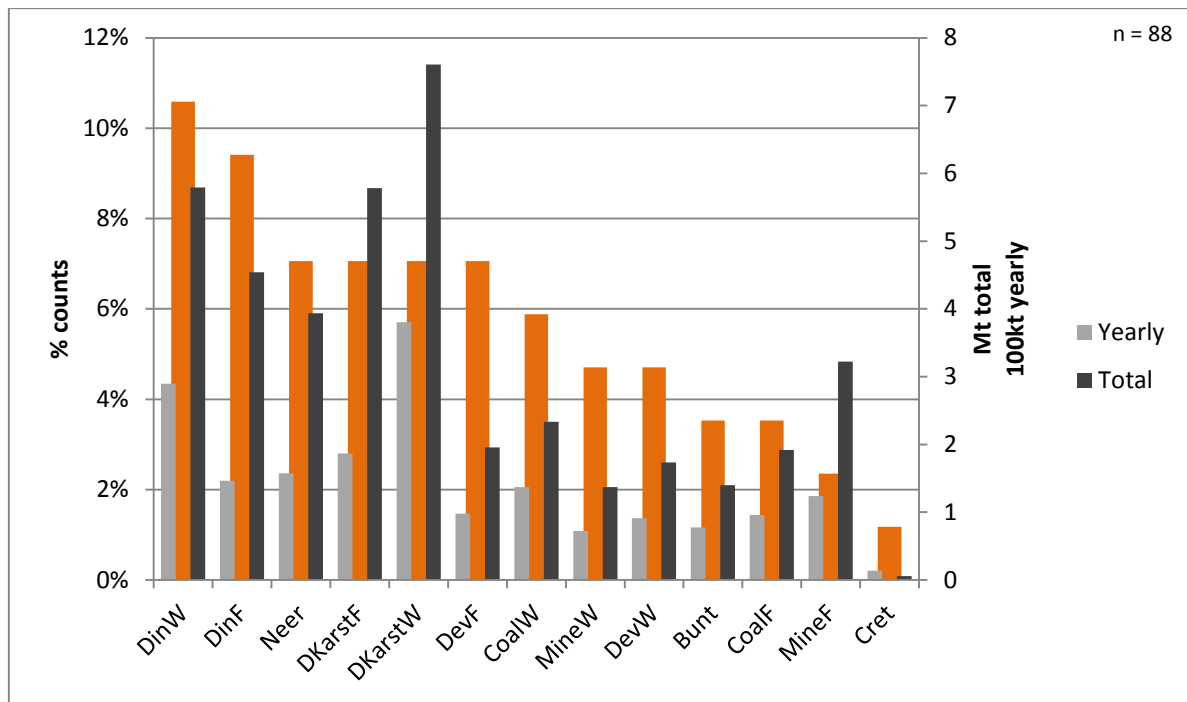


Figure 3.33. Matched total and yearly capacities, and probabilities (orange) for the Belgian reservoirs, for scenario 1. Reservoirs are ranked by probability. The dolomitised Dinantian reservoirs have around a 10% probability of being developed in scenario 1. Low probabilities are for the Cretaceous and the mines in the Flemish region, around 2% and lower.

In scenario 1 not much CO₂ is stored because of the low CO₂ price. If a CCS project is activated though, a fair amount of CO₂ is stored. The karstified Dinantian limestone and dolomitised Dinantian both in the Walloon region have the highest injectivity and total matched capacity. The Upper-Cretaceous on the other hand has a very low average total capacity, about 55 kt in total.

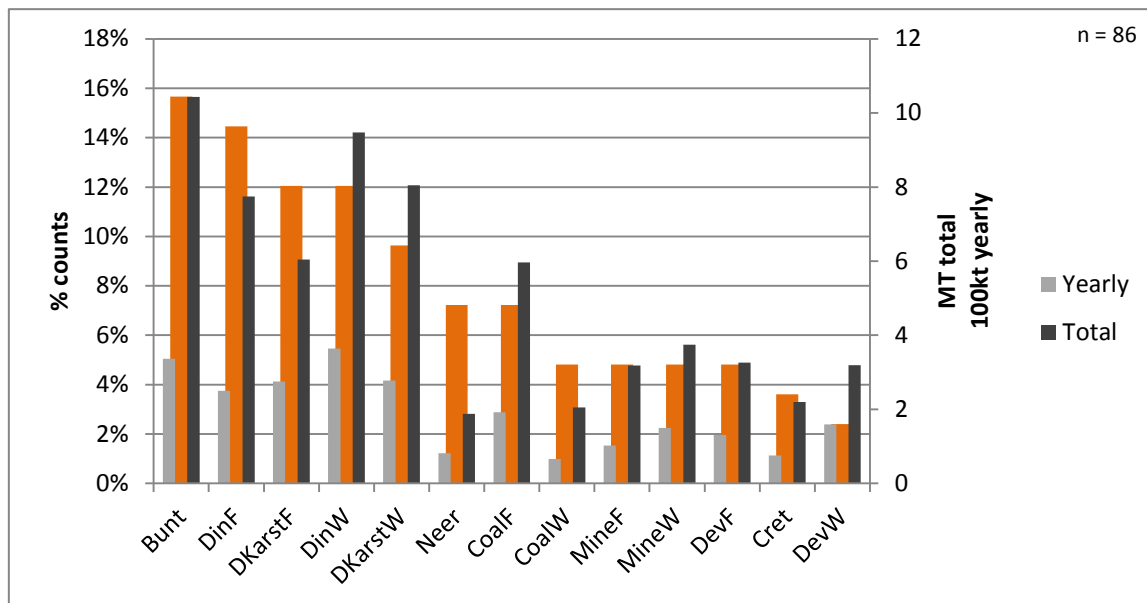


Figure 3.34. Matched total and yearly capacities, and probabilities (orange) for the Belgian reservoirs, for scenario 2. Reservoirs are ranked by probability. Like with the first scenario, the probability a reservoir is used provides the same image as the capacity graph, with highest probabilities for the Buntsandstein and Dinantian reservoirs.

In this scenario CCS is applied regularly. Six reservoirs have a total capacity of over 5 Mt: the Buntsandstein, coal seams in Flanders, and all Dinantian reservoirs. Cretaceous, Neeroeteren and coal seams in Flemish region reservoirs have the lowest matched total capacity.

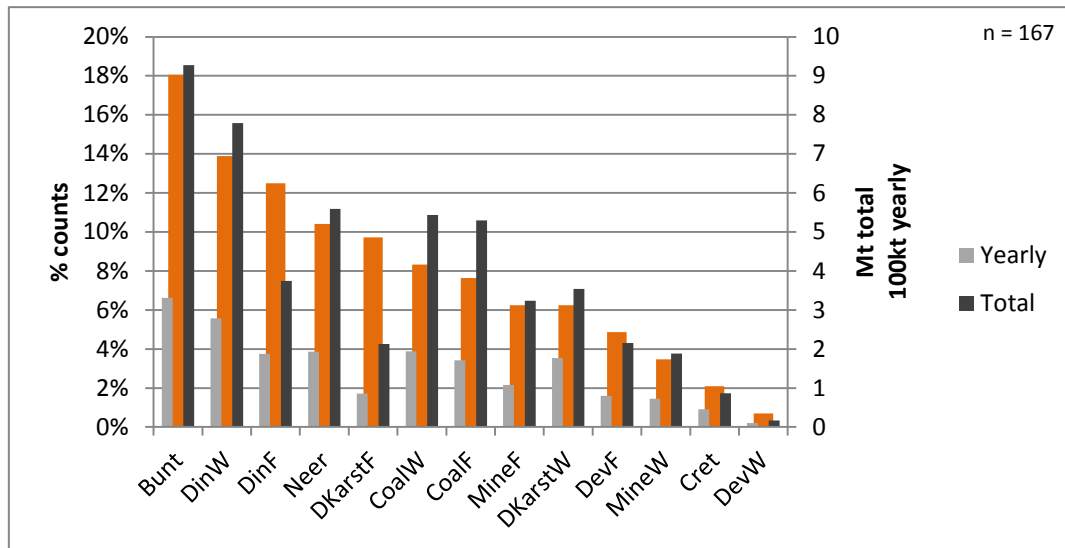


Figure 3.35. Matched total and yearly capacities, and probabilities (orange) for the Belgian reservoirs, for scenario 5. Reservoirs are ranked by probability. Buntsandstein and dolomitised Dinantian reservoirs have high probability of being developed. Cretaceous and Devonian in the Walloon region have a very low probability.

The Buntsandstein also has the largest yearly and total capacity, followed by the Dinantian in the Walloon region, the coal seam reservoirs and the Neeroeteren reservoir. Again Cretaceous and the Devonian in the Walloon region have the lowest capacities.

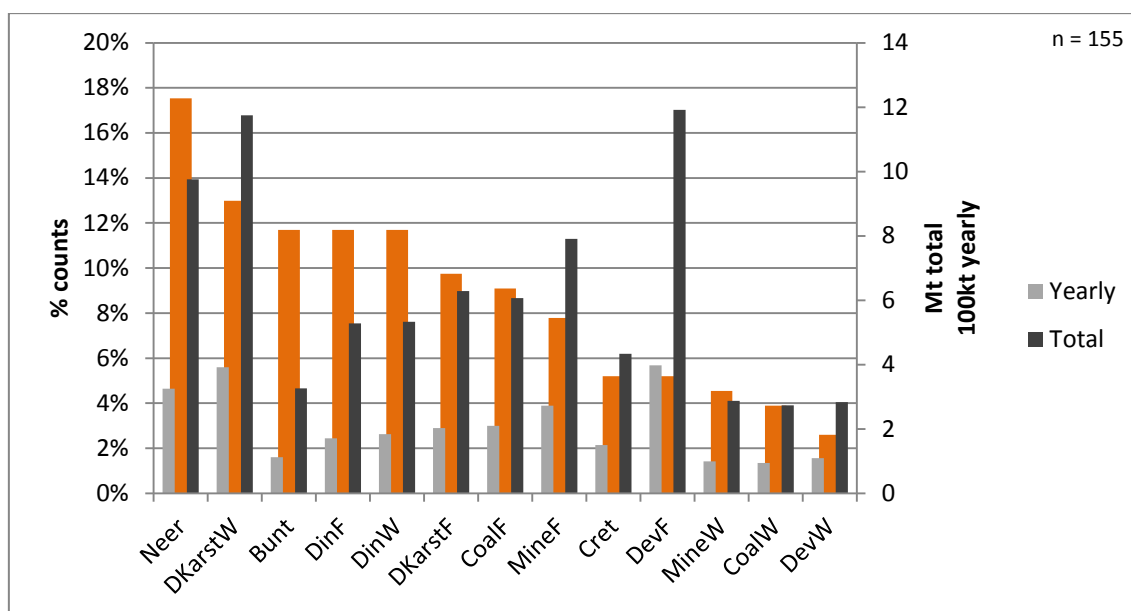


Figure 3.36. Matched total and yearly capacities, and probabilities (orange) for the Belgian reservoirs, for scenario 7. Reservoirs are ranked by probability. In this scenario the Neeroeteren reservoir is most likely to be developed, followed by the Dinantian and Buntsandstein reservoirs.

Highest capacity is surprisingly for the Devonian in the Flemish region since this reservoir has low probability of being developed; about the same image appears for the coal mines in the Flemish region. These reservoirs are thus a risk to develop, though if successfully developed a large capacity is available.

3.1.4.3. Dutch reservoirs

In all scenarios the Twente region was chosen in more than 75% of all Monte-Carlo calculations and the Utsira region in about 10 to 20%. No other reservoir is chosen, except for the Noord-Holland region for 37% in scenario 7. An explanation is delivered by looking at the storage costs and probabilities (see chapter 2.1.5 Storage). The Twente region is the only reservoir for the Netherlands where storage capacity is available from 3 €/tonne CO₂; all other reservoirs are available from 4 €/tonne or higher. Because no uncertainty data is available for the Dutch reservoirs, storage capacities are equal for a certain price point during all MC calculations. This enhances the unilateral distribution of reservoir choices. The Utsira region delivers a large capacity at all price points from 4€/tonne up, making it the second-best choice.

The choice for the Noord-Holland region for storage is not yet understood. Further research will be conducted using more detailed storage data for the Netherlands.

3.1.5. Conclusions: key messages

The results of the analysis of the four energy scenarios with the PSS II simulator can be summarized in following key messages.

3.1.5.1. CCS for industry is a likely economic option in the reference scenario

Even with a low CO₂ price of 20€/t, CCS is expected to become widely applied in industrial facilities, as is exemplified by the iron and steel sector where 70% of the production would rely on CCS technology.

CCS may under such circumstances also become part of the energy portfolio of Belgium, although on average not exceeding 10% of the energy production. Together with a phase out of nuclear energy, emissions from the power sector are therefore predicted to increase by a factor 2 compared to present day emissions.

3.1.5.2. Realistic, but high ETS prices are required to trigger large scale implementation of CCS in the power sector

Drastic reduction of the CO₂ emissions becomes feasible in scenarios where the CO₂ price exceeds 200€/t. In such situations, steel production will only come from CO₂ free production processes. CO₂ emissions in the power sector will also be effectively reduced compared to present day levels. However, PSS II predicts important effects of technology lock-in in scenarios where a phase out of nuclear energy is assumed.

3.1.5.3. High probability for near-zero emission in 2050 comes from combining nuclear and CCS power production

The deepest and most certain reductions are achieved in the scenario where there is no phase out of nuclear energy. When nuclear phase out is assumed, the emission trajectory strands at around 40% below current levels. This is because a too early phase out of nuclear energy will not always be compensated by the still immature and expensive CCS technology. Sustaining nuclear energy production, combined with CCS, is the only identified option that guarantees near-zero emissions from the power sector in 2050, although additional/alternative policy measures will be discussed in a following section (chapter 3.3. Comparison of some conclusions from the TIMES BE and PSS II models).

3.1.5.4. Capture ready does not automatically result in capture operational

Although capture ready plants are slightly more expensive than standard power plants, they are readily chosen. This is a logical investment decision in view of the uncertainties on the cost evolution of CO₂ emissions. Less intuitive is the observation that only a minority of the capture ready plants become capture operational. Initial in-depth analysis has shown that there is only a limited time window for making the additional economic investment to become CCS operational. Such effects can be prevented by adequate measures, but it is essential to realize that a capture ready plant is not a promise for a capture operational plant, and that further guarantees in that direction are usually required for real-world projects.

3.1.5.5. Developing domestic storage is justified

In spite of the importance of neighbouring regions for storing CO₂ captured in Belgium, the domestic storage potential is important. This is true for strategic reasons (Piessens et al., 2010), but it is also an economic reality. In about 50% of the PSS II simulations, domestic reservoirs are selected for the storage of CO₂ in spite of the relatively optimistic cost figures for reservoirs in some of the neighbouring countries.

3.1.5.6. Exporting CO₂ is necessary

The storage capacity of Belgium is currently poorly known. In view of the development time for storage projects, domestic storage is not realistic for early projects. When CCS will be fully deployed, the amounts of CO₂ to be captured and stored will probably be too large for the geological reservoirs in Belgium. International transport and storage of captured CO₂ will therefore be an essential element for CCS in Belgium.

3.1.5.7. Pipeline network planning is necessary for optimal cost-effectiveness

Careful planning of possible future CO₂ transporting pipelines will reduce the cost of transport. PSS II predicts pipeline networks with initially oversized pipelines being the most economical option in many cases. A backbone-type pipeline is likely to be constructed from the Antwerp and Ghent area towards the Rotterdam area in the Netherlands.

3.2. The European and Belgian TIMES model

The European and Belgian TIMES model used in this project are based on the model developed in the FP6 EU project NEEDS. The EU model covers 30 countries, the EU27 countries plus Norway, Switzerland and Iceland. For each country the full energy system is represented with four demand sectors (industry, residential, commercial and transport) and the supply sectors (electricity, fuel production, biomass and biofuel supply). Besides electricity and fuel trade the countries are also linked through trade in environmental certificates, allowing e.g. to define EU markets for CO₂ or for green certificates. The development of the Belgian TIMES model is also complementary to the development of the Flemish environmental cost model, supported by the Flemish environmental authorities.

The **extensions** of the Belgian TIMES model within this project covers following topics:

- Including new data on the non-electricity CO₂ capturing of which the steel sector is the most important. Data on CCS for refineries was not implemented into the TIMES model yet.
- Creation of a new model structure for the integration of CCS ready electricity power plants. This is now embedded in TIMES-BE, but not yet fully tested and therefore not used for the results presented here.
- Setting up a link with the PSS II model.

The update technologies for the different sectors was based on input from the cooperation with ULg, Ecofys, data available at VITO and on the technology 'briefs' elaborated within ETSAP (www.etsap.org) to which VITO also collaborated.

3.2.1. Overview of the scenarios

Different case studies covering issues related to sustainable energy (climate change, energy security, air quality) are examined with the model. In the choice of scenarios, attention was given to the importance of CCS as a climate mitigation technology and in relation to the option of using nuclear energy. The policy analysis is done both with the Belgian TIMES model and with the Pan European TIMES model. GEM-E3 (www.gem-e3.net), a computable general equilibrium model for the EU (25 countries) is used to derive the macroeconomic and sectoral evolution in Europe and in Belgium for the period 2010-2050 to be used for the generation of the TIMES reference scenario.

The scenarios cover the EU Climate policy perspectives and their implications for Belgium. Following is a list of the 8 scenario's that were run with TIMES. A short description of these scenarios is given in the table below. Four scenarios, with CCS allowed, were retained for the PSS II simulations.

Table 3.IV.

Scenario	Variants	Short description	Linked to and used by PSS II
Reference		No climate restrictions	X
NoNucGoCCS -58%		2050 climate restrictions, with nuclear fade-out	X
	-70%	With 70% emission reduction	
	More elastic	More elastic energy services demand	
	LowDemand	Low energy services demand	x
GoNucGoCCS -58%		2050 climate restrictions, no nuclear fade-out	X
NoNucNoCCS -58%		2050 climate restrictions, no nuclear fade-out	
GoNucNoCCS -58%		2050 climate restrictions, no nuclear fade-out	

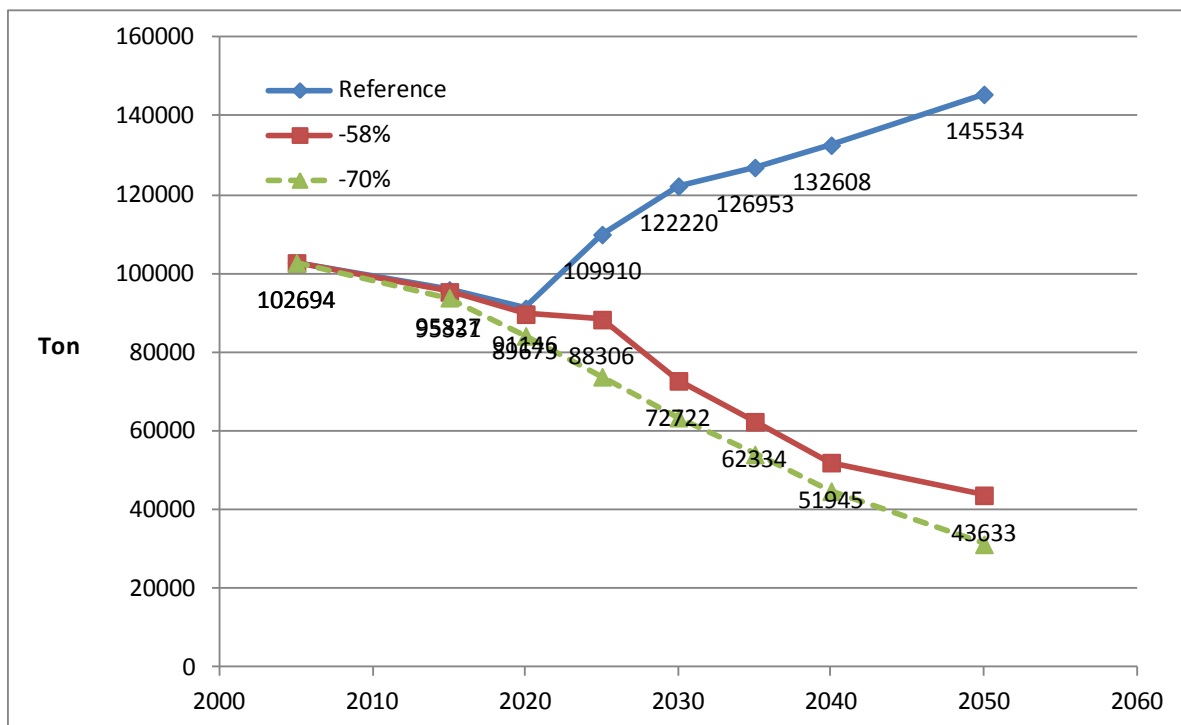


Figure 3.37. The CO₂ path of the TIMES Reference and -58% scenario (wrt 2005); the -70% was not discussed in this report but was a variant within the TUMATIM project.

In all climate scenarios, a CO₂ path of -70% wrt 2005 is implemented. This is equivalent to a reduction with 3% each year as from 2010. The EU Roadmap has an 80% reduction with respect to 1990 (that is 78% with respect to 2005).

3.2.2. The EU climate policy perspectives and their implications for Belgium

After Copenhagen, the EC has proposed to reach a 30% reduction in the EU GHG emissions by 2030. For 2050 an 80% reduction by 2050 is in line with the European commitment to limit global warming to 2°C max. These targets will be used to explore a range of policies allowing to reach them with the EU and the Belgian TIMES models.

The EU target is modeled with the Pan European model. This gives the cost optimal way to reach the target at EU level and their implications for Belgium in terms of cost and GHG reduction. With the Belgian model, we explored the impact on the emissions and on the cost of specific policy measures at the Belgian level such as the impact of including or excluding the option to use CCS.

3.2.3. Uncertainty issues with TIMES

Two different aspects of uncertainties are covered within the TIMES project: recurring uncertainties as on fuel prices and uncertainties with respect to the climate target and CCS. The latter is expected to be resolved within the time horizon.

3.2.3.1. Uncertainty on fuel prices

An extension of TIMES makes it possible to deviate from the risk neutral approach of the classical TIMES. The extension includes elements from the portfolio theory and is relatively new. It was not used in the comparison of the climate scenarios.

3.2.3.2. Uncertainty on the climate target and CCS

The climate change issue is full of uncertainty both regarding climate change itself and regarding the climate policy which will be put in place and the technologies to address this issue. We addressed some of these issues with stochastic TIMES:

- Uncertainty around the availability of carbon capture technology and storage , inclusive the retrofit possibility in the presence of a climate policy
- Uncertainty around the climate policy itself

The methodology of multi-stage stochastic programming was used and results can be found in the TUMATIM report.

3.2.4. Setting up links with PSS II

The main advantage of having both PSS II and Markal/TIMES is that the questions they can answer are different. Some of the important inputs and outputs of Markal/TIMES have been integrated in PSS II. The integration covers:

- INPUT: electricity and steel producing technologies data.
- OUTPUT: the amount of electricity produced from fossil or biomass resources.
- OUTPUT: the demand for steel.
- OUTPUT: data on the CO₂ price in the different scenarios.

These data have been fully aligned within the two models so that the outcomes can be compared. However, differences in approach may lead to differences in outcome. The PSS II model captures future uncertainties in a single strategy that is a combination of options and portfolio theory whereas until now, Markal/TIMES only covers one at the same time. Another reason for the results to be different is that Markal/TIMES captures the variation of the demand so that prices are timeslice dependent and choices might differ based on these prices.

3.3. Comparison of some conclusions from the TIMES BE and PSS II models

The evaluation of the implementation of CCS technologies in the energy sector has been evaluated with TIMES-BE and PSS II, two different models providing insights in energy policy. The results can readily be compared because they are based on essentially the same underlying data and assumptions. Differences may occur because the scope and approach of the models are different. PSS II is an ad-hoc model that forecasts future investment decisions for carbon capture and storage technologies and their direct alternatives (excluding nuclear and renewables). TIMES-BE is a complete energy model based on optimisation principles. For the scenario analysis of this project, TIMES was used with the classical approach that assumes perfect foresight. This assumption concerns both external pressures such as taxes or emission constraints and internal changes such as technology availability or cost reductions. By doing so, TIMES can anticipate and choose to increase investments in technology in order to be rewarded in the form of future cost decreases. Variants exist with flexible, limited foresight or where multistage, stochastic programming is used. Another variant was used within the TUMATIM project (Duerinck et al., submitted) to include risk aversion by including the portfolio theory. These variants are not covered by this comparison.

There is a soft data link between TIMES-BE and PSS II, and it are especially the ETS price of CO₂ and energy demand resulting from TIMES-BE calculations that are used in PSS II. Scenarios 1 (Reference scenario) and 2 (NoNucGoCCS) are best suited for comparison.

It should be clear that **the discussion below relates exclusively to the production of power from coal, gas and biomass**. TIMES-BE also provides results for the renewable and nuclear power, but these are taken out of the graphs below.

3.3.1. Results of the Reference scenario

The base scenario reflects the current policy, with moderate climate targets not exceeding those set by the Kyoto protocol and a phase out of nuclear energy. This is compatible with a CO₂ price that remains constant at 20€/t, while the demand for power increases gradually.

Looking at the portfolio of energy technologies that are implemented (Figure 3.38), there is a marked difference in newly built power production which starts earlier in PSS II. This is due to differences in the underlying dataset of existing power plants with the dataset of PSS II assuming an earlier closure of existing capacity (grey hatched area in Figure 3.38).

It can be observed (Figure 3.38b) that TIMES-BE predicts that fossil fuel power will dominantly (~60%) be produced from coal fired power plants without CCS, and the remainder from natural gas without CCS. Note that TIMES-BE does not evaluate CCS-ready technologies. The increasing share of fossil fuel power production without CCS increases the CO₂ emissions by a factor 2.5 (250%) in 2050 compared to 2010 levels (Figure 3.38d).

The average portfolio predicted by PSS II is also dominated by coal without CCS (around 80% in 2050, Figure 3.38a), although half of this represents capture ready technology. Only a marginal amount is retrofitted to become CCS operational. The future uncertainty on the CO₂ price, simulated by PSS II, warrants for a significant number of the installations the slightly higher investment costs for building a CCS-ready plant. During the simulation however, the CO₂ price remains low at only 20€/t which makes it uneconomic to retrofit an installation. Also coal with CCS is of minor importance. Natural gas without CCS is the second option, although its importance decreases towards 2050. The central use of biomass is clearly present, initially without CCS but with time increasingly with CCS. Although the share of coal without CCS is higher than in the TIMES-BE model, the use of biomass mitigates to some extent the emissions, which increase by a factor 2 (200%, Figure 3.38c) from 2010 to 2050. An increase of 200% is by far the most probable emission trajectory.

The output of the two models is well comparable for the Reference scenario. Coal without CCS for power production is the dominant option, followed by natural gas without CCS. The importance of fossil fuels without CCS leads to a steep increase of CO₂ emissions from the power sector.

A difference is the more prominent role of natural gas in TIMES-BE. This is triggered by short-term variability in demand requiring flexible production, an aspect that is ignored by PSS II where only average annual demand is taken into account. Interesting to note is that also a low ETS price can (under uncertainty) trigger the building of capture ready power plants, while CCS retrofits hardly occur.

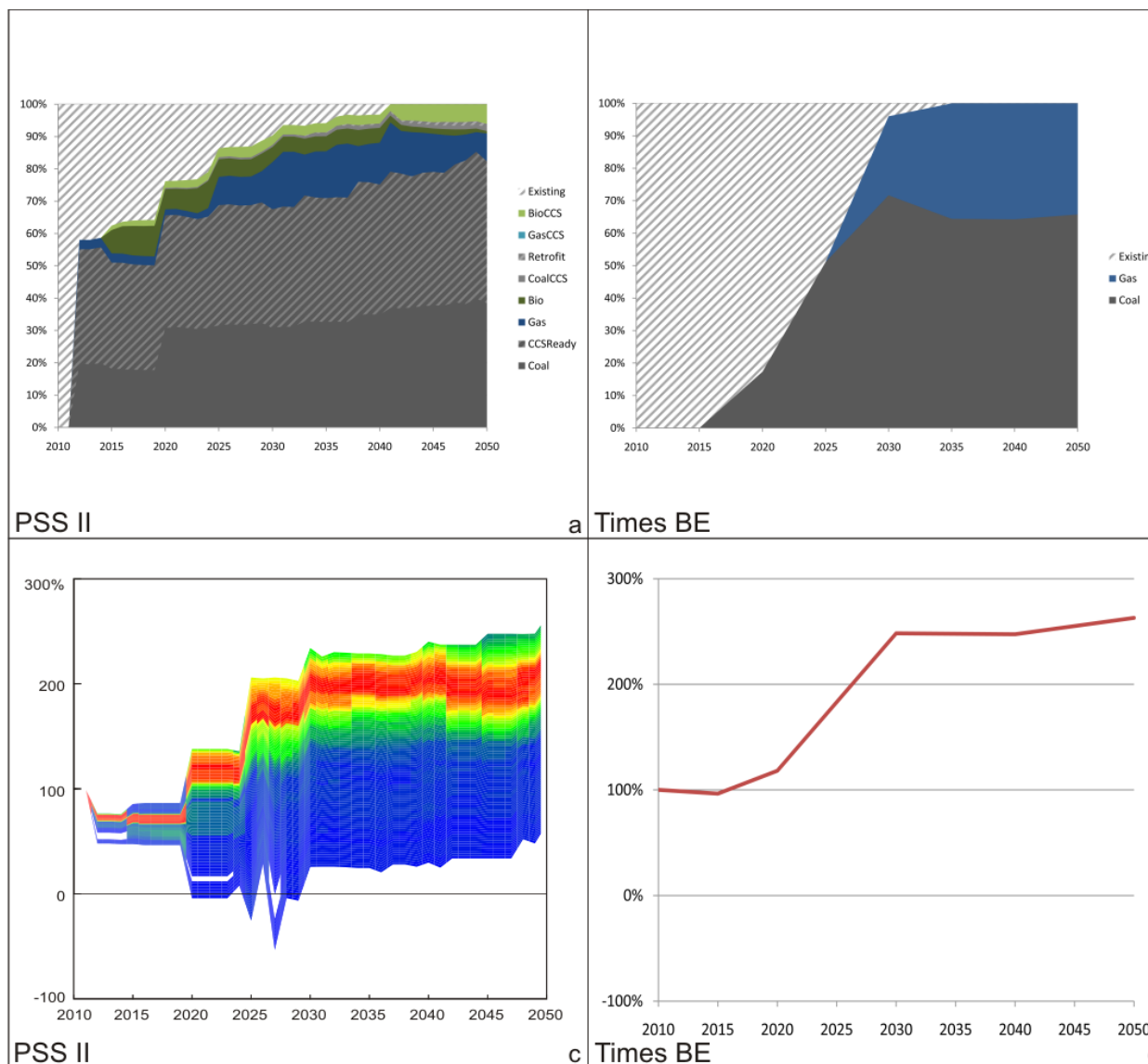


Figure 3.38. Results of the reference scenario for PSS II and Times BE. Only the results for the central use of coal, natural gas and biomass as a fuel are taken into account. (a) The technology portfolio, including existing and new plants by main technology groups, as predicted by PSS II between 2010 and 2050. Existing: Production of power from coal and natural gas in 2010, phasing out in the future. Bio/BioCCS: Central power production based on biomass, without/with CCS. Gas/GasCCS: Power based on natural gas, without/with CCS. Coal/CoalCCS: Power based on coal, without/with CCS. CCSReady: Power based on coal, with possibility to retrofit to become CCS operational. Retrofit: CCS ready plant retrofitted to be CCS operational. (b) Similar graph for TIMES-BE. (c) The corresponding CO₂ emissions from the different power technologies predicted by PSS II in (a). Red colours indicate the most probably path, blue the least probable. (d) Similar graph for TIMES-BE (without uncertainty).

3.3.2. Results for the NoNucGoCCS scenario

In the climate scenario NoNucGoCCS, nuclear energy is still phased out as scheduled, but a steeply increasing carbon price is assumed.

TIMES-The technology choices made in the previously discussed reference scenario has shown that PSS II and Times BE make comparable technology choices under conditions with a low CO₂ price, and that these are dominated by coal. In the NoNucGoCCS scenario, PSS II has to activate technologies early on, when the CO₂ price is still relatively low. This explains the importance of coal over natural gas before 2020 in PSS II. It is only after 2020 that the share of natural gas increases, a trend which is also anticipated by Times BE.

In Times BE this leads to a portfolio which is initially dominated by power production with natural gas, increasingly being replaced by coal, natural gas and biomass in combination with CCS (Figure 3.39b). This leads to near zero emission power production from fossil fuels and biomass by 2040 (Figure 3.39d).

The future outlook shown by PSS II is very different. The initial portfolio consists of coal-based power, dominantly as capture ready, with only a second place for natural gas (Figure 3.39a). Coal and natural gas with CCS become increasingly important from about 2025 onwards. In the Times BE portfolio these two groups occupy about 90% of the energy production by 2050, while in PSS II this is limited to only 50%. Part of the capture-ready potential is retrofitted to become CCS operational within the first 10 years, but after this, the remaining capture-ready infrastructure remains in the portfolio as CO₂ emitting sources in spite of the increasing CO₂ price. Partially, this can be explained by the model structure of PSS II which does not allow to turn off a power plant (see down). This effect is an example of technology lock-in in PSS II: natural gas without CCS and coal without CCS (including capture ready, not retrofitted installations) constitute 1/3rd of the total portfolio, and is a heritage from earlier investment decisions. Note again that capture ready technology is not automatically retrofitted to capture operational when CO₂ costs increase. In fact, it can be observed that retrofits are only installed within 10, at the latest 15 years after construction of the original facility. Time BE is capable of closing power plants early if this is economically sensible, and this happens in a significant degree with natural gas plants without CCS. In fact, the capacity is already reduced importantly after only 5 years of activity.

In PSS II, the share of natural gas increases together with biomass until around 2035. From then on, coal with CCS and especially natural gas with CCS continue to grow and take up about 50% of the energy portfolio. The emissions decrease compared to 2010, but only 40% on average by 2050 and a relatively high degree of uncertainty (Figure 3.39c).

The differences between the outlooks of TIMES-BE and PSS II are significant. Following points are important to understand when comparing both results:

- Due to different assumptions regarding existing fossil fuel power production, PSS II starts building new capacity already in 2011, while this is only in 2025 for TIMES-BE.
- PSS II does not allow closing utilities before the end of their life expectancy (25 or 40 years for most technologies). This is a viable option under most scenario conditions because large utilities in which longer discount times reduce the average electricity costs. This general rule is not necessarily true when operating costs strongly increase with time, which is the case in climate scenarios where the cost for CO₂ emissions rises nearly exponentially.
- The availability of biomass as fuel is assumed to be limited.
- There is no capture-ready technology for centralised power production from biomass.

For reasons which are difficult to identify, the investment decisions in PSS II are in favour of selecting biomass without CCS between 2020 and 2030. As a consequence, the total available capacity for biomass is already used, resulting in an only marginal role for biomass with CCS which would be selected after 2030. This is in contrast with the outlook of TIMES-BE, where the full potential of biomass is used in combination with CCS after 2030.

The effects of technology lock-in which are predicted by PSS II for especially capture ready coal-fired power plants, natural gas plants without CCS and biomass without CCS, lead to fundamental differences in the emission outlooks for the fossil fuel part of the power sector. According to TIMES-BE, emissions will steeply drop from 2020 onwards, when replacement of existing coal and natural gas plants starts, to reach nearly 0 in 2040. According to PSS II achieving these ultra low emissions is highly unlikely, and instead an on average reduction by about 40% compared to 2010 levels is predicted. As mentioned, this is due to the implicit assumption of PSS II that standard discount times of 40 years (25 for biomass) are optimal, which is not true when variable costs, including that for CO₂ emission, increase the way they do in the climate scenario NoNucGoCCS. Back-of-hand calculation shows that all non-CCS technology becomes so expensive around 2040 that they would be replaced by CCS alternatives, or that the plant is taken out of operation because variable costs are higher than the electricity price. If taken into account, the emissions predicted by PSS II would also surge to near zero but probably 5 to 10 years later than is foreseen by TIMES-BE.

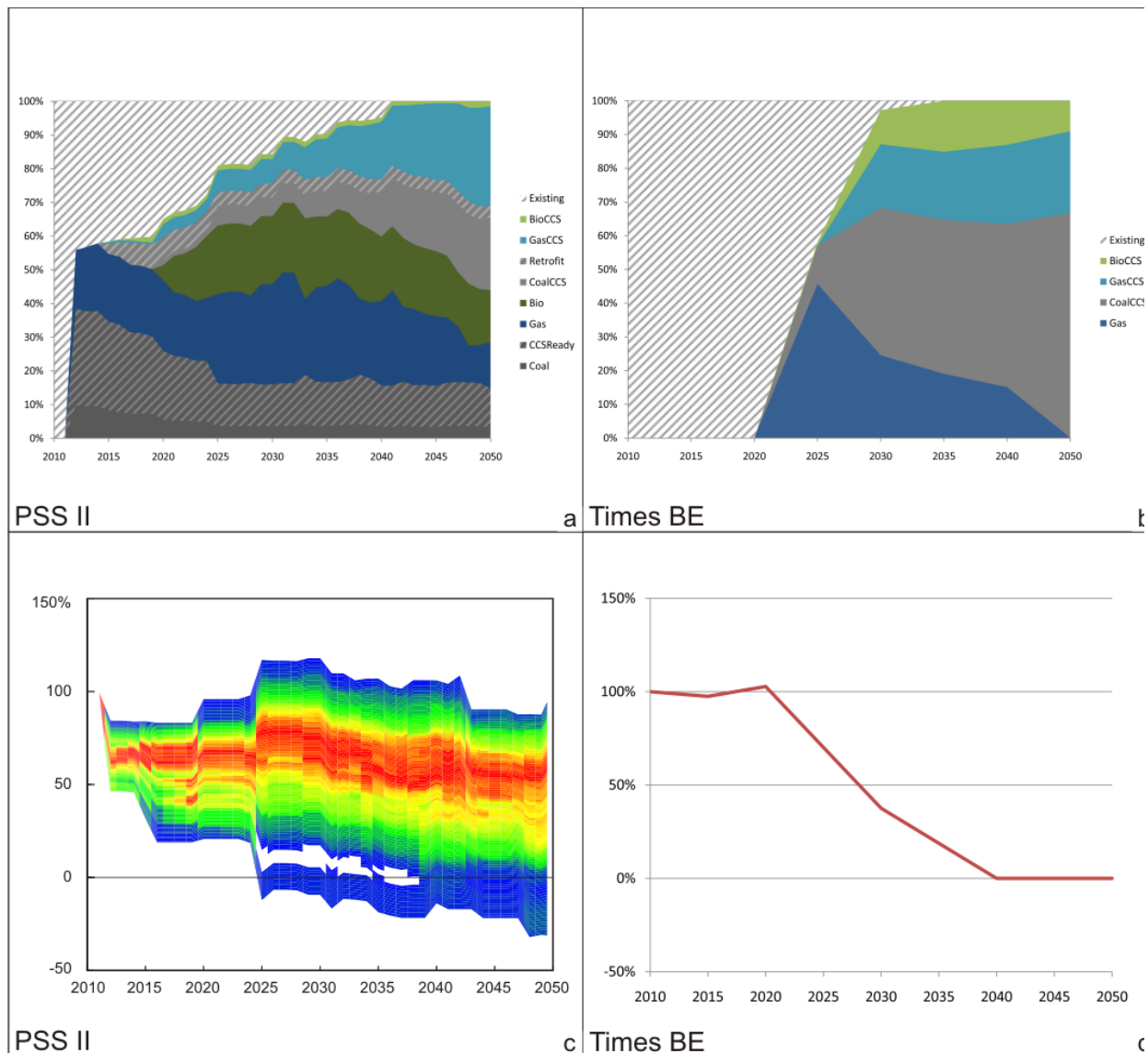


Figure 3.39.

Results of the climate scenario NoNucGoCCS from PSS II and TIMES-BE. Only the results for the central use of coal, natural gas and biomass as a fuel are taken into account. (a) The technology portfolio by main technology groups, as predicted by PSS II between 2010 and 2050. (b) Similar graph for TIMES-BE. (c) The corresponding CO₂ emissions from the different power technologies predicted by PSS II in (a). (d) Similar graph for TIMES-BE. Legends as in Figure 3.38.

3.3.3. The message behind the differences

It is beyond the scope of this report to analyse which of the two outlooks is technically most accurate. As a matter of fact, asking which of the forecasts is correct is posing the wrong question. It has been outlined earlier that the approach of PSS II is to make actual predictions on the energy portfolio and resulting CO₂ emissions by simulating investment decisions in a largely free, competitive market. Such forecasts may, but not necessarily need to, approximate the optimal energy choices proposed by Times BE.

Differences are most obvious in the climate scenario NoNucGoCCS, which includes the phasing out of nuclear capacity in Belgium. The TIMES-BE outlook provides a frame in which the fossil fuel power production is replaced by CCS technologies, leading in two decades to zero emissions from such sources. The corresponding CO₂ price that is needed to justify such choices appears is relatively high (exceeding 200€/t after 2035).

However, when a comparably high CO₂ price is assumed in PSS II, the investment decisions apparently do not result in a comparable steep drop in emissions. As has been concluded earlier, it must be clearly understood that the PSS II projections are unrealistic after 2040 because the implicit assumptions made by PSS II are violated. Nevertheless, some lessons can be learned from these uncorrected results:

- Early economic investments into less climate friendly technologies function as an unwanted technological heritage (technology lock-in for coal, gas and even biomass), which requires either high CO₂ costs or time to unlock.
- This technology lock-in can take different shapes:
- Traditional technology (state-of-the-art, but no CCS) that is optimal to build today and in the near future, but has a traditional life expectancy of 40 years (beyond 2050). These will be abandoned/replaced early when the CO₂ price reaches a certain level.
- So called 'future-compatible' technologies, in particular capture ready, which can however only be retrofitted economically within approximately the first 10 years. After this, they will behave as traditional technology and will be abandoned/replaced, rather than retrofitted.
- Investment decisions are taken based on a return on investment and risk in a competitive market, not directly to increase welfare (or reduce costs for society). Simulations based on market principles (PSS II) may approximate the ideal minimal cost-to-society (maximum welfare) solutions, but there is no guarantee that the two will coincide.

Policy makers, as well as project developers, should be well aware that the technology lock-in in capture ready installations can largely be avoided by requiring as much as possible up-front investments for the capture operational state. This reduces the additional investment needed to retrofit the installation, and will importantly stretch the economic time window for becoming CCS operational.

Lastly it needs to be emphasized that the results of both models, even if the differences are interesting and contain important lessons, do overall point in the same direction. The essential ones are highlighted below, including implicit ones which are easily overlooked:

- R&D funding for 'traditional' power production, including CCS, is urgent. It is clear that the technological improvements currently under development will play an important role in any climate scenario. The assumed availability and performance of technologies are realistic, but do require an R&D effort that exceeds the current engagements.
- Both PSS II and TIMES-BE (see also Duerinck et al., submitted) confirm that uncertainties are an essential and driving economic parameter, and need to be included in the modelling framework.
- It has also been shown that attributing uncertainty leads to a more diversified electricity mix. This is in fact a general lesson: the larger the technology portfolio, the more certain that climate targets will be met.

4. DISSEMINATION AND VALORISATION

4.1. Introduction

The methodology and results developed and obtained within the PSS-CCS projects were, are and will be disseminated in various ways. Firstly, the PSS-CCS phase I project ended with a public event and a press conference, both organised at the Royal Belgian Institute of Natural Sciences. A press overview is added hereafter. The PSS-CCS phase II and BeNe projects were also concluded with a public symposium at the RBINS. On several congresses and symposia abstracts were presented with posters and oral presentations. The PSS II simulator is also being used in other projects. An overview of all events and projects is given here, scientific and vulgarising articles are listed in chapter 5 (PUBLICATIONS).

4.2. PSS-CCS phase I

4.2.1. Organisation of dissemination events

Piessens K., Welkenhuysen K., Wambacq O., 2008. Symposium "Prospectives of Carbon Capture and Storage" of the PSS-CCS project. RBINS, Brussels, 27/06/2008. Piessens K. (convenor), Welkenhuysen K., Wambacq O. (organisation)

Piessens K., Welkenhuysen K., Wambacq O., Dejonghe L., 2008. Press conference of the PSS-CCS project. RBINS, Brussels, 08/07/2008. Piessens K. (convenor). Dejonghe L. (moderator), Welkenhuysen K., Wambacq O. (organisation)

4.2.2. Presentations at other events

- Fifth annual conference on carbon sequestration, abstract volume, Alexandria, Virginia, 8-11 May 2006. 1 oral presentation.
- AAPG conference "Challenging our Myths", Athens, Greece, 18-22 November 2007. 1 oral presentation.
- European Union Sustainable Energy Week. Brussels, Belgium, 28 January - 01 February 2008. 1 poster presentation
- Royal Belgian Institute of Natural Sciences Research Day. 24 November 2008. 1 poster presentation.
- TV newsitem on 17 December 2008. 13h Journaal, één.
- Hoorzitting Minaraad, Brussels, 3 October 2008. 1 oral presentation.

4.3. PSS-CCS phase II and BeNe

4.3.1. Organisation of dissemination events

Piessens K., Welkenhuysen K., 2011. Symposium "Treating uncertainty in energy systems and the role CCS can play" of the PSS-CCS II & BeNe projects. RBINS, Brussels, 26/05/2011. Piessens K. (convenor), Welkenhuysen K. (organisation).

4.3.2. Presentations at other events

Antarctica day. Brussels, Belgium, 15 February 2009. 1 poster presentation.

Studiedag Economische Zaken, 24 June 2009. 1 oral presentation.

Third International Conference Geologica Belgica "Challenges for the Planet: Earth Science's perspective". Ghent, Belgium, 14-15 September 2009. 1 poster presentation.

European Science Foundation Research Conference "CO₂ Geological Storage: Latest progress". Obergurgl, Austria, 22-27 November 2009. 1 poster presentation.

Fourth Strategic Energy Forum "A CO₂-lean society by 2050?". Brussel, Belgium, 10 December 2009. 1 poster presentation.

Vlaams-Europees verbindingsagentschap (VLEVA) workshop, Brussel, 03 February 2010. 1 oral presentation.

Second International Conference on Innovation for Sustainable Production. Bruges, Belgium, 18-21 April 2010. 4 oral presentations.

International Conference on Greenhouse Gas Technologies. Amsterdam, The Netherlands, 19-23 September 2010. 2 poster presentations.

Pipeline Technology Conference 2011, Hannover, Germany, 4-5 April 2011. 1 oral presentation.

Exploring Power Plant Emissions Reductions through cutting edge Technologies and Strategies conference (ExPPERTS EU), London, 27-28 September 2011. 1 oral presentation.

4.4. Dissemination and valorisation trough other projects

Within the framework of the EU funded project CGS Europe, a knowledge sharing and dissemination project on geological storage of CO₂, a task is foreseen for staff exchange between project partners (mostly geological surveys of most EU countries). It is within this task that a proposal was launched to receive up to four young scientists at the GSB-RBINS for a four week training with the PSS II simulator. The objective is to get acquainted with the simulator and its capabilities, feed data of their own region or country into the simulator and make projections for this region. A poster on this exchange proposal was presented at the CGS Europe knowledge sharing workshop on natural analogues in October 2011, and was received with much interest.

In another EU funded project, called ACCESS (Assistance in Clean Coal and Environmentally sound Storage Solutions, 2011-2012), the PSS II simulator is and will be used for assessing the storage potential and the importance for CCS in Kazakhstan.

A doctorate research was launched by Kris Welkenhuysen, starting in February 2011 (until February 2014) which is based on the PSS-CCS projects, the simulator and its results. The proposal, titled "Integration of geoscientific data and uncertainties in techno-economic forecasting on CO₂ capture and storage" has been accepted by the Arenberg Doctoral School at the K.U.Leuven.

5. PUBLICATIONS

The list of publications of the project PSS-CCS are grouped for those relating to phase one (PSS-CCS I) and phase two (PSS-CCS II and BeNe). A copy of each publication is added in Annex 1.

5.1. PSS-CCS phase I

5.1.1. Peer reviewed publications

Vandeginste, V. & Piessens, K., 2008. Pipeline design for a least-cost router application for CO₂ transport in the CO₂ sequestration cycle. *International Journal of Greenhouse Gas Control*, 2, p. 571-581.

5.1.2. Other publications

Piessens, K. & Laenen, B., 2006. Assessing the potential of carbon capture and storage in Belgium for the period 2010 - 2050: the Policy Support System for Carbon Capture and Storage (PSS-CCS). 5th annual conference on carbon sequestration, abstract volume, Alexandria, Virginia, 8-11/05/2006.

Piessens, K., 2006. Policy Support System for Carbon Capture and Storage: A New Tool for Looking into the Future of Belgium. *Greenhouse Issues*, 82, p.6-8.

Piessens, K., 2007. Dealing with Geological Uncertainties in Economic-Environmental Predictions on CCS: Approach of the Policy Support System for Carbon Capture and Storage. AAPG conference "Challenging our Myths", Athens, Greece, 18-22/11/2007.

Piessens, K., Dusar, M., Laenen, B., Mathieu, Ph. & Baele, J.-M. 2007. Carbon Capture and Storage (CCS). In: W. D'haeseleer (Ed.): *Belgium's Energy Challenges Towards 2030*. FOD Economie.

Piessens, K. (main author), 2008. Position paper on CCS. Written as member of the European Federation of Geologists and first distributed on the EU Sustainable Energy Week, Brussels, Belgium, 28/01-01/02/2008.

Piessens, K. & Dusar, M., 2008. Klimaatverandering door geologen. *Science connection*, 21, p.12-15.

Piessens, K. & Welkenhuysen, K. (main authors), 2008. Persmap voor persconferentie van het project PSS-CCS, 08/07/2008.

Baele, J.-M., 2008. The Walloon Region: Coal for storing CO₂. "Prospectives of CCS in Belgium", Brussels, Belgium, 27/06/2008. (oral presentation)

Hendriks, Ch., de Visser, E. & Brandsma, R., 2008. Belgian Source Inventory and International Storage Context. "Prospectives of CCS in Belgium", Brussels, Belgium, 27/06/2008. (oral presentation)

Laenen, B., 2008. Flanders and its Aquifers: Overview and Risk Assessment. "Prospectives of CCS in Belgium", Brussels, Belgium, 27/06/2008. (oral presentation)

Mathieu, Ph. & Bertrand, E., 2008. Capture of CO₂: the Power sector. "Prospectives of CCS in Belgium", Brussels, Belgium, 27/06/2008. (oral presentation)

Piessens, K. & Vandeginste, V., 2008. Between Sink and Source: Transport of CO₂. "Prospectives of CCS in Belgium", Brussels, Belgium, 27/06/2008. (oral presentation)

Piessens, K. & Welkenhuysen, K., 2008. Impact of CCS: Projections from the PSS-simulator. "Prospectives of CCS in Belgium", Brussels, Belgium, 27/06/2008. (oral presentation)

Piessens, K. & Welkenhuysen, K., 2008. Policy Support System for Carbon Capture and Storage: Projecting the implementation of CCS Technology. RBINS Research Day, Brussels, Belgium, 24/11/2008. (poster)

Welkenhuysen, K. & Piessens, K., 2008. CO₂ Capture and Storage. European Union Sustainable Energy Week, Brussels, Belgium, 28/01/2008-01/02/2008. (poster)

Piessens, K., Laenen, B., Mathieu, Ph., Baele, J.-M., Hendriks, Ch., Vandeginste, V., Welkenhuysen, K., Dreesen, R., Bierkens, J., Broothaers, M., Hildenbrand, S., Lagrou, D., Nijs, W., Bertrand, E., De Visser, E. & Brandsma, R., 2009. Final report of the project Policy Support System for Carbon Capture and Storage. Report for Belgian Science Policy Office on contract SD/CP/04a. 271p.

http://www.belspo.be/belspo/ssd/science/FinalReports/Reports/PSS-CCS_FinRep_2008.DEF.pdf

5.2. PSS-CCS phase II and BeNe

5.2.1. Peer reviewed publications

Piessens, K., Baele, J.-M., De Weireld, G., Dreesen R., Duser, M., Laenen, B., Mathieu, P. & Swennen, R. 2010. CO₂ Capture and Storage: Inevitable for a climate friendly Belgium. Royal Belgian Academy Council of Applied Science, 19 p.

5.2.2. Other publications

Dupont, N. & Baele, J.-M., 2009. Contribution of terrigenous rocks of South Belgian coal deposits in geological storage of CO₂: the sandstone case. European Geosciences Union General Assembly, 19-24/04/2011, Vienna, Austria. (poster presentation)

Laenen, B. & Ferket, H., 2009. Ondergrondse CO₂-opslag in België: Wat is er mogelijk en hoe beginnen we er aan? Studiedag Economische Zaken, 24-06-2009. (oral presentation)

Nijs, W., 2008. CCS possibilities for Iron and Steel, simulations with TIMES, New Dehli, ETSAP workshop, January 22, 2010

Novak, M.H., Piessens, K., Welkenhuysen, K., Gusbin, D., Stephenne, A., Cerheyuden, S., Stroobants, W., Hannon, E., Clerfayt, G. & Arnauts, F. 2009. Zero Emission fossil fuel Power plants Country profile – BELGIUM. Report for the ZEP Government Group, 12p. (unpublished)

Piessens, K., 2009. Opslag en afvang van CO₂: haalbaarheid voor België. Veiligheid & Milieu, jaargang 16, 6 extra, p.1-4.

Piessens, K., Baele, J.-M., Laenen, B., Chronopoulou, M., Welkenhuysen, K. & Dusar, M., 2009. Geographic and stratigraphic distribution of CO₂ storage opportunities in Belgium. Third Geologica Belgica International Conference "Challenges for the Planet: Earth Sciences' Perspective", Ghent, Belgium, 14-15/09/2009, p.84-85.

Piessens, K. & Welkenhuysen, K. 2009. Focus on national Carbon Capture and International Storage. Greenhouse Issues, 95, p.9-10.

Piessens, K. & Welkenhuysen K., 2009. Carbon Capture and Storage: Bridge to the Future. Antarctica Day 2009, 15/02/2009. (poster)

Welkenhuysen, K., Piessens, K., Baele, J.-M., Laenen, B. & Dusar, M., 2009. Update of Geological Storage Potential for CO₂ in Belgium. ESF-FWF-LFUI Conference on "CO₂ Geological Storage: Latest Progress", Obergurgl, Austria, 22-27/11/2009. (poster)

Welkenhuysen, K. & Piessens, K., 2009. Policy Support System for Carbon Capture and Storage – Projecting the implementation of CCS technology. 4th Strategic Energy Forum, Brussels, Belgium, 10/12/2009. (poster)

Zero Emissions Fossil Fuel Power Plants – Task Force Technology. 2009. Recommendations for research within EU and national programmes in support of deployment of CCS in Europe beyond 2020. 45p. Limited distribution. <http://www.zeroemissionsplatform.eu/library/publication/95-zep-report-on-long-term-ccs-rad.html>

Laenen, B. 2011. Is CCS also possible in Flanders? Vlaams-Europees verbindings-agentschap (VLEVA) workshop, Brussel, 03/02/2010. (oral presentation)

Broothaers, M., Lagrou, D. & Laenen, B., 2010. Potential reservoirs for underground CO₂ storage in deep aquifers in northern Belgium. Innovation for Sustainable Production (i-SUP 2010), Bruges, Belgium, 18-21/04/2010, p.28-31. (oral presentation)

Ferret, H. & Laenen, B., 2010. Risks and monitoring challenges for CO₂ sequestration in coal. Innovation for Sustainable Production (i-SUP 2010), Bruges, Belgium, 18-21/04/2010, p.22. (oral presentation)

Nijs, W. & Duerinck, J., 2010. CO₂ scenarios up to 2050, the role of CCS in steel production. Innovation for Sustainable Production (i-SUP 2010), Bruges, Belgium, 18-21/04/2010, p.5. (oral presentation)

Piessens, K. & Welkenhuysen, K., 2010. Establishing a priority list for the exploration of CO₂ reservoirs in Belgium. Innovation for Sustainable Production (i-SUP 2010), Bruges, Belgium, 18-21/04/2010, p.23-27. (oral presentation)

Piessens, K., 2010. Van wet naar praktijk: opslag en afvang van CO₂ in België. *Veligheid & Milieu*, jaargang 17, 5, p.1-4.

Piessens, K., 2010. Quantifying the CO₂ storage potential in Belgium: Working with theoretical capacities. *Energy Procedia*, 4, p.4905-4912. (poster at the 10th International Conference on Greenhouse Gas Control Technologies, Amsterdam, The Netherlands, 19-23/09/2010)

Welkenhuysen, K., Piessens, K., Baele, J.-M., Laenen, B. & Dusar, M., 2010. CO₂ storage opportunities in Belgium. *Energy Procedia*, 4, p.4913-4920. (poster at the 10th International Conference on Greenhouse Gas Control Technologies, Amsterdam, The Netherlands, 19-23/09/2010)

Welkenhuysen, K. & Piessens, K., 2011. Semi-optimised pipeline routing for CO₂ Capture and Storage. Pipeline Technology Conference 2011, Hannover, Germany, 4-5/04/2011. (oral presentation)

Baele, J.-M., 2011. Options for storing CO₂ in the Walloon Region. "Treating uncertainty in energy systems and the role CCS can play", Brussels, Belgium, 26/05/2011. (oral presentation)

Cochez, E., 2011. CO₂ Capturing Technologies. "Treating uncertainty in energy systems and the role CCS can play", Brussels, Belgium, 26/05/2011. (oral presentation)

Duerinck, J., 2011. Price elasticities in bottom-up and top-down models. "Treating uncertainty in energy systems and the role CCS can play", Brussels, Belgium, 26/05/2011. (oral presentation)

Ferket, H., 2011. Risks and monitoring challenges for CO₂-sequestration in coal. "Treating uncertainty in energy systems and the role CCS can play", Brussels, Belgium, 26/05/2011. (oral presentation)

Nijs, W. & Van Regemorter, D., 2011. A roadmap to a low carbon 2050 for Belgium. "Treating uncertainty in energy systems and the role CCS can play", Brussels, Belgium, 26/05/2011. (oral presentation)

Piessens, K., 2011. The Role of CCS. "Treating uncertainty in energy systems and the role CCS can play", Brussels, Belgium, 26/05/2011. (oral presentation)

Van Regemorter, D., Van Wortswinkel, L., Benoot, W. & Nijs, W., 2011. The Belgian and European TIMES model. "Treating uncertainty in energy systems and the role CCS can play", Brussels, Belgium, 26/05/2011. (oral presentation)

Welkenhuysen, K., 2011. Modelling the CCS chain. "Treating uncertainty in energy systems and the role CCS can play", Brussels, Belgium, 26/05/2011. (oral presentation)

Welkenhuysen, K., 2011. Combining geological, social and techno-economic parameters to successfully assess CO₂ reservoirs. Exploring Power Plant Emissions Reductions through cutting edge Technologies and Strategies conference (ExPPERTS EU), London, 27-28/09/2011. (oral presentation)

Emmanuel, R., 2011. Gaz de mine: une future ressource pour la Wallonie? Trends & tendances.be, 28/09/2011.

Broothaers, M., Baele, J.-M. & Piessens, K., in prep. Evaluation of potential sinks and estimation of total capacity for underground CO₂ sequestration in Belgium.

6. ACKNOWLEDGEMENTS

A special word of gratitude goes to the University of Utrecht and Andrea Ramírez and Machteld van den Broek in particular, for kindly providing storage and scenario data for the Netherlands and for establishing the contacts with the CATO-2 project. Tobias Wendt from E.ON and Marc Lanckzweirt from Antea Group are acknowledged for their help with the pipeline callibrations. The authors also wish to thank Peter Todd for providing the portfolio module in VBA, Mads Haahr from random.org for providing the random data and Peter John Acklam for the inverse normal distribution (<http://home.online.no/~pjacklam/notes/invnorm/>).

7. REFERENCES

3Siemens Fuel Gasification Technology GmbH, Halsbrücker Str. 34, 09599 Freiberg, Germany

Addis, M.A., 1997. Reservoir depletion and its effect on wellbore stability evaluation. *International Journal of Rock Mechanics and Mining Sciences*, 34, p.423.

Appelman, W. ; Rentz, O. ; Oertel, D. ; Berdowski, J. ; Jonker, J. ; Bloos, J. P. ; Richardson, S ; Passant, N. ; Pittman, S. ; Woodfield, M. ; van der Most, P., 2009. Chemical industry, ammonia production, EMEP/EEA emission inventory guidebook 2009

Arts, R., Chadwick, A. & Eiken, O., 2004. Recent Time-Lapse Seismic Data Show no Indication of Leakage at the Sleipner CO₂ Injection Site. In: Rubin, E.S., Keith, D.W. & Gilboy, C.F. (Eds.), *Proceedings of the 7th International Conference on Greenhouse Gas Control Technologies (GHGT-7)*, Vancouver, Canada, p.653-662.

Bachu, S., Bonijoly, D., Bradshaw, J., Burruss, R., Holloway, S., Christensen, N.P. & Mathiassen, O.M., 2007. CO₂ storage capacity estimation: Methodology and gaps. *International Journal of Greenhouse Gas Control*, 1(4), p.430-443.

Barker, D. J., Turner, S. A., Napier-Moore, P. A., Clark, M., & Davison, J. E., 2009. CO₂ Capture in the Cement Industry. *Energy Procedia*, 1(1), p. 87-94.

Bateson, L., Vellico, M., Beaubien, S.E., Pearce, J.M., Annunziatellis, A, Ciotoli, G., Coren, F, Lombardi, S. & Marsh, S., 2008. The application of remote sensing techniques to monitor CO₂ storage sites for surface leakage: method development and testing at Latera (Italy) where naturally produced CO₂ is leaking to the atmosphere. *Proceedings of the International Geoscience and remote sensing symposium (IJGGC)*, Boston, Massachusetts, USA, 2/3, p.388-400.

Bense, V., Van Balen, R.T. & De Vries, J., 2003. The impact of faults on hydrogeological conditions in the southeastern part of the Netherlands. *Netherlands Journal of Geosciences*, 82, p.41-52.

Bense, V. & Van Balen, R.T., 2004. The effect of fault relay and clay smearing on groundwater flow patterns in the Lower Rhine Embayment. *Basin Research*, 16, p.397-411.

Benson, S.M., Hoversten, M., Gasperikova, E. & Haines, M., 2005. Monitoring protocols and life-cycle costs for geological storage of carbon dioxide. In: Rubin, E.S., Keith, D.W. & Gilboy, C.F. (Eds.), *Proceedings of the 7th International Conference on Greenhouse Gas Control Technologies (GHGT-7)*, Vancouver, Canada, 2, p.1259-1265.

BERR, 2004. Review of environmental issues of underground coal gasification. Annex E: Permeability of coal seams, coal measures strata and faults. Report N° COAL R272, DTI / pub, URN 04/1880. Department of Business Enterprise & Regulatory Reform (BERR), UK.

Bertier, P., Swennen, R., Laenen, B., Lagrou, D. & Dreesen, R., 2005. Experimental identification of CO₂-water-rock interactions caused by sequestration of CO₂ in Westphalien and Buntsandstein sandstones of the Campine Basin (NE-Belgium). *Journal of Geochemical Exploration*, 89, p.10-14.

Bouckaert, J., Fock, W. & Vandenberghe, N., 1988. First results of the Belgian geotraverse 1986 (BELCORP). *Annales du la Société géologique de Belgique*, 111, p.279-290.

BREF, 2010. *Draft Reference Document on Best Available Techniques for Mineral Oil and Gas Refineries*, Institute for Prospective Technological Studies, Spain (Seville), European Commission, Directorate-General JRC Joint Research Centre.

Brekke, K.A. & Schieldrop, B., 2000. Investment in Flexible Technologies under Uncertainty. In: Brennan, M.J. & Trigeorgis (Eds.), *Project Flexibility, Agency, and Competition: New developments in the Theory and Application of Real Options*. Oxford University Press, New York, 357p.

Buchwalder J., Mernitz J., Harp G., , Hensmann M., Reuther C., Schingnitz M. (2004), *Development of injection of reduction gas into the blast furnace shaft*, Arcelor, Eisenhüttenstadt Germany and Betriebsforschungsinstitut VDEh-Institut für angewandte Forschung GmbH, Düsseldorf, Germany

Busch, A., Alles, S., Gensterblum, Y., Prinz, D., Dewhurst, D.N., Raven, M.D., Stanjek, H. & Krooss, B.M., 2008. Carbon dioxide storage potential of shales. *International Journal of Greenhouse Gas Control*, 2, p.297-308.

Celia, M.A. & Bachu, S., 2003. Geological storage of CO₂: is leakage unavoidable and unacceptable? In: Gale, J. & Kaya, Y. (Eds.), *Proceedings of the 6th International Conference on Greenhouse Gas Control Technologies*, Kyoto, Japan, 1, p.477-482.

Cembureau, 1999. A contribution from the European Cement Industry to the exchange of information and preparation of the IPPC BAT REFERENCE Document for the cement industry.

Clayton, J. L., Leventhal, J. S., Rice, D. D., Pashin, J. C., Mosher, B. & Czepiel, P., 1994. Atmospheric methane flux from coals: preliminary investigation of coal mines and geologic structures in the Black Warrior basin, Alabama. In: Howell, D. G. (Ed.), *The Future of Energy Gases: U.S. Geological Survey Professional Paper, 1570*, p.471-492.

Cloethingh, S., Cornu, T., Ziegler, P.A. & Beekman, F., 2006. Neotectonics and continental topography of the Northern Alpine Foreland. *Earth Science Reviews*, 74, p.127-196.

COPESEP, 1965. Jeumont-Marpent n°1, rapport de fin de sondage. Compagnie des Pétroles du Sud-est Parisien, 36p.

CRF tables UNFCCC, 2010. *National Inventory Submissions, Common Reporting Format, BEL-2010-2008-v1.4*, United Nations Framework Convention on Climate Change (UNFCCC)

De Beer, J., 2000. *Potential for industrial energy-efficiency improvement in the long term*, Springer, 31-mei-2000 - 254 pagina's

Daley, T. M, Myer, L., Hoversten, G. M. & Peterson, J. E., 2005. Borehole Seismic Monitoring of Injected CO₂ at the Frio Site. American Geophysical Union, 2005 fall meeting.

Davison, J., EAllam, R., White, V., Ivens, N., Simmonds, M., 2005. *Chapter 26, The oxyfuel baseline: Revamping heaters and boilers to oxyfiring by cryogenic air separation and flue gas recycle*, In *Carbon Dioxide Capture for Storage in Deep Geologic Formations – Results from the CO₂ capture project: Volume one: Capture and Separation of Carbon Dioxide from Combustion. Volume 1*, ed. D.C. Thomas, Elsevier, pp. 451-475.

Dejonghe, L., Delmer, A. & Hance, L., 1992. Les enseignements d'une campagne sismique conduite en Belgique, dans le Hainaut, selon l'axe Erquelines – Saint-Ghislain. *Annales de la Société Géologique Du Nord*. 1(2), 135-142.

Delmer, A. & Van Wichelen, P., 1980. Répertoire des puits naturels connus en terrain houiller du Hainaut. Geological Survey of Belgium Professional Paper, 172, 79p.

Delmer, A., Leclerq, V., Marlière, R. & Robaszynski, F., 1982. La géothermie en Hainaut et le sondage de Ghlin. *Annales de la Société Géologique du Nord*, 101, p.189-206.

Delmer, A., 2004. Tectonique du front varisque en Hainaut et dans le Namurois. Mémoires of the Geological Survey of Belgium, 50, 61 p.

Devleeschouwer, X., Declercq, P.-Y., Duser, M. & Debien, A., 2007. Contrasting ground movements revealed by radar interferometry over abandoned coal mines (Campine, Belgium). Abstract book of the Fringe 2007 Workshop, ESRIN-ESA, Frascati, Italy, p.123.

Devleeschouwer X., Declercq P.-Y., Flamion B., Brixko J., Timmermans A. & Vanneste J., 2008. Uplift revealed by radar interferometry around Liège (Belgium): a relation with rising mining groundwater. Abstract book of the Post-Mining GISOS 2008, Nancy, France.

DFG Energy, 2003. *Ammonia Cracking for Clean Electric Power Technology, WP 7 : Ammonia supply evaluation*, München (Germany)

Directive 2009/31/EC. On the geological storage of carbon dioxide and amending Council Directive 85/337/EEC, European Parliament and Council Directives 2000/60/EC, 2001/80/EC, 2004/35/EC, 2006/12/EC, 2008/1/EC and Regulation (EC) No 1013/2006.

<http://eur-lex.europa.eu/LexUriServ/LexUriServ.do?uri=OJ:L:2009:140:0114:0135:EN:PDF>

Dreesen, R.J.M., 1993. Seam thickness and geological hazards forecasting in deep coal mining: a feasibility study from the Campine collieries (N-Belgium). Bulletin de la Société Belge de Géologie, 101, p.209-254.

Dreesen, R., Bossiroy, D., Duser, M., Flores, R.M. & Verkaeren, P., 1995. Overview on the influence of syn-sedimentary tectonics and palaeo-fluvial systems on coal seam and sand body characteristics in the Westphalian C strata, Campine Basin, Belgium. In: Whateley, M.K.G. & Spiers, D.A. (Eds.), *European Coal Geology*, Geological Society Special Publication, 82, p.215-232.

Duerinck, J., Proost, S., Nijs, W., Van Regemorter, D., 2007. *MARKAL/TIMES, a model to support greenhouse gas reduction policies : final report*, Brussels (Belgium)

Duerinck J., Laes E., Michielsen H., Morbee J., Nijs W., Van Regemorter D., Van Wortswinkel L., & Vercammen D., submitted. Treating uncertainty and risk in energy systems with Markal/Times. Final Report. Brussels : Belgian Science Policy, 102 p. (Research Programme Science for a Sustainable Development)

Dupont, N. & Baele, J.-M., 2009. Contribution of terrigenous rocks of South Belgian coal deposits in geological storage of CO₂ : the sandstones case. EGU General Assembly , 19-24 April, Vienna, Austria.

EC, 2011a. Implementation of Directive 2009/31/EC on the Geological Storage of Carbon Dioxide. Guidance Document 1: CO₂ Storage Life Cycle Risk Management Framework. ISBN-13978-92-79-19833-5.

http://ec.europa.eu/clima/policies/lowcarbon/ccs/implementation/docs/gd1_en.pdf

EC, 2011b. Implementation of Directive 2009/31/EC on the Geological Storage of Carbon Dioxide. Guidance Document 2: Characterisation of the Storage Complex, CO₂ Stream Composition, Monitoring and Corrective Measures. ISBN-13 978-92-79-19834-2.

http://ec.europa.eu/clima/policies/lowcarbon/ccs/implementation/docs/gd2_en.pdf

EC, 2011c. Implementation of Directive 2009/31/EC on the Geological Storage of Carbon Dioxide. Guidance Document 3: Criteria for Transfer of Responsibility to the Competent Authority. ISBN-13 978-92-79-18472-7.

http://ec.europa.eu/clima/policies/lowcarbon/ccs/implementation/docs/gd3_en.pdf

EFMA, 2000. *Booklet No. 1 of 8: Production of Ammonia, Best Available Techniques for Pollution Prevention and Control in the European Fertilizer Industry*, European Fertilizer Manufacturers' Association, Brussels (Belgium)

Eggermont, L. 2010. Réinterprétation d'une section sismique dans le Bassin de Mons. Unpublished Master thesis, Faculté Polytechnique de Mons, 57p.

ENBW, consulted on 2009. www.enbw.com

Gasperikova, E. & Hoversten, G.M., 2008. Modeling the resolution of inexpensive, novel non-seismic geophysical monitoring tools to monitor CO₂ injection into Coal Beds. Appendix C to the Final Report of the project "Stored CO₂ and Methane Leakage Risk Assessment and Monitoring Tool Development: CO₂ Capture Project Phase 2 (CCP2)".

Gaussens, P., 1986. Manuel pour le transport et la distribution du gaz, tome 13: Stockages souterrains de gaz. Association technique de l'industrie du gaz en France, 333p.

Gentzis, T., Goodarzi, F., Cheung, F.K. & Laggoun-Défarge, F., 2008. Coalbed methane producibility from the Mannville coals in Alberta, Canada: a comparison of two areas. *International Journal of Coal Geology*, 74 (3-4), p.237-249.

Gibson-Poole, C.M., Daniel, R.F., Ennis-King, J., Rigg, A.J., Svendsen, L. & Watson, M.N., 2006. Using stratigraphic heterogeneity to maximize the efficiency of CO₂ geological storage. AAPG International Conference and Exhibition 2006, Perth, Western Australia. <http://www.co2crc.com.au/publications/>

Gielen, D., 2002. *CO₂ removal in the iron and steel industry*; 1 National Institute for Environmental Studies, 16-2 Onogawa Tsukuba, Ibaraki 305-0053, Japan May 2002

Groessens, E., Conil, R., & Hennebert, M., 1979. Le Dinantien au sondage de Saint-Ghislain, stratigraphie et paléontologie. Mémoires of the Geological Survey of Belgium, 22, 137p.

Groshong, R. H., Jr., Cox, M. H., Pashin, J. C. & McIntyre, M. R., 2003. Relationship between gas and water production and structure in southeastern Deerlick Creek coalbed methane field, Black Warrior basin, Alabama. Proceedings of the 2003 International Coalbed Methane Symposium, Tuscaloosa, Alabama, U.S.A. ,0306, 12p.

Gunter, W.D., Mavor, M.J. & Robinson, J.R., 2005. CO₂ storage and enhanced methane production: field testing at Fenn-Big Valley, Alberta, Canada, with applications. In: Rubin, E.S., Keith, D.W. & Gilboy, C.F. (Eds.), Proceedings of the 7th International Conference on Greenhouse Gas Technologies (GHGT-7), Vancouver, Canada, 1, p.413-422.

Harris, J.M., Kovscek, A.R., Orr, F.M., Zoback, M.D. and investigators, 2007. Geological storage of CO₂. GCEP 2007 Technical Report 2.4.6, 98p.

He, Xuezhong, Arvid, Jon, Lie, Sheridan, Edel, Hägg, May-Britt, 2009. *CO₂ Capture by Hollow Fibre Carbon Membranes: Experiments and Process Simulations*; Department of Chemical Engineering, Norwegian University of Science and Technology, N-7491 Trondheim, Norway

Hellevang, H., 2006. Interactions between CO₂, saline water and minerals during geological storage of CO₂. PhD thesis of the University of Bergen, Norway. https://bora.uib.no/bitstream/1956/1551/28/MainThesis_Hellevang.pdf

Hendriks, C., de Visser, E., Jansen, D., Carbob, M., Jan Ruijg, G., Davisonc, J., 2009. *Capture of CO₂ from Medium-scale Emission Sources*, Energy Procedia, pp. 1497–1504.

Hillis, R. R., 2001, Coupled changes in pore pressure and stress in oil fields and sedimentary basins. *Petroleum Geoscience*, 7, p.419–425.

IEA – EET – ETPD, 2004. *Hydrogen supply cost explained. Background information for the WEIO 2003 assumptions*

IEA, 2005. *Task 16: Hydrogen from carbon containing materials, subtask C, Small-scale Reformers for Stationary Hydrogen Production with Minimum CO₂- emissions*, Hydrogen Implementing Agreement (HIA), International Energy Agency

IEA and Vattenfall Europe Generation, 2005. *International oxy-combustion network for CO₂ capture*, workshop in Cottbus, Germany, November 2005.

IEA, 2006. *Hydrogen production and storage ,R&D priorities and gaps*, Hydrogen Implementing Agreement (HIA), Organisation for Economic Co-operation and Development, International Energy Agency, Paris (France)

IEA GHG, 2007. *CO₂ capture from medium scale combustion installations*, International Energy Agency, Greenhouse Gas R&D Programme, Report Number 2007/7

IEA, 2008a. *Energy Technology Analysis, CO₂ capture and storage, a key carbon abatement option*, International Energy Agency, Paris (France)

IEA, 2008b. *Energy Technology Perspectives 2008, Scenarios and strategies to 2050*, International Energy Agency, Paris (France)

IEA, 2009. *Energy Technology Perspectives*

IPCC, 2005. *IPCC Special report on Carbon dioxide capture and storage*, Prepared by Working Group III of the Intergovernmental Panel on Climate Change [Metz, B., O. Davidson, H. C. de Coninck, M. Loos, and L. A. Meyer (eds.)]. Cambridge University Press, Cambridge, United Kingdom and New York, NY, USA, 442 pp.

IPIECA, 2007. *The oil and gas industry and climate change*, IPEACE June 2007, http://www.ipieca.org/activities/climate_change/downloads/publications/siaf_climatechange.pdf

Jacobson Jr., J., Silver, E.A. & Pickles, W.L., 2007. Direct CO₂ and CH₄ area wide anomalous gas detection using Remote Sensing. CCP2 Storage Monitoring and Verification Conference, Pittsburg, Pennsylvania.

Jin, G. & Pashin, J.C., 2008. Discrete fracture network models of the SECARB carbon sequestration test site, Deerlick Creek Field, Black Warrior Basin, Alabama. 2008 International Coalbed & Shale Gas Symposium, 0821, 8p.

Kehlhofer, R., Bachmann, R., Nielson, H., Warner, J. , 1999. *Combined-Cycle Gas & Steam Turbine Power Plants*, 2nd Edition, 1999.

Kharaka, Y.K., Cole, D.R., Hovorka, S.D., Gunter, W.D., Kanauss, K.G., Freifeild, B.M., 2006. Gas-water-rock interactions in Frio Formation following CO₂ injection: implications for the storage of greenhouse gases in sedimentary basins. *Geology*, 34, p.577–580.

Kieke, D., 2008. Stored CO₂ and Methane Leakage Risk Assessment and Monitoring Tool Development: CO₂ Capture Project Phase 2 (CCP2), Final Report presented to the DOE, DE-FC26-05NT42211.

Kuby, M.J., Middleton, R.S. & Bielicki, M., 2011. Analysis of cost savings from networking pipelines in CCS infrastructure systems. *Energy Procedia*, 4, p.2808-2815.

Lacquement, F. 1997. Retraitement d'un profil sismique dans le Nord de la France : M146. Université des Sciences et Technologies de Lille I, Compagnie Générale de Géophysique, rapport interne, 49p.

Laenen, B., Van Tongeren, P., Dreesen, R. & Duser, M., 2004. Carbon dioxide sequestration in the Campine Basin and the adjacent Roer Valley Graben (North Belgium): an inventory. In: Baines, S.J. and Worden, R.H. (Eds.), 2004. Geological storage of carbon dioxide. Geological Society of London Special Publication, 233, p.193-210.

Lagrou, D., 2002. Ondergrondse opslag van CO₂: ontwerp voor brochure. In opdracht van ANRE, VITO-rapport 2002/ETE/R/004.

Langenaeker, V., 2000. The Campine Basin: stratigraphy, structural geology, coalification and hydrocarbon potential for the Devonian to Jurassic. *Aardkundige Mededelingen*, 10, 142p. & 4 maps.

Leclerq, V., 1980. Le sondage de Douvrain. Professional Paper of the Geological Survey of Belgium, 170, 51p.

Lüth, S., Giese, R., Bergmann, P., Götz, J., Ivanova, A., Juhlin, C., Juhojuntti, N., Kashubin, A. & Cosma, C., 2010. Seismic monitoring of CO₂-injection at Ketzin: time-lapse observations at different scales. Proceedings of the Geodarmstadt 2010 Conference, Darmstadt, SDGG 68, p.365.

Markowitz, H.M., 1987. Mean-Variance Analysis in Portfolio Choice and Capital Markets. Wiley, Milton Keynes, 379p.

Martens, A., Germain, A., Proost, S., Palmers, G., 2006. *Part 1: Sustainable consumption and production patterns, Development of tools to evaluate the potential of sustainable hydrogen in Belgium*, Scientific Support Plan For a Sustainable Development Policy (SPSD II), Brussels (Belgium), Belgian Science Policy

Mavor, M.J., Gunter, W.D., Robinson, J.R., Law, D.H-S. & Gale, J., 2002. Testing for CO₂ sequestration and enhanced methane production from coal. SPE paper 75680, SPE Gas Technology Symposium, Calgary, 14p.

Mazumder, S. & Wolf, K.H., 2008. Differential swelling and permeability change of coal in response to CO₂ injection for ECBM. *International Journal of Coal Geology*, 74, p.123-138.

Melien, T., 2005. *Chapter 3, Economic and Cost Analysis for CO₂ Capture Costs in The CO₂ Capture Project Scenarios*, In *Carbon Dioxide Capture for Storage in Deep Geologic Formations – Results from the CO₂ capture project: Volume one: Capture and Separation of Carbon Dioxide from Combustion*. Volume 1, ed. D.C. Thomas, Elsevier, pp. 47-87.

Mello, L.F., Pimentaa R., Mourea G., Pravia O., Gearhartb L., Milios P., Melienc T., 2008. *A technical and economical evaluation of CO₂ capture from FCC units*, Energy Procedia, Elsevier.

Mello, L. F., Moure, G.T., Pravia, O.R.C., Gearhart, L., Milios, P. B., 2009. *Chapter 3: Oxy-Combustion for CO₂ Capture from Fluid Catalytic Crackers (FCC)*, In *Carbon Dioxide Capture for Storage in Deep Geologic Formations – Results from the CO₂ capture project: Volume three: Advances in CO₂ Capture and Storage Technology Results (2004-2009)*. Volume 3, ed. L.I. Eide, CPLPress.

Mito, S., Xue, Z. & Ohsumi, T., 2008. Case study of geochemical reactions at the Nagaoka CO₂ injection site, Japan. *International Journal of Greenhouse Gas Control* 2, p.309-318.

Moel, A. & Tufano, P., 2000. Bidding for the Antamina Mine: Valuation and Incentives in a Real Options Context. In: Brennan, M.J. & Trigeorgis (Eds.), *Project Flexibility, Agency, and Competition: New developments in the Theory and Application of Real Options*. Oxford University Press, New York, 357p.

Myer, L.R., Hoversten, G.M. & Gasperikova, E., 2002. Sensitivity and Cost of Monitoring Geologic Sequestration Using Geophysics. 6th International Conference on Greenhouse Gas Control Technologies (GHGT-6), Kyoto, Japan.

Myer, L.R., 2003. Geomechanical risks in coal bed carbon dioxide sequestration. LBNL, Berkeley, CA LBNL-53250.

Nelson, C.R., Evans, J.M., Sorensen, J.A., Steadman, E.N. & Harju, J.A., 2005. Factors affecting the potential for CO₂ leakage from geological sinks. NETL Topical Report from the PCO₂R partnership.

<http://www.undeerc.org/pcor/newsandpubs/pdf/FactorsAffectingPotential.pdf>

NETL, 2009. Best practices for monitoring, verification and accounting of CO₂ stored in deep geological formations. National Energy Technology Laboratory (NETL) of the US Department of Energy (DOE), DOE/NETL-311/081508.

Nijs, W., Simbolotti, G., Tosato, G.C., Van Wortswinkel, L., 2009. IEA ETSAP - Technology Brief I02 - May 2010 - www.etsap.org

Nijs, W. & Vanregemorter, D., 2007. Markal/Times, a model to support greenhouse gas reduction policies, VITO and CES KULeuven.

http://www.belspo.be/belspo/home/publ/pub_ostc/CPen/rCP22_en.pdf

Nordbotten, J.M., Celia, M.A. & Bachu, S., 2004. Analytical solutions for leakage rates through abandoned wells. *Water Resources Research* 40, W04204, 10p., doi:10.1029/2003WR002997.

NRC, 2004. *The Hydrogen Economy: Opportunities, Costs, Barriers, and R&D Needs*, Prepared by the Committee on Alternatives and Strategies for Future Hydrogen Production and Use, Board on Energy and Environmental Systems of the National Research Council, The National Academies Press, Washington, DC.

Nygaard, R. & Lavoie, R., 2009. Project cost estimate Wabamun area CO₂ sequestration project (WASP), University of Calgary and Energy Environmental Systems Group (EES) – Institute for Sustainable Energy, Environment and Economy (ISEEE), 19p.

Olroyd, G.C., McPherson, M.J. & Morris, L.H., 1971. Investigations into sudden abnormal emissions for firedamp from the floor strata of the Silkstone seam at Cortonwood Colliery, *The Mining Engineer*, 130, p.577-593.

Oudinot, A., Schepers, K. & Reeves, S., 2007. "Gas Injection and Breakthrough Trends as Observed in ECBM Sequestration Pilot Projects and Field Demonstrations", 2007 International Coalbed Methane Symposium, 0714, Tuscaloosa, AL.

Pacala S. & Socolow R. 2004. Stabilization wedges: solving the climate problem for the next 50 years with current technologies. *Sciences* 305, p. 968-972.

Pagnier, H., van Bergen, F. & Krzystalik, P., 2006. Reduction of CO₂ Emissions by means of CO₂ Storage in Coal Seams in the Silesian Coal Basin of Poland, Final Report.

Pashin, J. C., Carroll, R. E., Groshong, R. H., Jr., Raymond, D. E., McIntyre, M. & Payton, W. J., 2003. Geologic screening criteria for sequestration of CO₂ in coal: quantifying potential of the Black Warrior coalbed methane fairway, Alabama. Annual Technical Progress Report, U.S. Department of Energy, National Technology Laboratory, contract DEFC-00NT40927, 190p.

Pashin, J. C., Carroll, R. E., Groshong, R. H., Jr., Raymond, D. E., McIntyre, M. & Payton, W. J., 2004. Geologic screening criteria for sequestration of CO₂ in coal: quantifying potential of the Black Warrior coalbed methane fairway, Alabama. Final Report, U.S. Department of Energy, National Energy Technology Laboratory, contract DE-FC26-00NT40927, 276p.

Piessens, K. & Dusar, M., 2004. Feasibility of CO₂ sequestration in abandoned coal mines in Belgium. *Geologica Belgica*, 7 (3-4), p.165-180.

Piessens, K., 2009. Carbon Capture and Storage in Belgium: significance of geological constraints. Third International Conference *Geologica Belgica 2009 "Challenges for the Planet: Earth Sciences' Perspective"*, Ghent, Belgium, p.42-43.

Piessens, K., Laenen, B., Mathieu, Ph., Baele, J.-M., Hendriks, Ch., Vandeginste, V., Welkenhuysen, K., Dreesen, R., Bierkens, J., Broothaers, M., Hildenbrand, S., Lagrou, D., Nijs, W., Bertrand, E., De Visser, E. & Brandsma, R., 2009. Final report of the project Policy Support System for Carbon Capture and Storage. Report for Belgian Science Policy Office on contract SD/CP/04a. 271p.

http://www.belspo.be/belspo/ssd/science/FinalReports/Reports/PSS-CCS_FinRep_2008.DEF.pdf

Piessens, K., Baele, J.-M., De Weireld, G., Dreesen, R., Dusar, M., Laenen, B., Mathieu, P. & Swennen, R., 2010. CO₂ Capture and Storage: inevitable for a climate friendly Belgium. Royal Belgian Academy Council of Applied Sciences, 19p.

Piessens, K. & Welkenhuysen, K., 2010. Establishing a preliminary priority list for the exploration of CO₂ reservoirs in Belgium. *Proceedings of Innovation for Sustainable Production 2010 (i-SUP 2010)*, session Carbon Capture and Storage. Bruges, Belgium, p.23-27.

Piessens, K., 2011. Quantifying the CO₂ storage potential in Belgium: Working with theoretical capacities. *Energy Procedia*, 4, p.4905-4912.

Piessens, K., in press. The conceptual model for an abandoned coal mine reservoir. In: International workshop on CO₂ storage in Carboniferous Formations and Abandoned Coal Mines. Beijing, China, p. 15, Balkema publishers.

Pitman, J.K., Pashin, J.C., Hatch, J. R. & Goldhaber, M.B., 2003. Origin of minerals in joint and cleat systems of the Pottsville Formation, Black Warrior basin, Alabama: implications for coalbed methane generation and production. American Association of Petroleum Geologists Bulletin, 87, p.713-731.

Pone, J.D.N., Halleck, P.M. & Mathews, J.P., 2009. Methane and Carbon Dioxide Sorption and Transport Rates in Coal at In-situ Conditions. Energy Procedia 1, p.3121-3128.

Powergen Europe, 2009. *CO₂ CAPTURE BY ANTISUBLIMATION: From the laboratory to the power plant*; Denis Clodic, Mourad Younes, Rima El Hitti, François Giger - Mines Paris-Tech, EDF, France

Pöttgens, J.J. & Van Herk, J.M., 2000. Ground movements over abandoned coalmines in relation to rising mine waters in Limburg (The Netherlands). French Mining Congress, Paris, 9p.

Quan, Y. & Harris, J.M., 2006. Integration of active and passive seismic data for monitoring CO₂ storage in coal. GCEP Research Symposium, Stanford University, U.S.A.

Rafiqul, I., Weber, C., Lehmann, B., Voss, A., 2005. *Energy efficiency improvements in ammonia production—perspectives and uncertainties*, Energy 30 (2005), Elsevier, pp. 2487–2504

Reeves, S.R. & Schoeling, L., 2000. Geological Sequestration of CO₂ in Coalseams: Reservoir Mechanisms Field Performance and Economics. In: Williams, D., Durie, B., McMullan, P., Paulson, C. & Smith, A. (Eds.), Proceedings of the International Conference on Greenhouse Gas Control Technologies (GHGT-5), Cairns, Australia.

Reeves, S.R., Taillefert, A. Pekot, L. & Clarkson, C., 2003. The Allison Unit CO₂ – ECBM Pilot: A Reservoir Modeling Study, Topical Report, DOE Contract No. DE-FC26-00NT40924.

Reeves, S.R. & Oudinot, A., 2005. The Allison Unit CO₂-ECBM Pilot: A Reservoir and Economic Analysis. Proceedings of the International Coalbed Methane Symposium, Tuscaloosa, AL, U.S.A.

Reeves, S.R., 2005. The Coal-Seq Project: Key Results from Field, Laboratory, and Modeling Studies. In: Wilson, M., Morris, T., Gale, J. and Thambimuthu, K. (Eds.): Proceedings of 7th International Conference on Greenhouse Gas Control Technologies, 2, p.399-403.

Reeves, S.R., Harpalani, S. & Gasem, K., 2008. Results, status and future activities of the Coal-Seq consortium. 7th Annual Conference on Carbon Capture & Sequestration, Pittsburgh, PA, Paper 544.

Reumont, M., 2011. Contribution des roches terrigènes du Carbonifère continental du Hainaut au stockage géologique du CO₂ – cas des pélites. Unpublished Master thesis, Faculté Polytechnique de Mons, 55p.

Ripepi, N.S., 2009. Carbon Dioxide Storage in Coal Seams with Enhanced Coalbed Methane Recovery: Geologic Evaluation, Capacity Assessment and Field Validation of the Central Appalachian Basin. PhD thesis of Virginia Polytechnic Institute & State University, 247p.

RISC, 2009. CO₂ Injection Well Cost Estimation, Report prepared for the Carbon Storage Taskforce, 17p.

Rosenqvist, T., 2004. *Principles of Extractive Metallurgy*, Tapir Academic Press, 2nd edition

Rutqvist J. & Tsang, C.-F., 2003. TOUGH-FLAC: A numerical simulator for analysis of coupled thermal hydrologic mechanical processes in fractured and porous geological media under multiphase flow conditions. TOUGH Symposium, Berkeley, CA.

Schmöle P., Bodo Lungen H., 2004. *Hot metal production in the blast furnace from an ecological point of view*, Steel Institute VDEh, Düsseldorf, Germany, Presented at the 2nd International Meeting on Ironmaking and 1st International Symposium on Iron Ore, Vitoria, Brazil, 12 to 15 September, 2004

Schulz, H.M., Mulders, F.M., Geel, C., Carlsen, I.M. & Mjaaland, S., 2005. Review existing preventive and corrective action technologies regarding leakage through rock and faults. CASTOR technical report no. WP3.5.2, BGR Hannover, Germany.

Shi, J.-Q., Durucan, S. & Fujioka, M., 2008. A reservoir simulation study of CO₂ injection and N₂ flooding at the Ishikari coalfield CO₂ storage pilot project, Japan. International Journal of Greenhouse Gas Control, 2, p.47-57.

Simbeck, D.R., 2005. *Hydrogen Costs with CO₂ Capture*. M. Wilson, T. Morris, J. Gale and K. Thambimuthu (eds.): Proceedings of 7th International Conference on Greenhouse Gas Control Technologies. Volume II: Papers, Posters and Panel Discussion, Elsevier Science, Oxford UK, 1059-1066.

Smith, L.K. & Reeves, S.R., 2002. Scoping Equilibrium Geochemical Modeling to Evaluate the Potential for Precipitate Formation when Sequestering CO₂ in San Juan Basin Coals. Topical Report, DOE Contract No. DE-FC26-00NT40924.

Socolow R. 2011. Wedges reaffirmed. Bulletin of the Atomic Scientists. <http://www.thebulletin.org/web-edition/features/wedges-reaffirmed>

Streit, J.E. & Hillis, R.R., 2004. Estimating fault stability and sustainable fluid pressures for underground storage of CO₂ in porous rocks. *Energy*, 29, p.1445-1456.

Stuffken, J., 1957. De mijngasafgifte van koollagen. PhD thesis of the Delft Technical University, faculty Mijnbouw. Delft, the Netherlands.

Switzer, L., Rosen, L., Thompson, D., Sirman, J., Howard, H., Bool, L., 2005. *Chapter 32, Cost and Feasibility Study on the Praxair Advanced Boiler for the CO₂ Capture Project's Refinery Scenario*, In Carbon Dioxide Capture for Storage in Deep Geologic Formations – Results from the CO₂ capture project: Volume one: Capture and Separation of Carbon Dioxide from Combustion. Volume 1, ed. D.C. Thomas, Anon, Elsevier, pp. 561-579.

Tingay, M. R. P., Hillis, R. R., Morley, C. K., King, R. C., Swarbrick, R. E. & Damit, A. R., 2009. Present-day stress and neotectonics of Brunei: Implications for petroleum exploration and production. *AAPG Bulletin*, 93(1), p.75–100.

Van Bergen, F., Winthaegen, P., Pagnier, H., A., Krzystolik, P., Jura, B., Skiba, J., & van Wageningen, N., 2008. Monitoring of CO₂ in the enhanced coalbed methane pilot site in Kaniów (Poland). *Energy Procedia*, 1, p.3407-3414.

Van Bergen, F., 2009. Effect of coal matrix swelling on enhanced coalbed methane production – a field and laboratory study. PhD dissertation from the university of Utrecht (the Netherlands); *Geologica Ultraiectina, Mededelingen van de Faculteit Geowetenschappen Universiteit Utrecht*, 315, 196p.

Van Bergen, F., Krzystolik, P., van Wageningen, N., Pagnier, H., Jura, B., Skiba, J., Winthaegen, P. and Kobiela, Z., 2009. Production of gas from coal seams in the Upper Silesian coal basin in Poland in the post-injection period of an ECBM pilot site. *International Journal of Coal Geology*, 77, p.175-187.

Valenti, G., Bonalumi, D., Macchi, E., 2009. *Energy and exergy analyses for the carbon capture with the Chilled Ammonia Process (CAP)*; Politecnico di Milano – Dipartimento di Energia, P.zza L. da Vinci, 32, 20133 Milano, Italy

Van Straelen, J., Geuzebroek, F., Goodchild, N., Protopapas, G., Mahony, L., 2009. *CO₂ capture for refineries, a practical approach*, International Journal of Greenhouse Gas Control 4 (2010), pp. 316–320.

Van Wees, J.-D., Orlic, B., Van Eijs, R., Zijl, W., Jongerius, P., Schreppers, G.J., Hendriks, M. & Cornu, T., 2003. Integrated 3D geomechanical modelling for deep subsurface deformation in the eastern Netherlands. In: Nieuwland, D.A. (Ed.), *New insights into structural interpretation and modeling*. Geological Society of London Special Publication, 212, p.313-328.

Vandeginste, V. & Piessens, K., 2008. Pipeline design for a least-cost router application for CO₂ transport in the CO₂ sequestration cycle. International Journal of Greenhouse Gas Control, 2(4), p.571-581.

Vidas, H., Hugman, R. & Clapp, C., 2009. Analysis of geologic sequestration costs for the United States and implications for climate change mitigation. Energy Procedia 1, p.4281-4288.

Welkenhuysen, K. & Piessens, K., 2011a. Semi-optimised pipeline routing for CO₂ Capture and Storage. Proceedings of the Pipeline Technology Conference 2011, Hannover, Germany, p.60.

Welkenhuysen, K. & Piessens, K., 2011b. The CCS potential from technical, economic and geological data and uncertainties: international outreach. 2nd CGS Europe Knowledge Sharing Workshop, Maria Laach, Germany, 19-23/10/2011. (poster)

Welkenhuysen, K., Piessens, K., Baele, J.-M., Laenen, B. & Duser, M., 2011. CO₂ storage opportunities in Belgium. Energy Procedia, 4, p.4913-4920.

White, D.J., Burrowes, G., Davis, T., Hajnal, Z., Hirsche, K., Hutcheon, I., Majer, E., Rostron, B. & Whittaker, S., 2004. Greenhouse gas sequestration in abandoned oil reservoirs: The International Energy Agency Weyburn pilot project. GSA Today, 14 (7), p.4-10.

Wo, S., Liang, J.T. and Myer & L.R., 2005. CO₂ storage in coalbeds: risk assessment of CO₂ and methane leakage. In: Thomas, D.C. & Benson, S.M. (Eds.), *Carbon dioxide capture for storage in deep geologic formations*, 2.

Wolf, K.-H.A.A., Barzandji, O.H., Bruining, J. & Ephraim, R., 2001. CO₂ injection in and CH₄ production from coal seams: laboratory experiments and image analysis for simulations. Proceedings of the First National Conference on Carbon Sequestration, 13p. Nr.: DOE/NETL;2001/1144.

Xu, T., Apps, J.A. & Pruess, K., 2004. Numerical simulation of CO₂ disposal by mineral trapping in deep aquifers. Applied Geochemistry, 19, p.917-936.

Yamaguchi, S., Ohga, K., Fujioka, M. & Muto, S., 2004. Prospect of CO₂ sequestration in the Ishikari coalfield, Japan. In: Rubin, E.S., Keith, D.W., Gilboy, C.F. (Eds.), Proceedings of the 7th International Conference on Greenhouse Gas Control Technologies, 1, p.423–430.

ZEP, 2008. The EU technology platform for Zero Emission fossil fuel Power plants, *Recommendations for RTD, support actions and international collaboration activities within FP7 energy work programmes and national RTD programmes in support of deployment of CCS in Europe*.

ZEP, 2011a. The Cost of CO₂ Capture, Transport and Storage. European Technology Platform for Zero Emission Fossil Fuel Power Plants, 51p. <http://www.zeroemissionsplatform.eu/downloads/811.html>

ZEP, 2011b. The Cost of CO₂ Transport. European Technology Platform for Zero Emission Fossil Fuel Power Plants, 53p. <http://www.zeroemissionsplatform.eu/downloads/813.html>

ZEP, 2011c. The Cost of CO₂ Capture. European Technology Platform for Zero Emission Fossil Fuel Power Plants, 53p. <http://www.zeroemissionsplatform.eu/downloads/812.html>

Zhou, W., Stenhouse, M. & Arthur, R., 2005. Assessment of potential well leakage in the Weyburne Site using a stochastic approach. Conference proceedings of the Fourth Annual Conference on Carbon Capture and Sequestration DOE/NETL, 9p.

8. ANNEXES

THE ANNEXES ARE AVAILABLE ON OUR WEBSITE

http://www.belspo.be/belspo/SSD/science/pr_climate_en.stm